The spin structure of the proton from JLab to the LHC

Charlotte Van Hulse
VUB

ODYSSEUS Top science in Flanders fwo

CNUGS26
26 May 2026 to 12 June 2026
Jefferson Lab

How it started

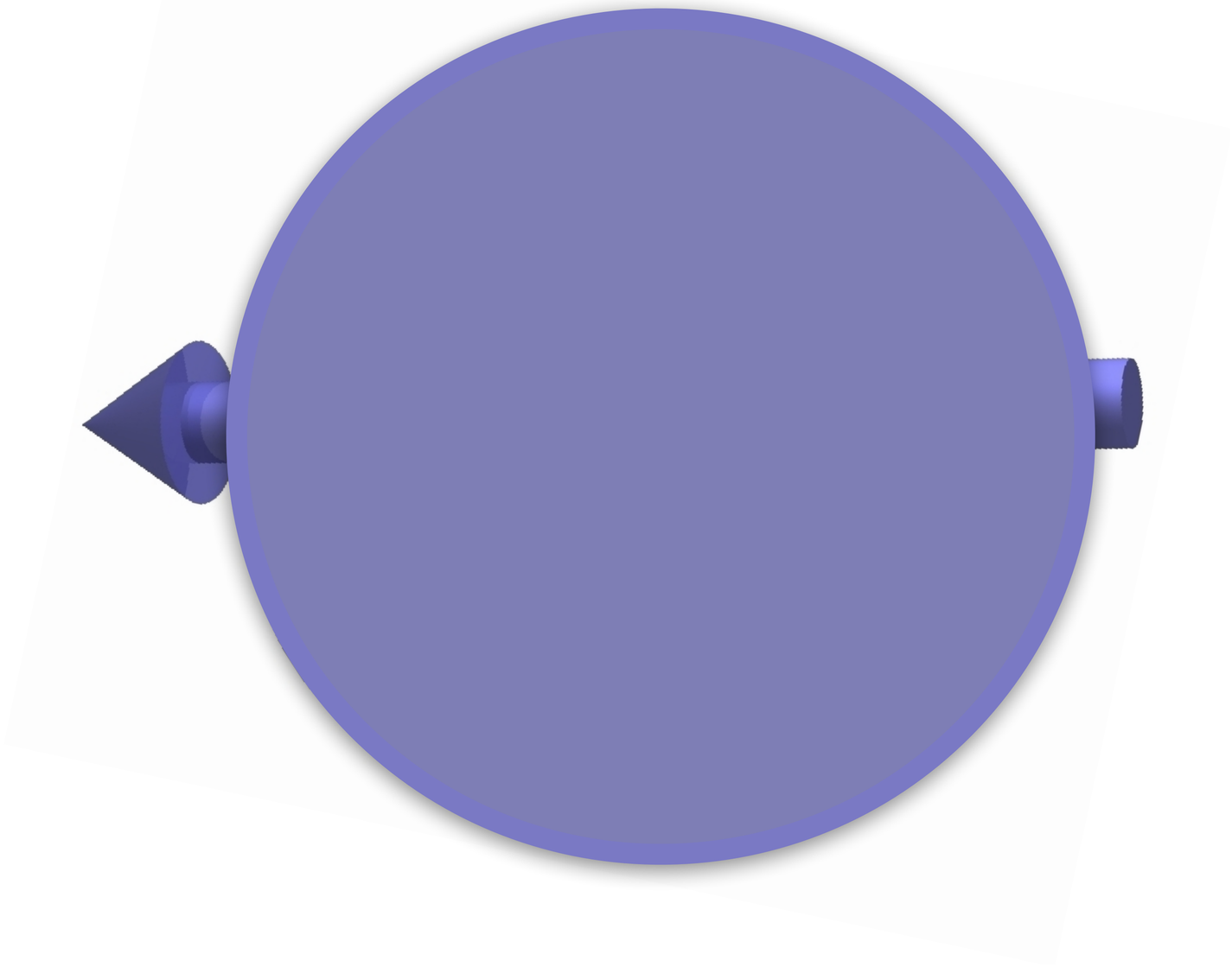

How it started

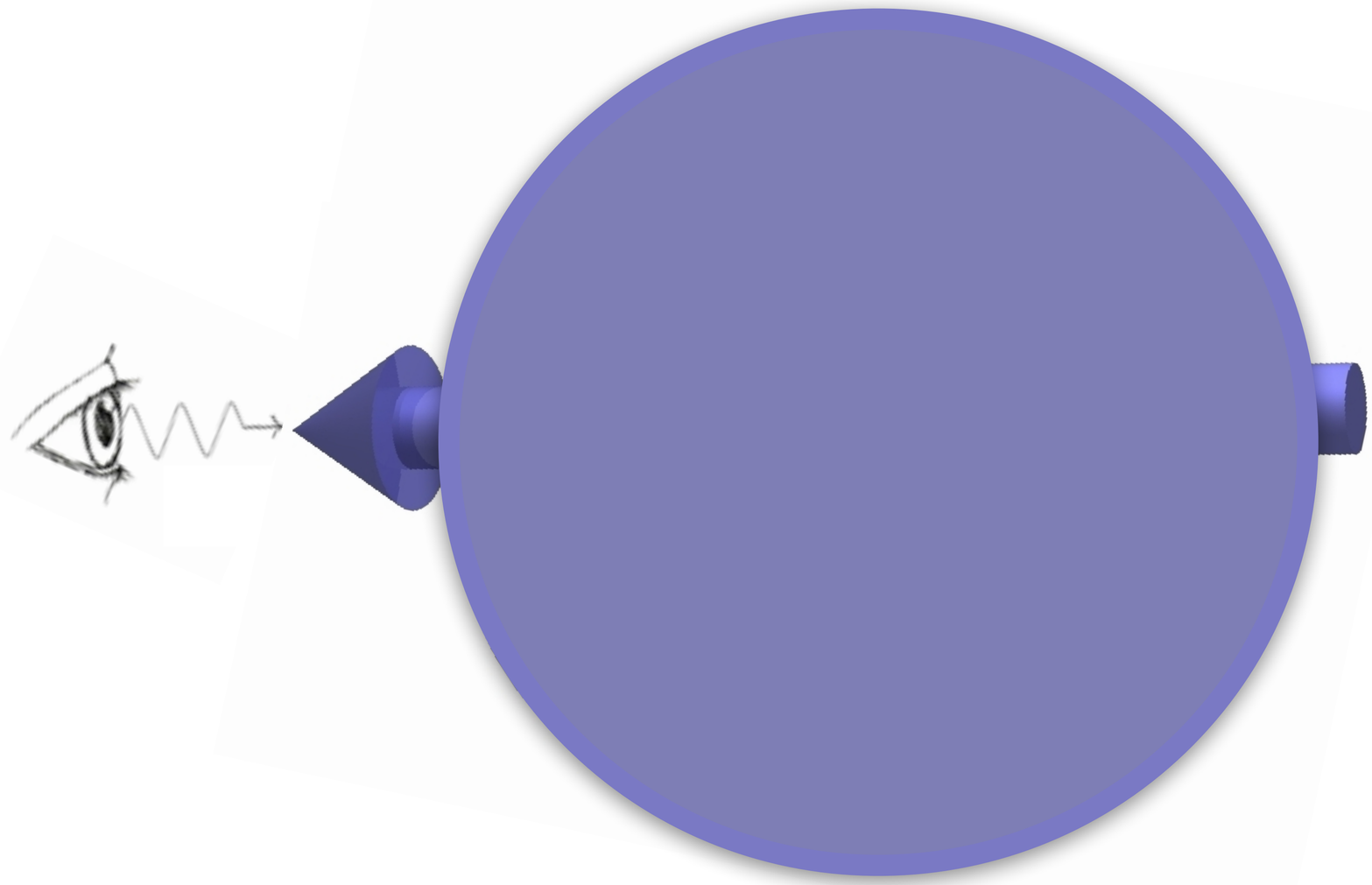

How it started

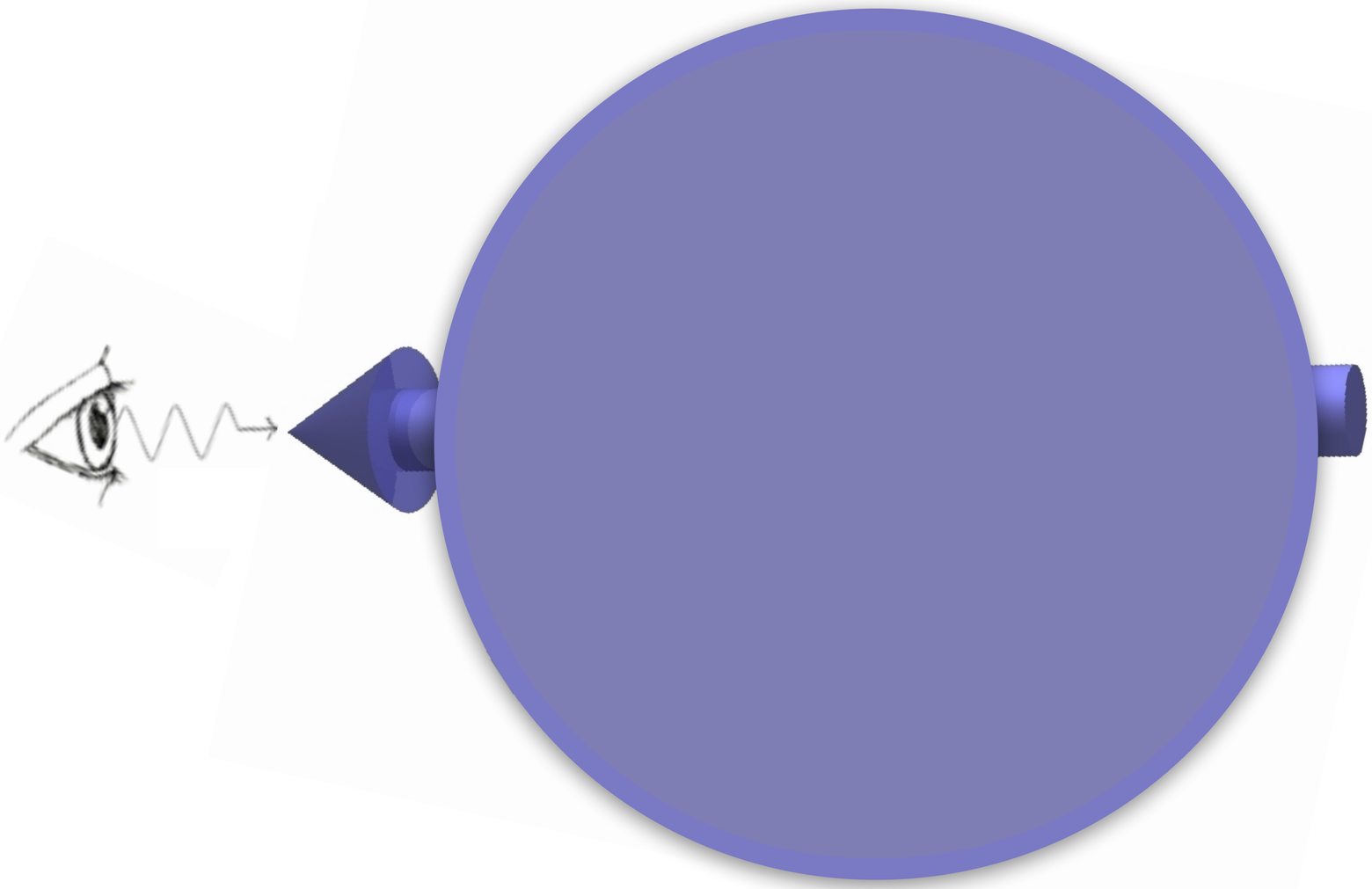

Proton spin = $\frac{1}{2}$

What is its origin?

How it started

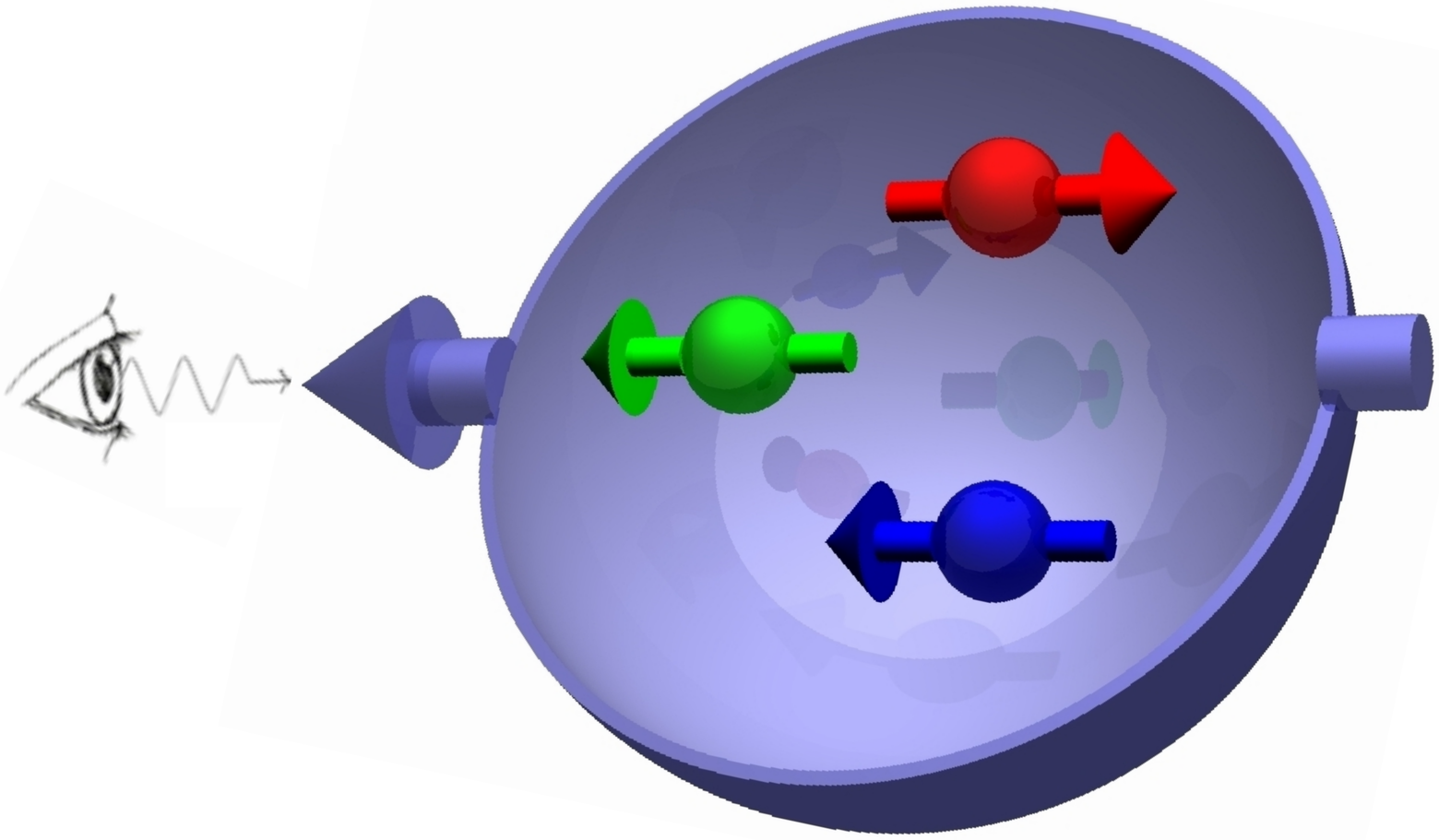

- Naive constituent quark model:

$$\frac{1}{2} = \sum \text{quark spin}$$

$$= \frac{1}{2}\Delta\Sigma$$

How it started

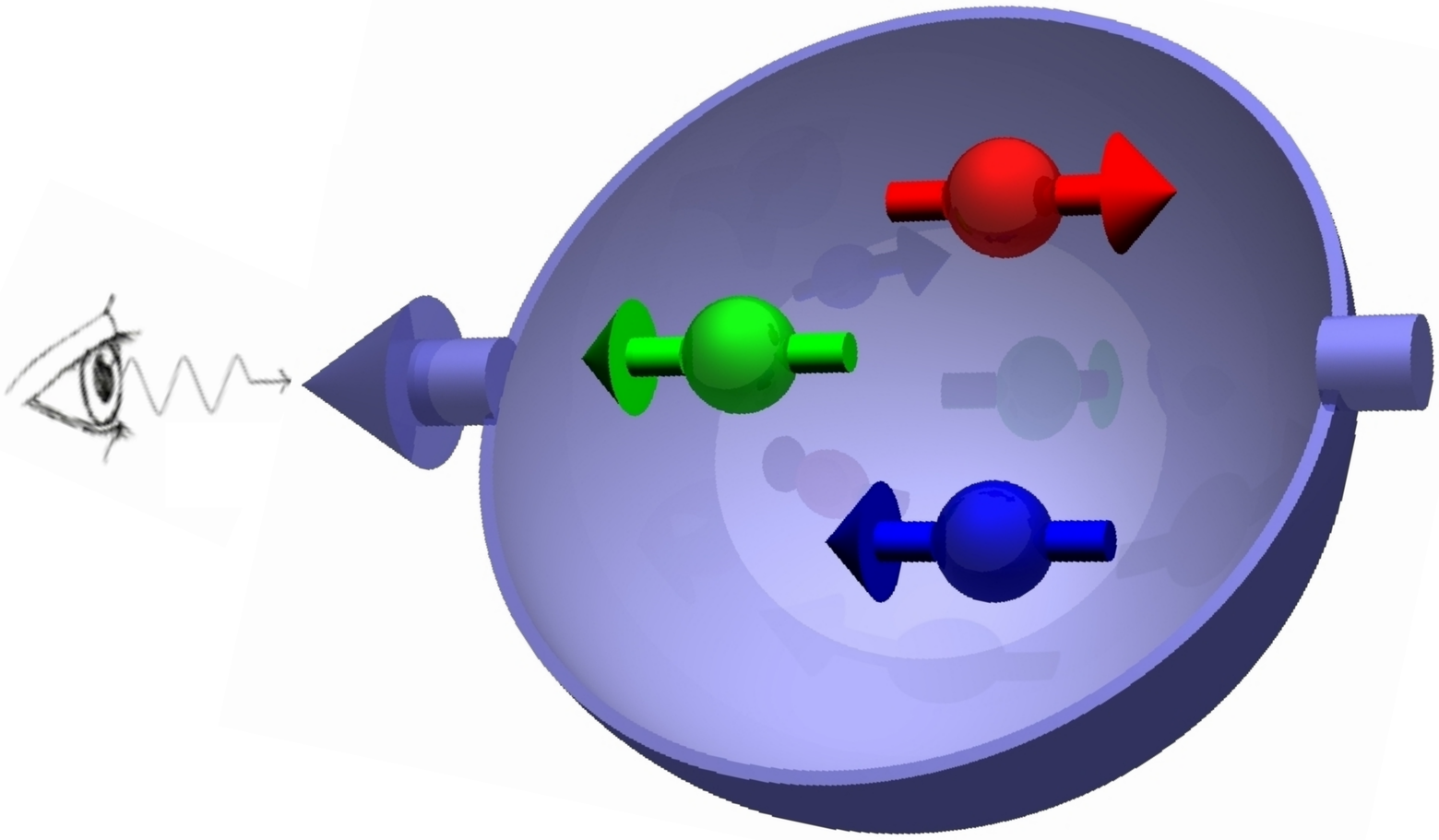

- Naive constituent quark model:

$$\frac{1}{2} = \sum \text{quark spin}$$

$$= \frac{1}{2}\underbrace{\Delta\Sigma}_{1}$$

How it started

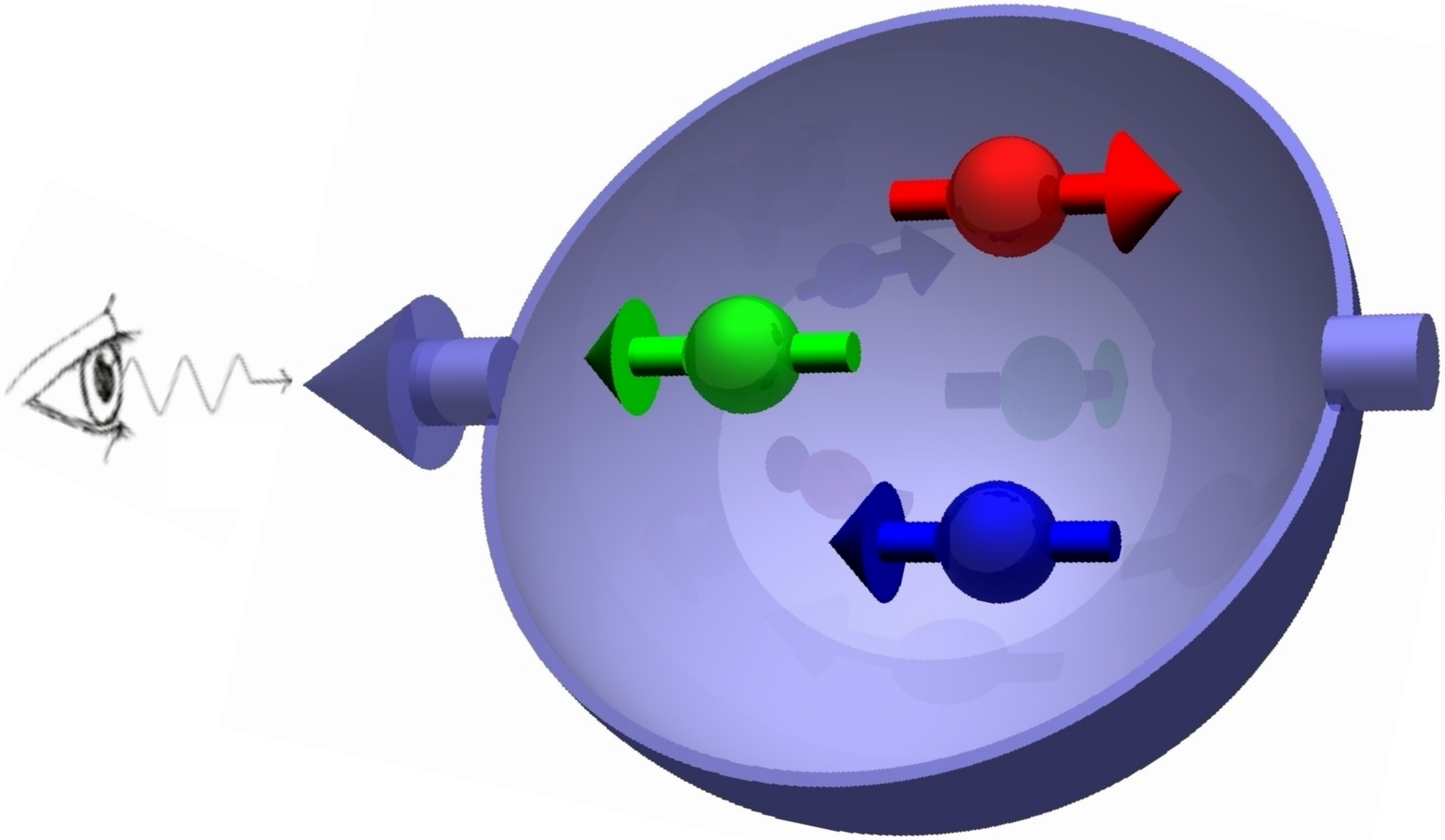

- Naive constituent quark model:

$$\frac{1}{2} = \sum \text{quark spin}$$

$$= \frac{1}{2}\underbrace{\Delta\Sigma}_{1}$$

- Add relativistic corrections

$$\Delta\Sigma \approx 0.65$$

How it started

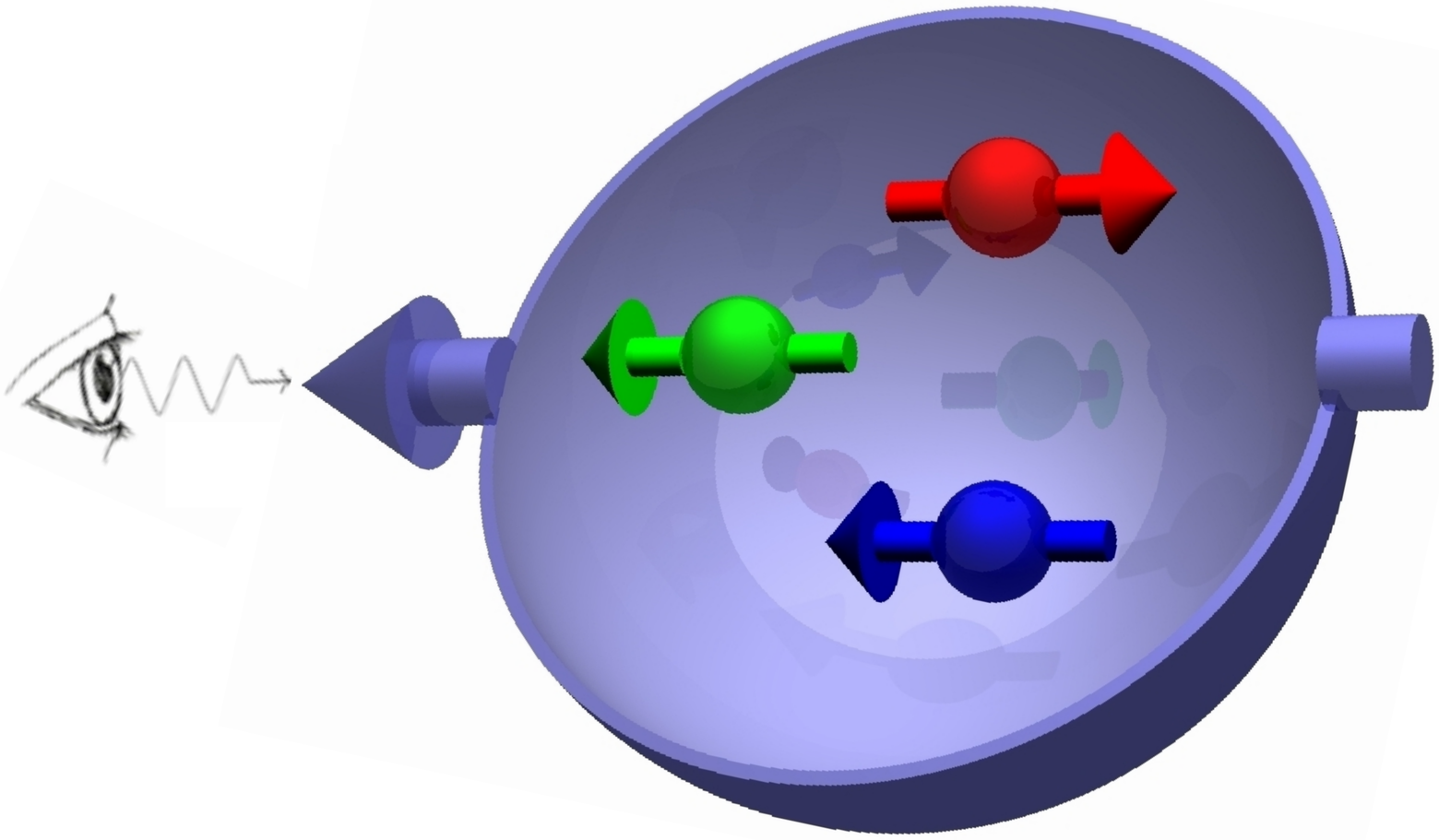

- Naive constituent quark model:

$$\frac{1}{2} = \sum \text{quark spin}$$

$$= \frac{1}{2}\underbrace{\Delta\Sigma}_{1}$$

- Add relativistic corrections

$$\Delta\Sigma \approx 0.65$$

- First measurement: EMC 1988

$$\Delta\Sigma = \Delta u + \Delta\bar{u} + \Delta d + \Delta\bar{d} + \Delta s + \Delta\bar{s}$$

with $\Delta q = \overrightarrow{q} - \overleftarrow{q}$: helicity parton distribution function (PDF)

How it started

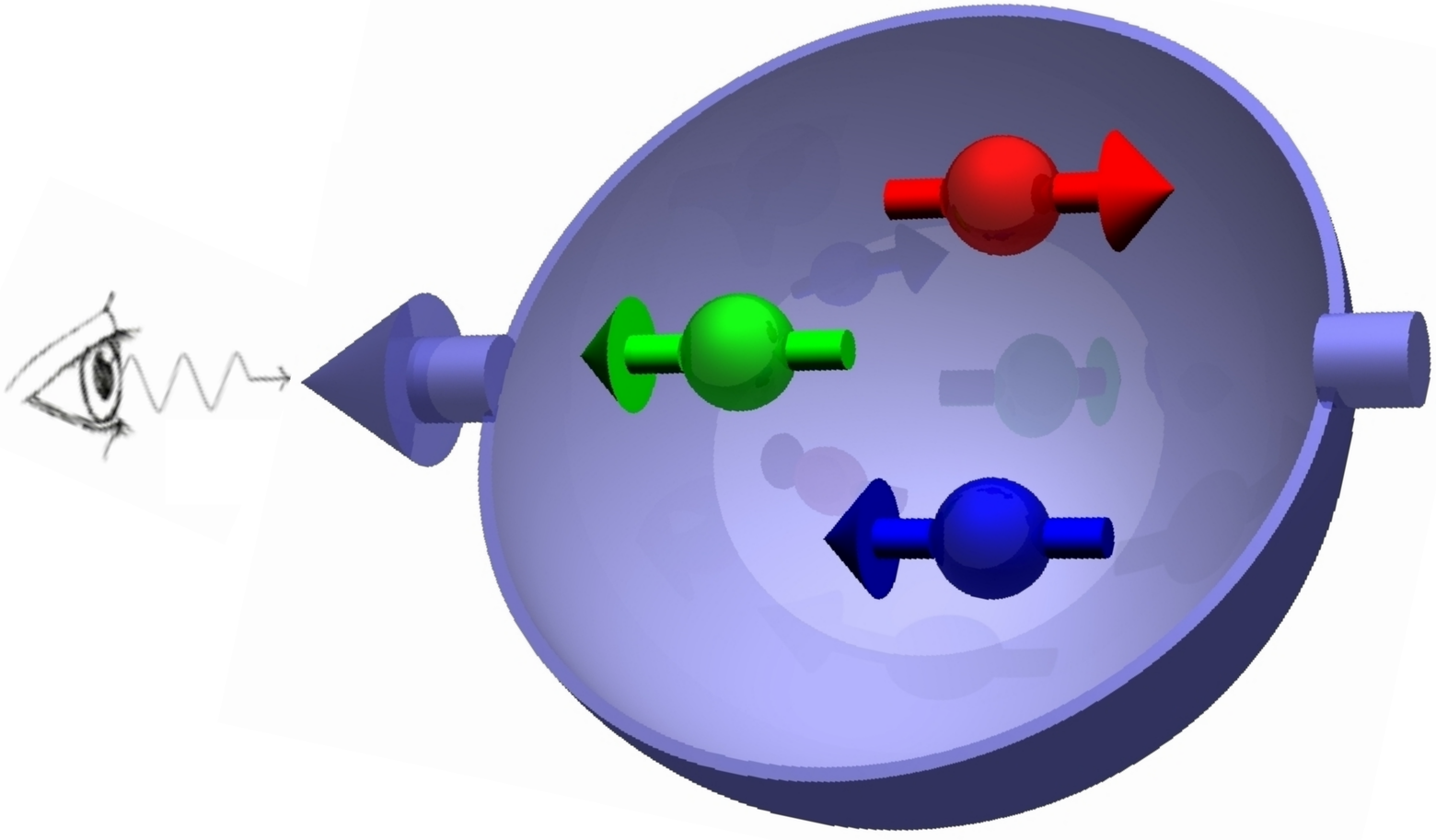

- Naive constituent quark model:

$$\frac{1}{2} = \sum \text{quark spin}$$

$$= \frac{1}{2}\underbrace{\Delta\Sigma}_{1}$$

- Add relativistic corrections

$$\Delta\Sigma \approx 0.65$$

- First measurement: EMC 1988

$$\Delta\Sigma = \Delta u + \Delta\bar{u} + \Delta d + \Delta\bar{d} + \Delta s + \Delta\bar{s}$$

$$= 0.14 \pm 0.09 \pm 0.21$$

with $\Delta q = \overrightarrow{q} - \overleftarrow{q}$: helicity parton distribution function (PDF)

How it started

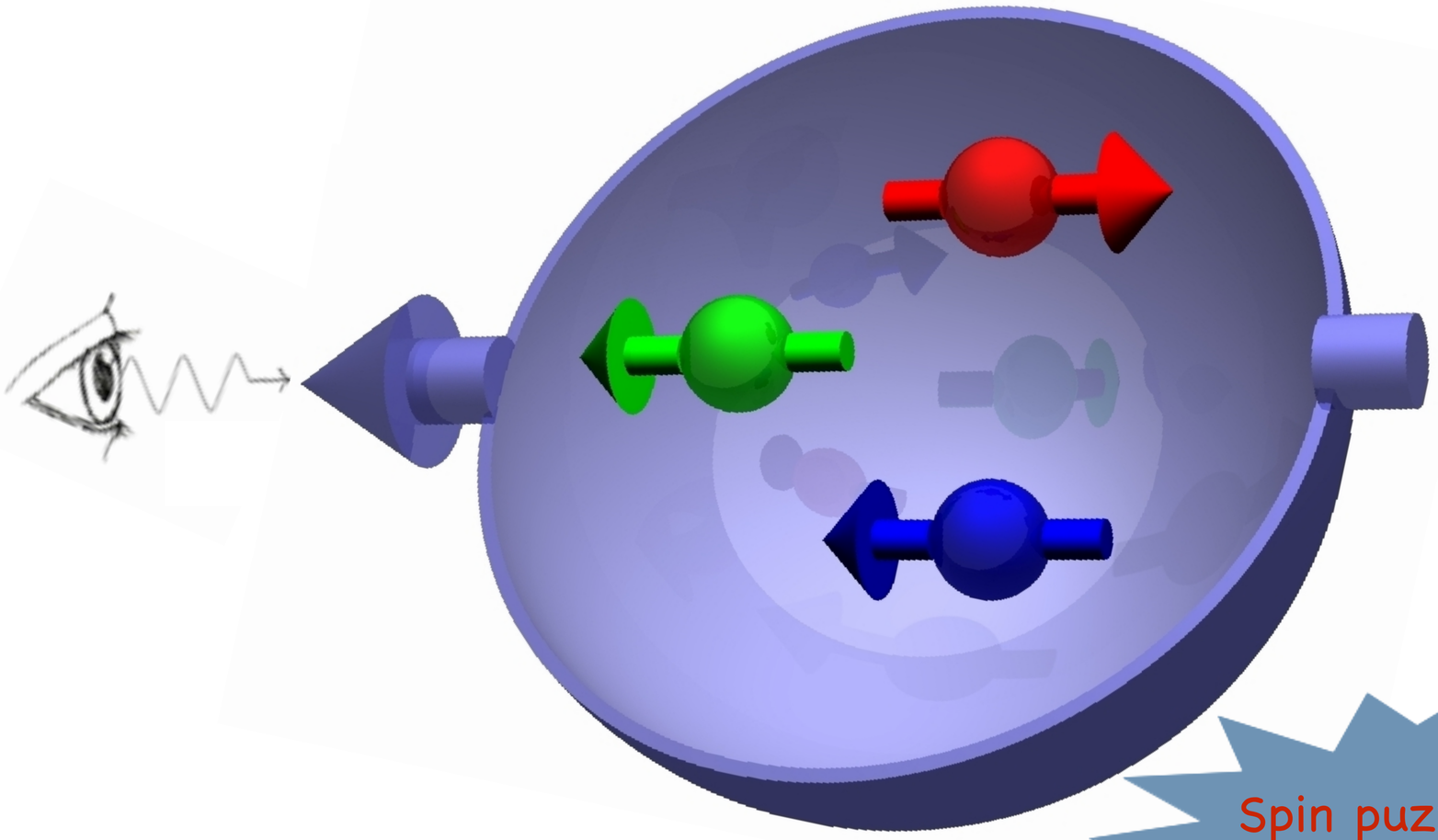

- Naive constituent quark model:

$$\frac{1}{2} = \sum \text{quark spin}$$

$$= \frac{1}{2}\underbrace{\Delta\Sigma}_{1}$$

- Add relativistic corrections

$$\Delta\Sigma \approx 0.65$$

Spin puzzle

First measurement: EMC 1988

$$= \Delta u + \Delta\bar{u} + \Delta d + \Delta\bar{d} + \Delta s + \Delta\bar{s}$$

$$= 0.14 \pm 0.09 \pm 0.21$$

with $\Delta q = \overrightarrow{q} - \overleftarrow{q}$: helicity parton distribution function (PDF)

How it started

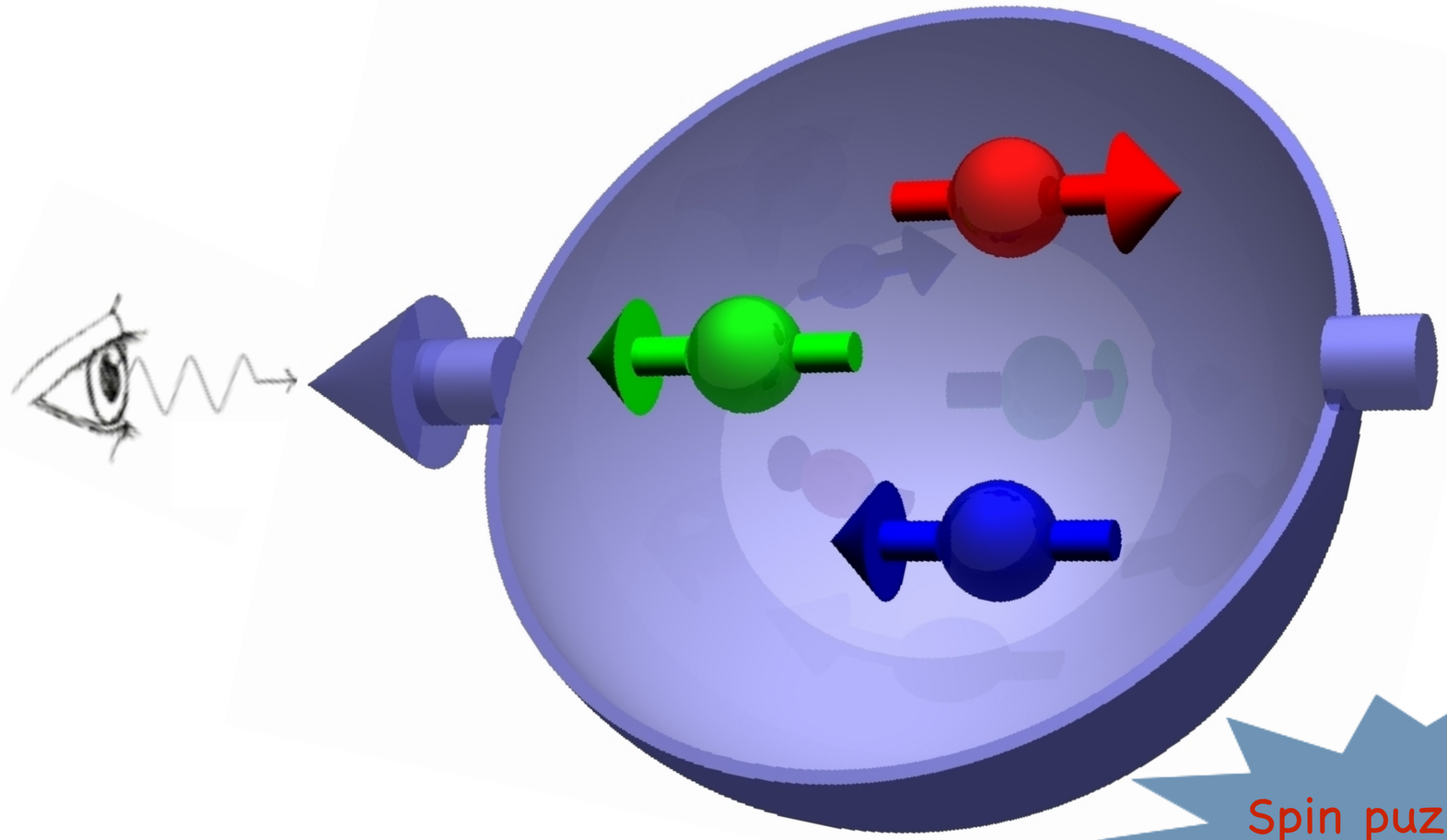

- Naive constituent quark model:

$$\frac{1}{2} = \sum \text{quark spin}$$

$$= \frac{1}{2}\underbrace{\Delta\Sigma}_{1}$$

- Add relativistic corrections

$$\Delta\Sigma \approx 0.65$$

First measurement: EMC 1988

Spin puzzle

$$= \Delta u + \Delta\bar{u} + \Delta d + \Delta\bar{d} + \Delta s + \Delta\bar{s}$$

$$0.09 \pm 0.21$$

Spin crisis!

$\rightarrow$

with $\Delta q = q$ tion distribution function (PDF)

How it started

Spin puzzle

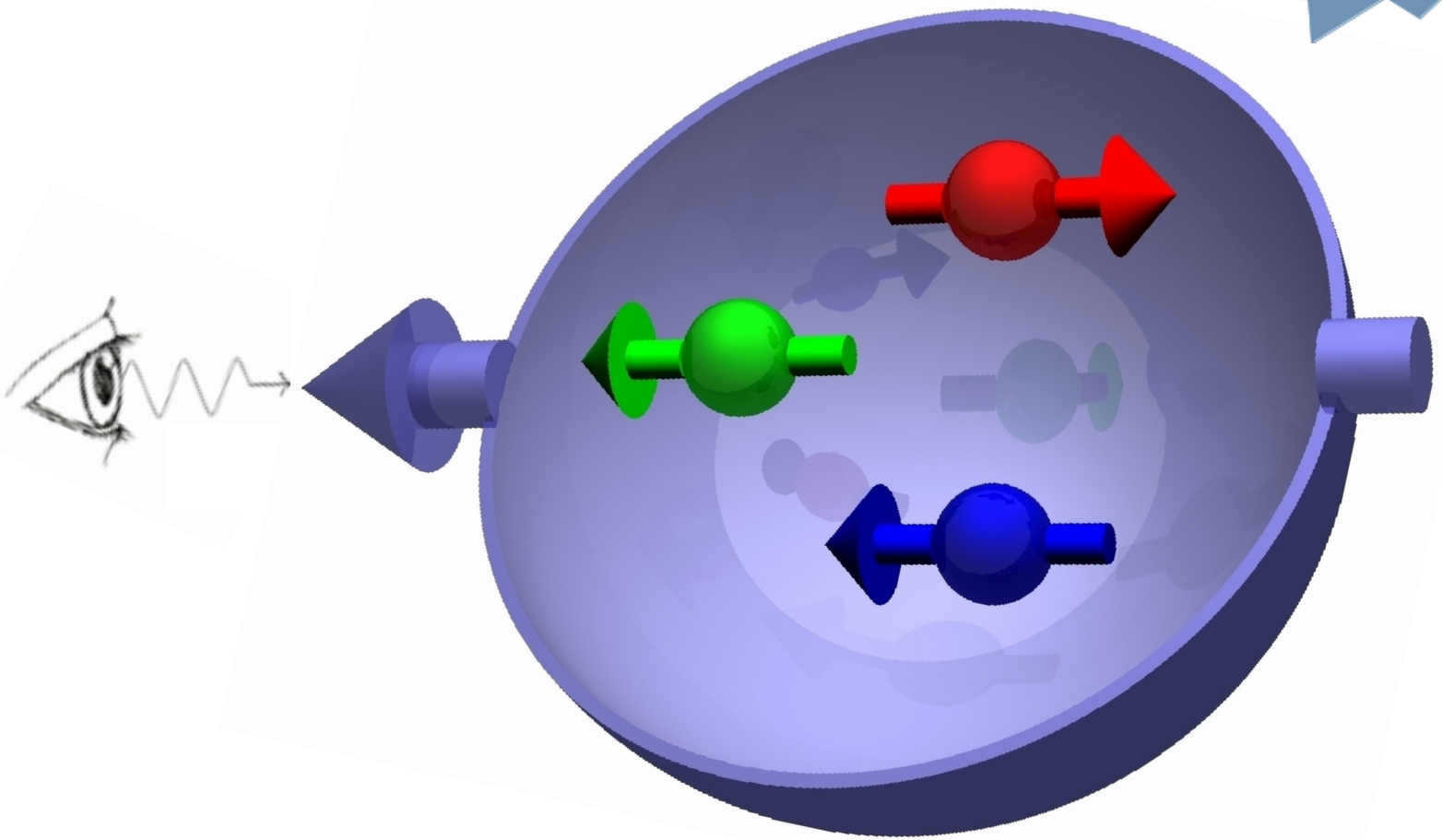

Birth of new experiments:
SMC, HERMES, JLAb, COMPASS

How it started

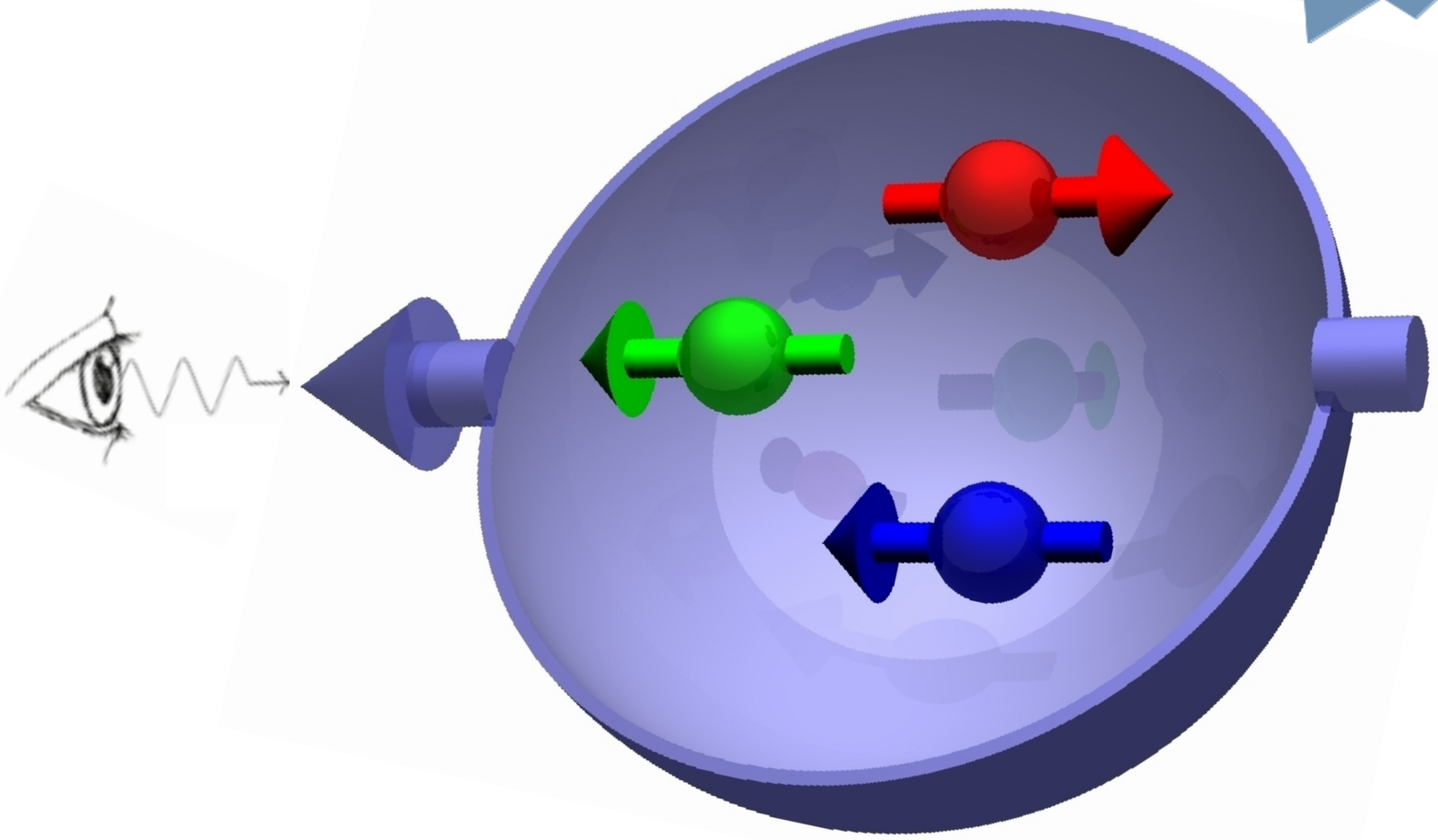

Spin puzzle

Birth of new experiments:
SMC, HERMES, JLAb, COMPASS

- Check EMC result

How it started

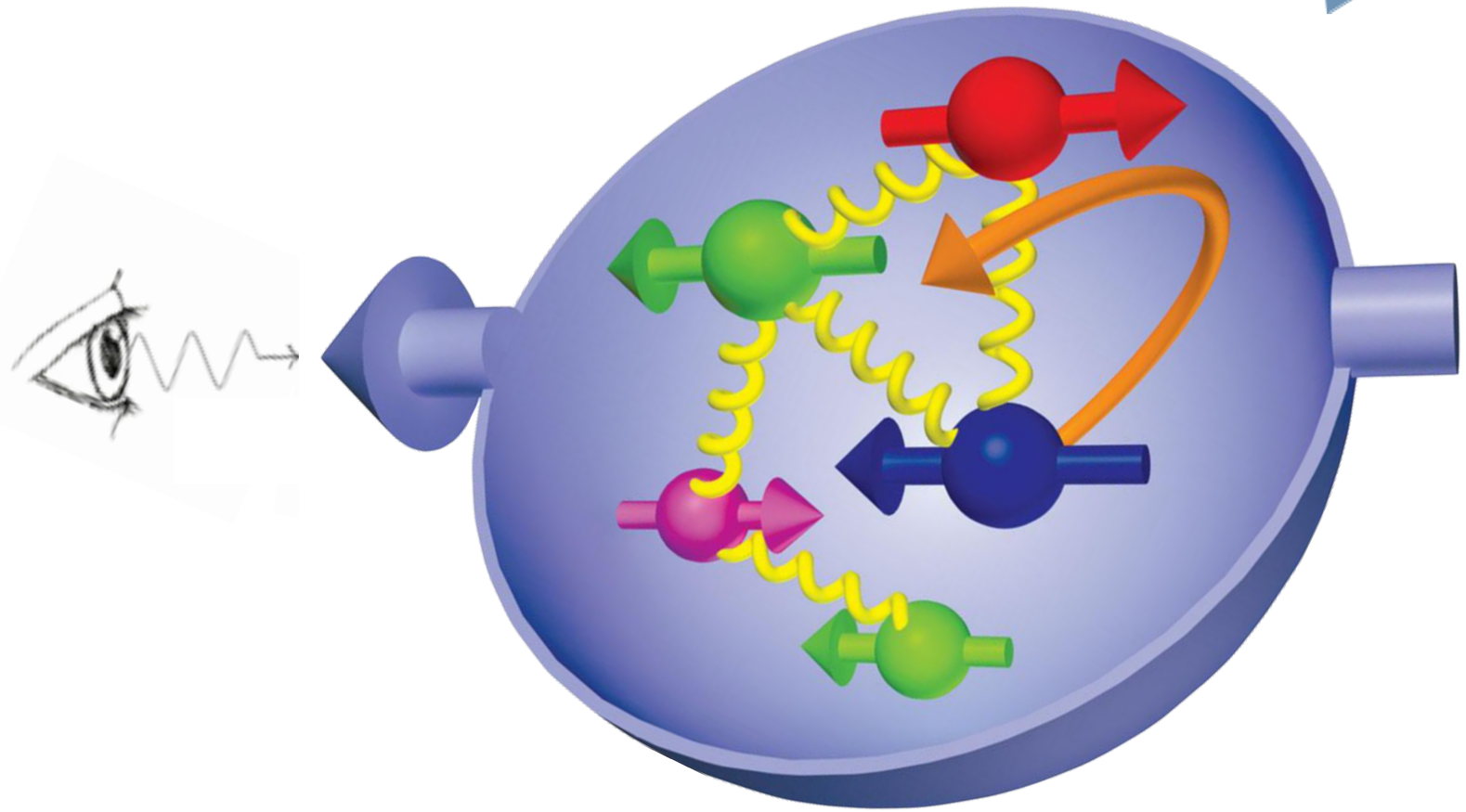

Spin puzzle

Birth of new experiments:
SMC, HERMES, JLAb, COMPASS

- Check EMC result
- Find missing contributions

How it started

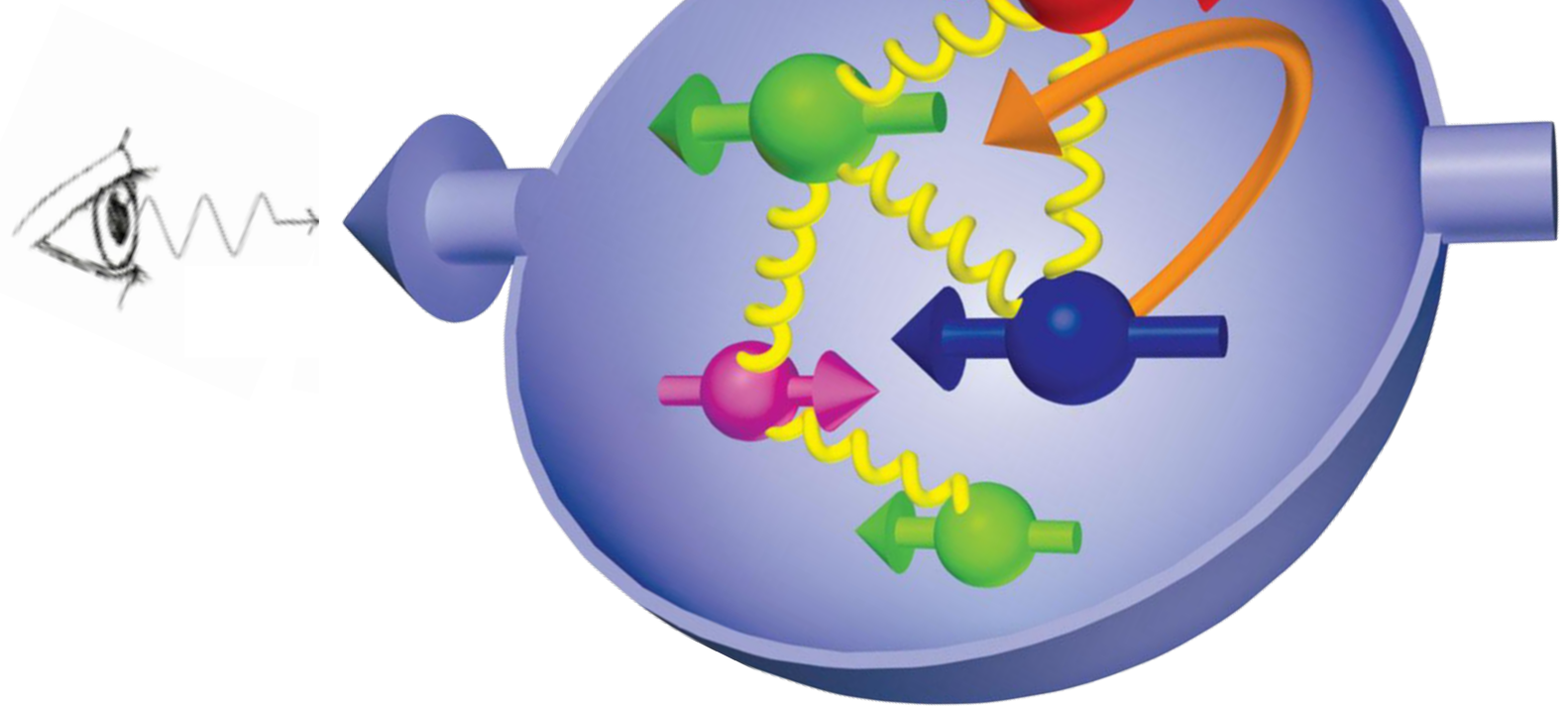

Spin puzzle

Birth of new experiments:
SMC, HERMES, JLAb, COMPASS

- Check EMC result
- Find missing contributions

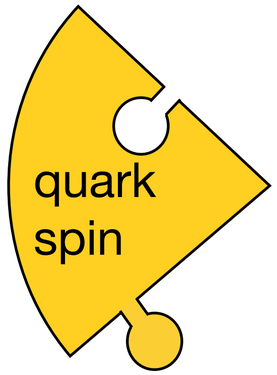

How it started

Spin puzzle

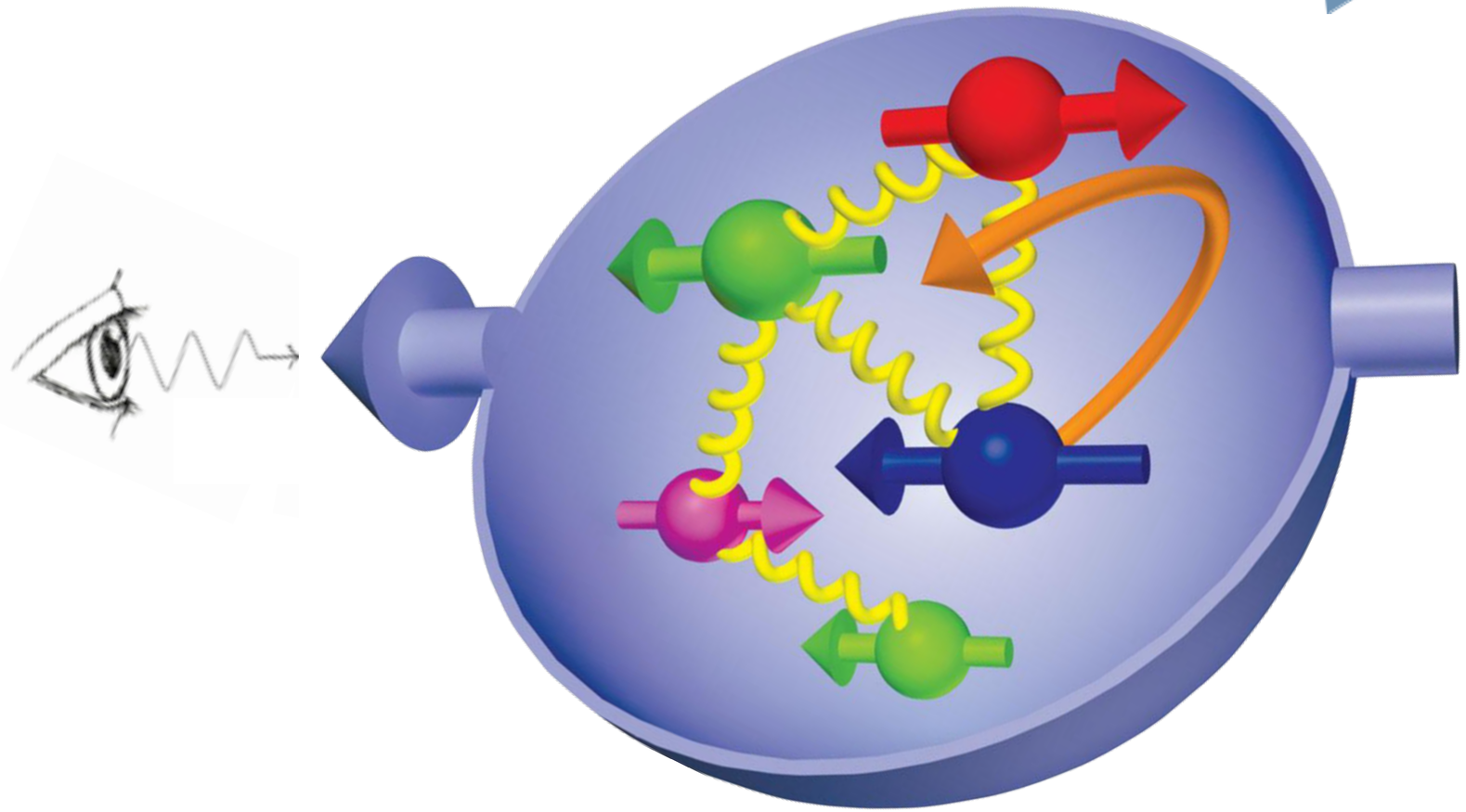

Birth of new experiments:
SMC, HERMES, JLAb, COMPASS

- Check EMC result
- Find missing contributions

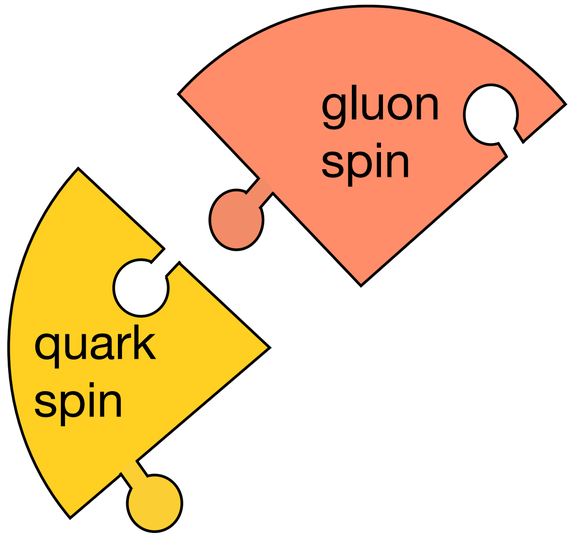

How it started

Spin puzzle

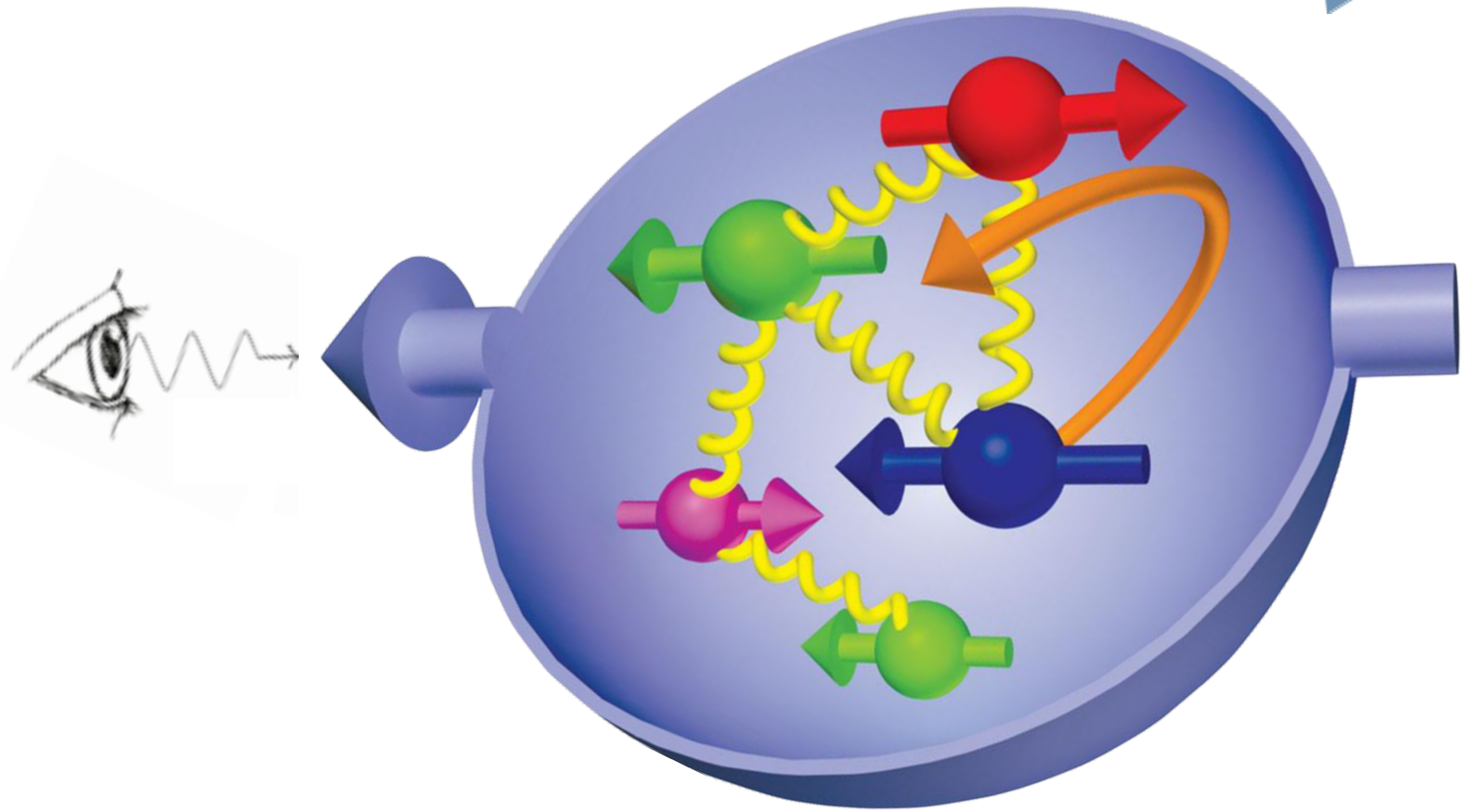

Birth of new experiments:
SMC, HERMES, JLAb, COMPASS

- Check EMC result
- Find missing contributions

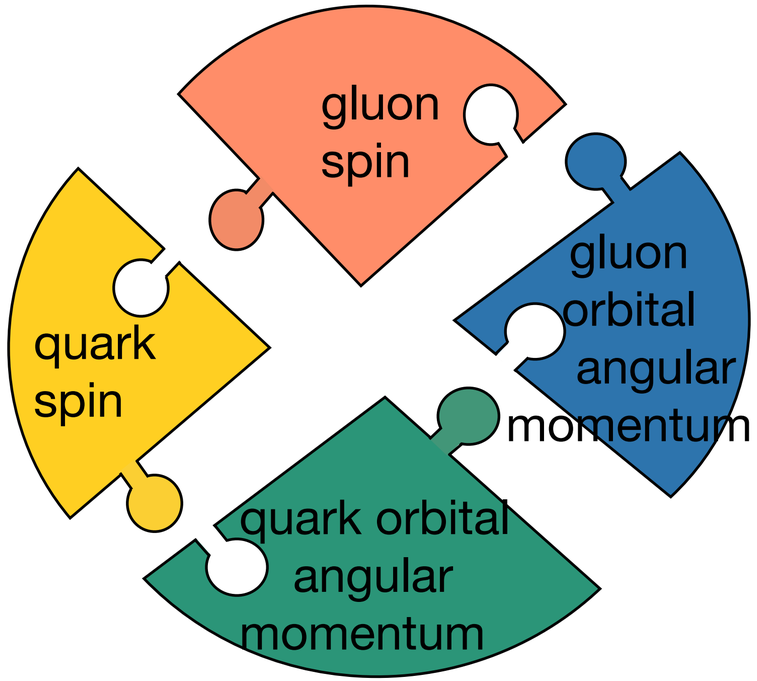

Experiments studying spin

$e^+ + e^-$ and $\vec{e} + \vec{p}, \vec{D}, \overrightarrow{He}$

SLAC NATIONAL ACCELERATOR LABORATORY

Jefferson Lab

$\vec{e} + \vec{p}, \vec{D}, \overrightarrow{He}$

$\vec{p}\,\vec{p}$ collider

BROOKHAVEN NATIONAL LABORATORY

$\vec{e} + \vec{p}, \vec{D}, \overrightarrow{He}$

DESY

COMPASS $\vec{\mu} + \vec{p}$ & $\pi + \vec{p}$

CERN

LHC $p + p$

KEK High Energy Accelerator Research Organization

$e^+ + e^-$

Access to partons and their helicity

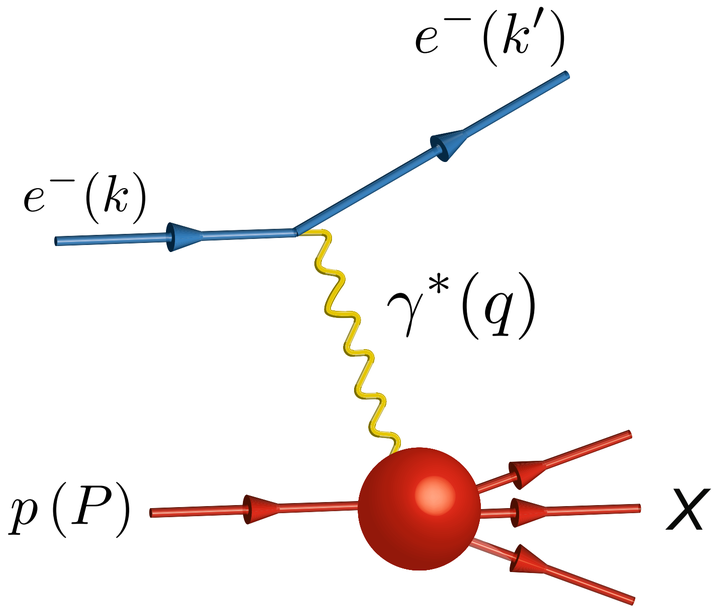

$$Q^2 = -\,q^2$$

Highly virtual photon:

$Q^2 \gg 1$ GeV^2

provides hard scale of process

→ factorisation

$$x_B = \frac{Q^2}{2P\,.\,q}$$

Access to partons and their helicity

Longitudinally polarised lepton beam

Longitudinally polarised proton beam or fixed target

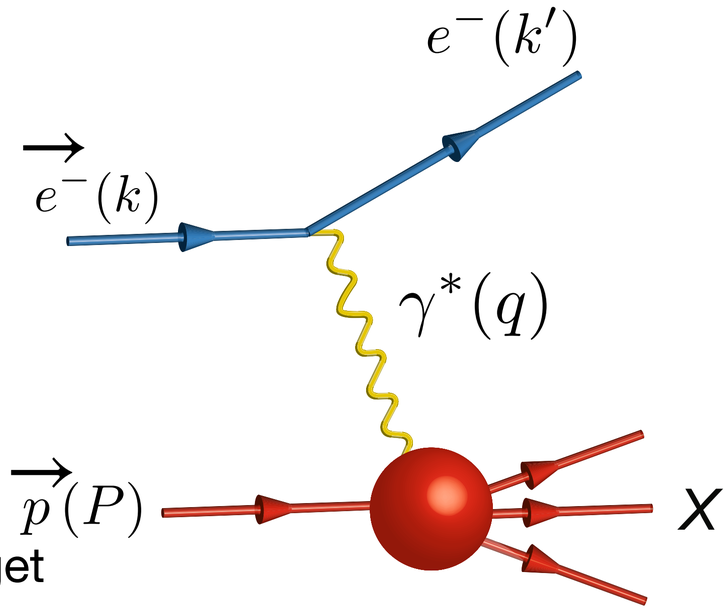

$$Q^2 = -q^2$$

Highly virtual photon:

$Q^2 \gg 1\ \text{GeV}^2$

provides hard scale of process

→ factorisation

$$x_B = \frac{Q^2}{2P \cdot q}$$

Measurement of the quark spin contribution

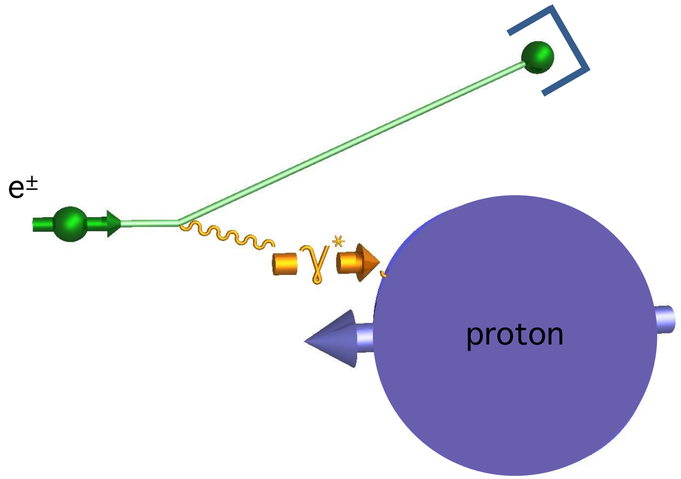

- longitudinally polarised proton
- longitudinally polarised $e^{\pm}$ or $\mu^{\pm}$ beam
- count…

Measurement of the quark spin contribution

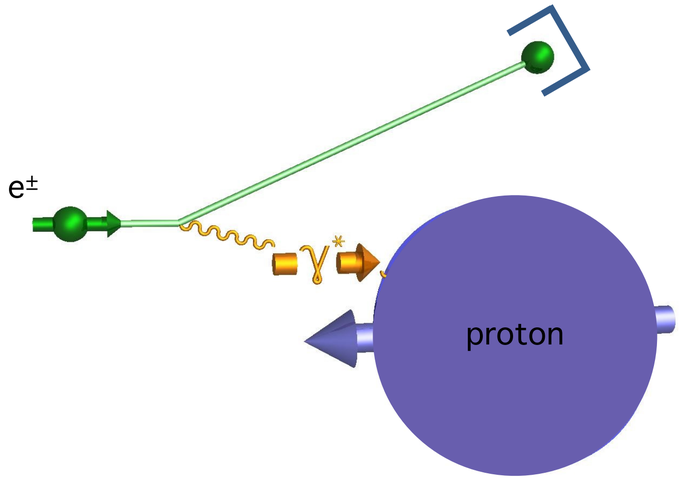

- longitudinally polarised proton
- longitudinally polarised $e^{\pm}$ or $\mu^{\pm}$ beam
- count… 0 2 4 6 8 0

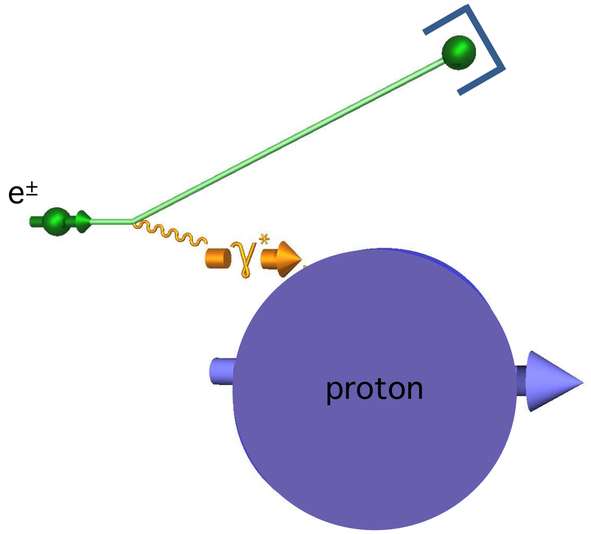

- flip proton spin and count… 0 2 4 6 8 0

Measurement of the quark spin contribution

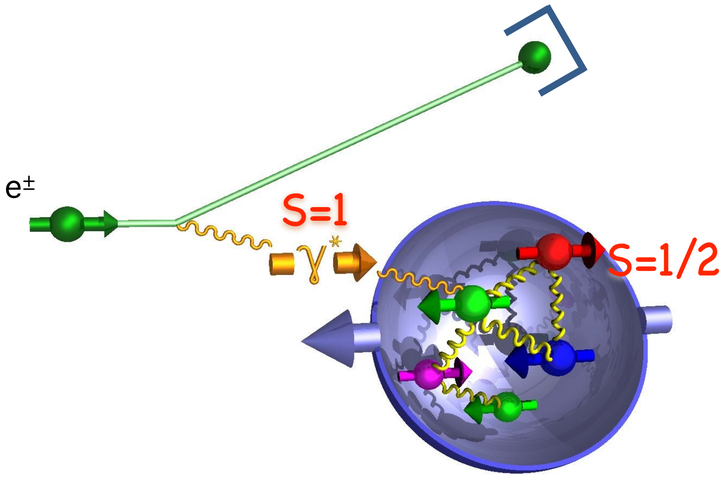

- longitudinally polarised proton
- longitudinally polarised $e^{\pm}$ or $\mu^{\pm}$ beam
- count…

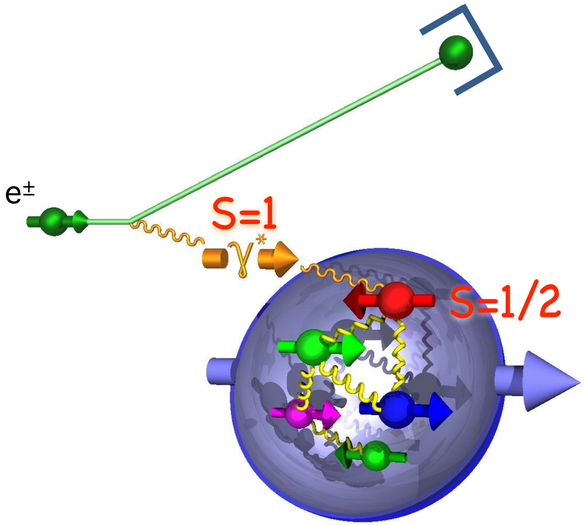

- flip proton spin and count…

Measurement of the quark spin contribution

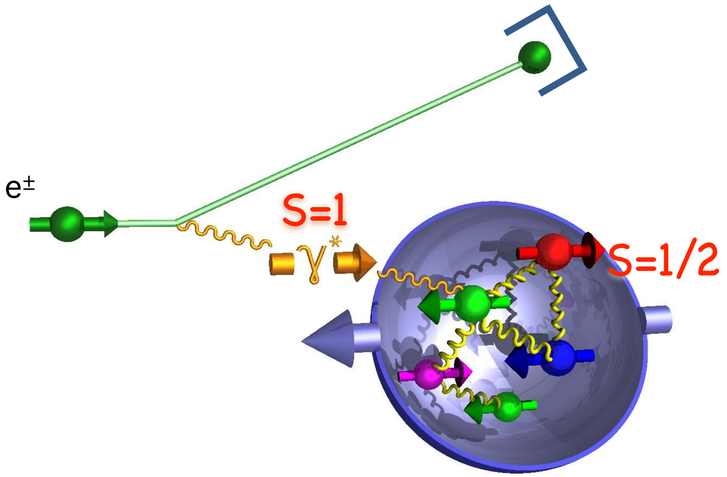

- longitudinally polarised proton
- longitudinally polarised $e^{\pm}$ or $\mu^{\pm}$ beam
- count…

Access to quarks with spin aligned to proton spin

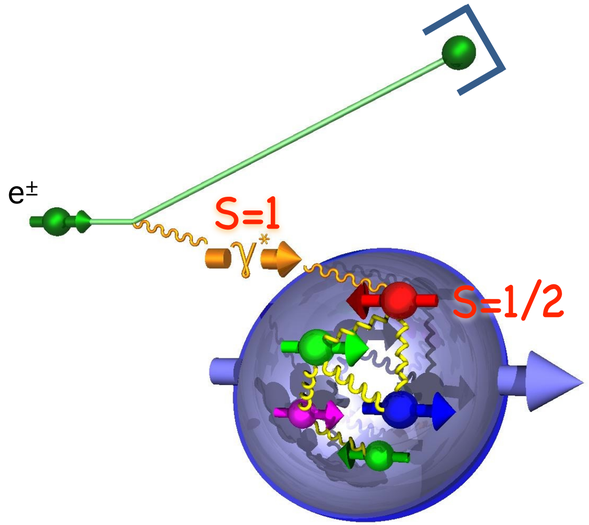

- flip proton spin and count…

Access to quarks with spin anti-aligned to proton spin

Measurement of the quark spin contribution

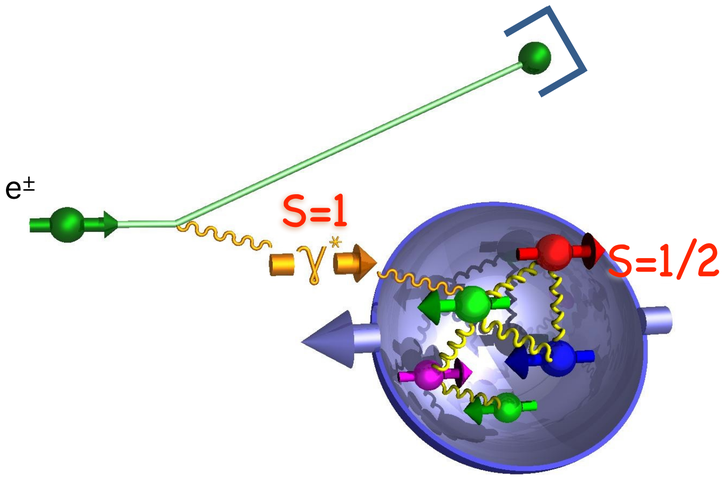

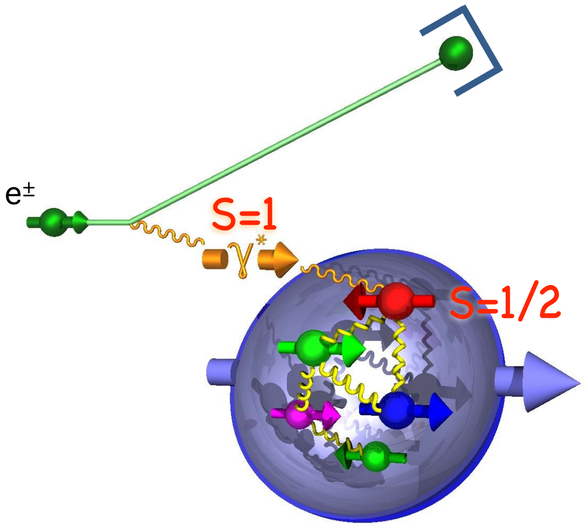

Measurement of the quark spin contribution

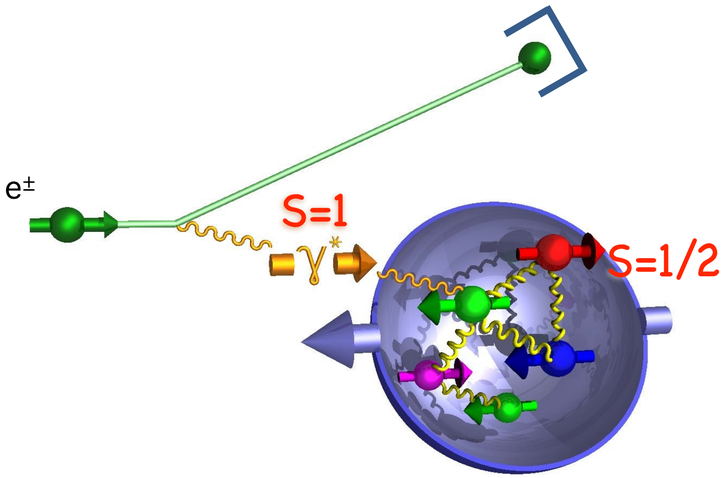

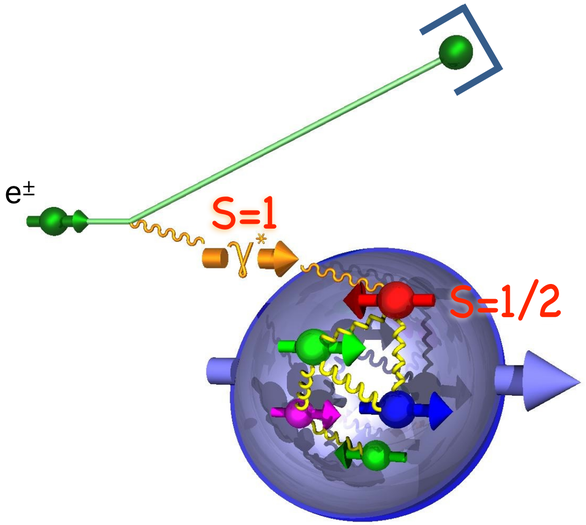

Asymmetry: $$A_{LL} = \frac{\frac{\overleftarrow{\rightarrow}}{N} - \frac{\overrightarrow{\rightarrow}}{N}}{\frac{\overleftarrow{\rightarrow}}{L} \quad \frac{\overrightarrow{\rightarrow}}{L}}(x_B, Q^2)$$

$$\frac{\frac{\overleftarrow{\rightarrow}}{N} + \frac{\overrightarrow{\rightarrow}}{N}}{\frac{\overleftarrow{\rightarrow}}{L} \quad \frac{\overrightarrow{\rightarrow}}{L}}$$

Measurement of the quark spin contribution

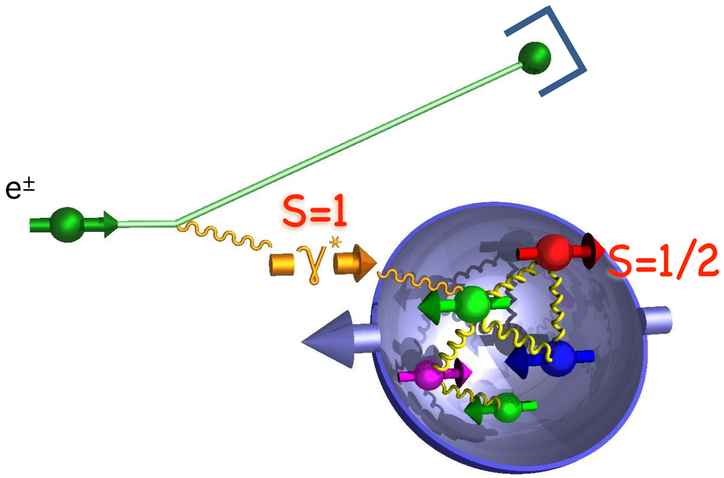

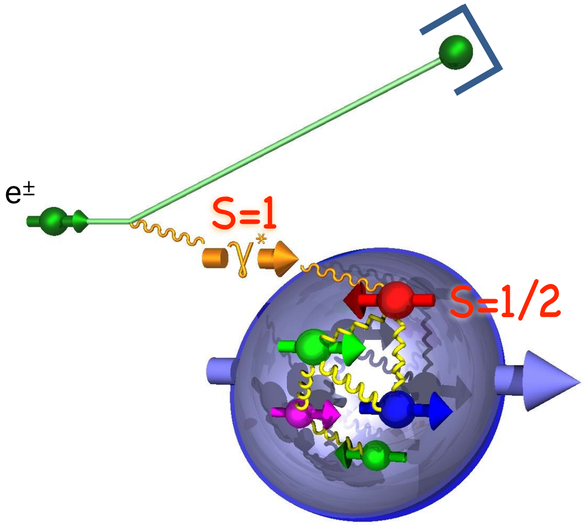

Asymmetry: $$A_{LL} = \frac{\overleftarrow{\overrightarrow{N}} - \overrightarrow{\overrightarrow{N}}}{\overleftarrow{\overrightarrow{L}} \quad \overrightarrow{\overrightarrow{L}}}(x_B, Q^2)$$

$$\overleftarrow{\overrightarrow{N}} + \overrightarrow{\overrightarrow{N}}$$
$$\overleftarrow{\overrightarrow{L}} \quad \overrightarrow{\overrightarrow{L}}$$

precise luminosity determination

Measurement of the quark spin contribution

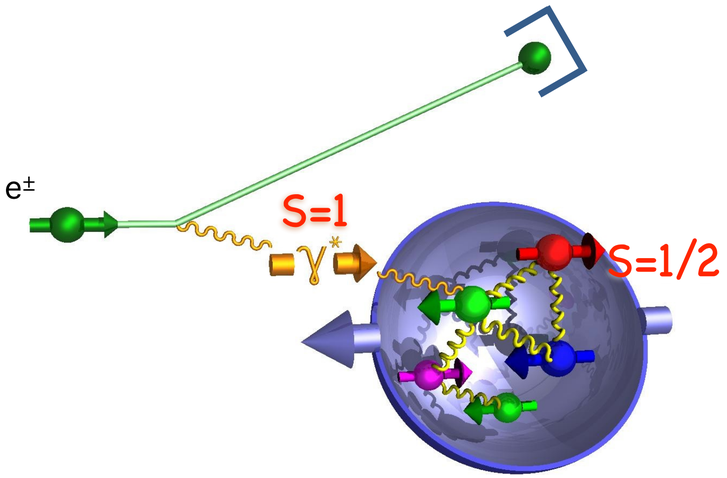

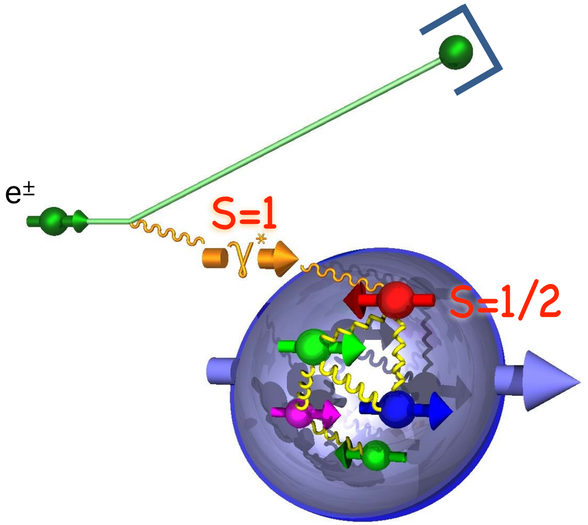

Asymmetry: $A_{LL} = \dfrac{\overleftarrow{\overrightarrow{N}} - \overrightarrow{\overrightarrow{N}}}{\overleftarrow{\overrightarrow{N}} + \overrightarrow{\overrightarrow{N}}}(x_B, Q^2)$ $\overleftarrow{\overrightarrow{L}}$ $\overrightarrow{\overrightarrow{L}}$

precise luminosity determination

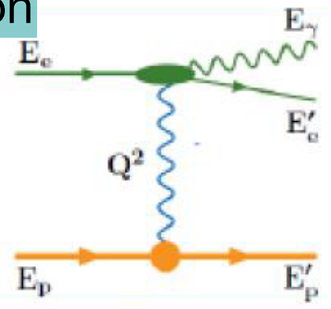

Measurement of the quark spin contribution

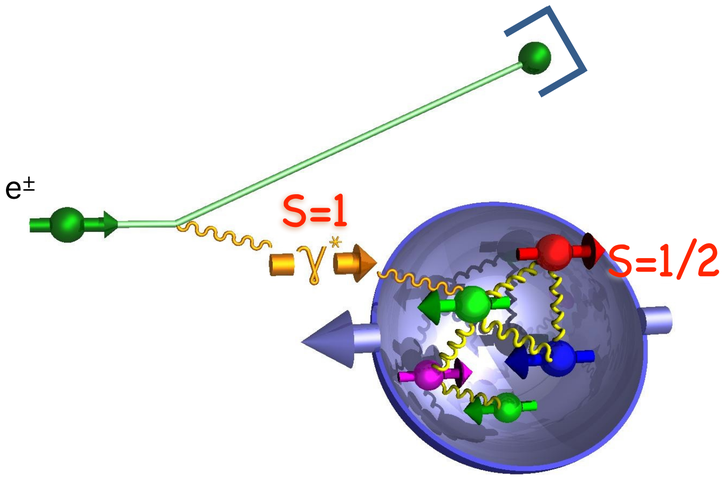

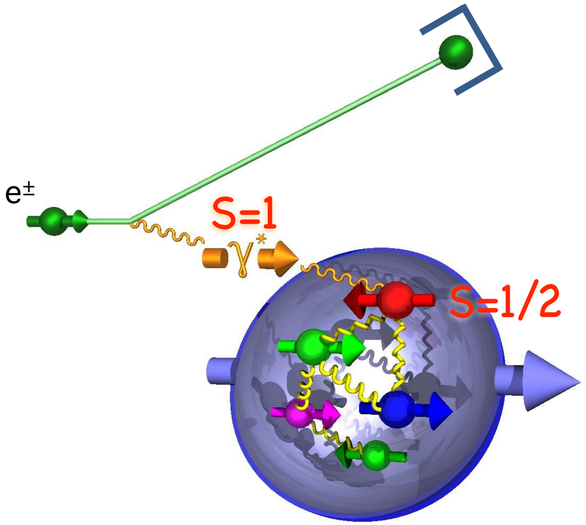

high polarisation

Asymmetry: $A_{LL} = \dfrac{\overleftarrow{\overrightarrow{N}} - \overrightarrow{\overrightarrow{N}}}{\overleftarrow{\overrightarrow{L}} + \overrightarrow{\overrightarrow{L}}}(x_B, Q^2)$

precise luminosity determination

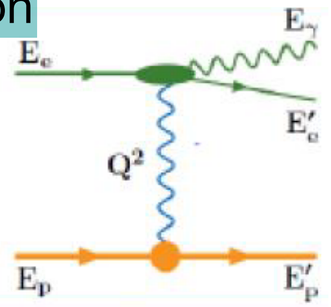

Measurement of the quark spin contribution

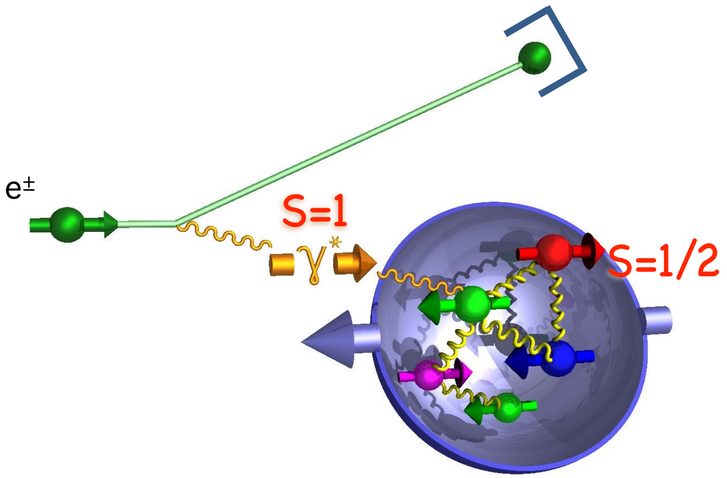

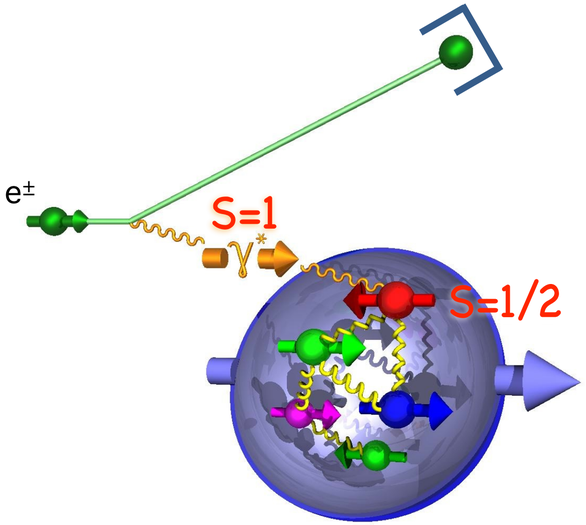

high polarisation

Asymmetry: $A_{LL} = \dfrac{\frac{\overleftarrow{N}}{\overleftarrow{L}} - \frac{\overrightarrow{N}}{\overrightarrow{L}}}{\frac{\overleftarrow{N}}{\overleftarrow{L}} + \frac{\overrightarrow{N}}{\overrightarrow{L}}}(x_B, Q^2) \propto g_1(x, Q^2) = \frac{1}{2}\sum_q e_q^2 \Delta q(x, Q^2)$

precise luminosity determination

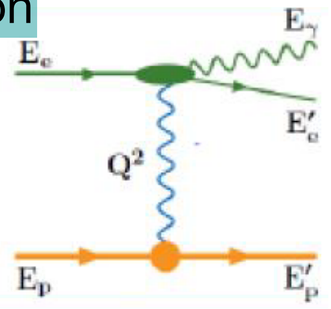

Polarised DIS experiments

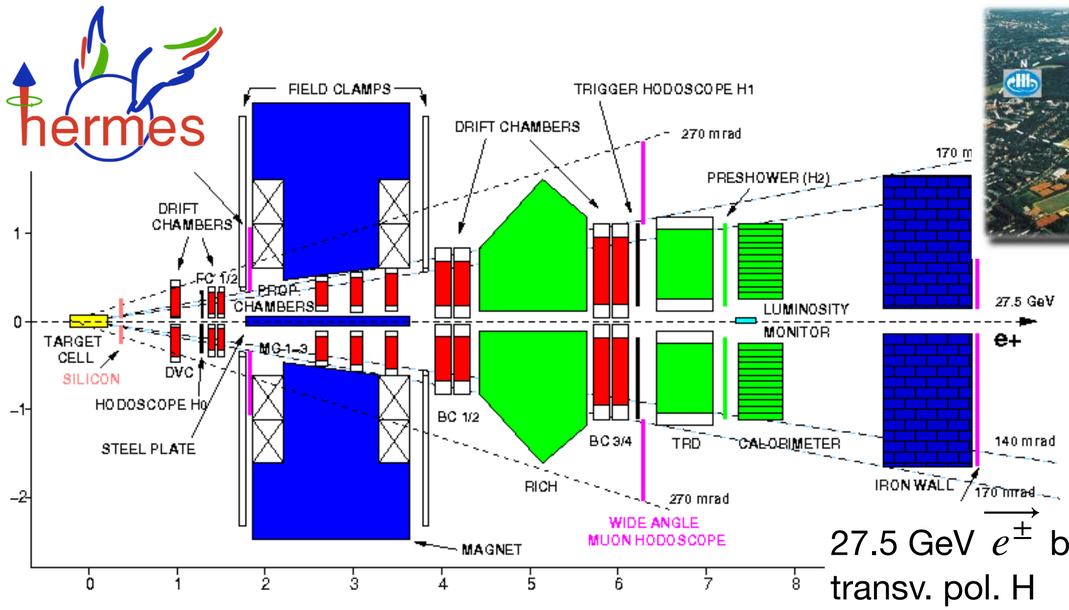

data taking
1995 — 2007

27.5 GeV $\overrightarrow{e^{\pm}}$ beam off gas target:
transv. pol. H
long. pol. H, D, He
unpol. H, D, He, Ne, Kr, Xe

Polarised DIS experiments

Jefferson Lab

$\overrightarrow{e^-}$ beam off gas and solid target:
long. and transv. pol. H, D, He

data taking
6 GeV: 2000 — 2012
12 GeV: 2009 –

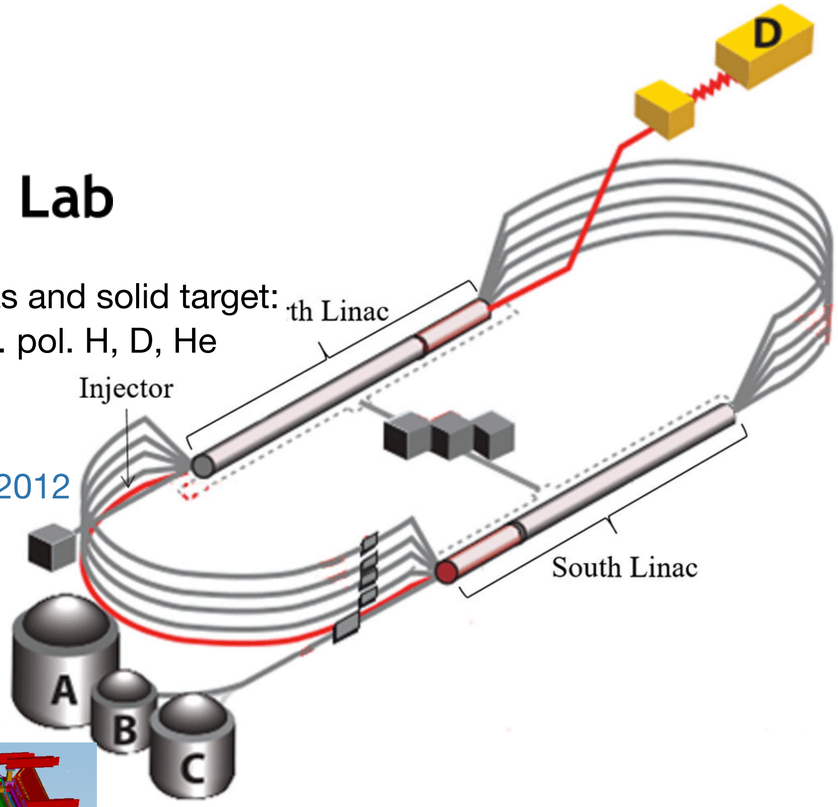

CLAS12 in Hall B

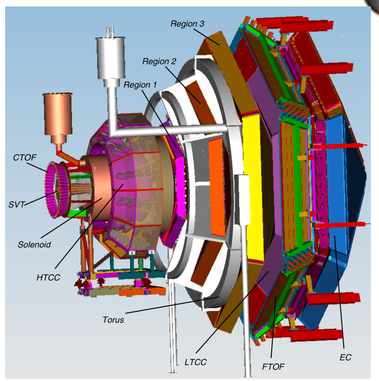

hermes

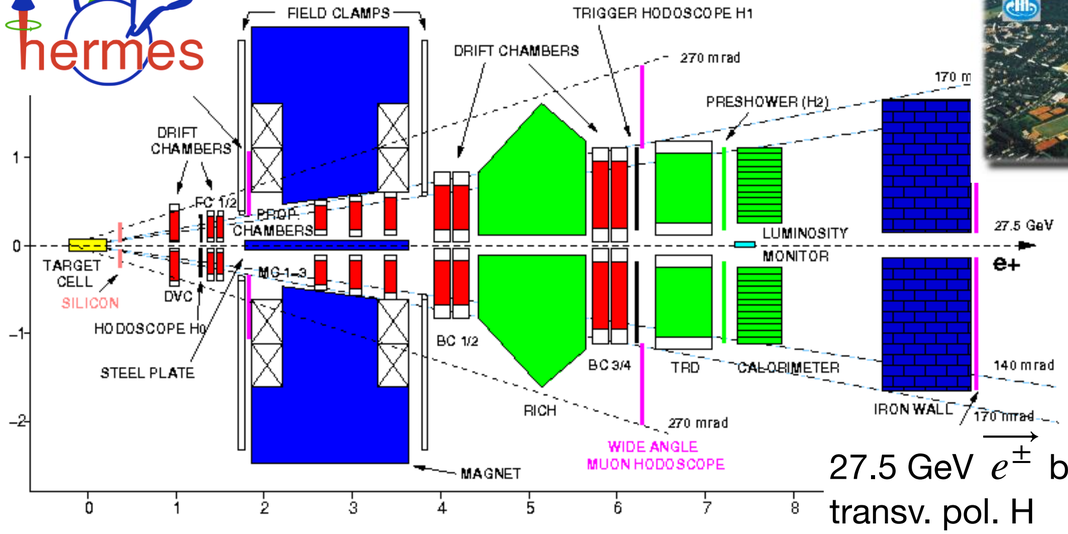

data taking
1995 — 2007

27.5 GeV $\overrightarrow{e^{\pm}}$ beam off gas target:
transv. pol. H
long. pol. H, D, He
unpol. H, D, He, Ne, Kr, Xe

Polarised DIS experiments

Jefferson Lab

$\overrightarrow{e^-}$ beam off gas and solid target:
long. and transv. pol. H, D, He

data taking
6 GeV: 2000 — 2012
12 GeV: 2009 –

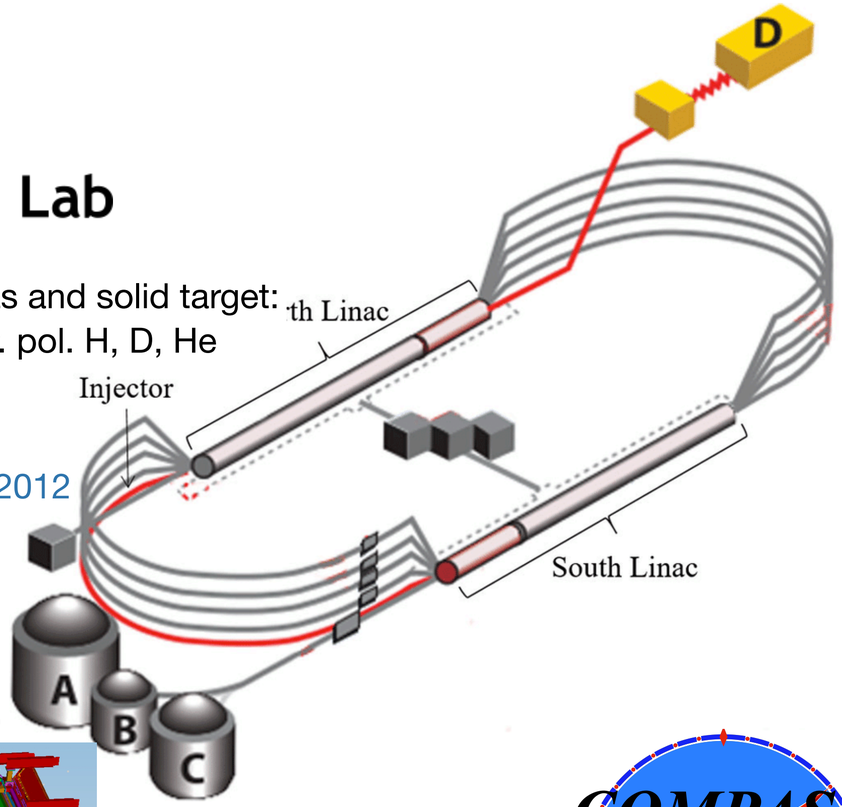

CLAS12 in Hall B

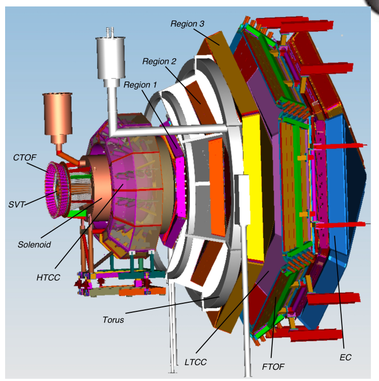

hermes

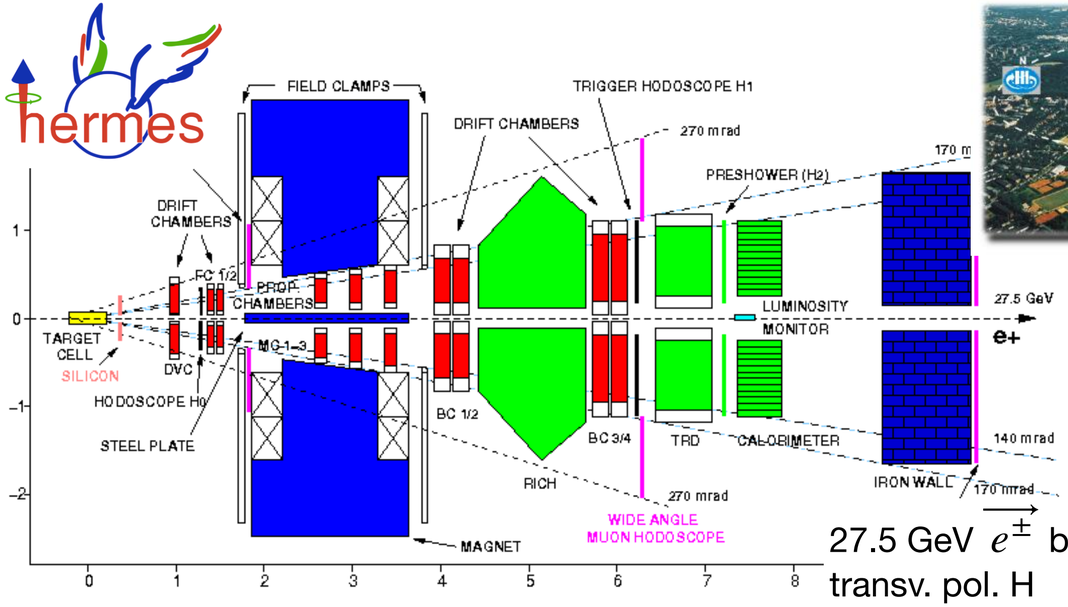

data taking
1995 — 2007

27.5 GeV $\overrightarrow{e^\pm}$ beam off gas target:
transv. pol. H
long. pol. H, D, He
unpol. H, D, He, Ne, Kr, Xe

COMPASS

25 years
1997 - 2022

data taking
2002 — 2022

160–200 GeV $\overrightarrow{\mu^\pm}$ beam off solid target:
long. and transv. pol H and D

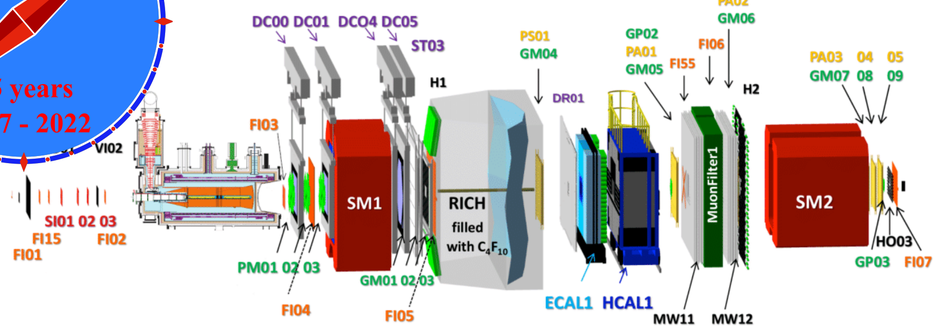

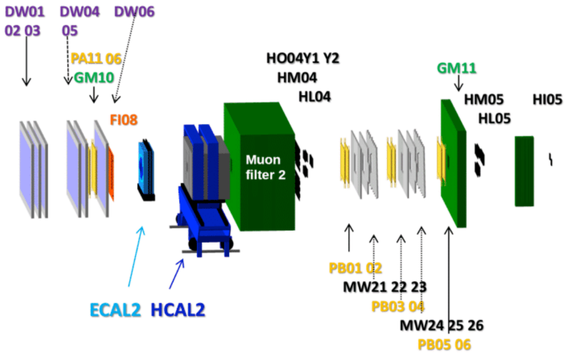

The asymmetry

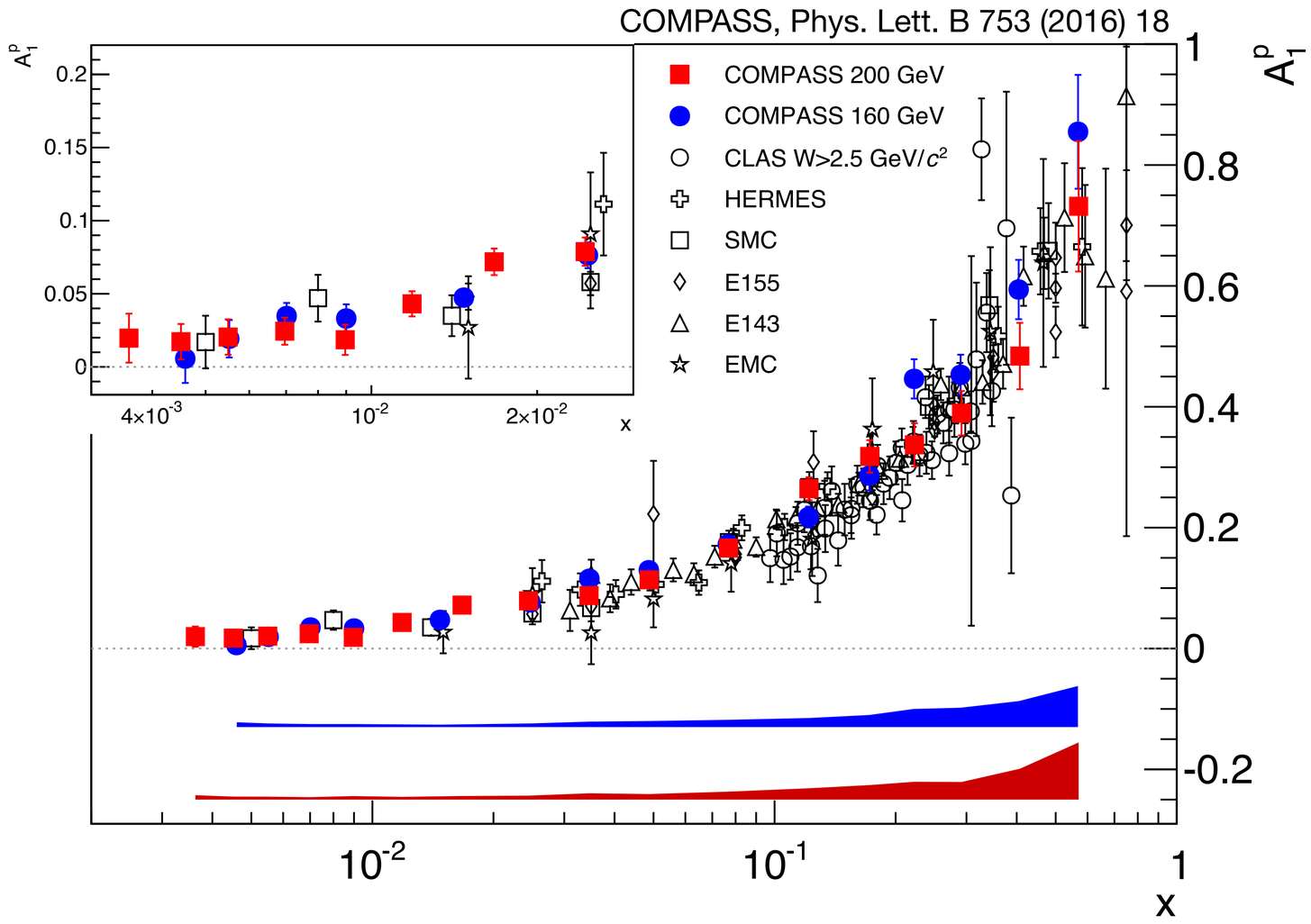

The asymmetry

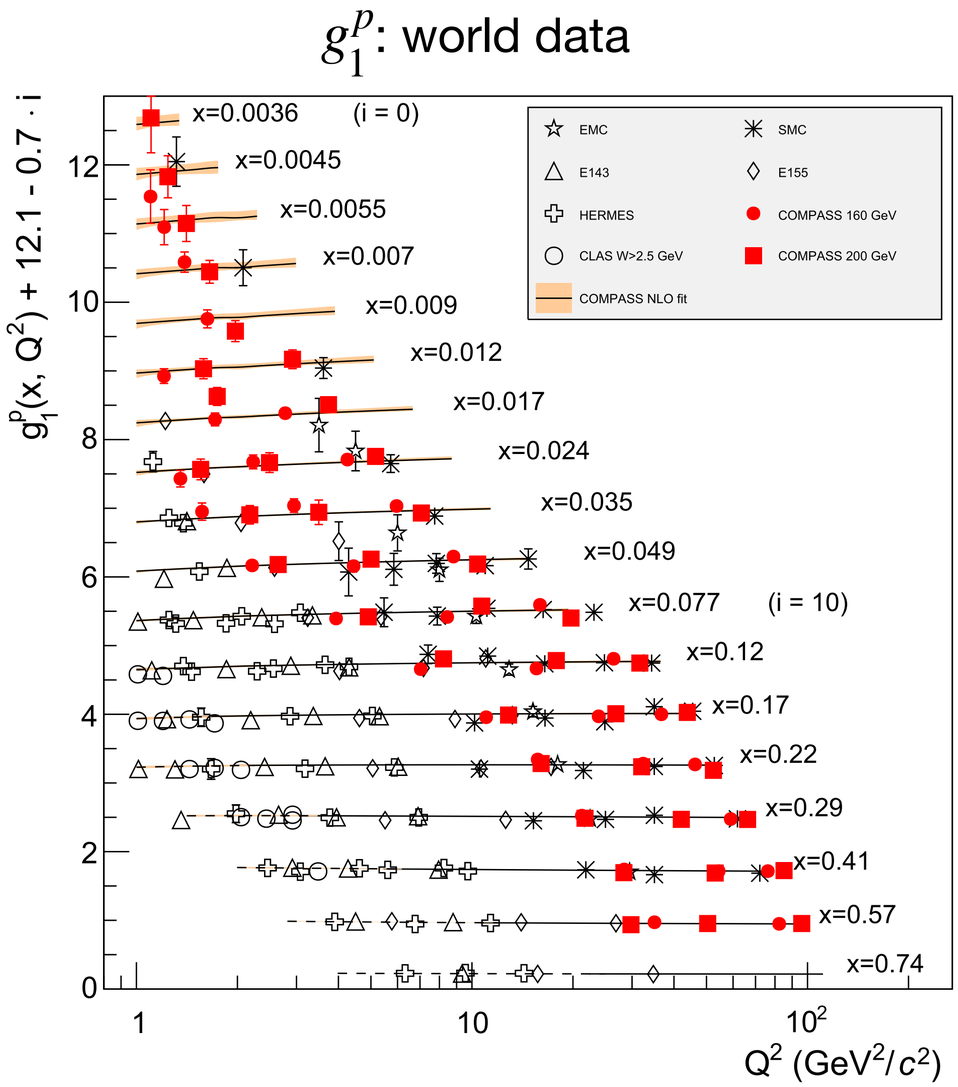

The asymmetry

g_1^p: world data

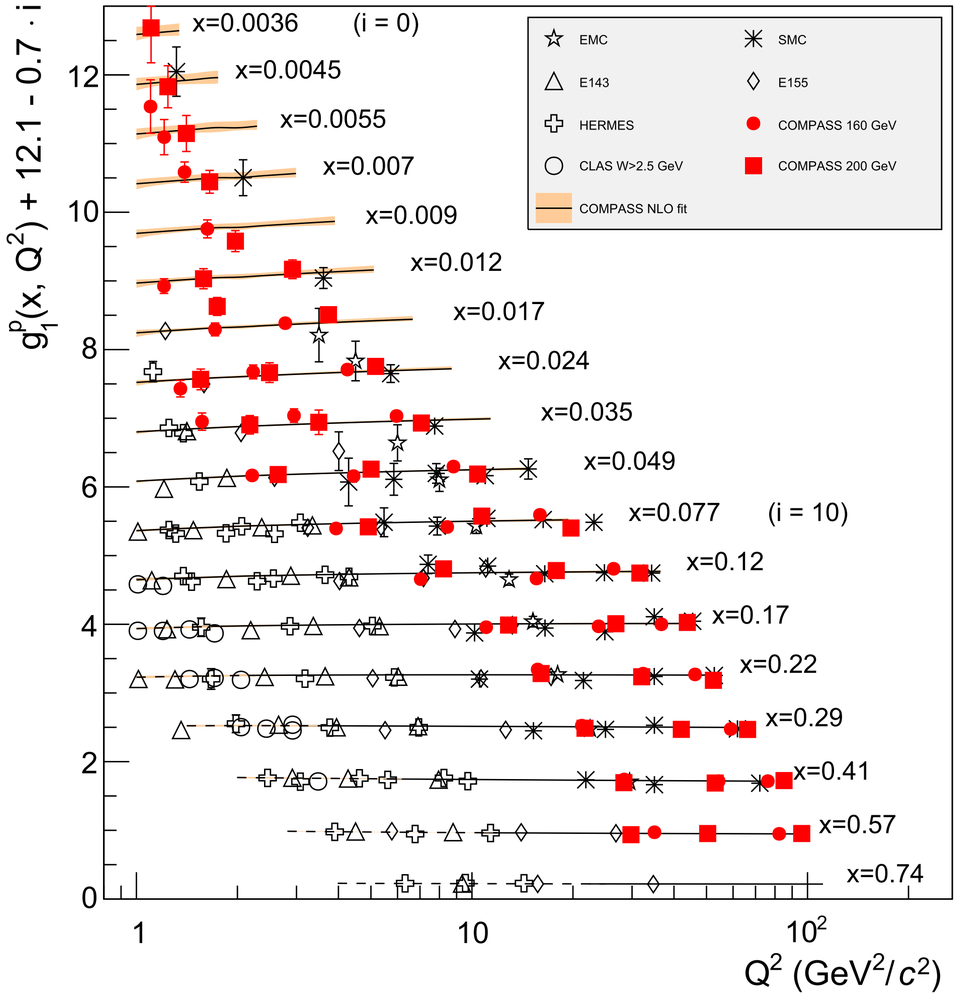

$$\int dx g_1(x, Q^2) = \frac{1}{36}\left(4\Delta\Sigma + 3\Delta q_3 + \Delta q_8\right)$$

Δq_3 from neutron β decay

Δq_8 from hyperon β decay

The asymmetry

g_1^p: world data

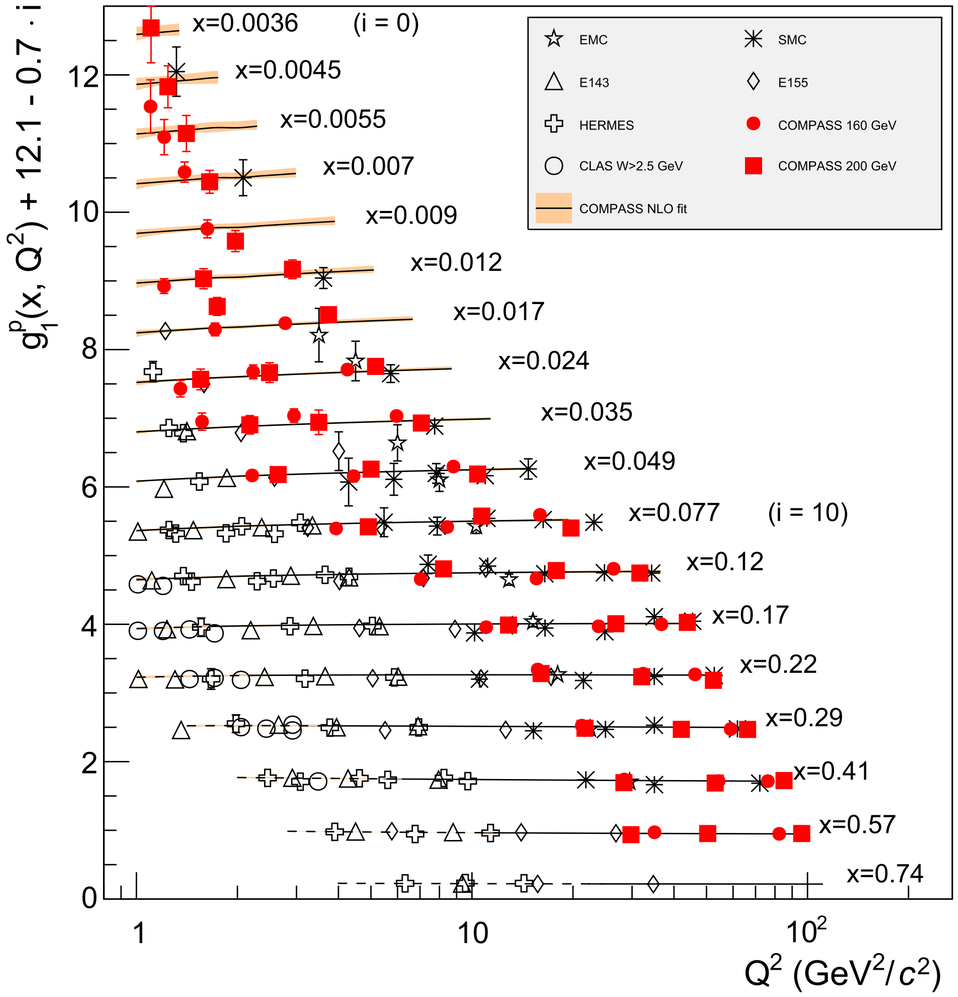

$$\int dx g_1(x, Q^2) = \frac{1}{36}\left(4\Delta\Sigma + 3\Delta q_3 + \Delta q_8\right)$$

Δq_3 from neutron β decay

Δq_8 from hyperon β decay

$\Delta\Sigma$

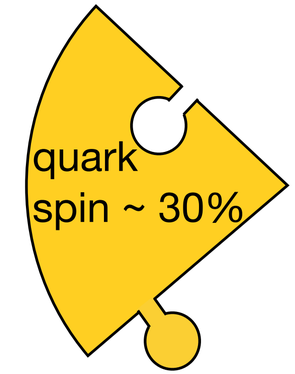

Quark flavour dependent helicity: single-hadron production in semi-inclusive DIS

$$Q^2 = -q^2$$

$$x_B = \frac{Q^2}{2P \cdot q}$$

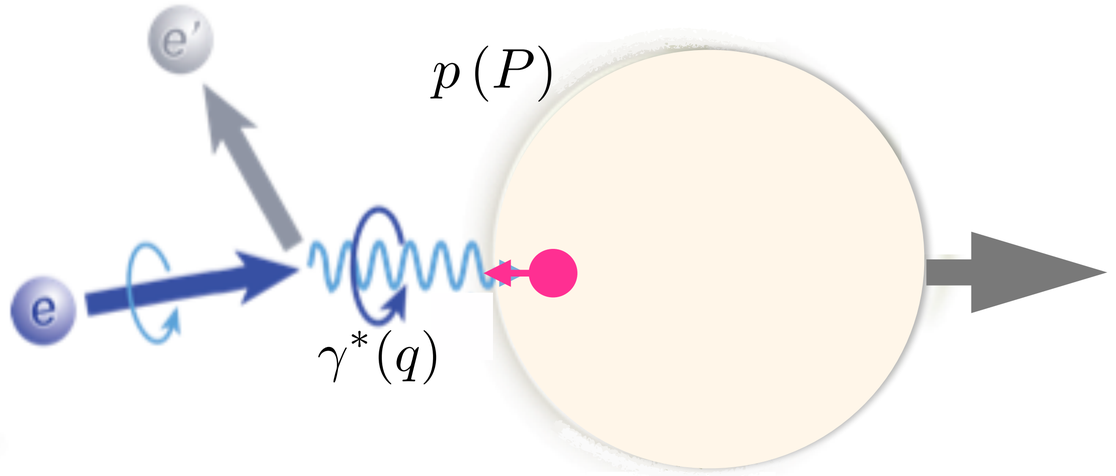

Quark flavour dependent helicity: single-hadron production in semi-inclusive DIS

$$Q^2 = -q^2$$

$$x_B = \frac{Q^2}{2P \cdot q}$$

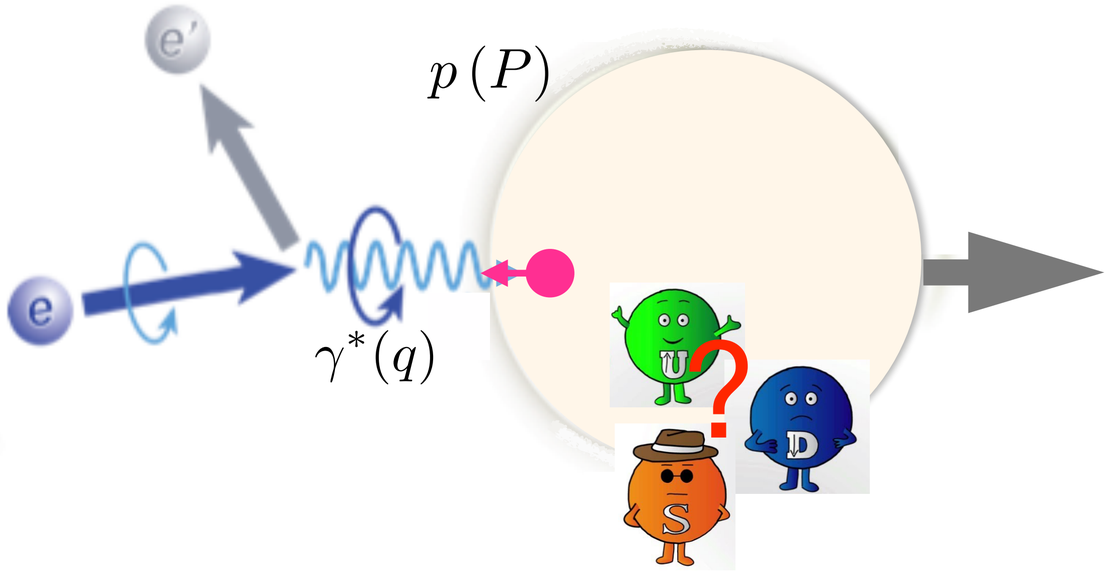

Quark flavour dependent helicity: single-hadron production in semi-inclusive DIS

$$Q^2 = -q^2$$

$$x_B = \frac{Q^2}{2P \cdot q}$$

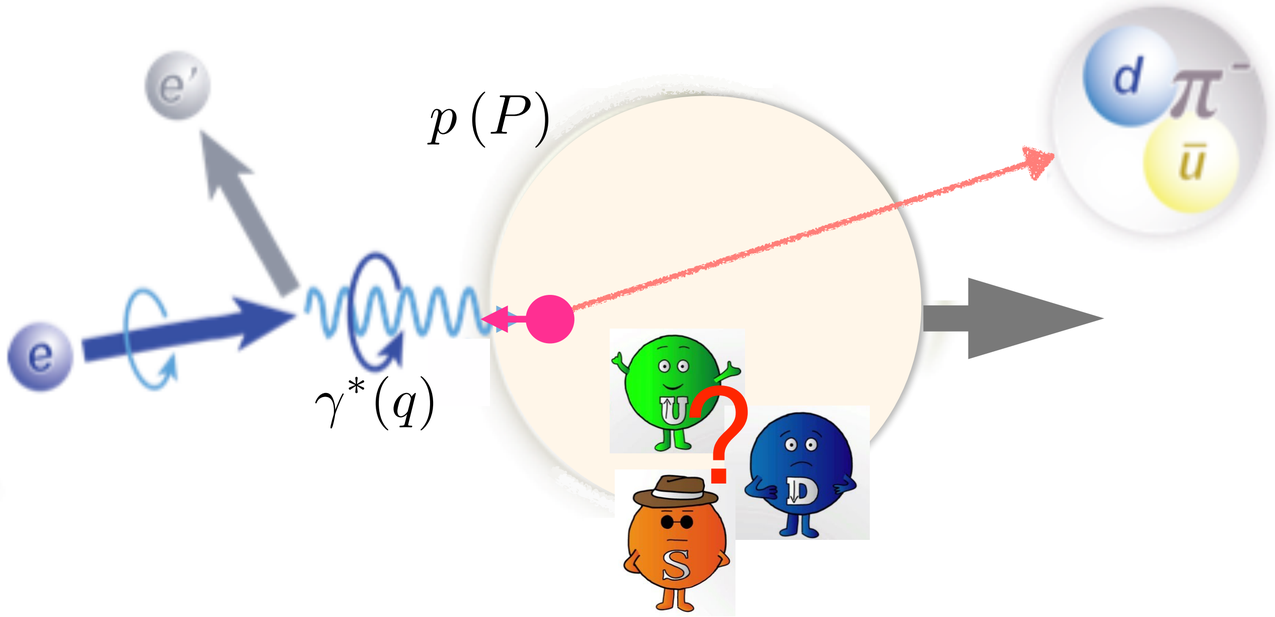

Detect a hadron!

Quark flavour dependent helicity: single-hadron production in semi-inclusive DIS

$$Q^2 = -q^2$$

$$x_B = \frac{Q^2}{2P \cdot q}$$

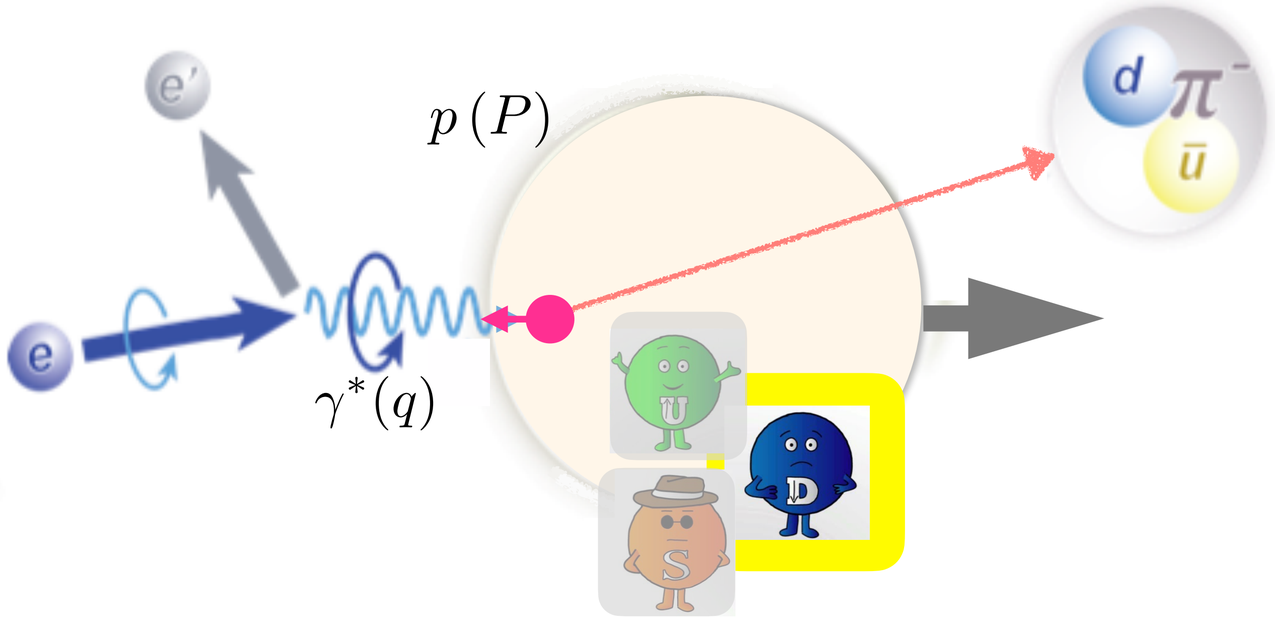

Detect a hadron!

Quark flavour dependent helicity: single-hadron production in semi-inclusive DIS

$$Q^2 = -q^2$$

$$x_B = \frac{Q^2}{2P \cdot q}$$

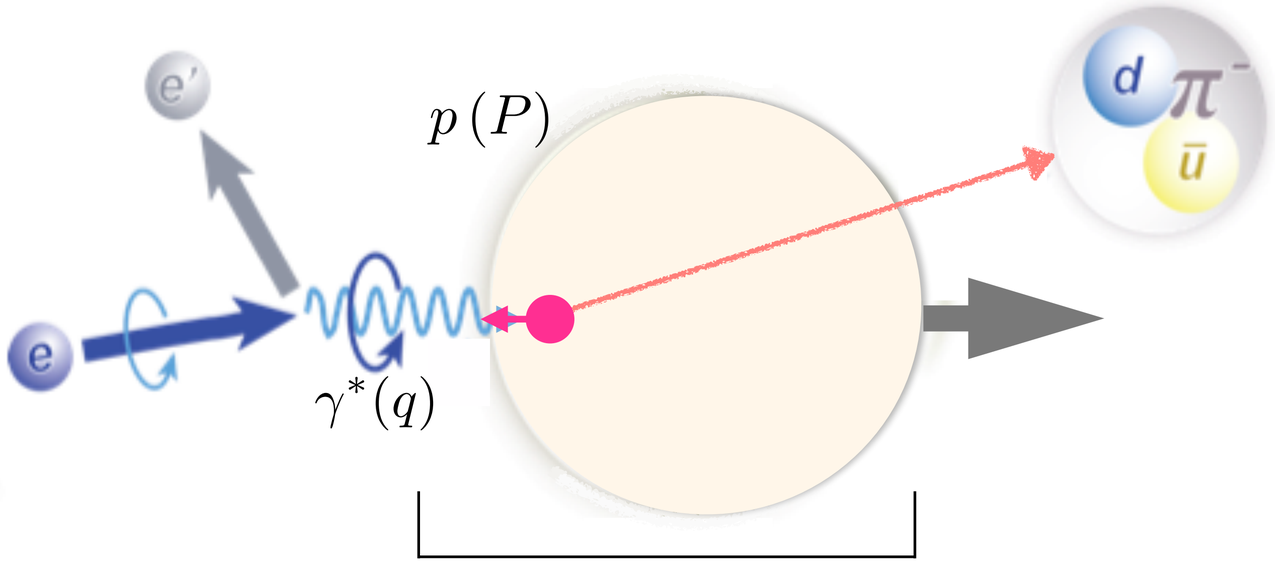

Detect a hadron!

parton distribution function $PDF(x_B, Q^2)$

Quark flavour dependent helicity: single-hadron production in semi-inclusive DIS

$$Q^2 = -q^2$$

$$x_B = \frac{Q^2}{2P \cdot q}$$

$$z \overset{\text{lab}}{=} \frac{E_h}{E_{\gamma *}}$$

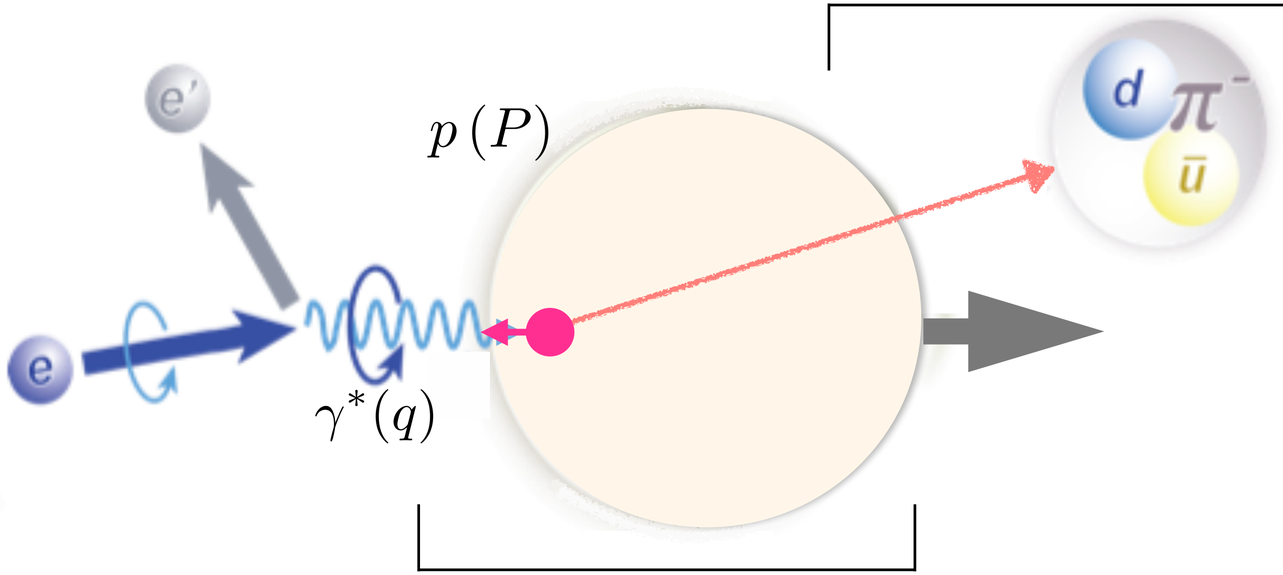

Quark flavour dependent helicity: single-hadron production in semi-inclusive DIS

fragmentation function:

- e^+e^- annihilation
- semi-inclusive DIS
- pp collisions

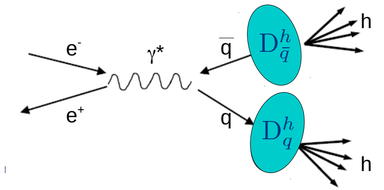

fragmentation function $FF(z, Q^2)$

$$Q^2 = -q^2$$

$$x_B = \frac{Q^2}{2P \cdot q}$$

$$z \overset{\text{lab}}{=} \frac{E_h}{E_{\gamma *}}$$

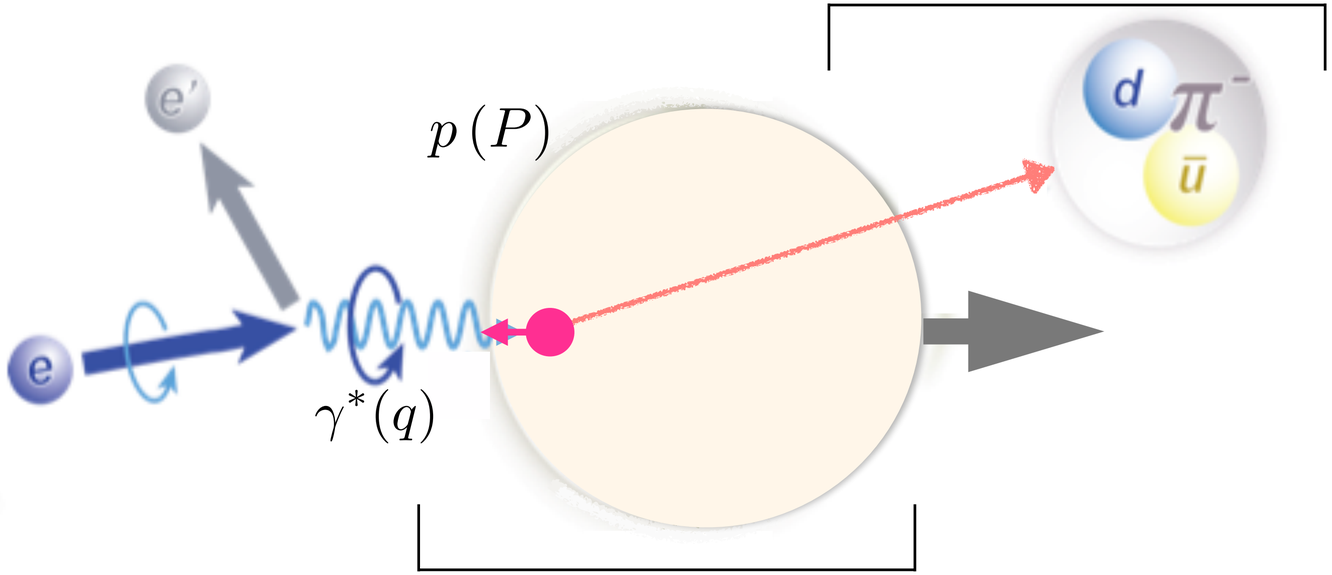

Detect a hadron!

parton distribution function $PDF(x_B, Q^2)$

Quark flavour dependent helicity: single-hadron production in semi-inclusive DIS

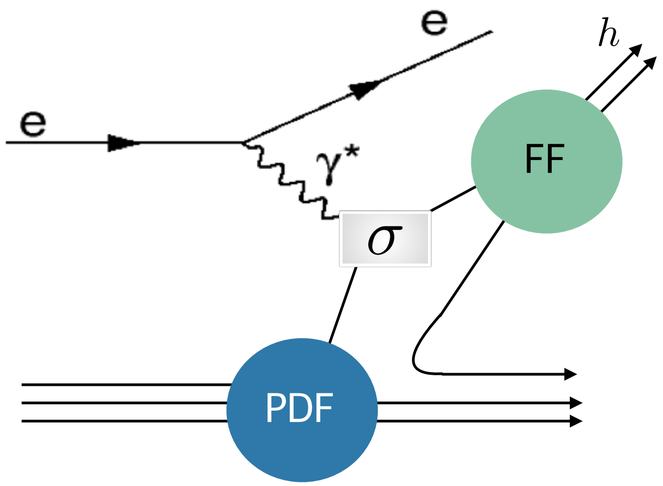

Asymmetry: $$\frac{\frac{\overleftrightarrows}{N^h}}{\overleftrightarrows{L}} - \frac{\frac{\overrightarrow{\rightarrow}}{N^h}}{\overrightarrow{\rightarrow}{L}} \Big/ \frac{\frac{\overleftrightarrows}{N^h}}{\overleftrightarrows{L}} + \frac{\frac{\overrightarrow{\rightarrow}}{N^h}}{\overrightarrow{\rightarrow}{L}} (x_B, Q^2, z)$$

$$\propto \sum_q e_q^2 \left[\Delta q \otimes w_1 D_1^{q \to h} \right]$$

FF

Semi-inclusive measurements
→ access to flavour-dependent quark spin contribution

Single-hadron asymmetry from semi-inclusive DIS

HERMES, Phys. Rev. D **99** (2019) 11, 112001

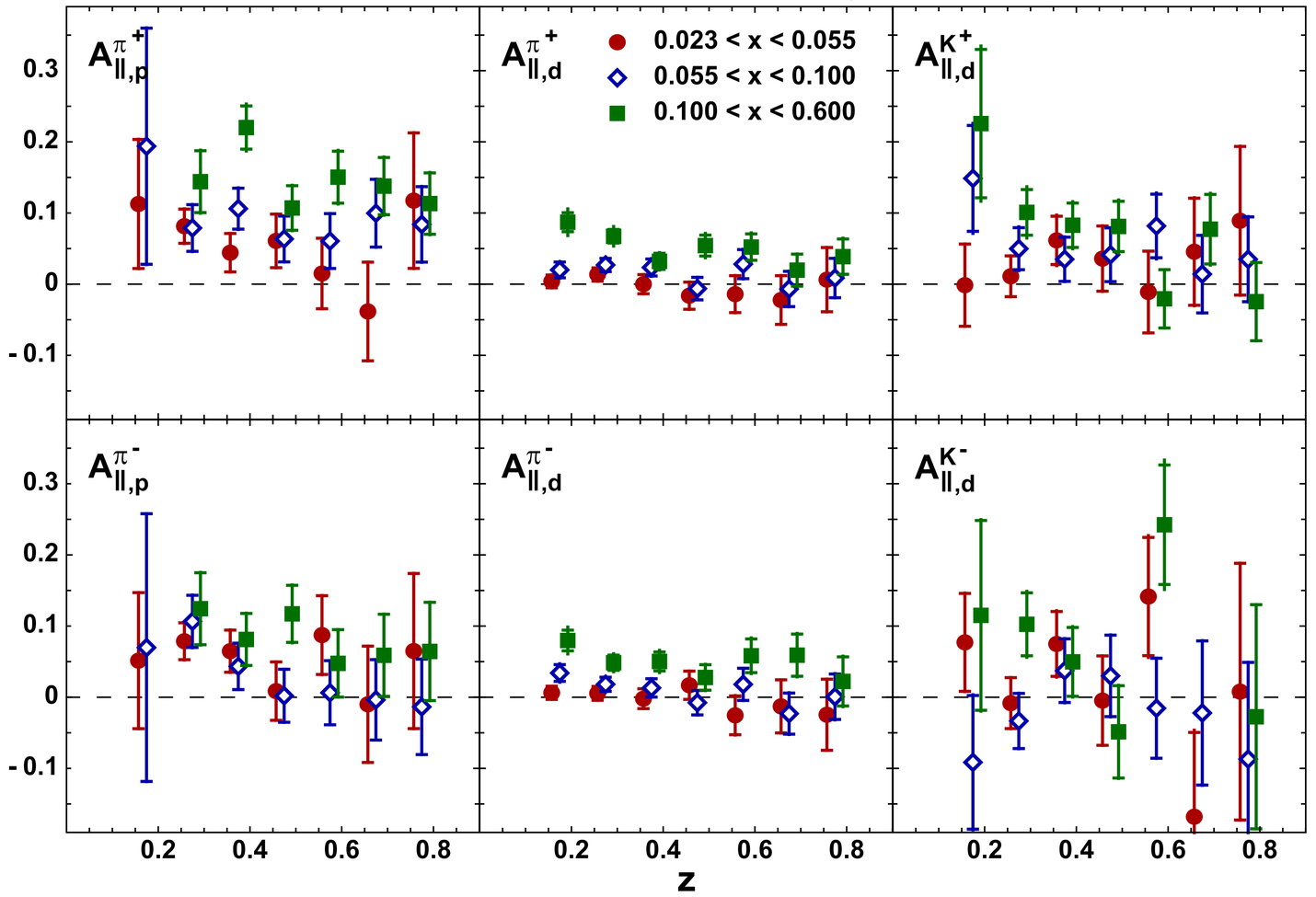

Single-hadron asymmetry from semi-inclusive DIS

At leading order and leading twist

$$A_1^h(x, Q^2, z) = \frac{\sum_q e_q^2 \Delta q(x, Q^2) D_q^h(z, Q^2)}{\sum_q e_q^2 q(x, Q^2) D_q^h(z, Q^2)}$$

and assuming $D^{q \to h^+} = D^{\bar{q} \to h^-}$:

$$A_{1,d}^{h^+ - h^-} = \frac{4\Delta u_v + \Delta d_v}{4u_v + d_v}$$

$$A_{1,p}^{h^+ - h^-} = \frac{4\Delta u_v - \Delta d_v}{4u_v - d_v}$$

Single-hadron asymmetry from semi-inclusive DIS

At leading order and leading twist

$$A_1^h(x, Q^2, z) = \frac{\sum_q e_q^2 \Delta q(x, Q^2) D_q^h(z, Q^2)}{\sum_q e_q^2 q(x, Q^2) D_q^h(z, Q^2)}$$

and assuming $D^{q \to h^+} = D^{\bar{q} \to h^-}$:

$$A_{1,d}^{h^+ - h^-} = \frac{4\Delta u_v + \Delta d_v}{4u_v + d_v}$$

$$A_{1,p}^{h^+ - h^-} = \frac{4\Delta u_v - \Delta d_v}{4u_v - d_v}$$

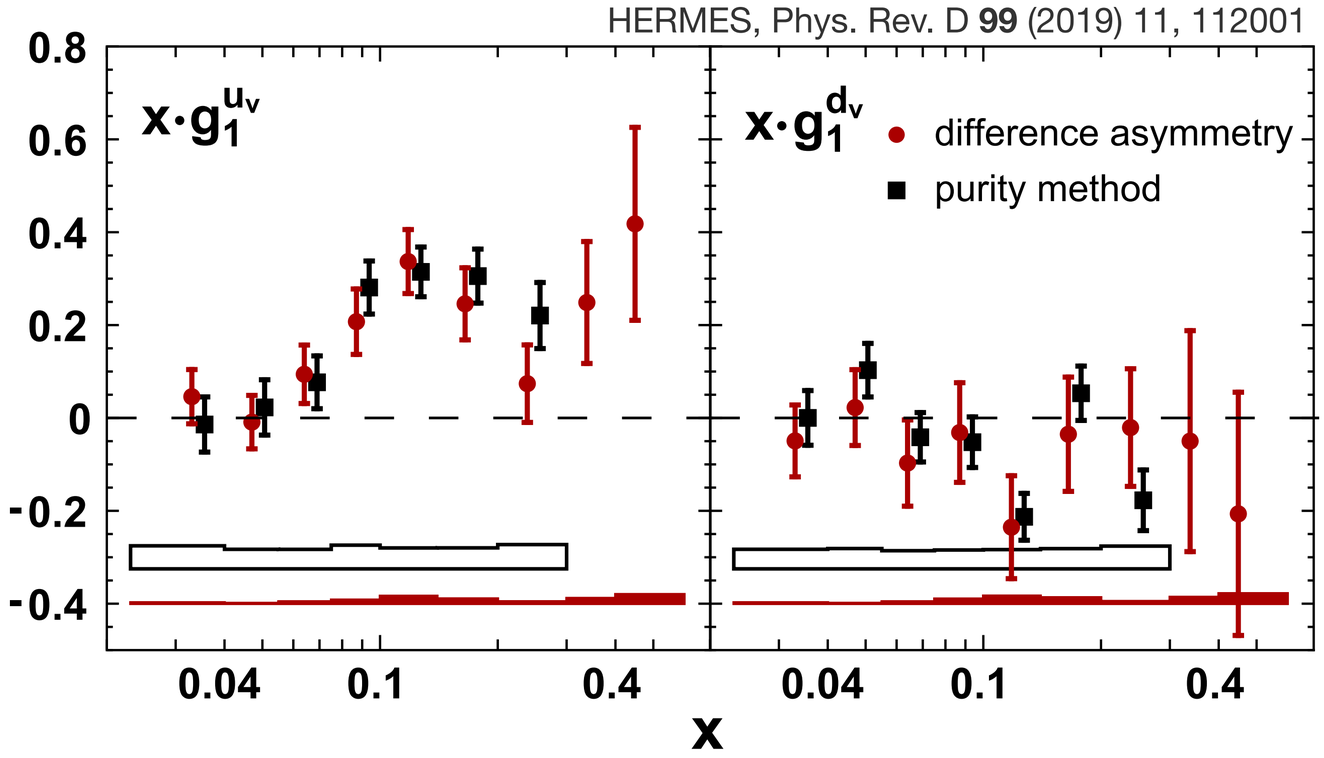

Access to helicity distributions through pp collisions

Weak interaction: only coupling to left-handed fermions and right-handed anti-fermions: $u_L \bar{d}_R \rightarrow W^+$ and $\bar{u}_R d_L \rightarrow W^-$

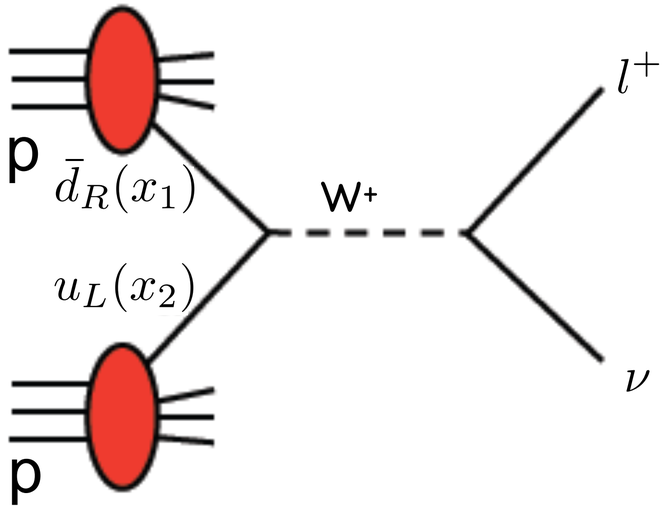

Access to helicity distributions through pp collisions

Weak interaction: only coupling to left-handed fermions and right-handed anti-fermions: $u_L \bar{d}_R \rightarrow W^+$ and $\bar{u}_R d_L \rightarrow W^-$

$$\vec{N} \sim \vec{\vec{d}}(x_1)u(x_2) + \vec{\overleftarrow{u}}(x_1)\bar{d}(x_2)$$

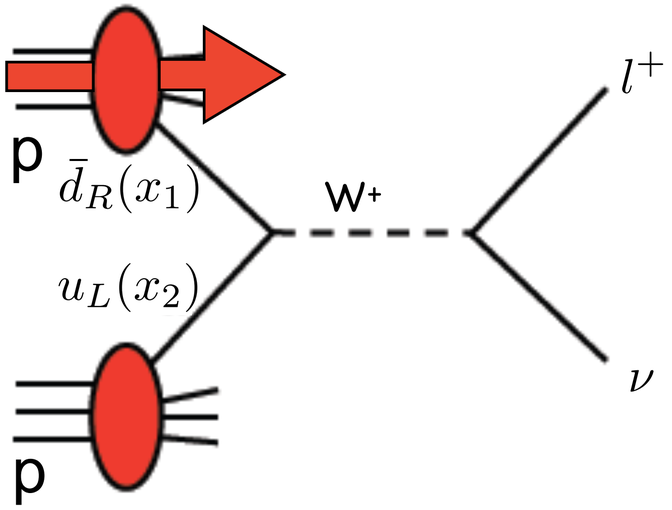

Access to helicity distributions through pp collisions

Weak interaction: only coupling to left-handed fermions and right-handed anti-fermions: $u_L \bar{d}_R \to W^+$ and $\bar{u}_R d_L \to W^-$

$$\vec{N} \sim \vec{\vec{d}}(x_1)u(x_2) + \vec{\overleftarrow{u}}(x_1)\bar{d}(x_2)$$

$$\overleftarrow{N} \sim \overleftarrow{\vec{d}}(x_1)u(x_2) + \overleftarrow{\overleftarrow{u}}(x_1)\bar{d}(x_2)$$

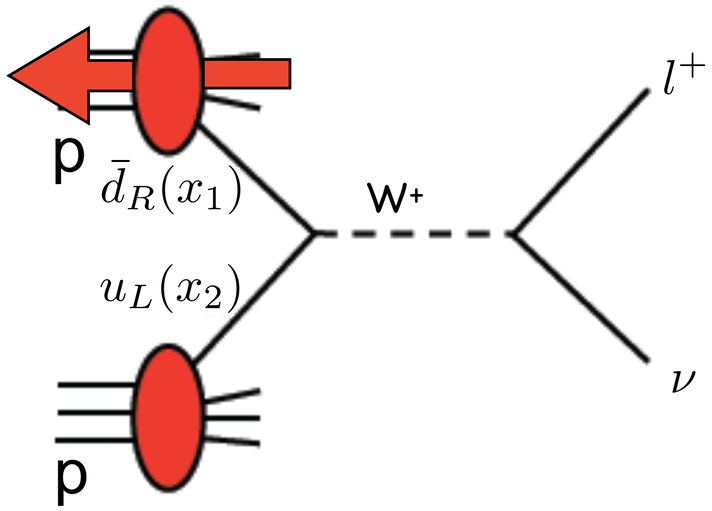

Access to helicity distributions through pp collisions

Weak interaction: only coupling to left-handed fermions and right-handed anti-fermions: $u_L \bar{d}_R \to W^+$ and $\bar{u}_R d_L \to W^-$

$$\vec{N} \sim \vec{\vec{d}}(x_1)u(x_2) + \vec{\overleftarrow{u}}(x_1)\bar{d}(x_2)$$

$$\overleftarrow{N} \sim \vec{\overleftarrow{d}}(x_1)u(x_2) + \overleftarrow{\overleftarrow{u}}(x_1)\bar{d}(x_2)$$

$$\rightarrow \quad A_L^{W^+} = \frac{\vec{N} - \overleftarrow{N}}{\vec{N} + \overleftarrow{N}}$$

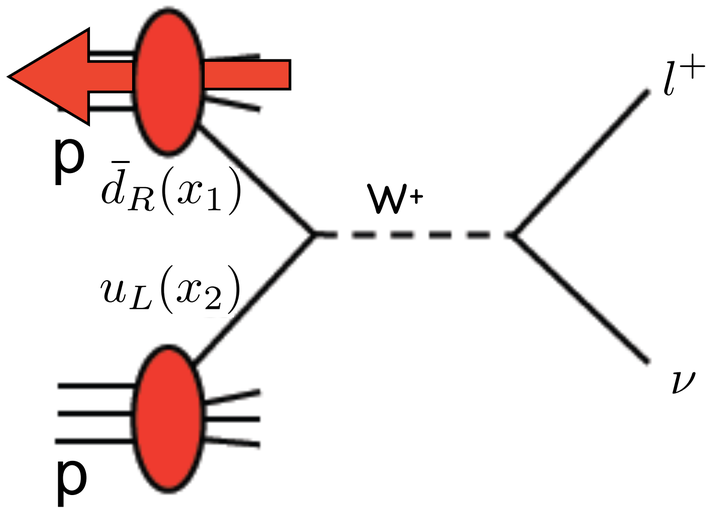

Access to helicity distributions through pp collisions

Weak interaction: only coupling to left-handed fermions and right-handed anti-fermions: $u_L \bar{d}_R \to W^+$ and $\bar{u}_R d_L \to W^-$

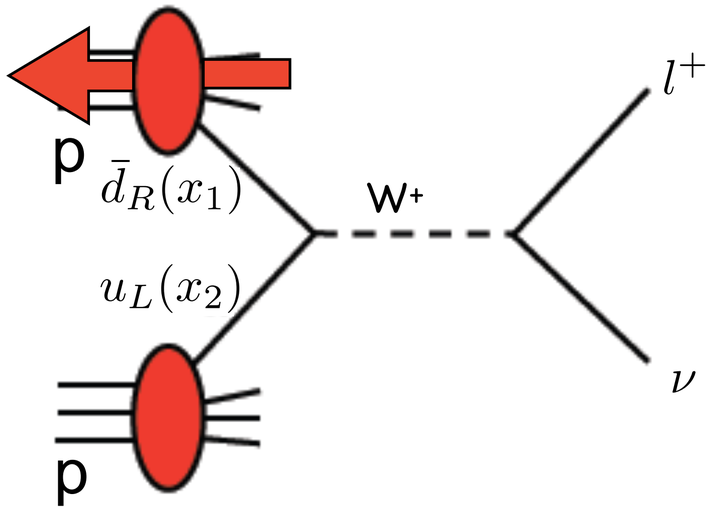

$$\overrightarrow{N} \sim \overrightarrow{\overrightarrow{d}}(x_1)u(x_2) + \overrightarrow{\overleftarrow{u}}(x_1)\bar{d}(x_2)$$

$$\overleftarrow{N} \sim \overleftarrow{\overrightarrow{d}}(x_1)u(x_2) + \overleftarrow{\overleftarrow{u}}(x_1)\bar{d}(x_2)$$

$$\to \quad A_L^{W^+} = \frac{\overrightarrow{N} - \overleftarrow{N}}{\overrightarrow{N} + \overleftarrow{N}} = \frac{\overrightarrow{\overrightarrow{d}}(x_1)u(x_2) + \overrightarrow{\overleftarrow{u}}(x_1)\bar{d}(x_2) - \overleftarrow{\overrightarrow{d}}(x_1)u(x_2) - \overleftarrow{\overleftarrow{u}}(x_1)\bar{d}(x_2)}{\overrightarrow{\overrightarrow{d}}(x_1)u(x_2) + \overrightarrow{\overleftarrow{u}}(x_1)\bar{d}(x_2) + \overleftarrow{\overrightarrow{d}}(x_1)u(x_2) + \overleftarrow{\overleftarrow{u}}(x_1)\bar{d}(x_2)}$$

Access to helicity distributions through pp collisions

Weak interaction: only coupling to left-handed fermions and right-handed anti-fermions: $u_L \bar{d}_R \to W^+$ and $\bar{u}_R d_L \to W^-$

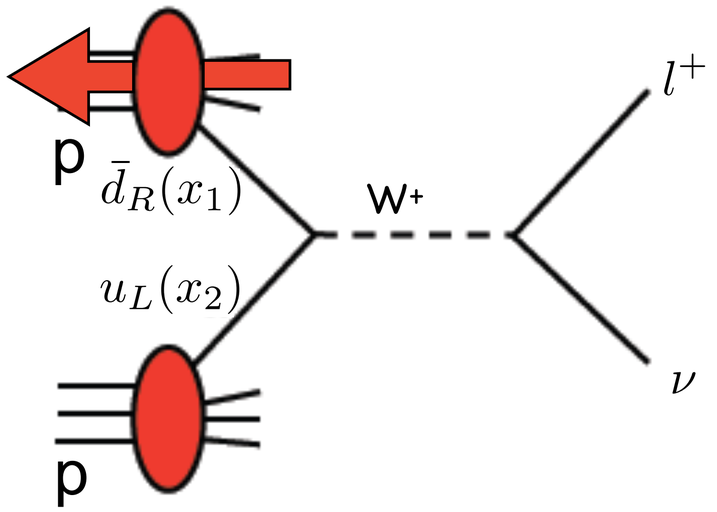

$$\overrightarrow{N} \sim \overrightarrow{\overrightarrow{d}}(x_1)u(x_2) + \overrightarrow{\overleftarrow{u}}(x_1)\bar{d}(x_2)$$

$$\overleftarrow{N} \sim \overleftarrow{\overrightarrow{d}}(x_1)u(x_2) + \overleftarrow{\overleftarrow{u}}(x_1)\bar{d}(x_2)$$

$$\to \quad A_L^{W^+} = \frac{\overrightarrow{N} - \overleftarrow{N}}{\overrightarrow{N} + \overleftarrow{N}} = \frac{\overrightarrow{\overrightarrow{d}}(x_1)u(x_2) + \overrightarrow{\overleftarrow{u}}(x_1)\bar{d}(x_2) - \overleftarrow{\overrightarrow{d}}(x_1)u(x_2) - \overleftarrow{\overleftarrow{u}}(x_1)\bar{d}(x_2)}{\overrightarrow{\overrightarrow{d}}(x_1)u(x_2) + \overrightarrow{\overleftarrow{u}}(x_1)\bar{d}(x_2) + \overleftarrow{\overrightarrow{d}}(x_1)u(x_2) + \overleftarrow{\overleftarrow{u}}(x_1)\bar{d}(x_2)}$$

$$= \frac{\Delta\bar{d}(x_1)u(x_2) - \Delta u(x_1)\bar{d}(x_2)}{\bar{d}(x_1)u(x_2) + u(x_1)\bar{d}(x_2)}$$

Access to helicity distributions through pp collisions

Weak interaction: only coupling to left-handed fermions and right-handed anti-fermions: $u_L \bar{d}_R \to W^+$ and $\bar{u}_R d_L \to W^-$

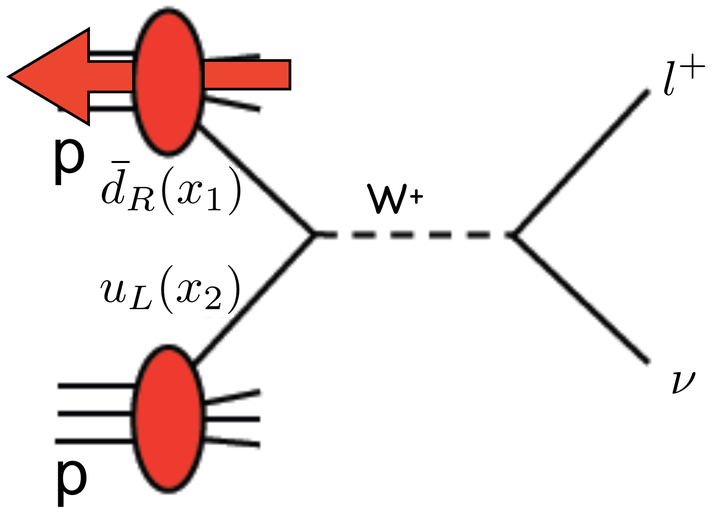

$$\overrightarrow{N} \sim \overrightarrow{\overrightarrow{d}}(x_1)u(x_2) + \overrightarrow{\overleftarrow{u}}(x_1)\bar{d}(x_2)$$

$$\overleftarrow{N} \sim \overleftarrow{\overrightarrow{d}}(x_1)u(x_2) + \overleftarrow{\overleftarrow{u}}(x_1)\bar{d}(x_2)$$

$$\to \quad A_L^{W^+} = \frac{\overrightarrow{N} - \overleftarrow{N}}{\overrightarrow{N} + \overleftarrow{N}} = \frac{\overrightarrow{\overrightarrow{d}}(x_1)u(x_2) + \overrightarrow{\overleftarrow{u}}(x_1)\bar{d}(x_2) - \overleftarrow{\overrightarrow{d}}(x_1)u(x_2) - \overleftarrow{\overleftarrow{u}}(x_1)\bar{d}(x_2)}{\overrightarrow{\overrightarrow{d}}(x_1)u(x_2) + \overrightarrow{\overleftarrow{u}}(x_1)\bar{d}(x_2) + \overleftarrow{\overrightarrow{d}}(x_1)u(x_2) + \overleftarrow{\overleftarrow{u}}(x_1)\bar{d}(x_2)}$$

$$= \frac{\Delta\bar{d}(x_1)u(x_2) - \Delta u(x_1)\bar{d}(x_2)}{\bar{d}(x_1)u(x_2) + u(x_1)\bar{d}(x_2)} \xrightarrow{x_1 \gg x_2} \frac{-\Delta u(x_1)}{u(x_1)}$$

Access to helicity distributions through pp collisions

Weak interaction: only coupling to left-handed fermions and right-handed anti-fermions: $u_L \bar{d}_R \to W^+$ and $\bar{u}_R d_L \to W^-$

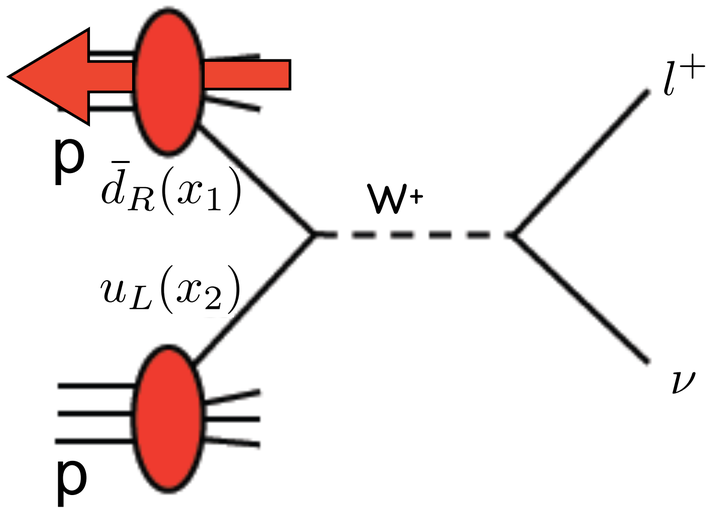

$$\overrightarrow{N} \sim \overrightarrow{\overrightarrow{d}}(x_1)u(x_2) + \overrightarrow{\overleftarrow{u}}(x_1)\bar{d}(x_2)$$

$$\overleftarrow{N} \sim \overleftarrow{\overrightarrow{d}}(x_1)u(x_2) + \overleftarrow{\overleftarrow{u}}(x_1)\bar{d}(x_2)$$

$$\to \quad A_L^{W^+} = \frac{\overrightarrow{N} - \overleftarrow{N}}{\overrightarrow{N} + \overleftarrow{N}} = \frac{\overrightarrow{\overrightarrow{d}}(x_1)u(x_2) + \overrightarrow{\overleftarrow{u}}(x_1)\bar{d}(x_2) - \overleftarrow{\overrightarrow{d}}(x_1)u(x_2) - \overleftarrow{\overleftarrow{u}}(x_1)\bar{d}(x_2)}{\overrightarrow{\overrightarrow{d}}(x_1)u(x_2) + \overrightarrow{\overleftarrow{u}}(x_1)\bar{d}(x_2) + \overleftarrow{\overrightarrow{d}}(x_1)u(x_2) + \overleftarrow{\overleftarrow{u}}(x_1)\bar{d}(x_2)}$$

$$= \frac{\Delta\bar{d}(x_1)u(x_2) - \Delta u(x_1)\bar{d}(x_2)}{\bar{d}(x_1)u(x_2) + u(x_1)\bar{d}(x_2)} \quad \begin{cases} x_1 \gg x_2 \to \dfrac{-\Delta u(x_1)}{u(x_1)} \\ x_2 \gg x_1 \to \dfrac{\Delta\bar{d}(x_1)}{\bar{d}(x_1)} \end{cases}$$

Access to helicity distributions through pp collisions

Weak interaction: only coupling to left-handed fermions and right-handed anti-fermions: $u_L \bar{d}_R \to W^+$ and $\bar{u}_R d_L \to W^-$

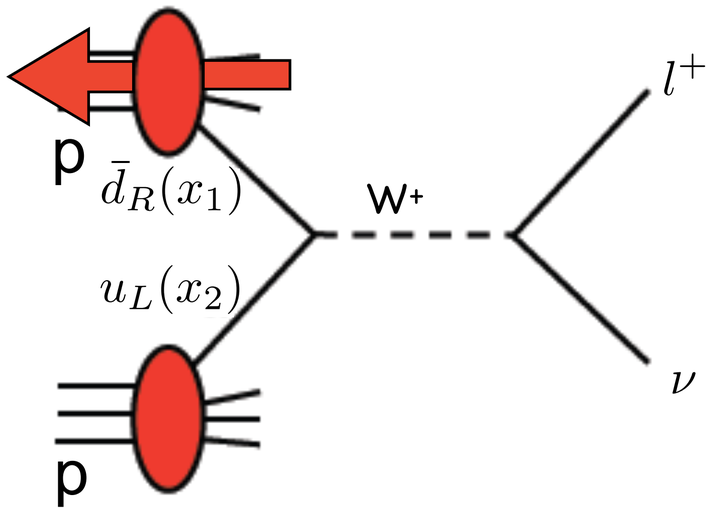

$$\overrightarrow{N} \sim \overrightarrow{\overrightarrow{d}}(x_1)u(x_2) + \overrightarrow{\overleftarrow{u}}(x_1)\bar{d}(x_2)$$

$$\overleftarrow{N} \sim \overleftarrow{\overrightarrow{d}}(x_1)u(x_2) + \overleftarrow{\overleftarrow{u}}(x_1)\bar{d}(x_2)$$

$$\to \quad A_L^{W^+} = \frac{\overrightarrow{N} - \overleftarrow{N}}{\overrightarrow{N} + \overleftarrow{N}} = \frac{\overrightarrow{\overrightarrow{d}}(x_1)u(x_2) + \overrightarrow{\overleftarrow{u}}(x_1)\bar{d}(x_2) - \overleftarrow{\overrightarrow{d}}(x_1)u(x_2) - \overleftarrow{\overleftarrow{u}}(x_1)\bar{d}(x_2)}{\overrightarrow{\overrightarrow{d}}(x_1)u(x_2) + \overrightarrow{\overleftarrow{u}}(x_1)\bar{d}(x_2) + \overleftarrow{\overrightarrow{d}}(x_1)u(x_2) + \overleftarrow{\overleftarrow{u}}(x_1)\bar{d}(x_2)}$$

$$= \frac{\Delta\bar{d}(x_1)u(x_2) - \Delta u(x_1)\bar{d}(x_2)}{\bar{d}(x_1)u(x_2) + u(x_1)\bar{d}(x_2)}$$

$x_1 \gg x_2$: $\dfrac{-\Delta u(x_1)}{u(x_1)}$

$x_2 \gg x_1$: $\dfrac{\Delta\bar{d}(x_1)}{\bar{d}(x_1)}$

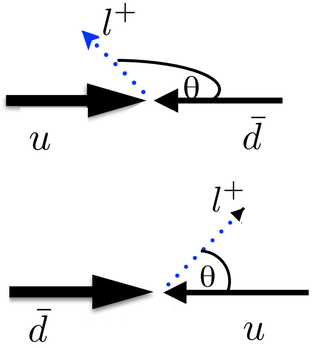

Access to helicity distributions through pp collisions

Weak interaction: only coupling to left-handed fermions and right-handed anti-fermions: $u_L \bar{d}_R \to W^+$ and $\bar{u}_R d_L \to W^-$

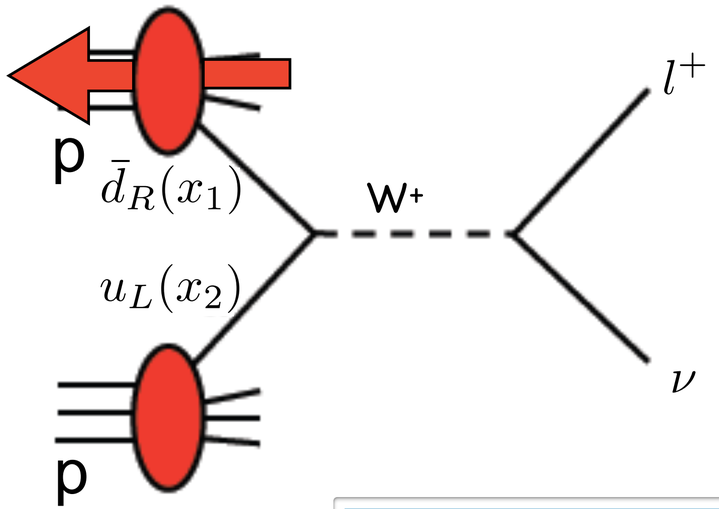

$$\overrightarrow{N} \sim \overrightarrow{\overrightarrow{d}}(x_1)u(x_2) + \overrightarrow{\overleftarrow{u}}(x_1)\bar{d}(x_2)$$

$$\overleftarrow{N} \sim \overleftarrow{\overrightarrow{d}}(x_1)u(x_2) + \overleftarrow{\overleftarrow{u}}(x_1)\bar{d}(x_2)$$

$$\to \quad A_L^{W^+} = \frac{\overrightarrow{N} - \overleftarrow{N}}{\overrightarrow{N} + \overleftarrow{N}} = \frac{\overrightarrow{\overrightarrow{d}}(x_1)u(x_2) + \overrightarrow{\overleftarrow{u}}(x_1)\bar{d}(x_2) - \overleftarrow{\overrightarrow{d}}(x_1)u(x_2) - \overleftarrow{\overleftarrow{u}}(x_1)\bar{d}(x_2)}{\overrightarrow{\overrightarrow{d}}(x_1)u(x_2) + \overrightarrow{\overleftarrow{u}}(x_1)\bar{d}(x_2) + \overleftarrow{\overrightarrow{d}}(x_1)u(x_2) + \overleftarrow{\overleftarrow{u}}(x_1)\bar{d}(x_2)}$$

- Complementary access to Δq
- No need for FFs
- Higher Q^2 than (fixed-target) DIS

$$= \frac{\Delta\bar{d}(x_1)u(x_2) - \Delta u(x_1)\bar{d}(x_2)}{\bar{d}(x_1)u(x_2) + u(x_1)\bar{d}(x_2)}$$

$x_1 \gg x_2$: $\dfrac{-\Delta u(x_1)}{u(x_1)}$

$x_2 \gg x_1$: $\dfrac{\Delta\bar{d}(x_1)}{\bar{d}(x_1)}$

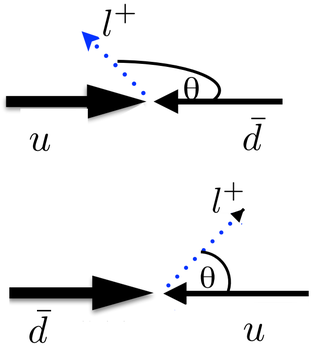

Polarised pp collisions

RHIC

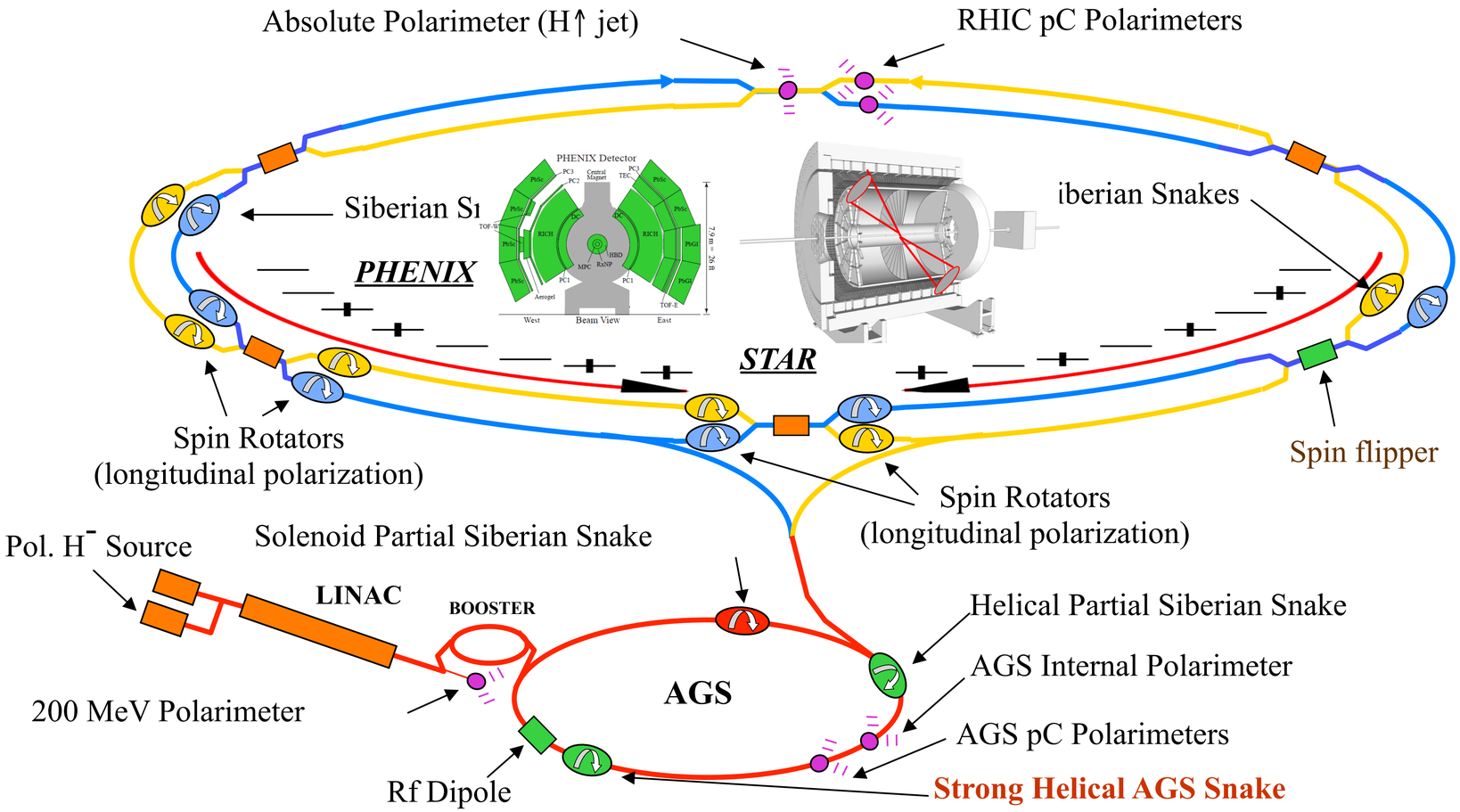

data taking
2000 — 2026

- Polarisation direction changes from bunch to bunch
- Spin rotators provide choice of spin orientation

Longitudinal single-spin asymmetry in pp collisions

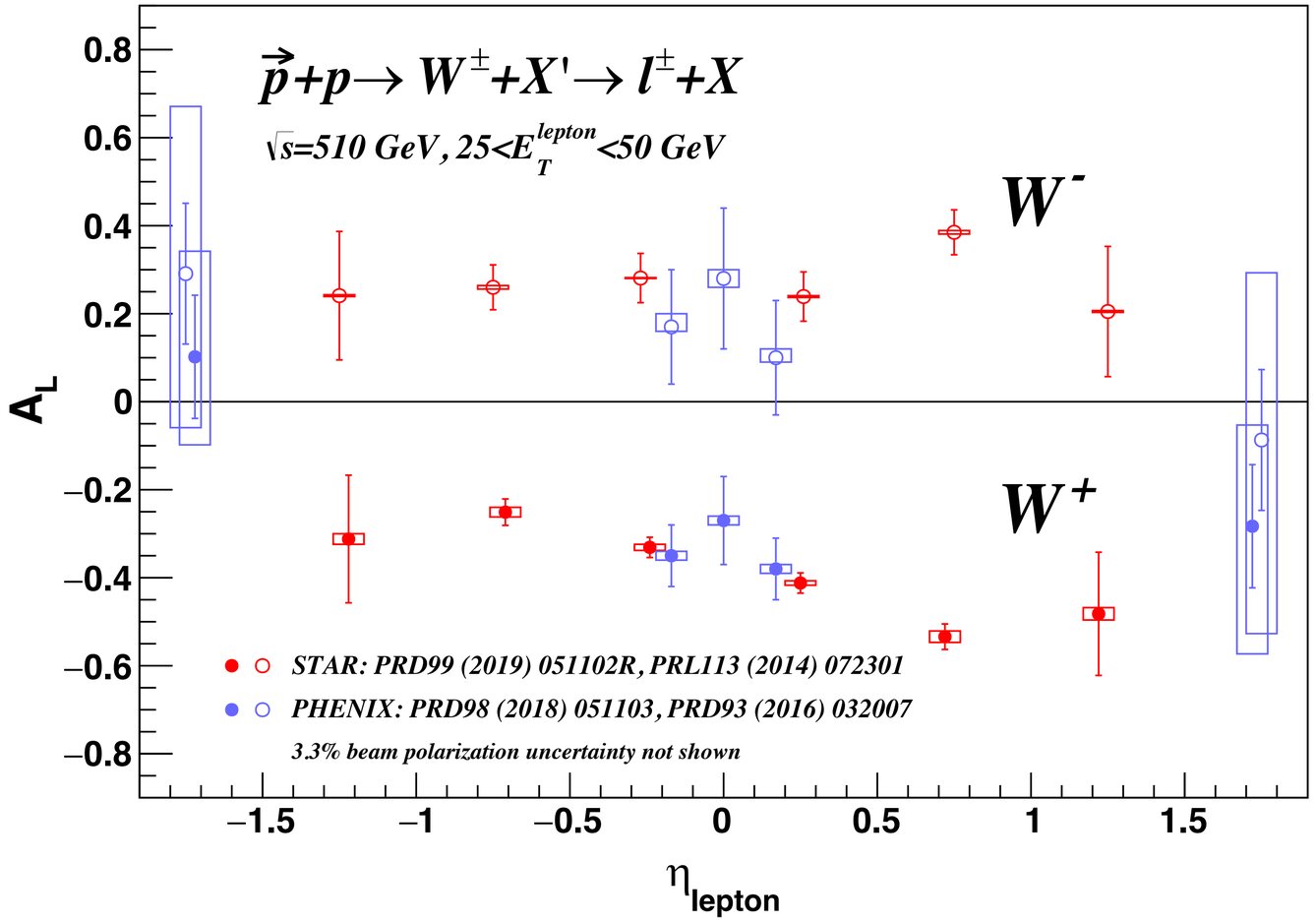

Longitudinal single-spin asymmetry in pp collisions

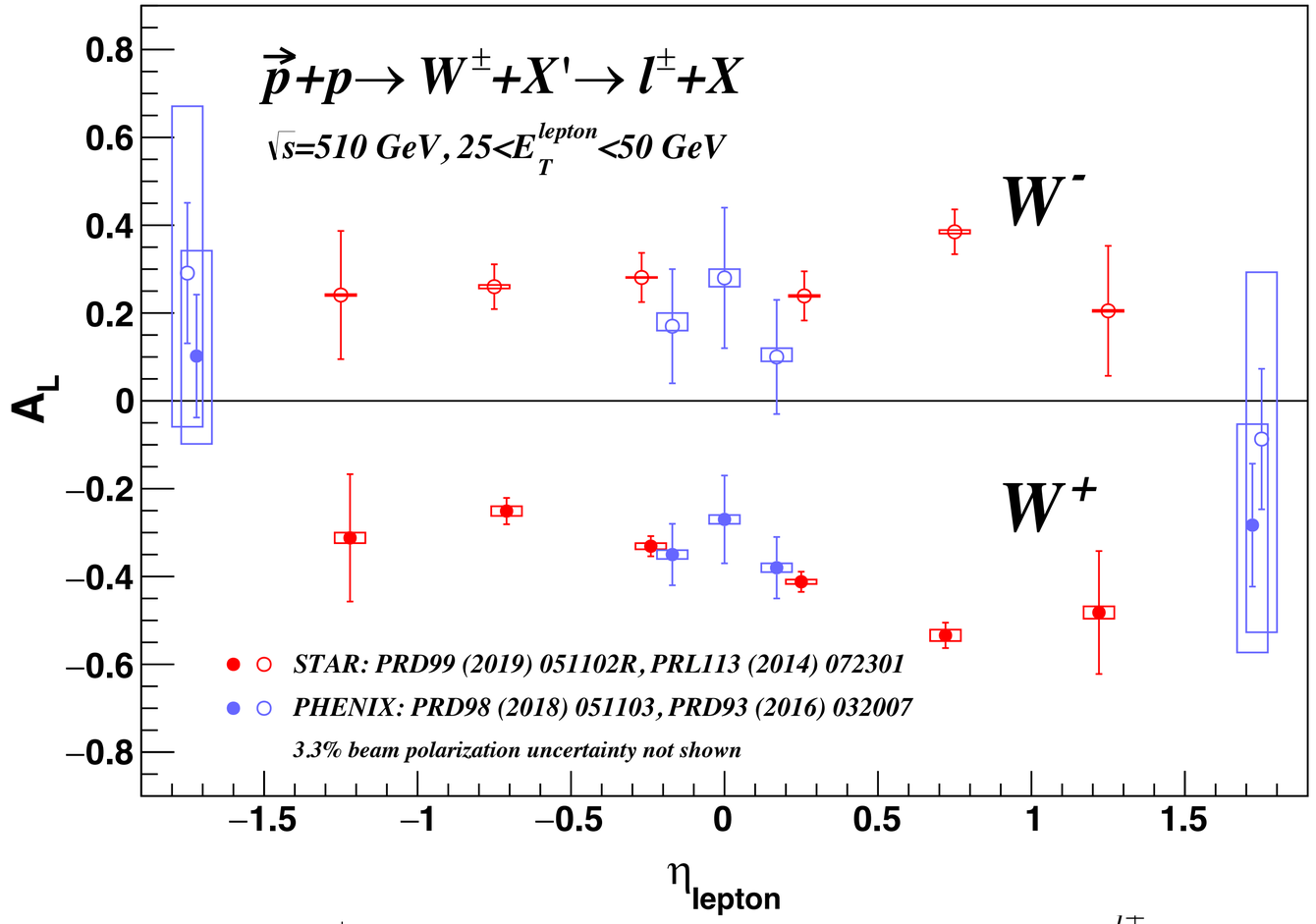

W^+ production:

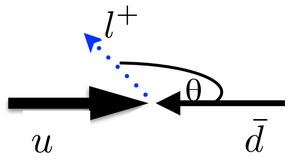

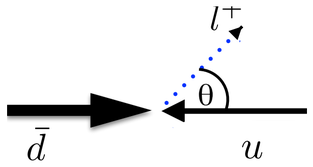

Longitudinal single-spin asymmetry in pp collisions

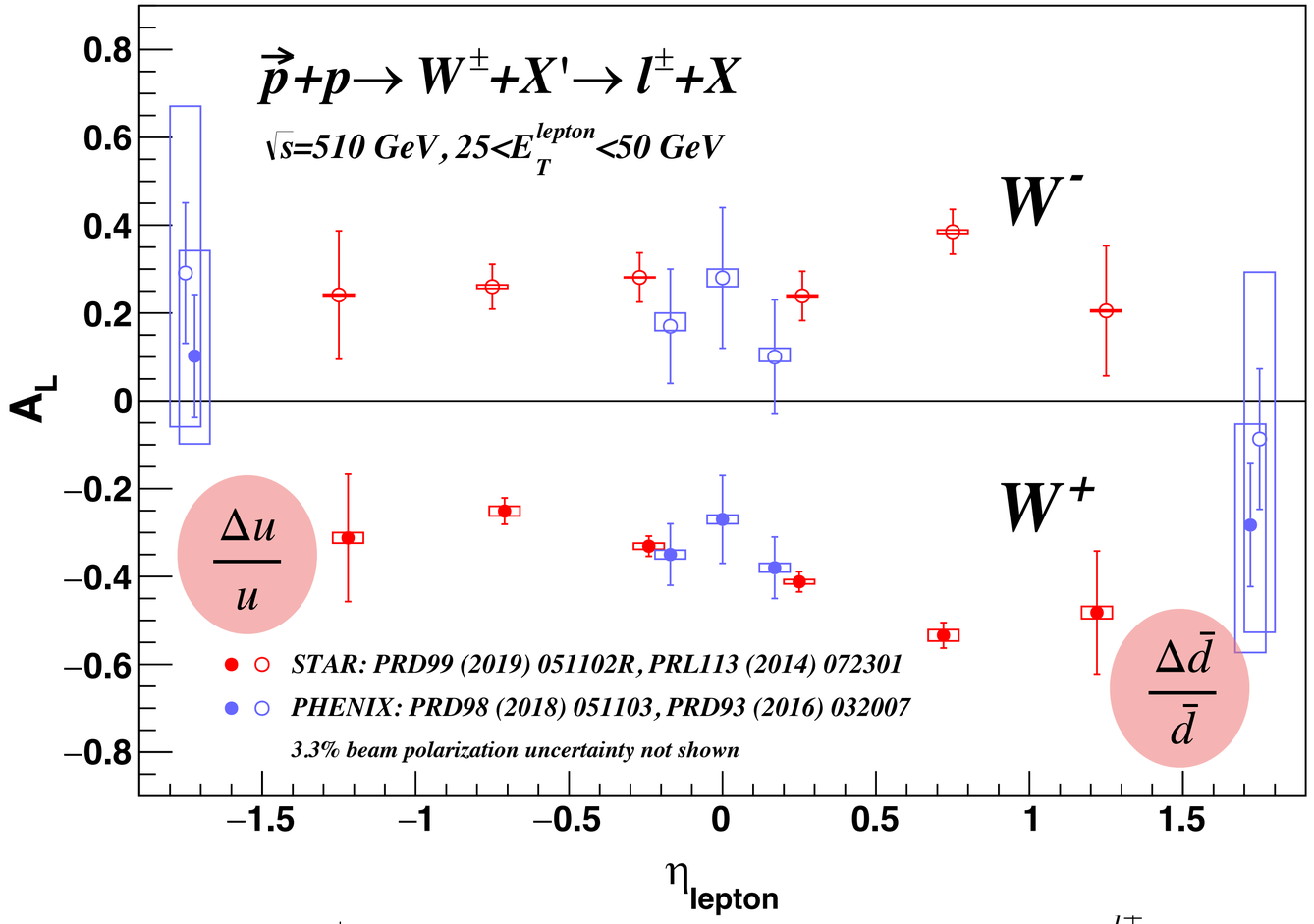

W^+ production:

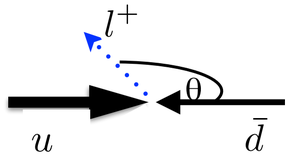

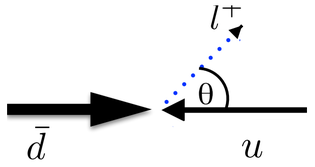

Longitudinal single-spin asymmetry in pp collisions

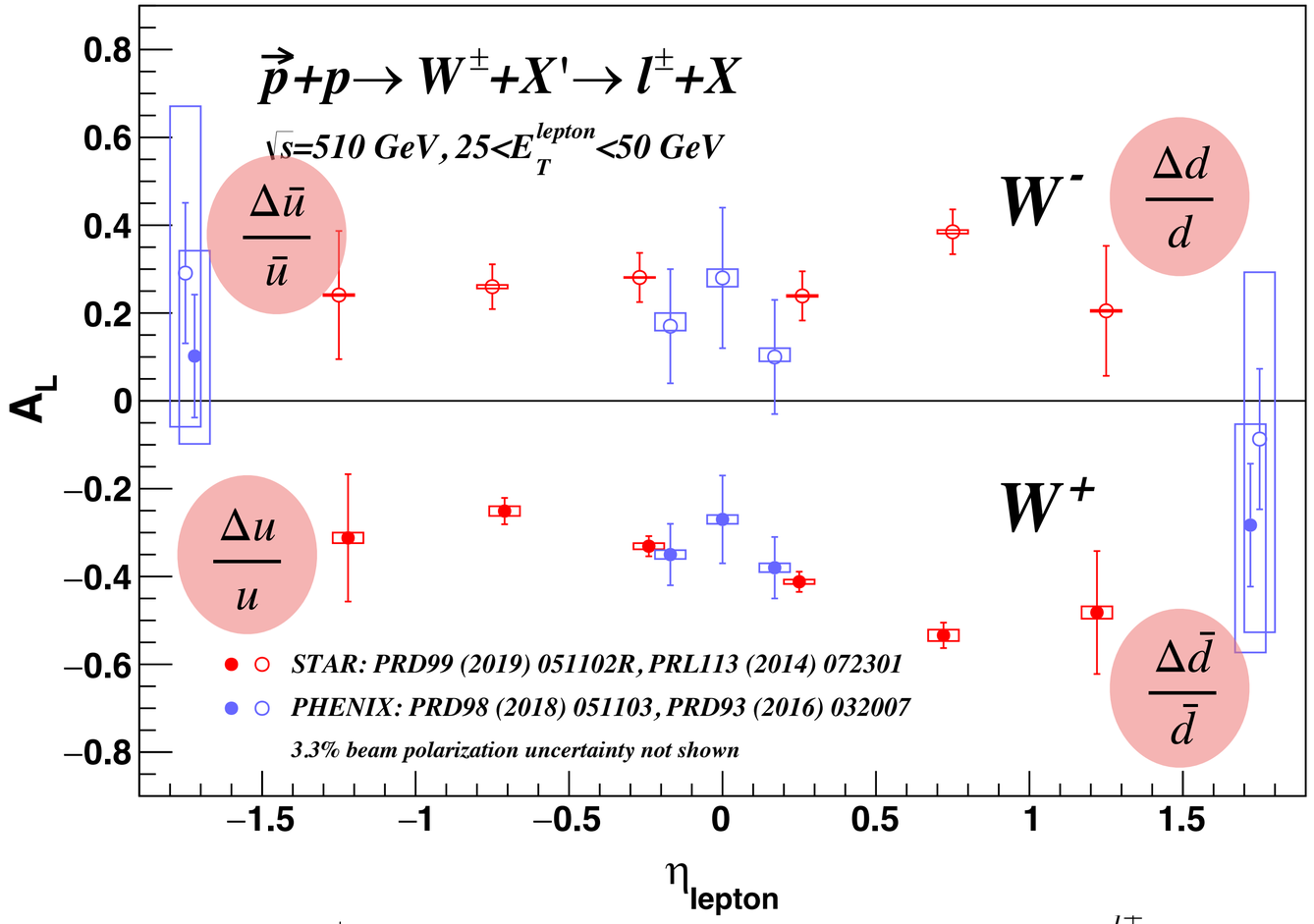

W^+ production:

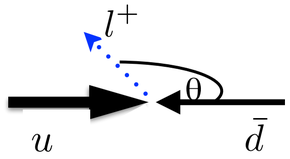

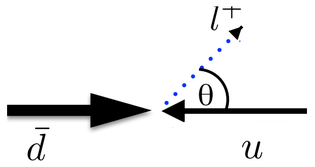

Global fits: quark helicity PDFs

Data:

- inclusive DIS
- SIDIS
- e^+e^- annihilation

JAM Collaboration,
Phys. Rev. Lett. **119** (2017) 132001

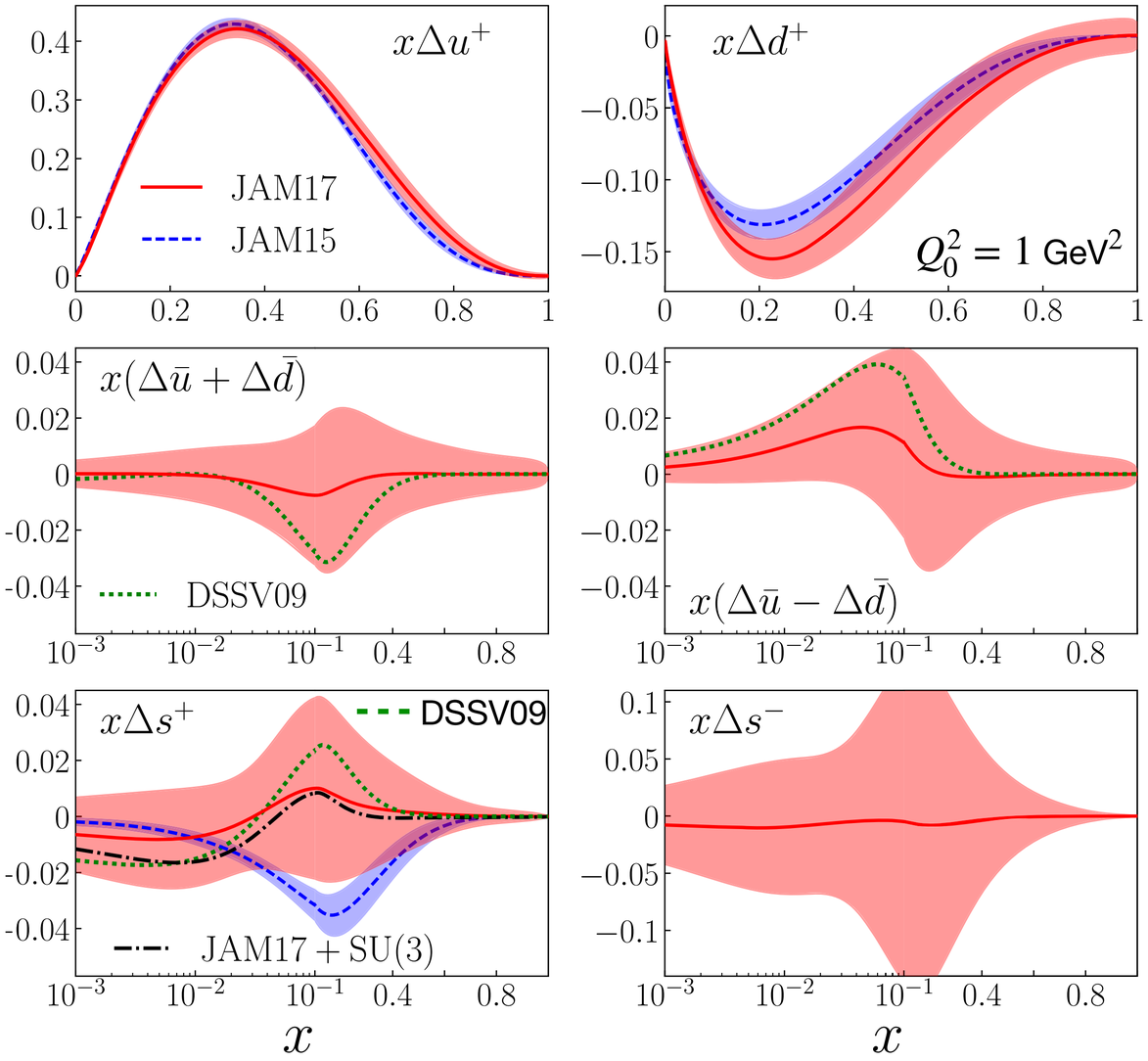

Global fits: quark helicity PDFs

Data:
- inclusive DIS
- SIDIS
- e^+e^- annihilation

JAM Collaboration,
Phys. Rev. Lett. **119** (2017) 132001

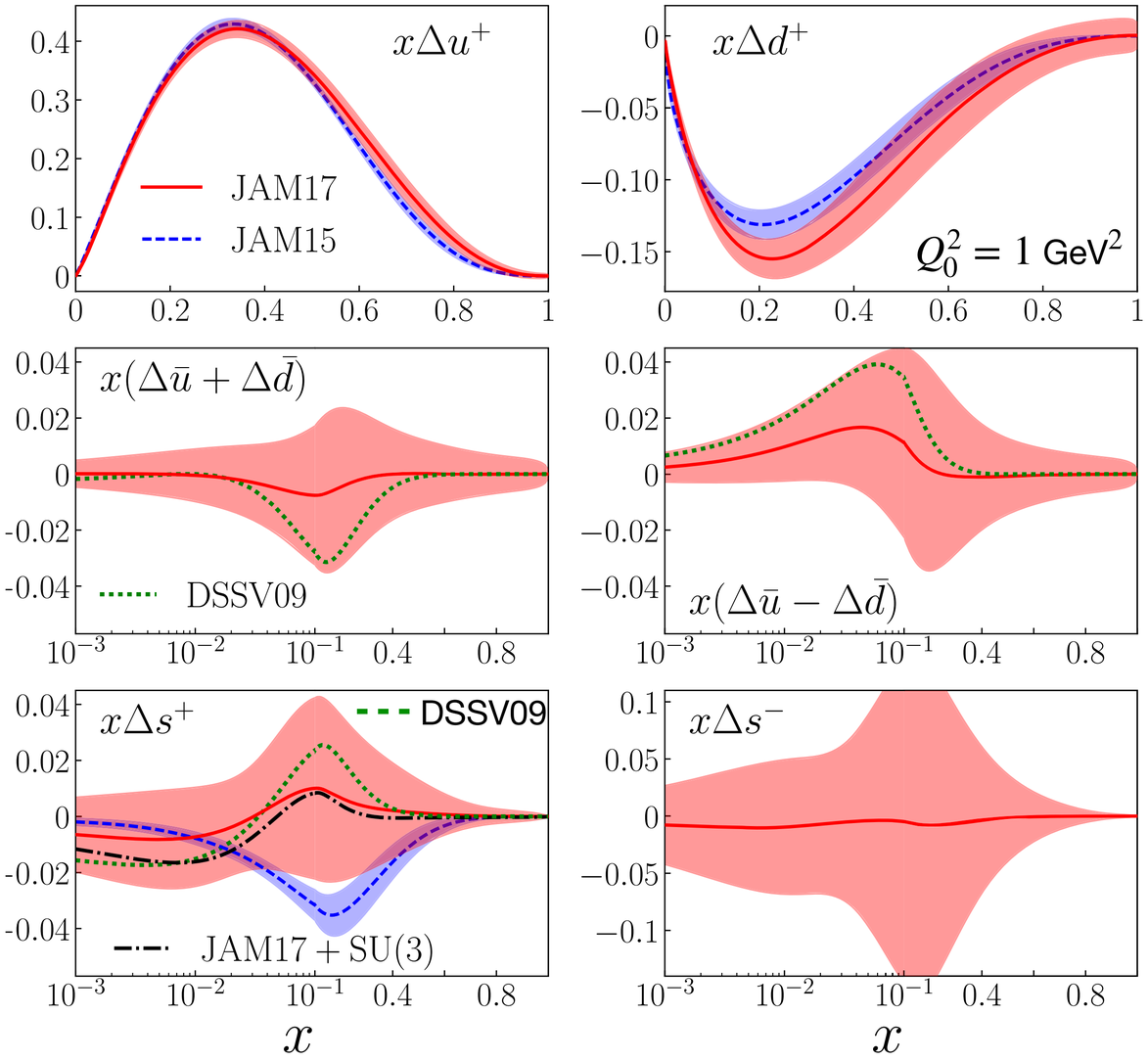

$\Delta q^+ = \Delta q + \Delta\bar{q}$:
largely determined by inclusive DIS data

Global fits: quark helicity PDFs

Data:
- inclusive DIS
- SIDIS
- e^+e^- annihilation

JAM Collaboration,
Phys. Rev. Lett. **119** (2017) 132001

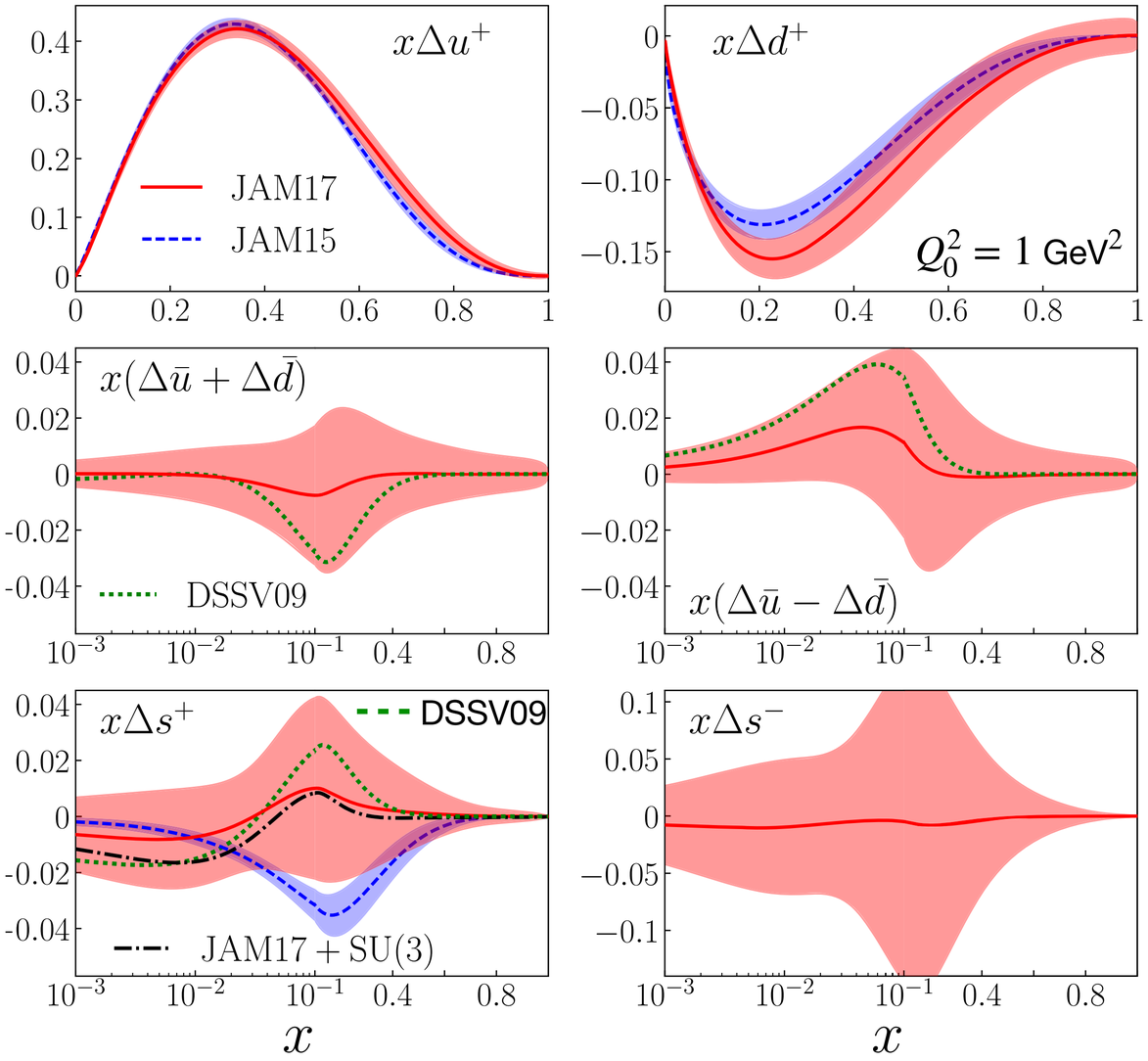

$\Delta q^+ = \Delta q + \Delta\bar{q}$:
largely determined by inclusive DIS data

SIDIS: distinguish between q and $\bar{q}$

$\Delta\bar{u} - \Delta\bar{d}$ slightly positive

Global fits: quark helicity PDFs

Data:
- inclusive DIS
- SIDIS
- e^+e^- annihilation

JAM Collaboration,
Phys. Rev. Lett. **119** (2017) 132001

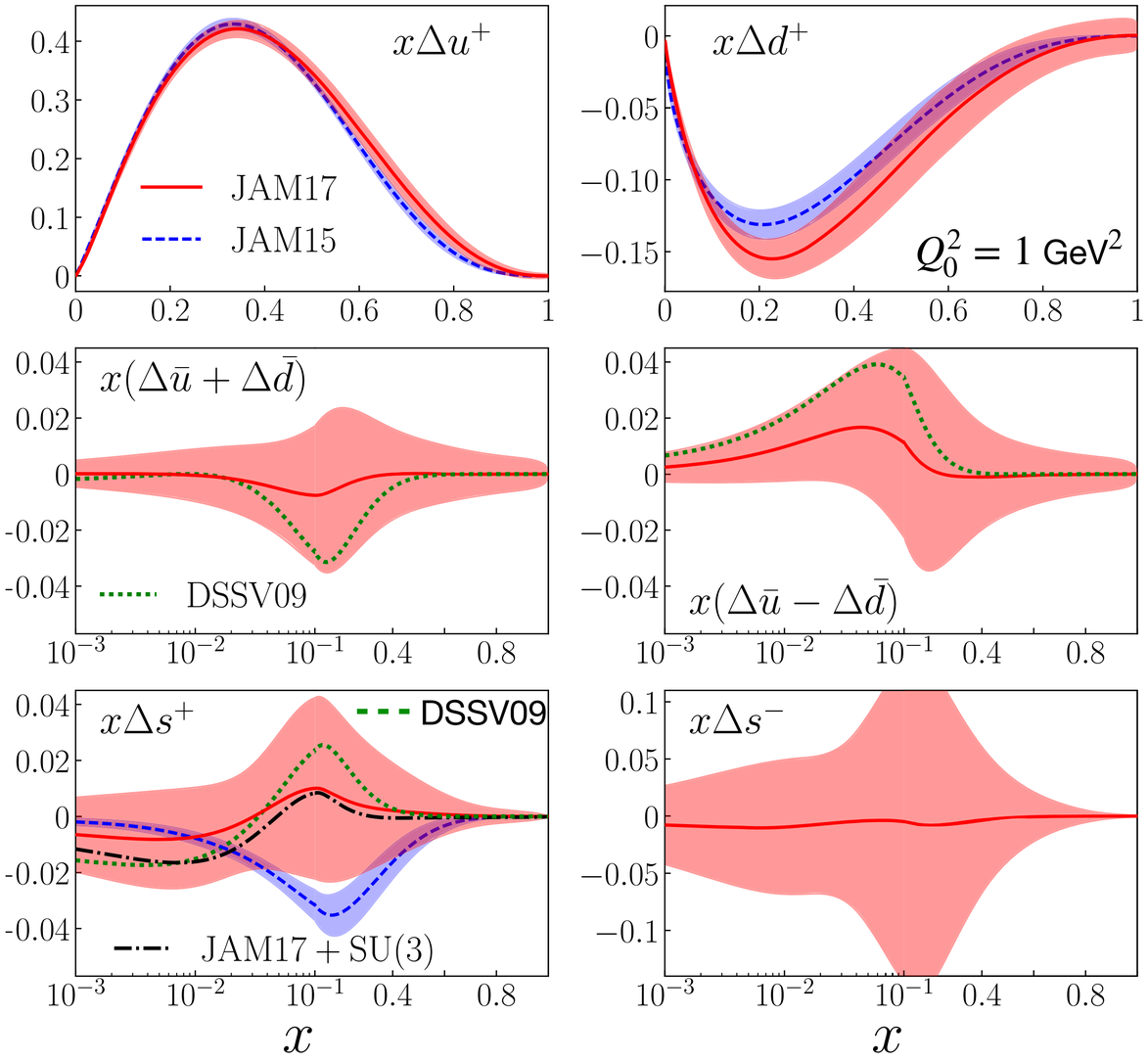

$\Delta q^+ = \Delta q + \Delta\bar{q}$:
largely determined by inclusive DIS data

SIDIS: distinguish between q and $\bar{q}$

$\Delta\bar{u} - \Delta\bar{d}$ slightly positive

DSSV+RHIC $W\,A_L$ data: $\Delta\bar{u} > \Delta\bar{d}$

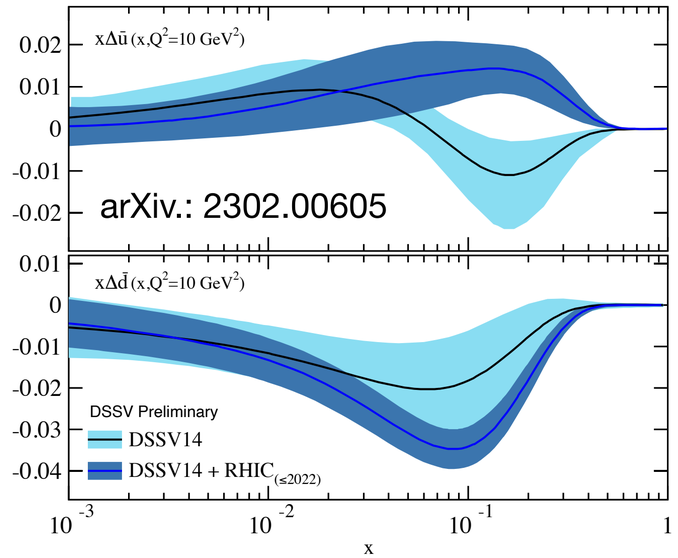

Global fits: quark helicity PDFs

Data:
- inclusive DIS
- SIDIS
- e^+e^- annihilation

JAM Collaboration,
Phys. Rev. Lett. **119** (2017) 132001

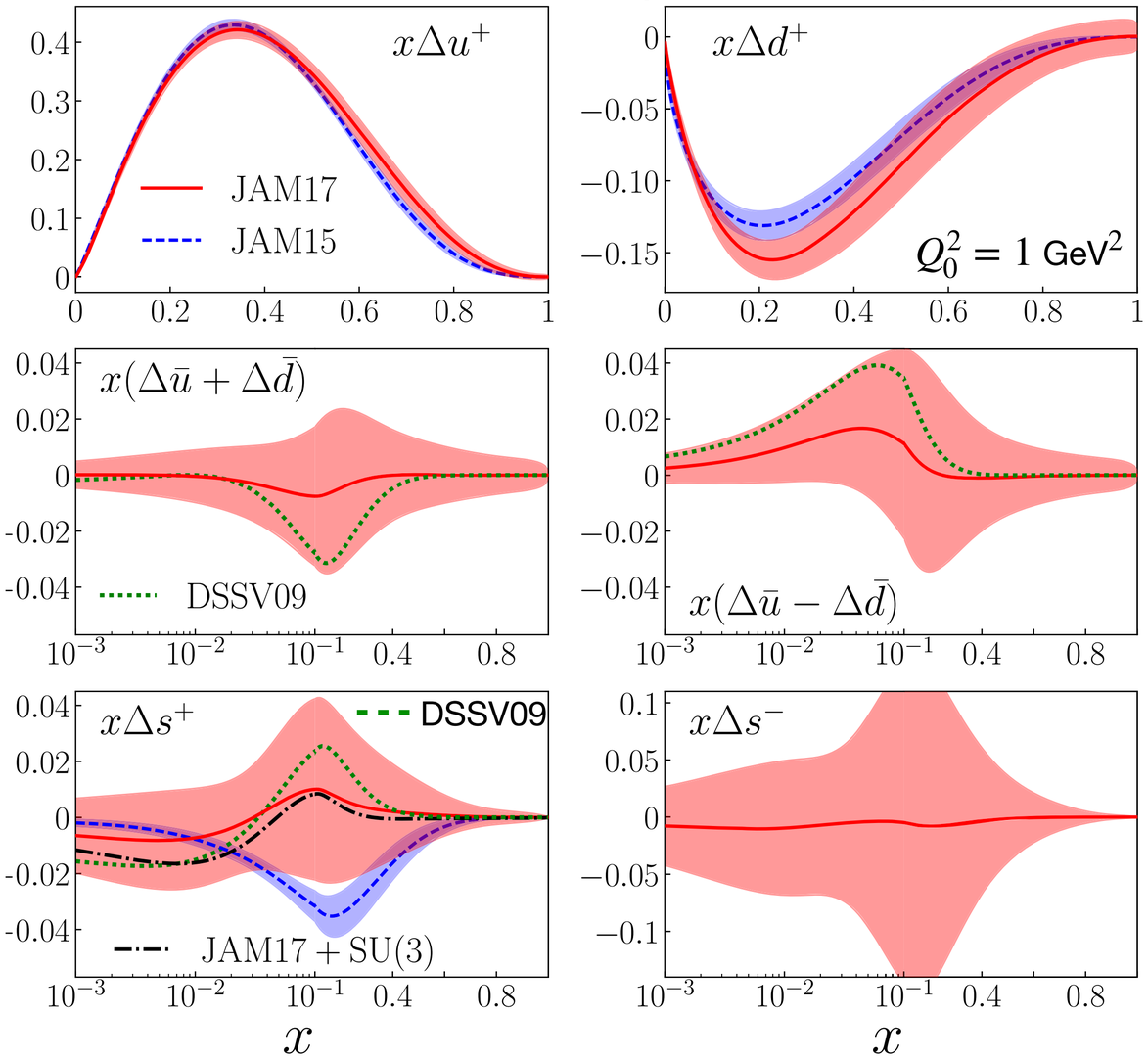

$\Delta q^+ = \Delta q + \Delta\bar{q}$:
largely determined by inclusive DIS data

SIDIS: distinguish between q and $\bar{q}$

$\Delta\bar{u} - \Delta\bar{d}$ slightly positive

STAR, Phys. Rev. D **99** (2019) 051102

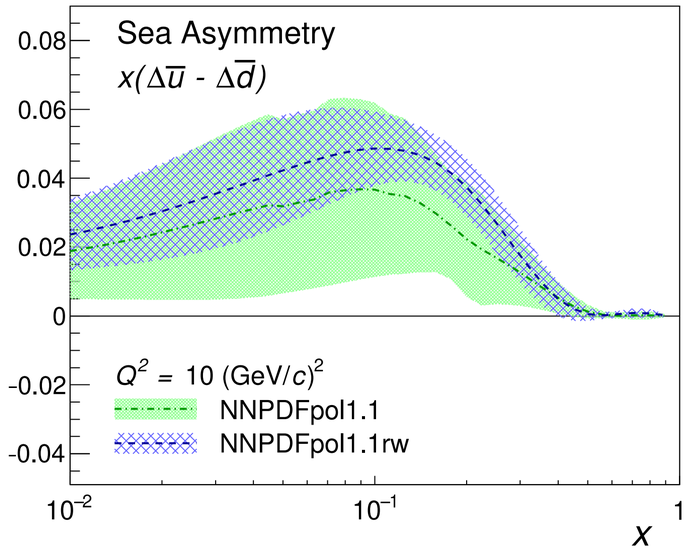

Global fits: quark helicity PDFs

Data:
- inclusive DIS
- SIDIS
- e^+e^- annihilation

JAM Collaboration,
Phys. Rev. Lett. **119** (2017) 132001

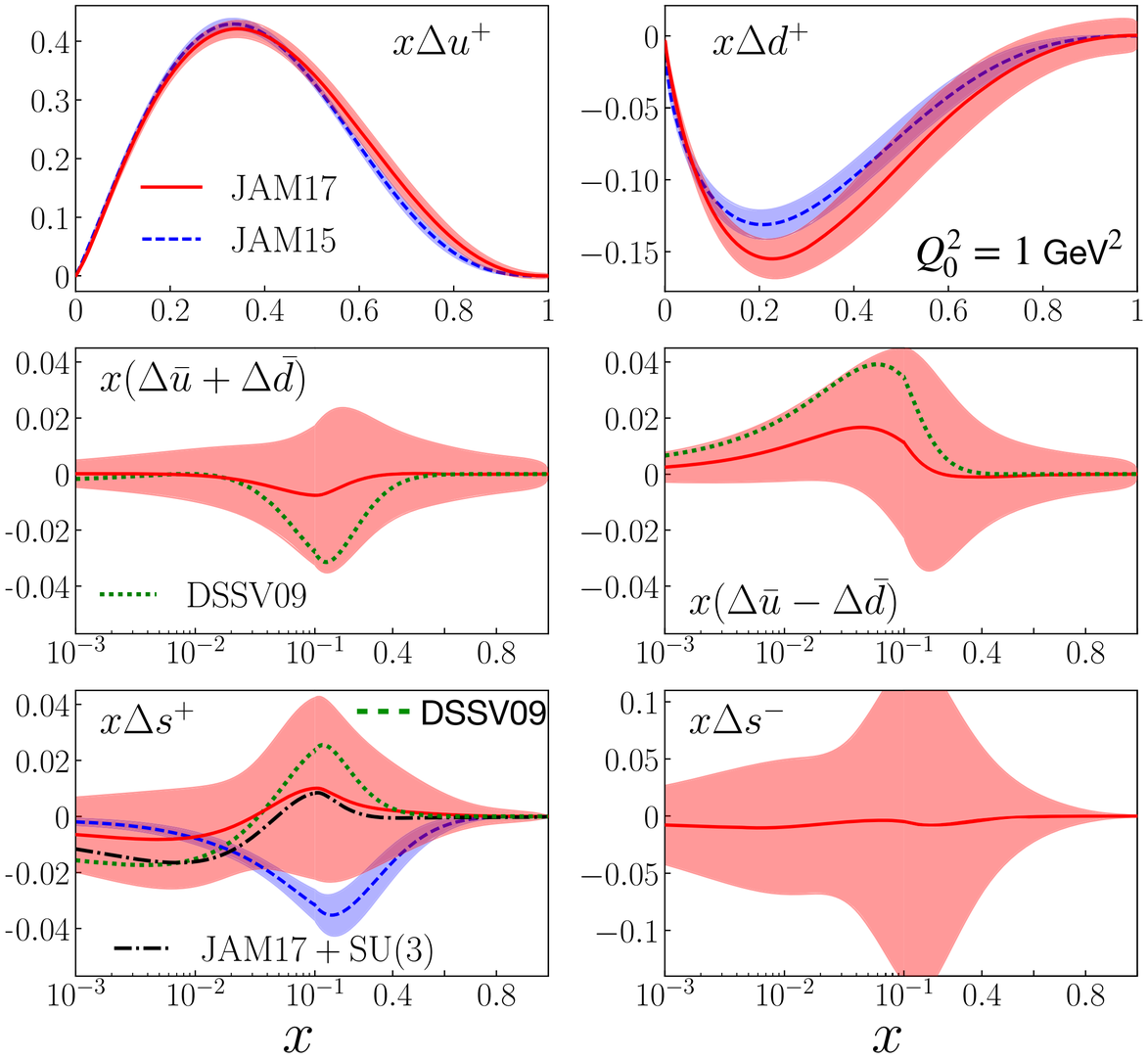

$\Delta q^+ = \Delta q + \Delta\bar{q}$:
largely determined by inclusive DIS data

SIDIS: distinguish between q and $\bar{q}$

$\Delta\bar{u} - \Delta\bar{d}$ slightly positive

STAR, Phys. Rev. D **99** (2019) 051102

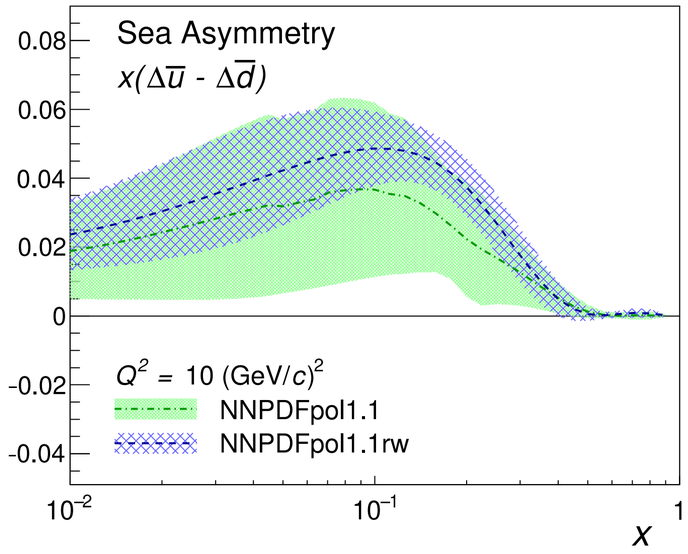

Δs^+:
Consistent with 0

Slightly >0 at intermediate x

Shape determined by SIDIS K data

Gluon helicity

g_1^p: world data

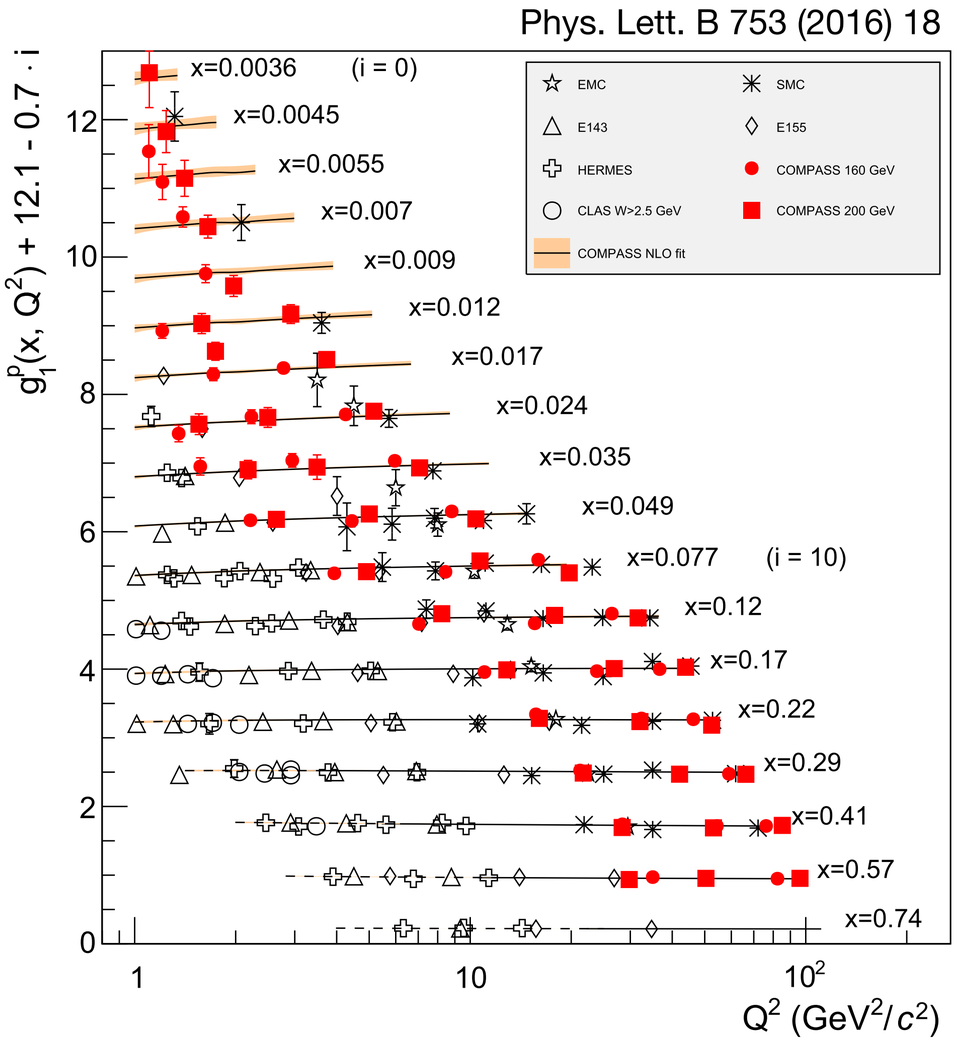

scaling violation from $g_1(x,Q^2)$

Gluon helicity

g_1^p: world data

Phys. Lett. B 753 (2016) 18

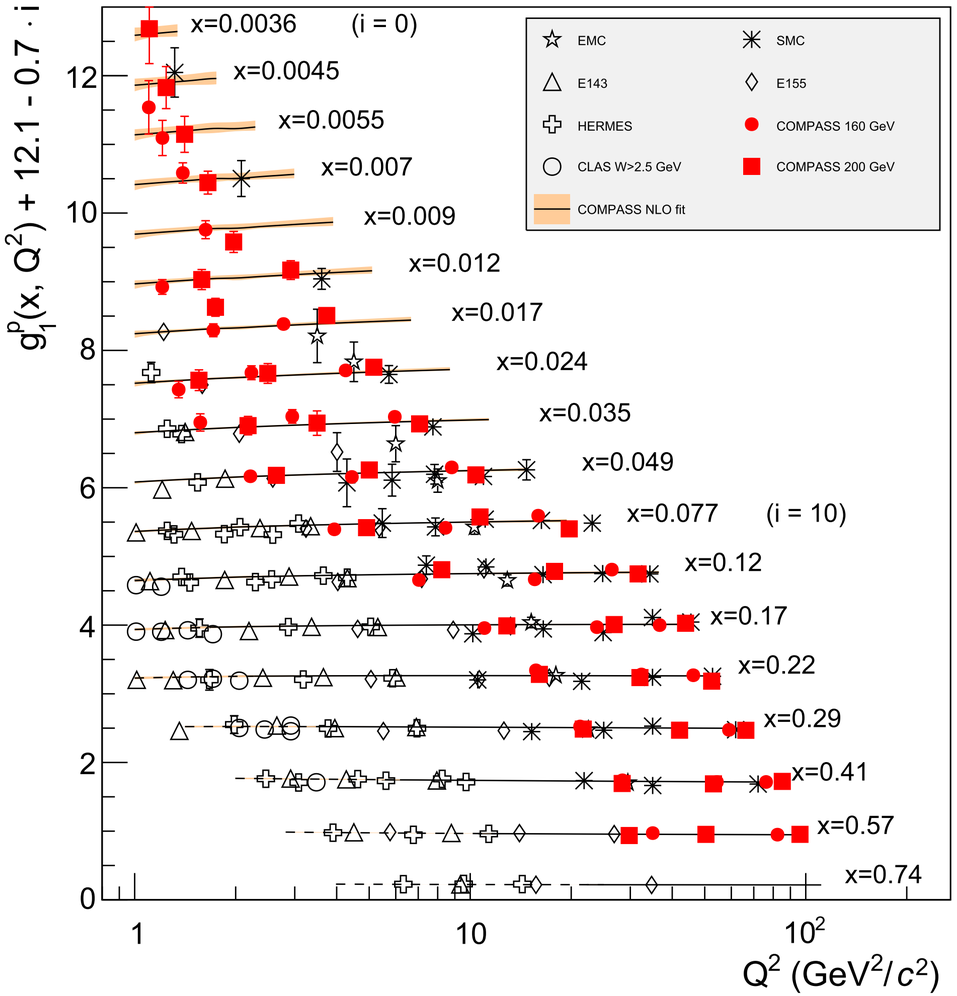

scaling violation from $g_1(x,Q^2)$

$$\frac{dg_1(x,Q^2)}{d\ln Q^2} \propto -\Delta g(x,Q^2)$$

⟶ gluon spin

Double-spin asymmetry in pp collisions

Inclusive DIS: gluons only enter at NLO

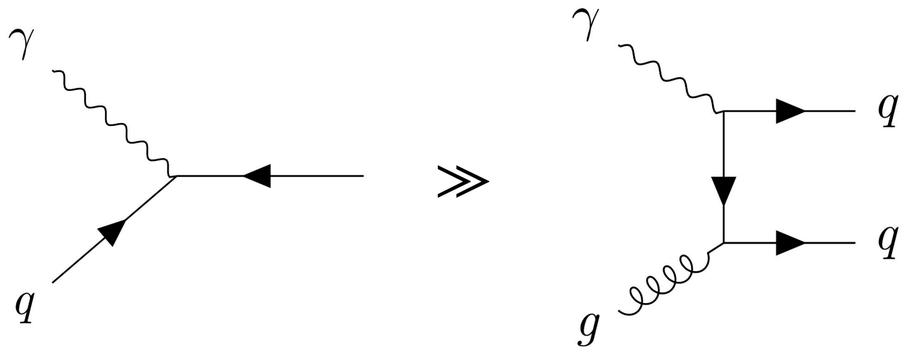

pp collisions: gluons enter at LO

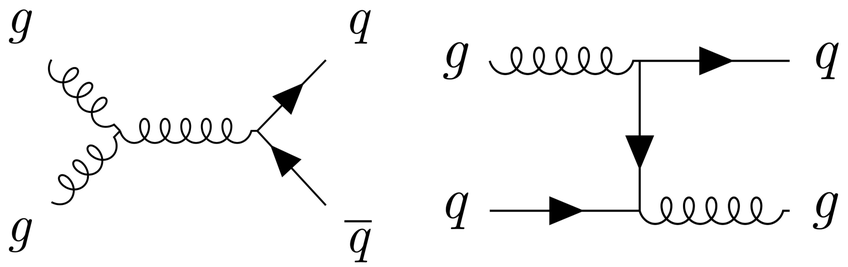

- Inclusive jet production
- Inclusive dijet production
- π^0 and $\pi^{\pm}$ production
- Direct photon production

Double-spin asymmetry in pp collisions

Inclusive DIS: gluons only enter at NLO

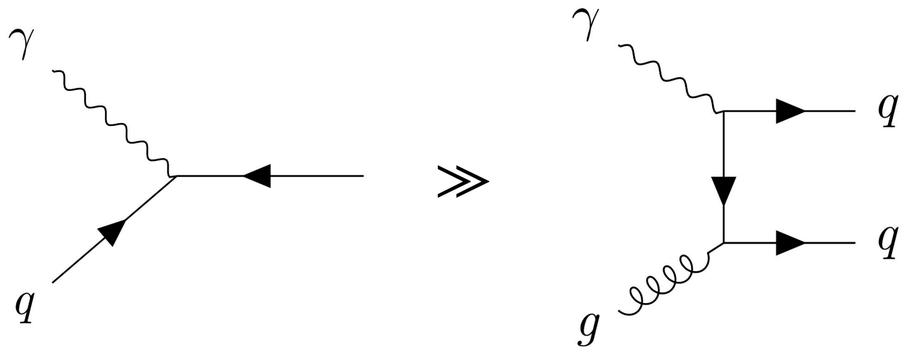

- Increased sensitivity to gluons:
  - heavy-quark production
  - high-p_T hadrons

pp collisions: gluons enter at LO

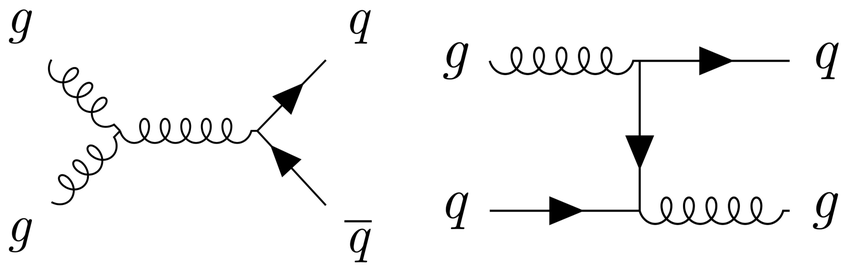

- Inclusive jet production
- Inclusive dijet production
- π^0 and $\pi^{\pm}$ production
- Direct photon production

Longitudinal double-spin asymmetry in pp collisions

$$A_{LL} = \frac{\frac{\vec{\vec{N}}^{\text{dijet}}}{\vec{\vec{L}}} - \frac{\vec{\overleftarrow{N}}^{\text{dijet}}}{\vec{\overleftarrow{L}}}}{\frac{\vec{\vec{N}}^{\text{dijet}}}{\vec{\vec{L}}} + \frac{\vec{\overleftarrow{N}}^{\text{dijet}}}{\vec{\overleftarrow{L}}}}(x_B, Q^2)$$

$$\propto \frac{\Delta f(x_1, Q^2)\Delta f(x_2, Q^2)}{f(x_1, Q^2) f(x_2, Q^2)}$$

Longitudinal double-spin asymmetry in pp collisions

$$A_{LL} = \frac{\vec{\vec{N}}^{\text{dijet}} - \vec{\overleftarrow{N}}^{\text{dijet}}}{\vec{\vec{L}} \quad \vec{\overleftarrow{L}}}(x_B, Q^2)$$
$$\vec{\vec{N}}^{\text{dijet}} + \vec{\overleftarrow{N}}^{\text{dijet}}$$
$$\vec{\vec{L}} \quad \vec{\overleftarrow{L}}$$

$$\propto \frac{\Delta f(x_1, Q^2)\Delta f(x_2, Q^2)}{f(x_1, Q^2) f(x_2, Q^2)}$$

probed partons

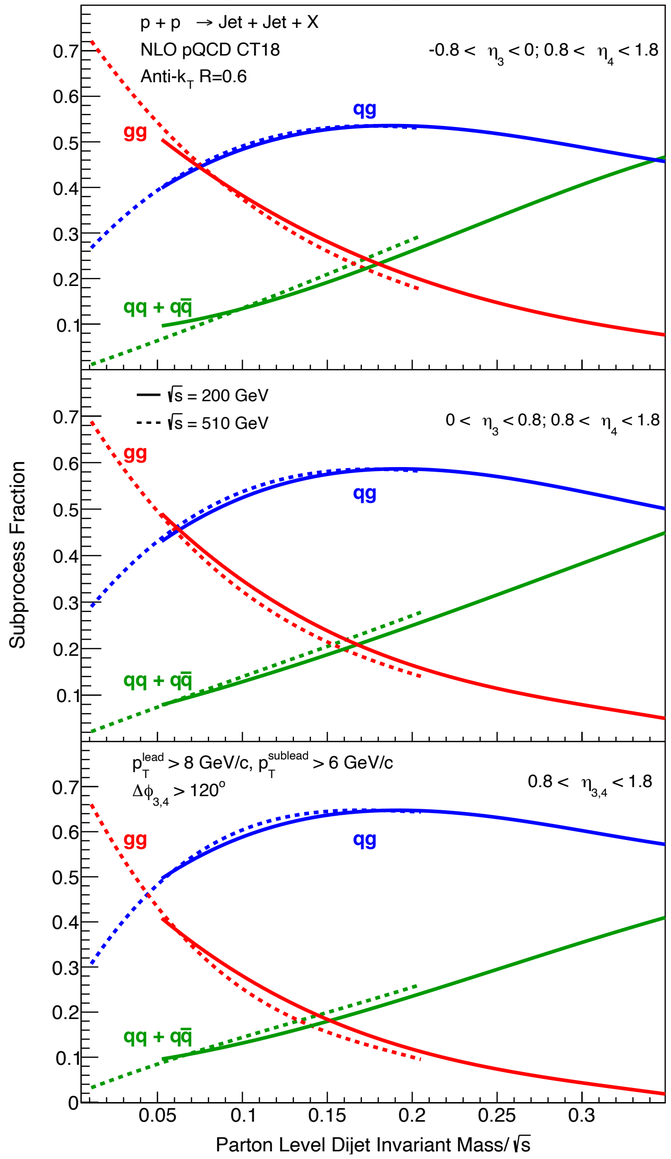

Longitudinal double-spin asymmetry in pp collisions

$$A_{LL} = \frac{\frac{\vec{N}^{\text{dijet}}}{\vec{L}} - \frac{\overleftarrow{N}^{\text{dijet}}}{\overleftarrow{L}}}{\frac{\vec{N}^{\text{dijet}}}{\vec{L}} + \frac{\overleftarrow{N}^{\text{dijet}}}{\overleftarrow{L}}}(x_B, Q^2)$$

$$\propto \frac{\Delta f(x_1, Q^2)\Delta f(x_2, Q^2)}{f(x_1, Q^2) f(x_2, Q^2)}$$

probed partons

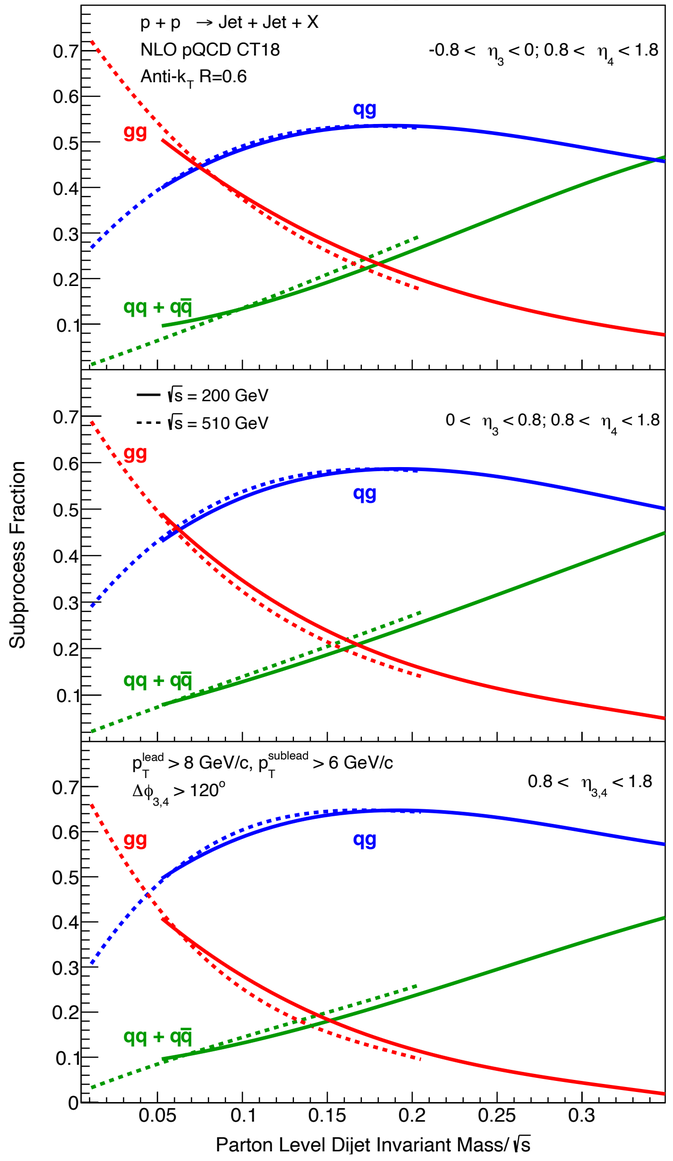

probed x region

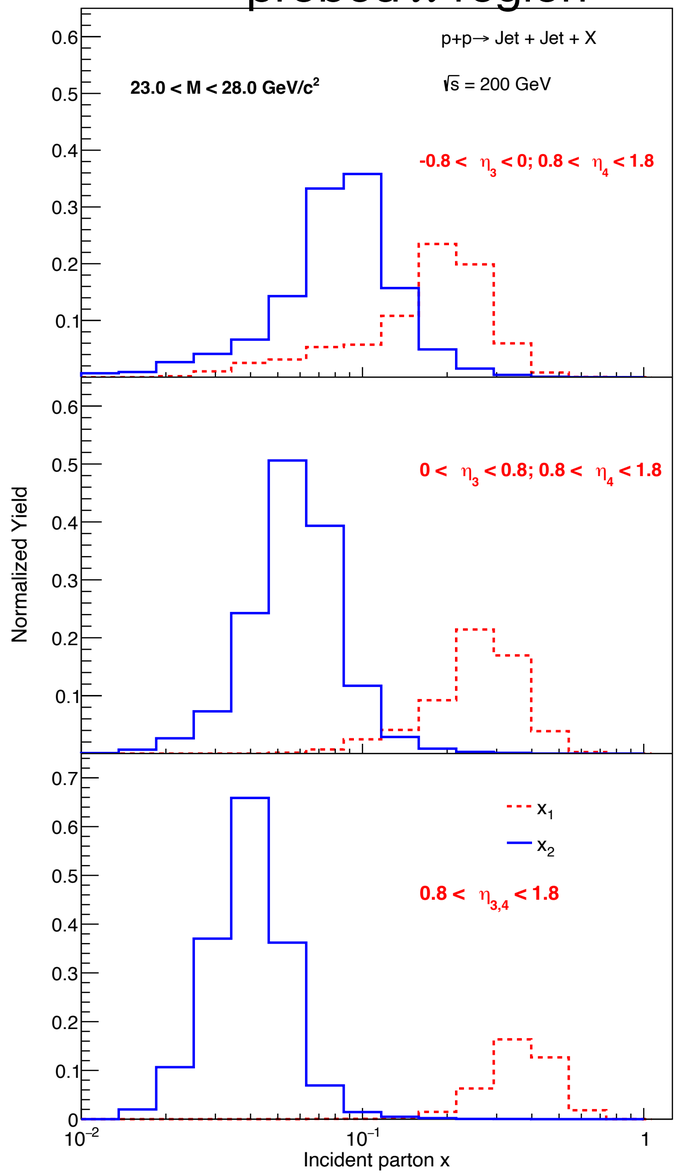

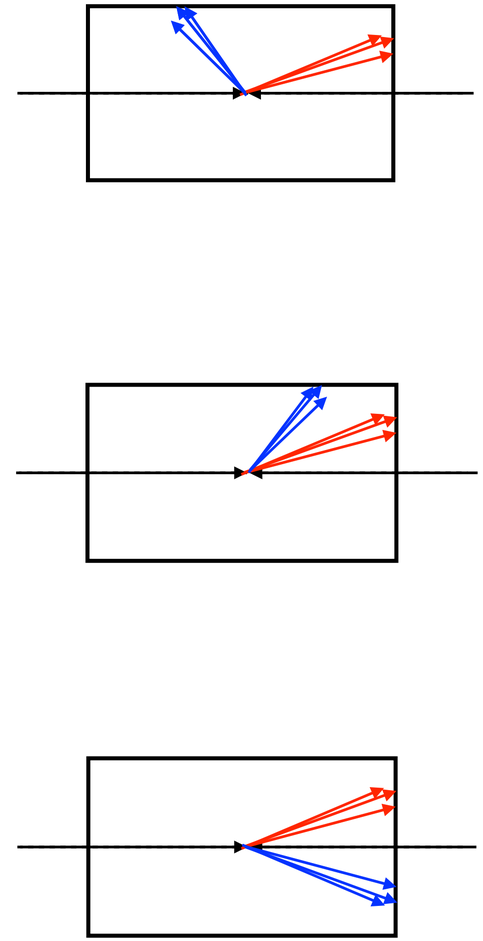

Longitudinal double-spin asymmetry measurement

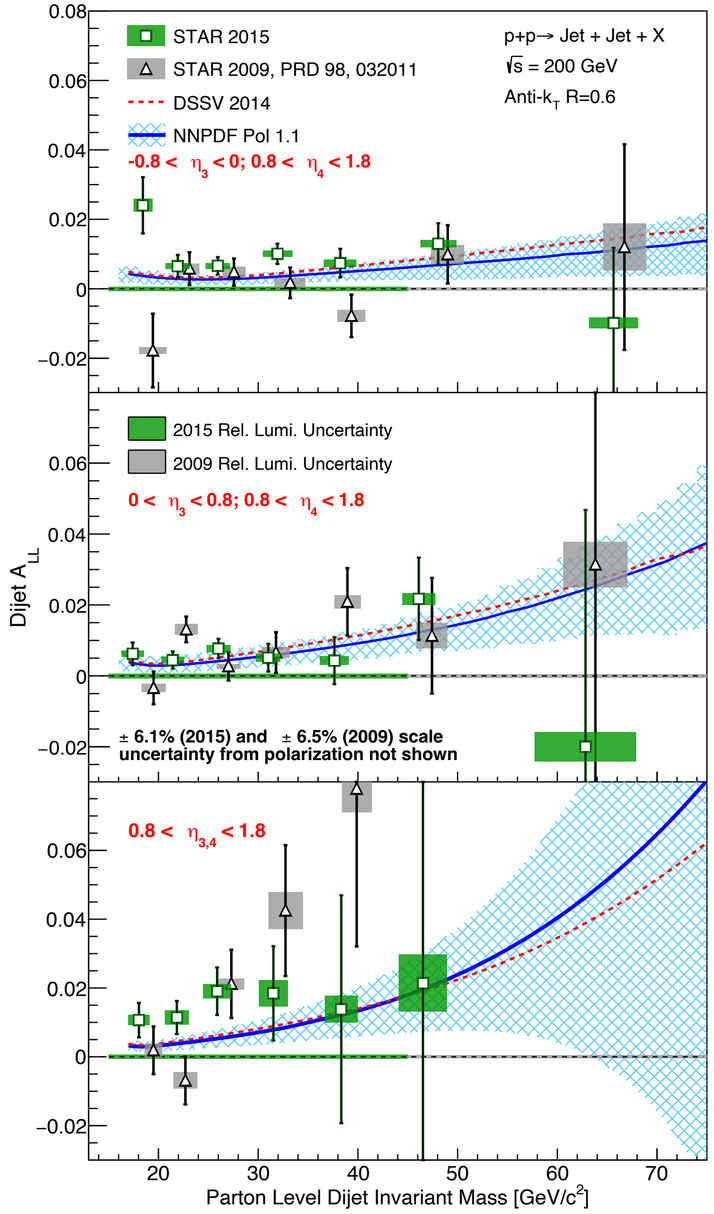

Global fits: gluon helicity PDF

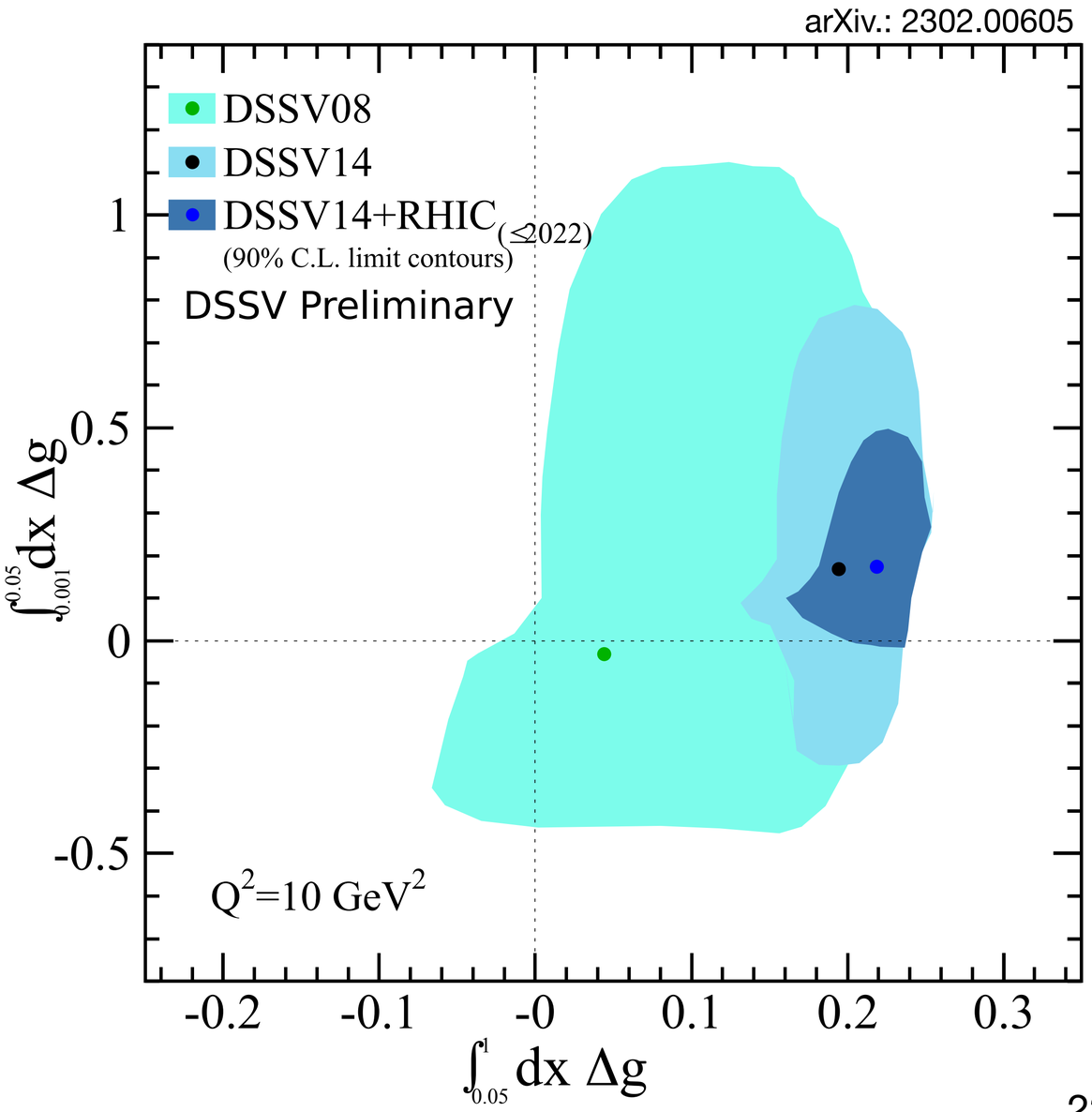

(SI)DIS provide limited constraints on ΔG

RHIC jet and pion A_{LL} data:

$\Delta G > 0$ for $x > 0.05$

Future: probing the valence region with CLAS12

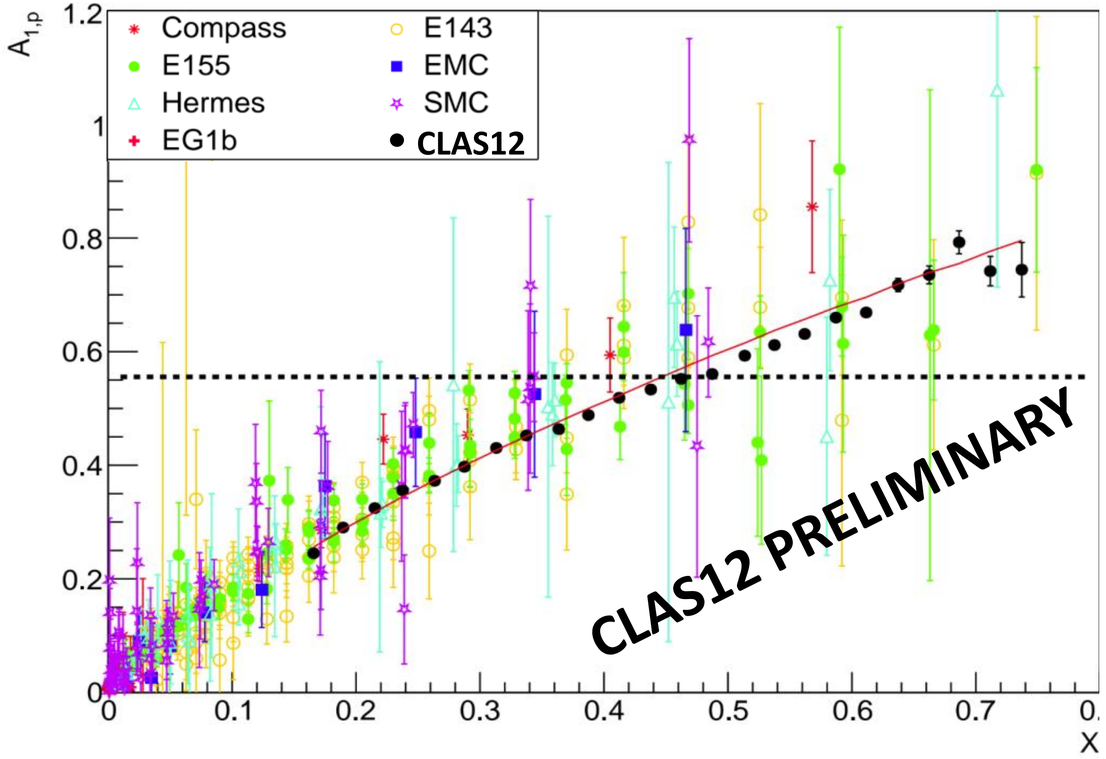

S. Niccolai, DIS2026

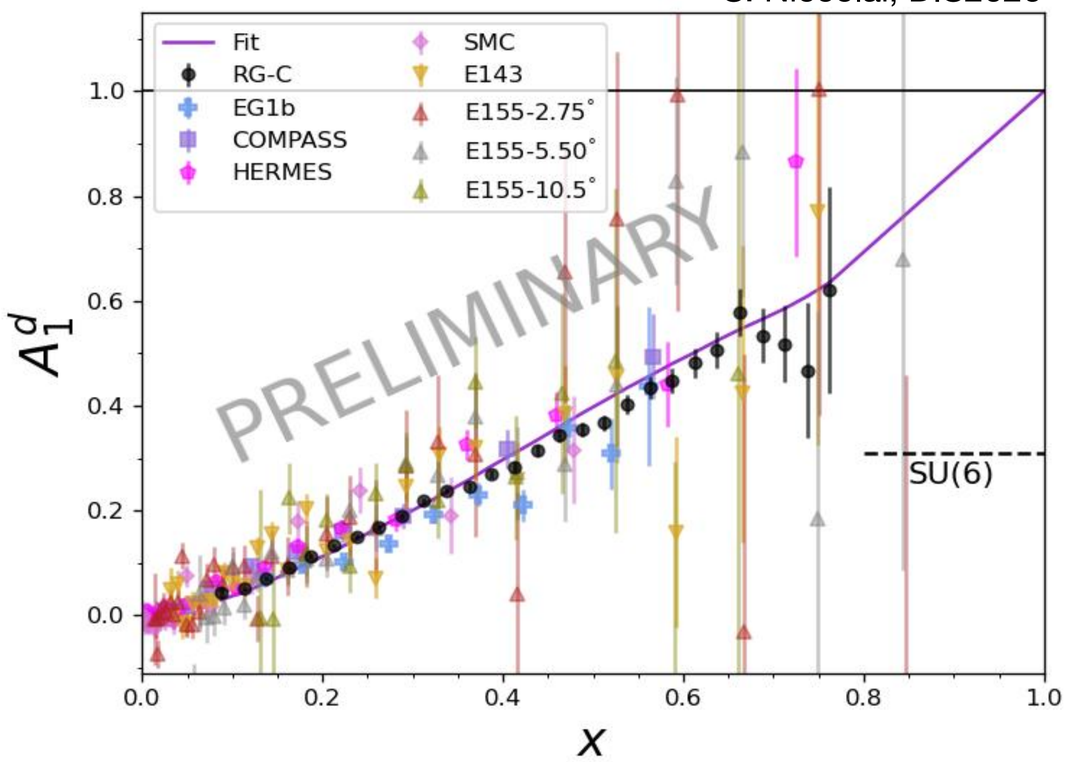

Valence region

Flavour decomposition combining p and D data

Future: the electron-ion collider (EIC)

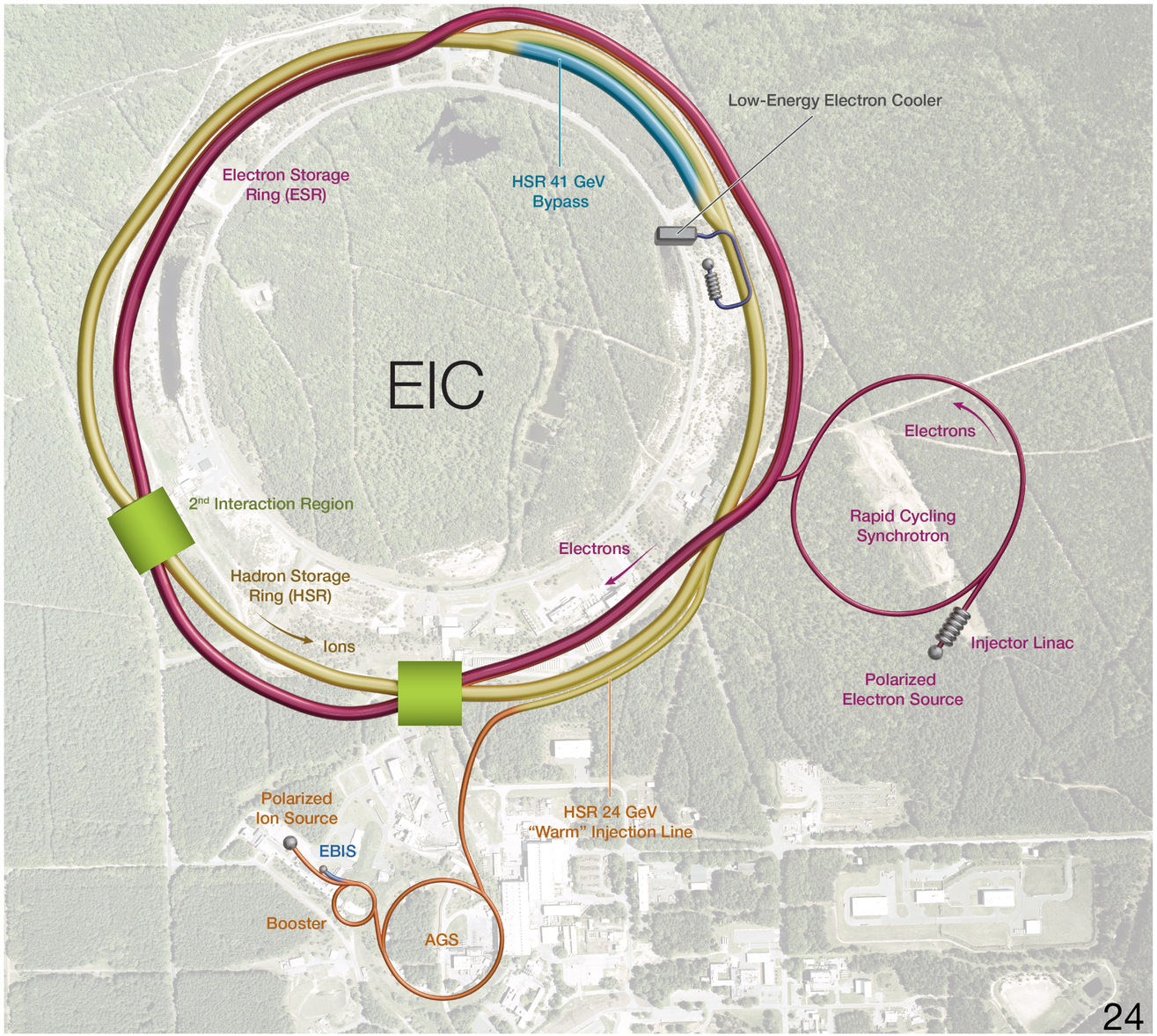

- Based on RHIC:
  - use exiting hadron storage ring
    energy: 41, 100–275 GeV
  - add electron storage ring in RHIC tunnel
    energy: 5–10 GeV

Future: the electron-ion collider (EIC)

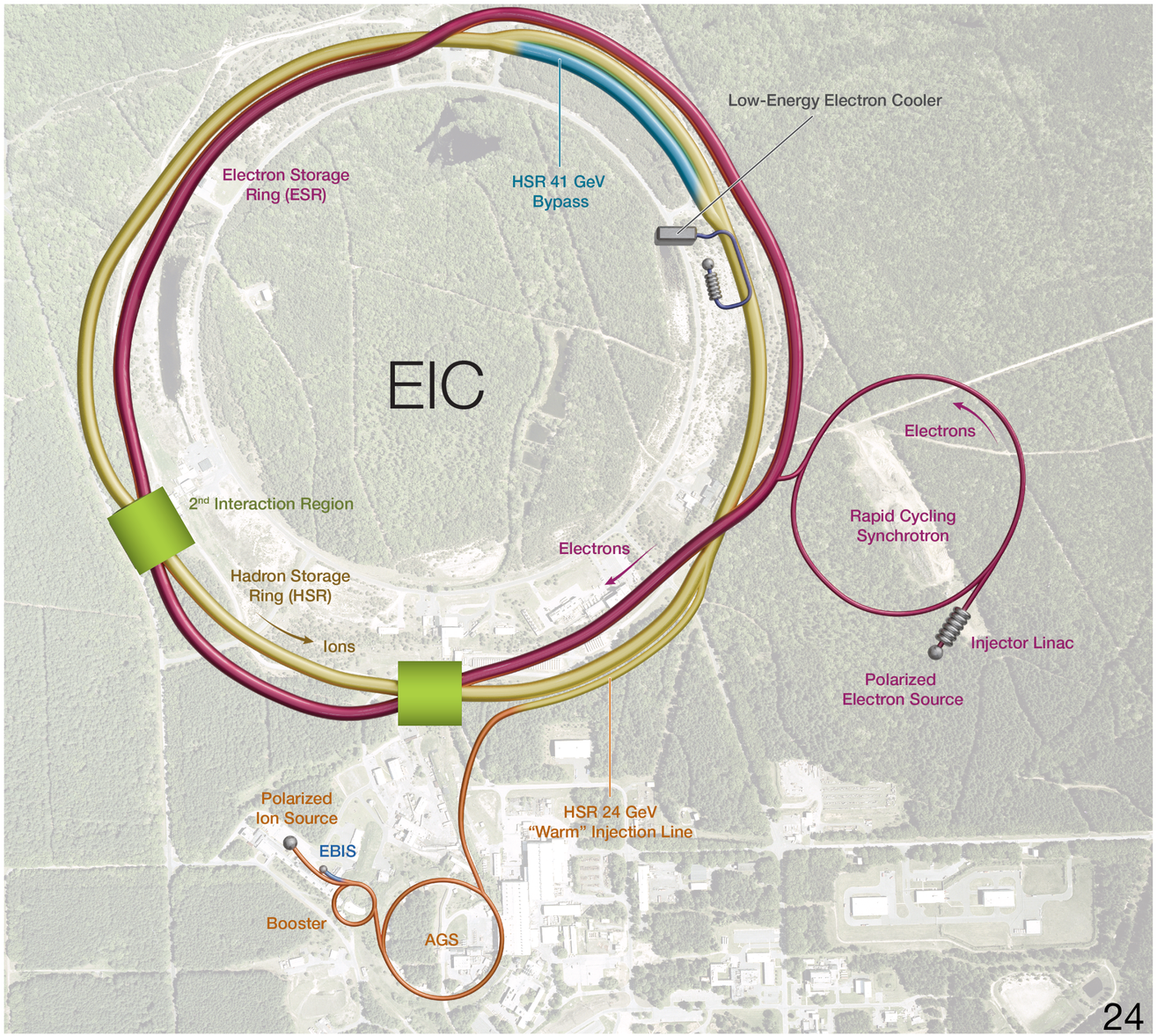

- Based on RHIC:
  - use exiting hadron storage ring
    energy: 41, 100–275 GeV
  - add electron storage ring in RHIC tunnel
    energy: 5–10 GeV

$\rightarrow \sqrt{s} = 29 - 100$ GeV (140 GeV upgradable)

Future: the electron-ion collider (EIC)

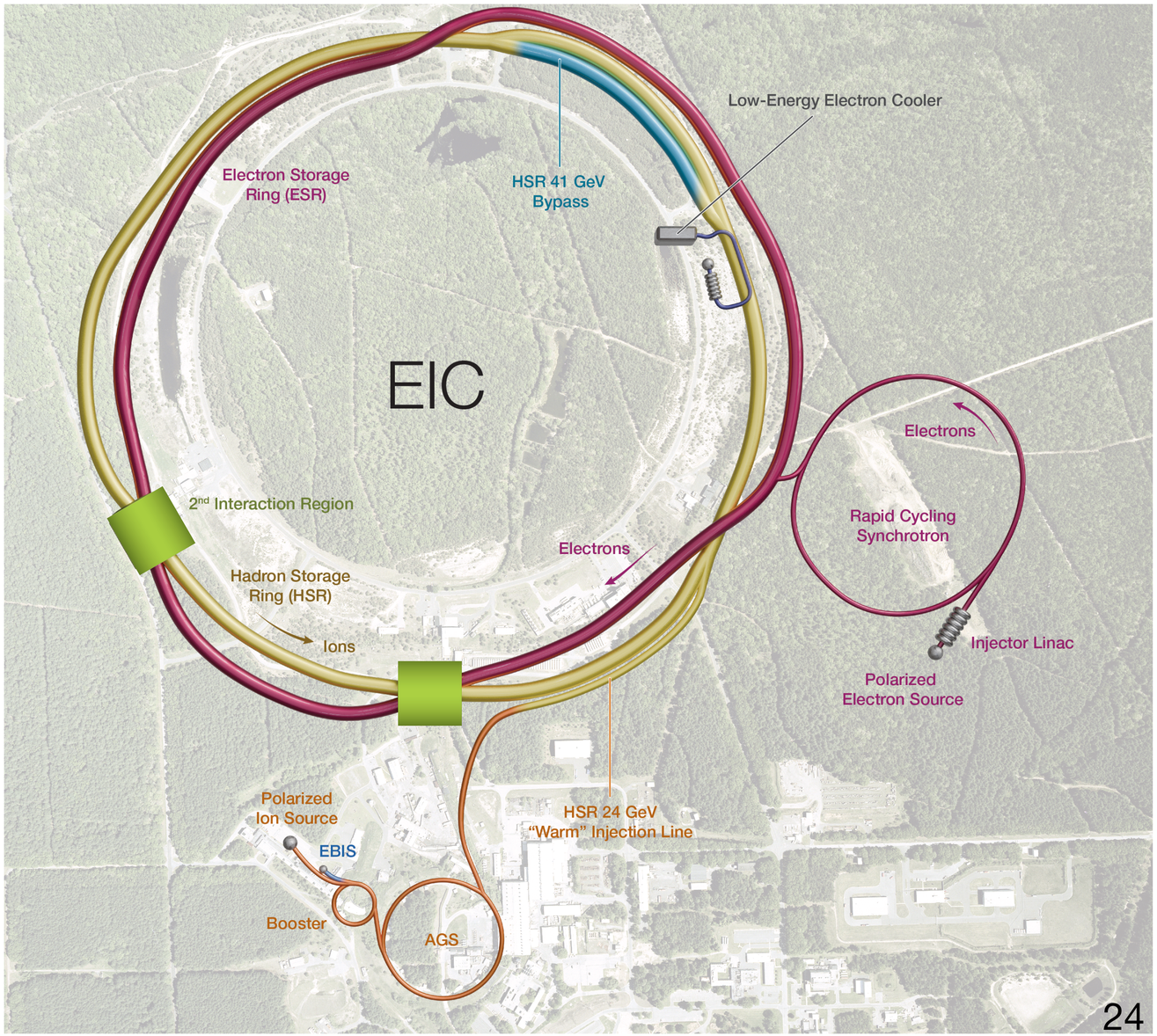

- Based on RHIC:
  - use exiting hadron storage ring
    energy: 41, 100–275 GeV
  - add electron storage ring in RHIC tunnel
    energy: 5–10 GeV

  $\rightarrow \sqrt{s} = 29 - 100$ GeV (140 GeV upgradable)

- $\vec{e} + \vec{p}^{\uparrow}, \overrightarrow{He}^{\uparrow}$

  ~ 70% polarisation

Future: the electron-ion collider (EIC)

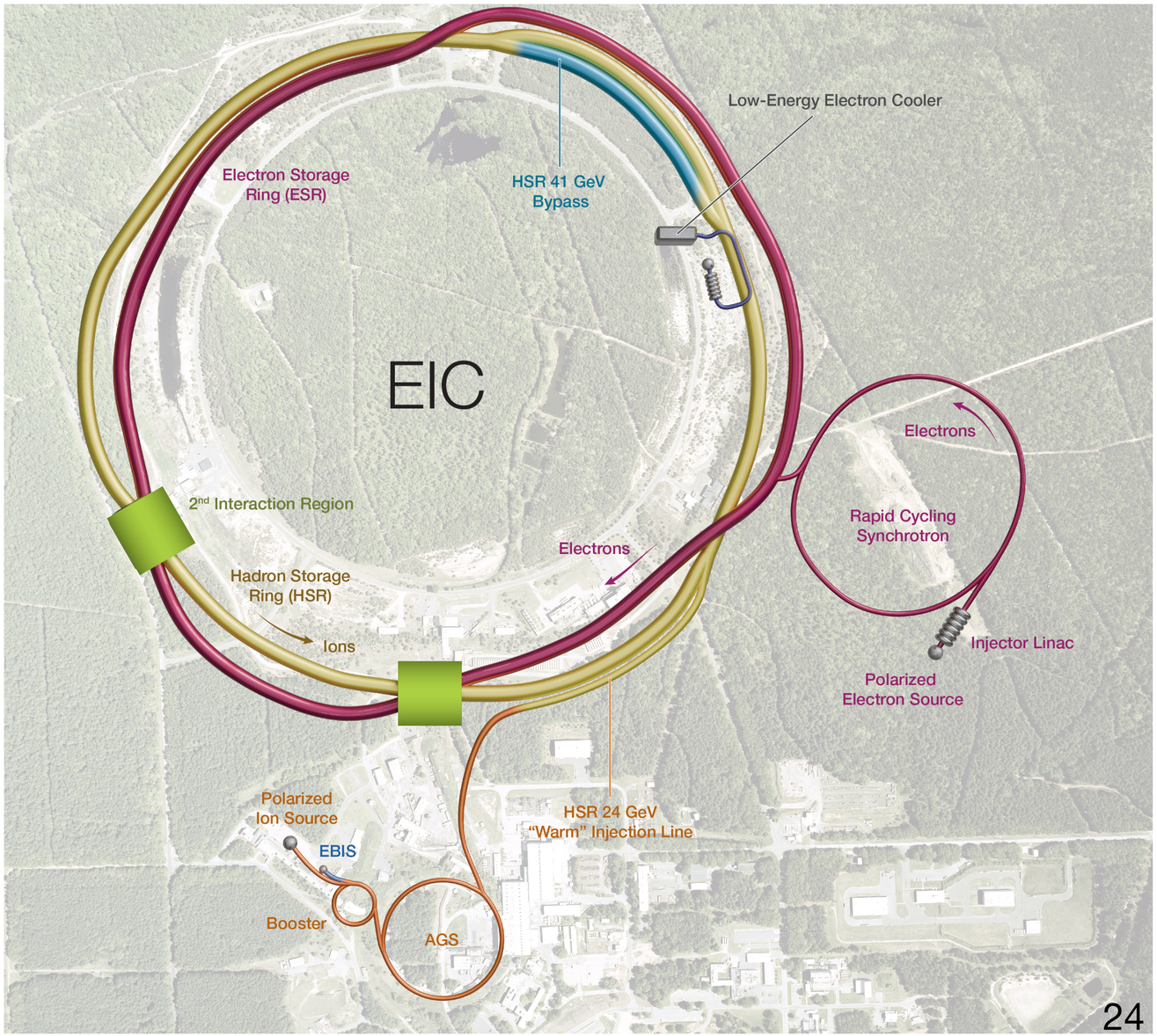

- Based on RHIC:
  - use exiting hadron storage ring
    energy: 41, 100–275 GeV
  - add electron storage ring in RHIC tunnel
    energy: 5–10 GeV

  $\rightarrow \sqrt{s} = 29 - 100$ GeV (140 GeV upgradable)

- $\vec{e} + \vec{p}^{\uparrow}, \overrightarrow{He}^{\uparrow}$

  ~ 70% polarisation

  + heavier, unpolarised ions, up to Uranium

Future: the electron-ion collider (EIC)

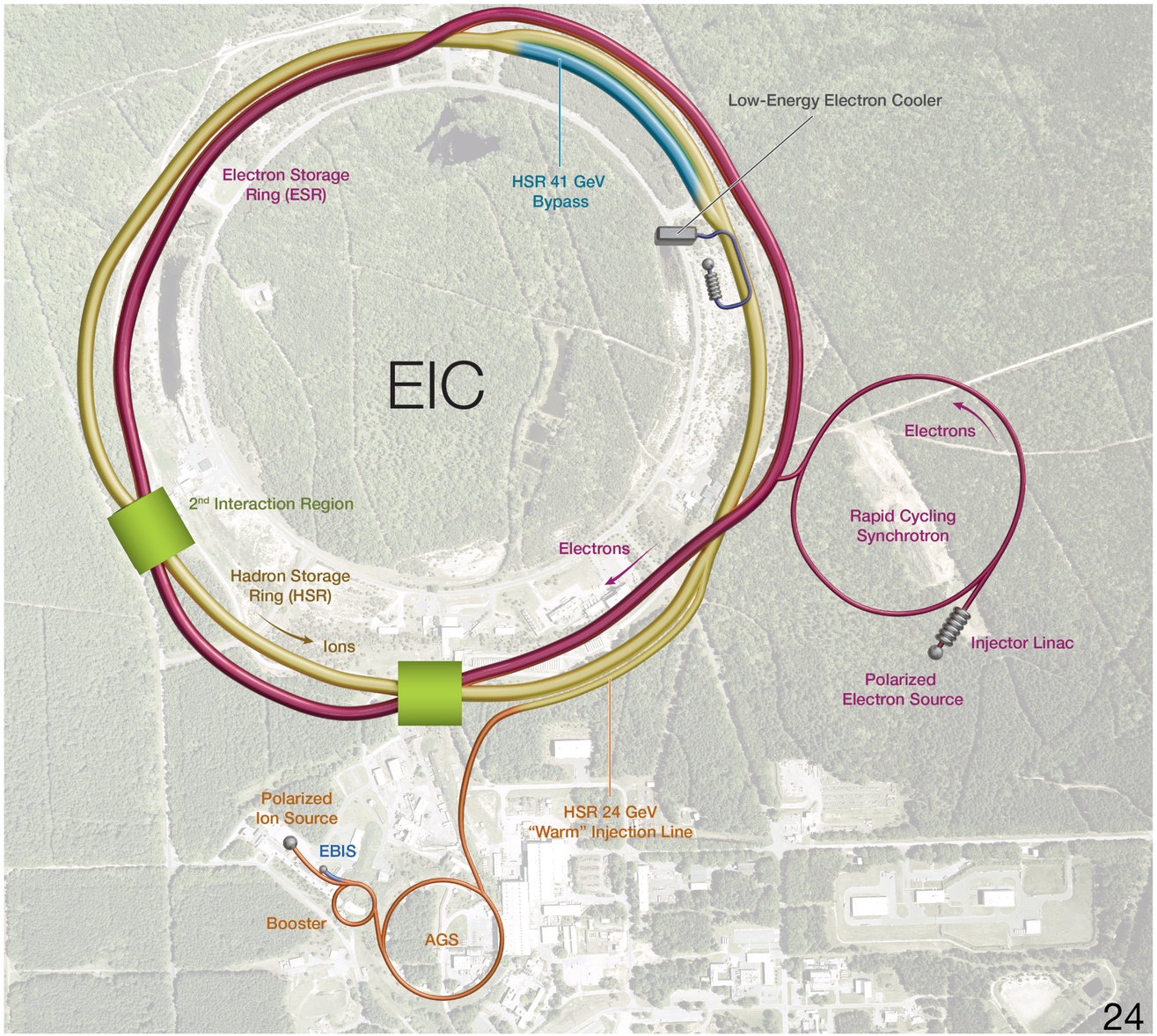

- Based on RHIC:
  - use exiting hadron storage ring
    energy: 41, 100–275 GeV
  - add electron storage ring in RHIC tunnel
    energy: 5–10 GeV

  $\rightarrow \sqrt{s} = 29 - 100$ GeV (140 GeV upgradable)

- $\vec{e} + \vec{p}^{\uparrow}, \overrightarrow{He}^{\uparrow}$

  ~ 70% polarisation

  + heavier, unpolarised ions, up to Uranium

- $\mathscr{L} = 10^{33-34}\,\mathrm{cm}^{-2}\,\mathrm{s}^{-1}$

  $\leftrightarrow \mathscr{L}_{\mathrm{int}} = 10 - 100\,\mathrm{fb}^{-1}/\mathrm{year}$

Future: the electron-ion collider (EIC)

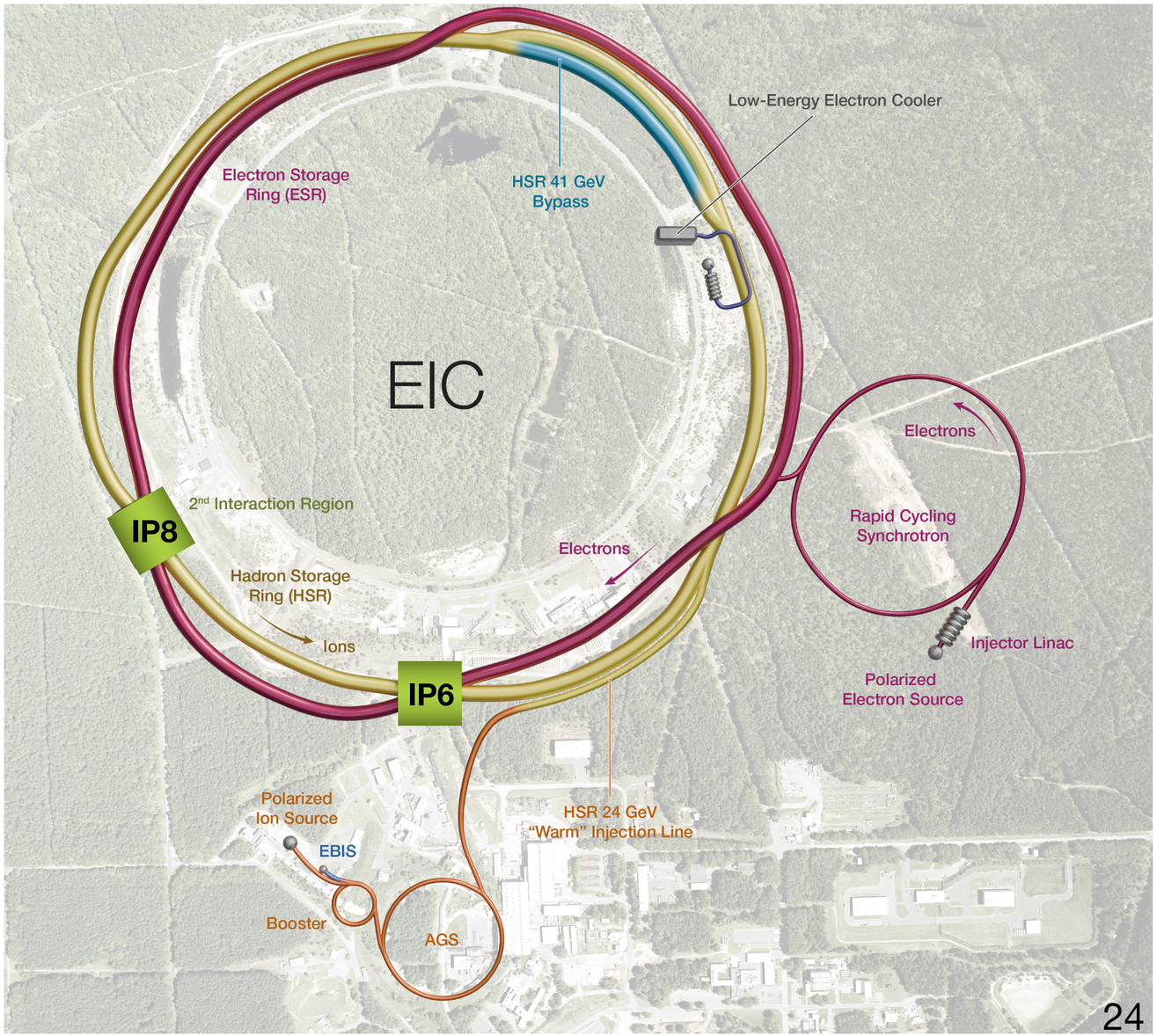

- Based on RHIC:
  - use exiting hadron storage ring
    energy: 41, 100–275 GeV
  - add electron storage ring in RHIC tunnel
    energy: 5–10 GeV

  $\rightarrow \sqrt{s} = 29 - 100$ GeV (140 GeV upgradable)

- $\vec{e} + \vec{p}^{\uparrow}, \overrightarrow{He}^{\uparrow}$

  ~ 70% polarisation

  + heavier, unpolarised ions, up to Uranium

- $\mathscr{L} = 10^{33-34}\,\mathrm{cm}^{-2}\,\mathrm{s}^{-1}$

  $\leftrightarrow \mathscr{L}_{\mathrm{int}} = 10 - 100\,\mathrm{fb}^{-1}/\mathrm{year}$

Future: the electron-ion collider (EIC)

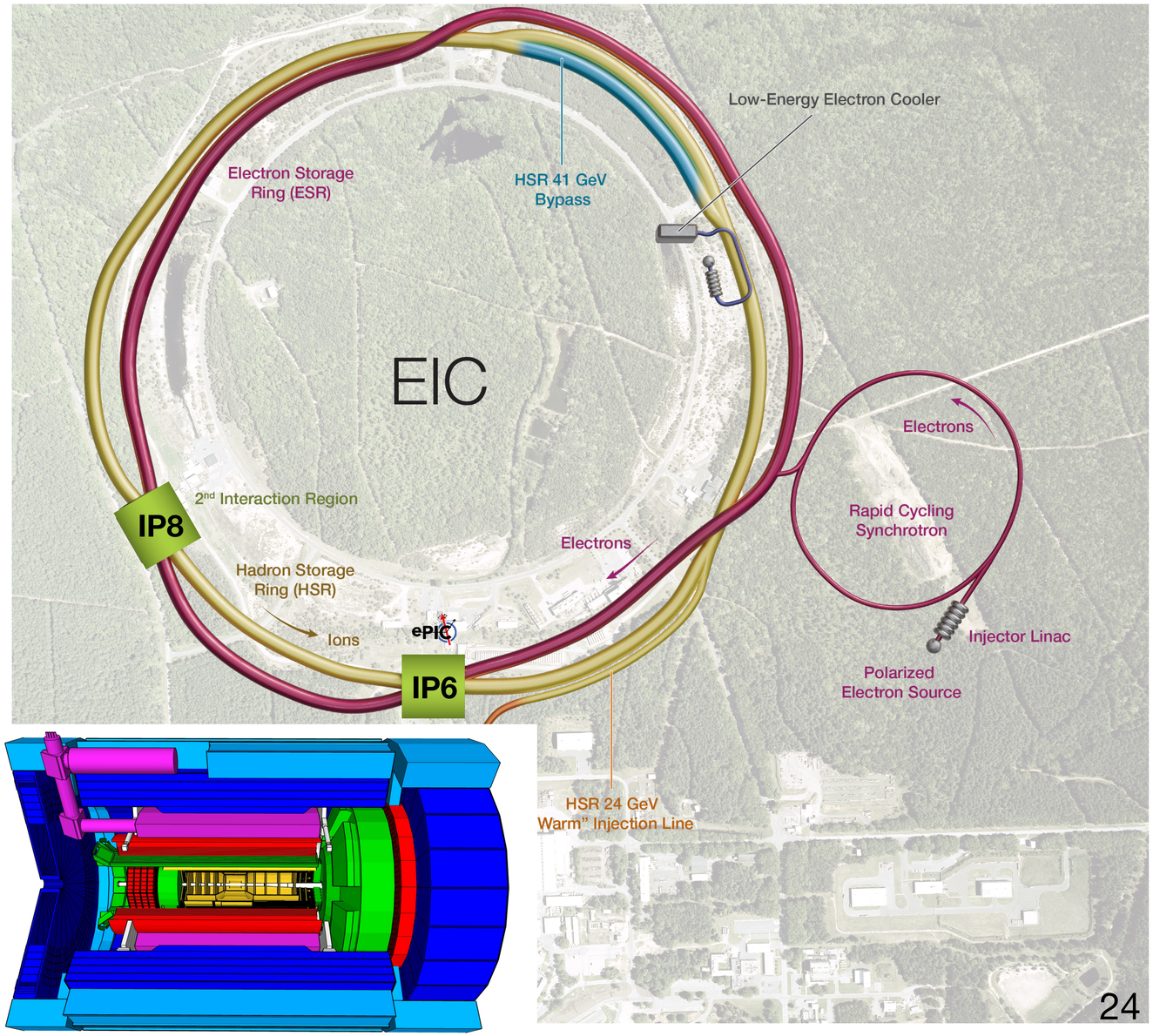

- Based on RHIC:
  - use exiting hadron storage ring
    energy: 41, 100–275 GeV
  - add electron storage ring in RHIC tunnel
    energy: 5–10 GeV

  $\rightarrow \sqrt{s} = 29 - 100$ GeV (140 GeV upgradable)

- $\vec{e} + \vec{p}^{\uparrow}, \overrightarrow{He}^{\uparrow}$

  ~ 70% polarisation

  + heavier, unpolarised ions, up to Uranium

- $\mathscr{L} = 10^{33-34}\,\mathrm{cm}^{-2}\,\mathrm{s}^{-1}$

  $\leftrightarrow \mathscr{L}_{\mathrm{int}} = 10 - 100\,\mathrm{fb}^{-1}/\mathrm{year}$

The various data-collection stages

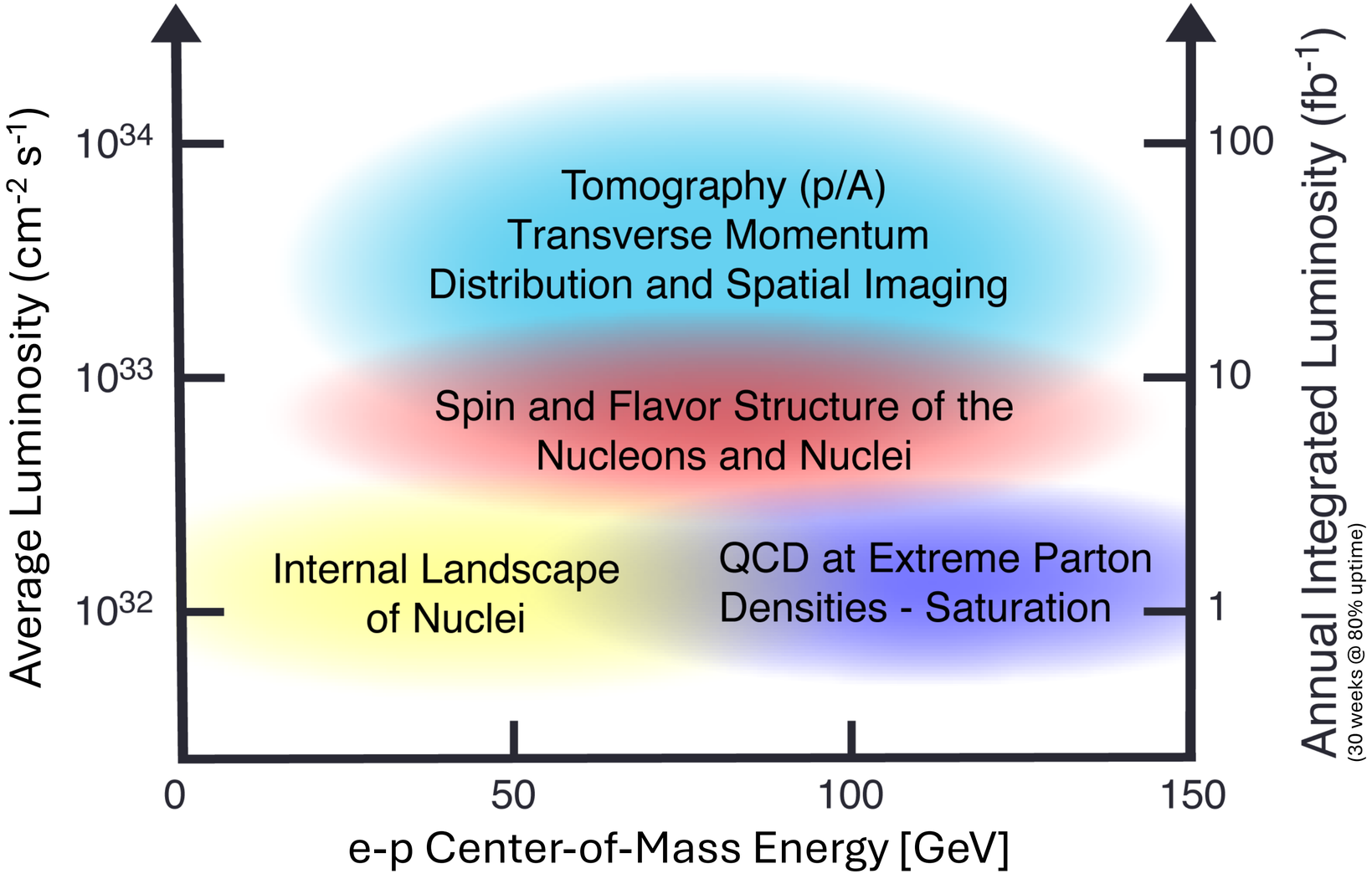

The various data-collection stages

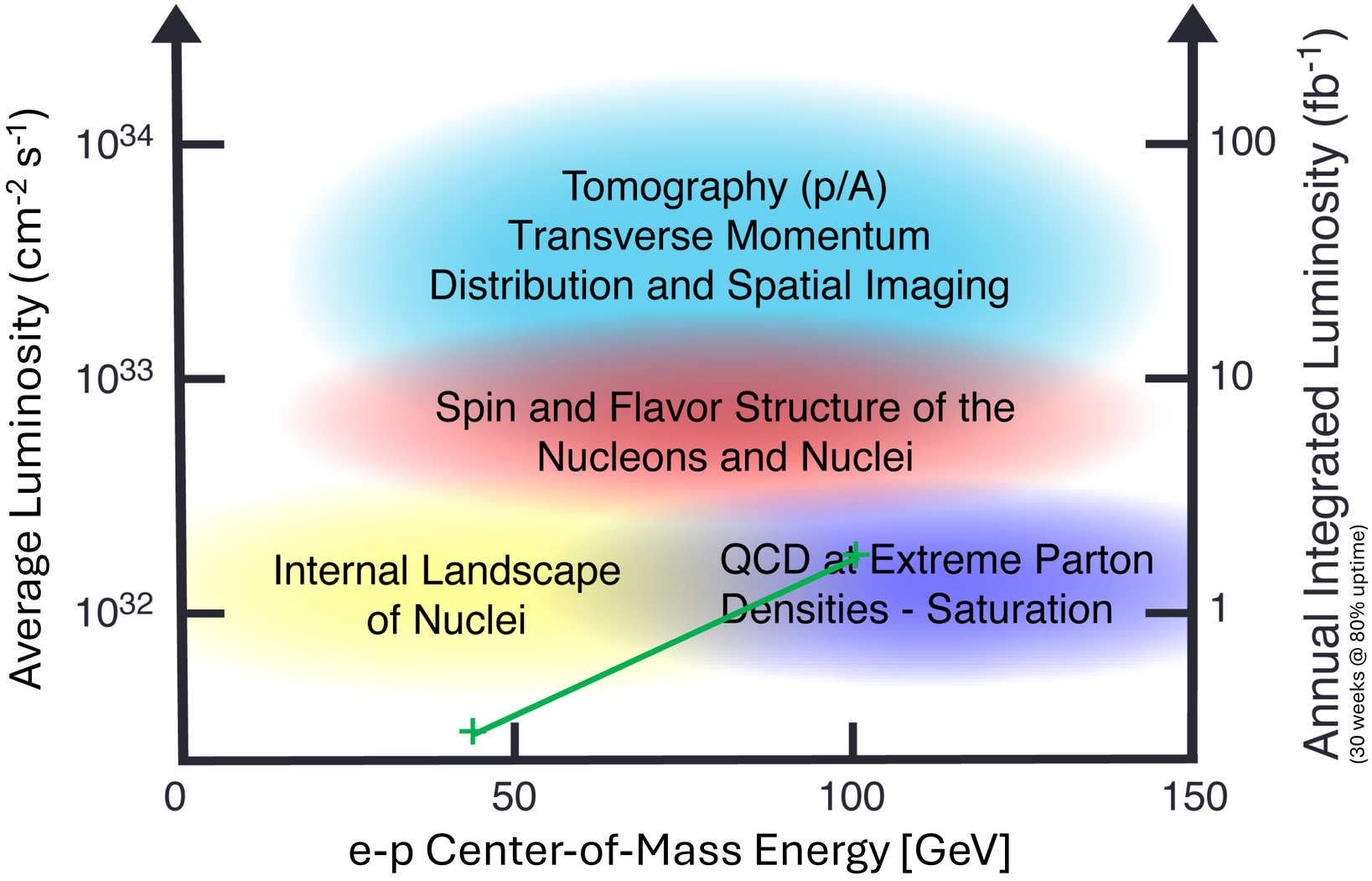

+ EIC
  - SRF for 7nC/bunch
  - no 394 MHz crab cavities
  - no low energy cooling
  - no 41 GeV bypass

The various data-collection stages

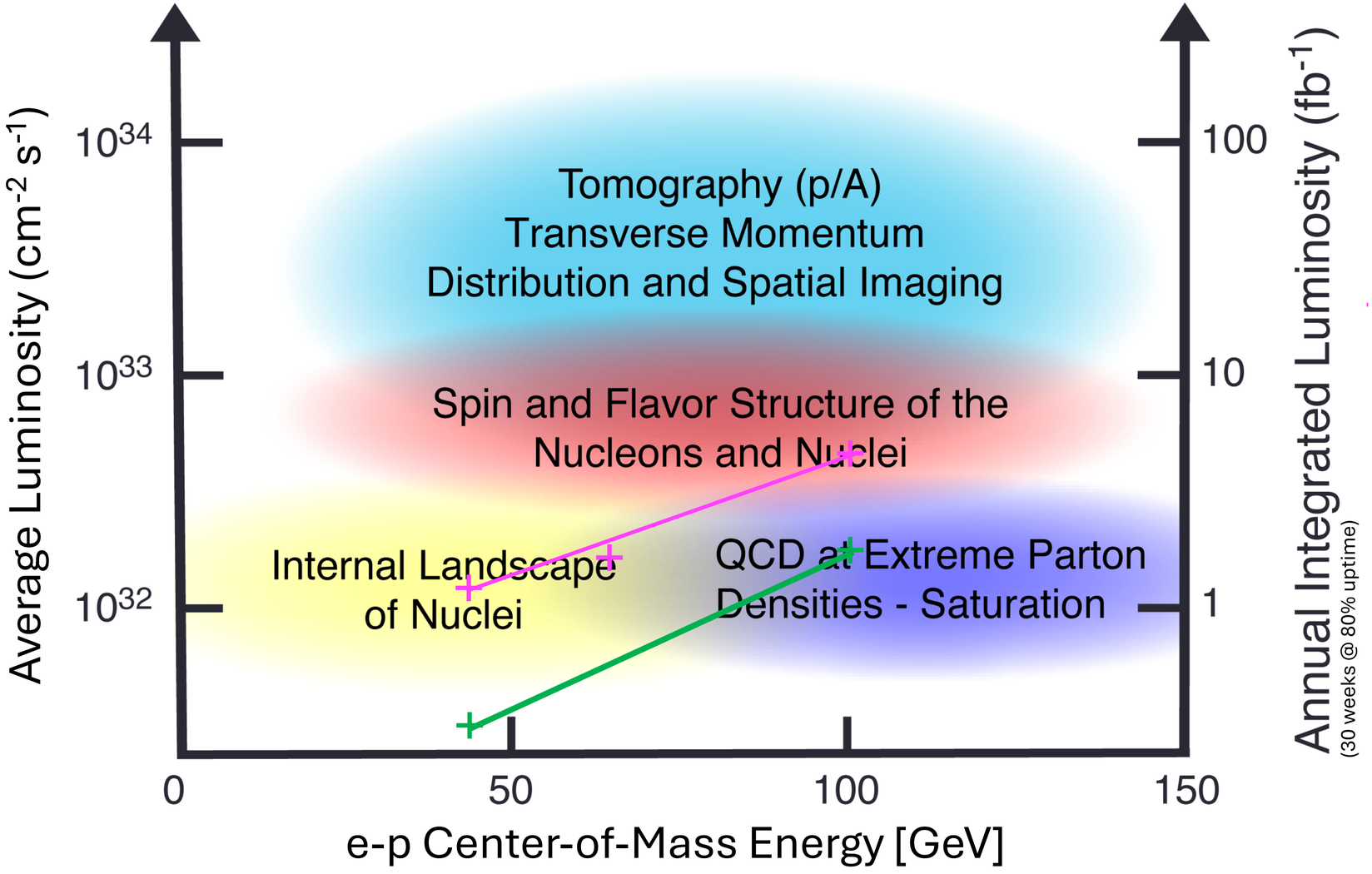

+ EIC
  - SRF for 7nC/bunch
  - no 394 MHz crab cavities
  - no 41 GeV bypass

+ EIC
  - SRF for 7nC/bunch
  - no 394 MHz crab cavities
  - no low energy cooling
  - no 41 GeV bypass

The various data-collection stages

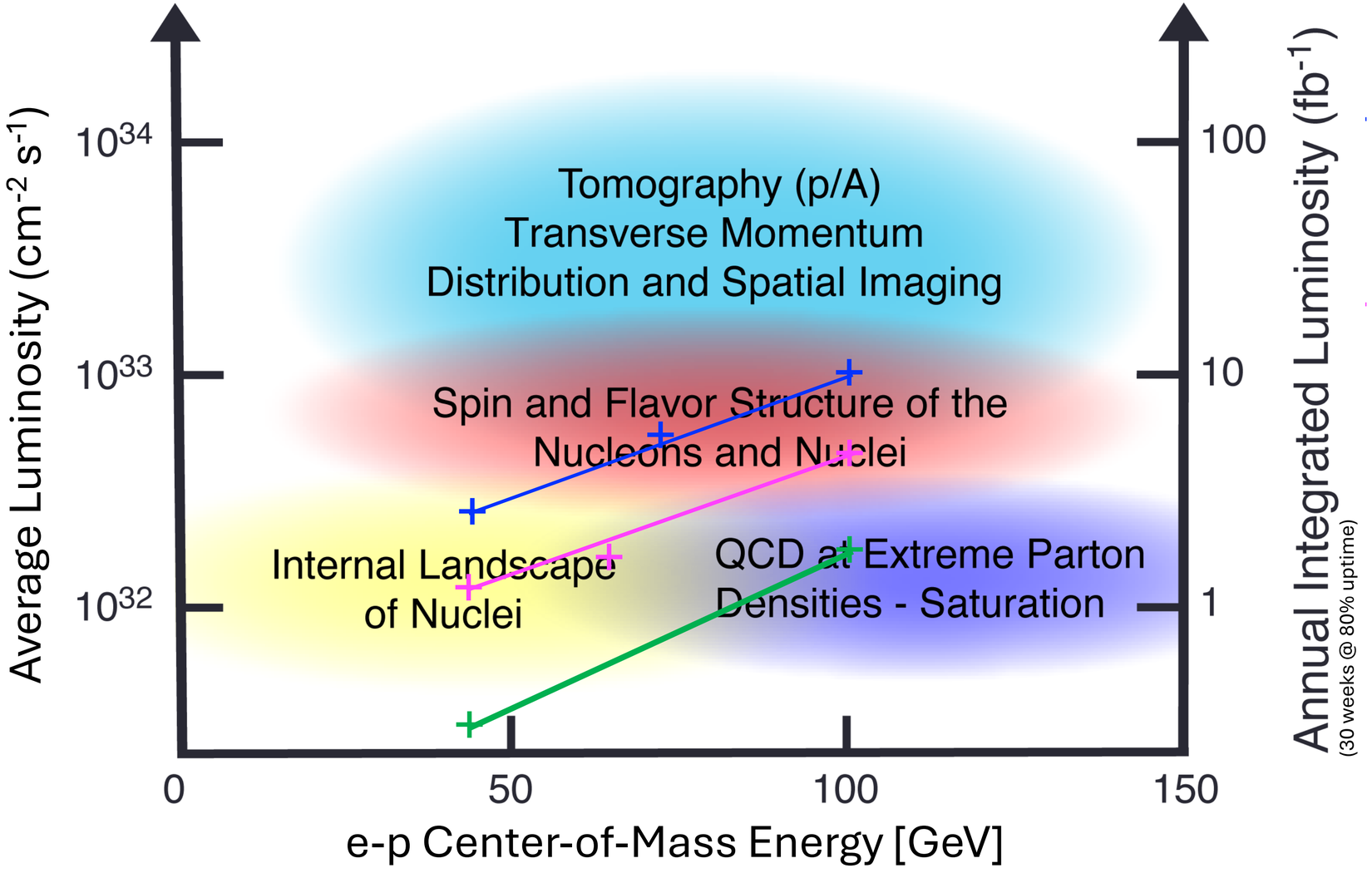

+ EIC
  - SRF for 7nC/bunch
  - no 41 GeV bypass

+ EIC
  - SRF for 7nC/bunch
  - no 394 MHz crab cavities
  - no 41 GeV bypass

+ EIC
  - SRF for 7nC/bunch
  - no 394 MHz crab cavities
  - no low energy cooling
  - no 41 GeV bypass

The various data-collection stages

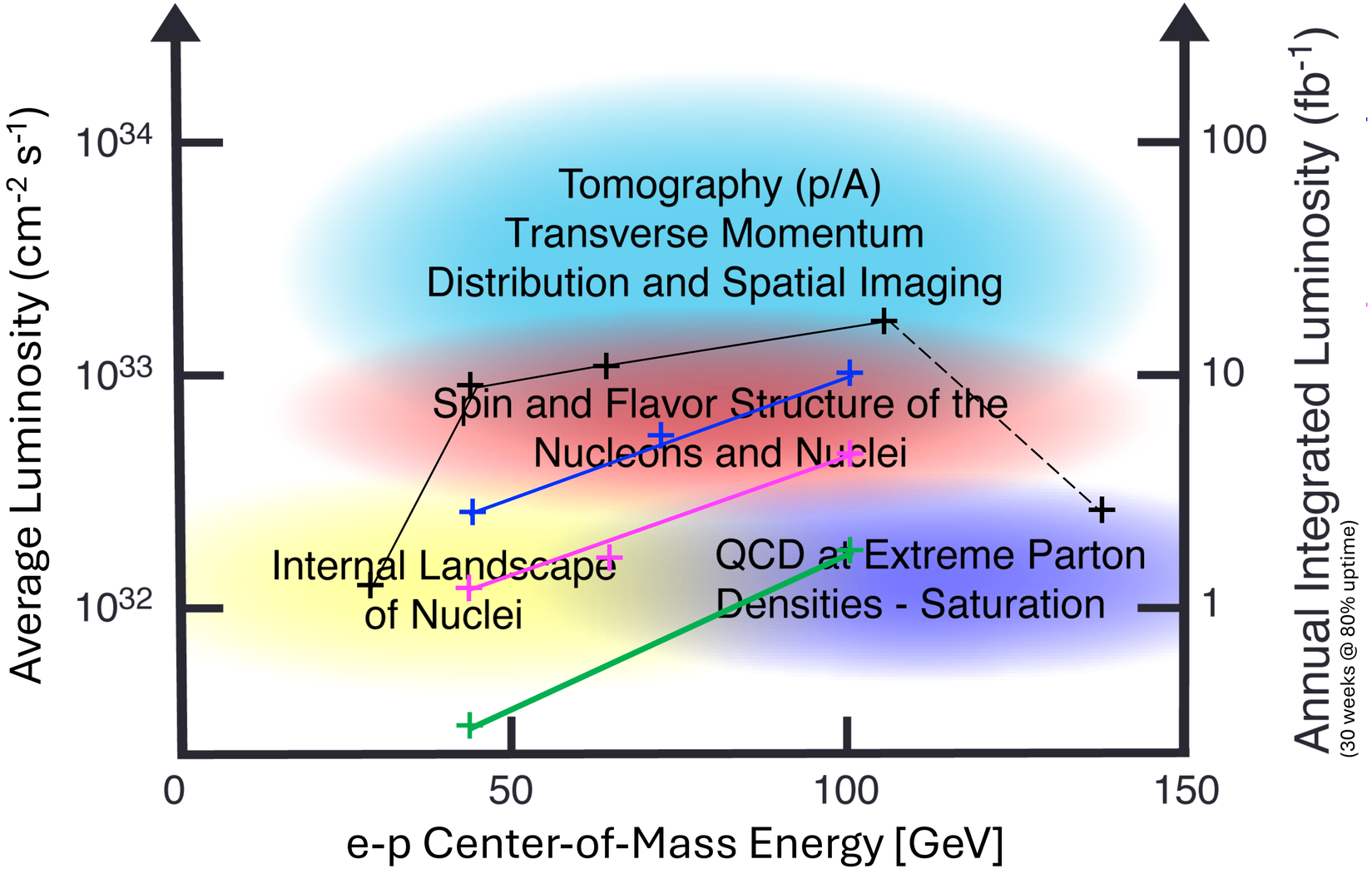

+ EIC Full Capability
  - - - 140 GeV (upgrade)

+ EIC
  - SRF for 7nC/bunch
  - no 41 GeV bypass

+ EIC
  - SRF for 7nC/bunch
  - no 394 MHz crab cavities
  - no 41 GeV bypass

+ EIC
  - SRF for 7nC/bunch
  - no 394 MHz crab cavities
  - no low energy cooling
  - no 41 GeV bypass

Luminosity and centre-of-mass energy: ep collisions

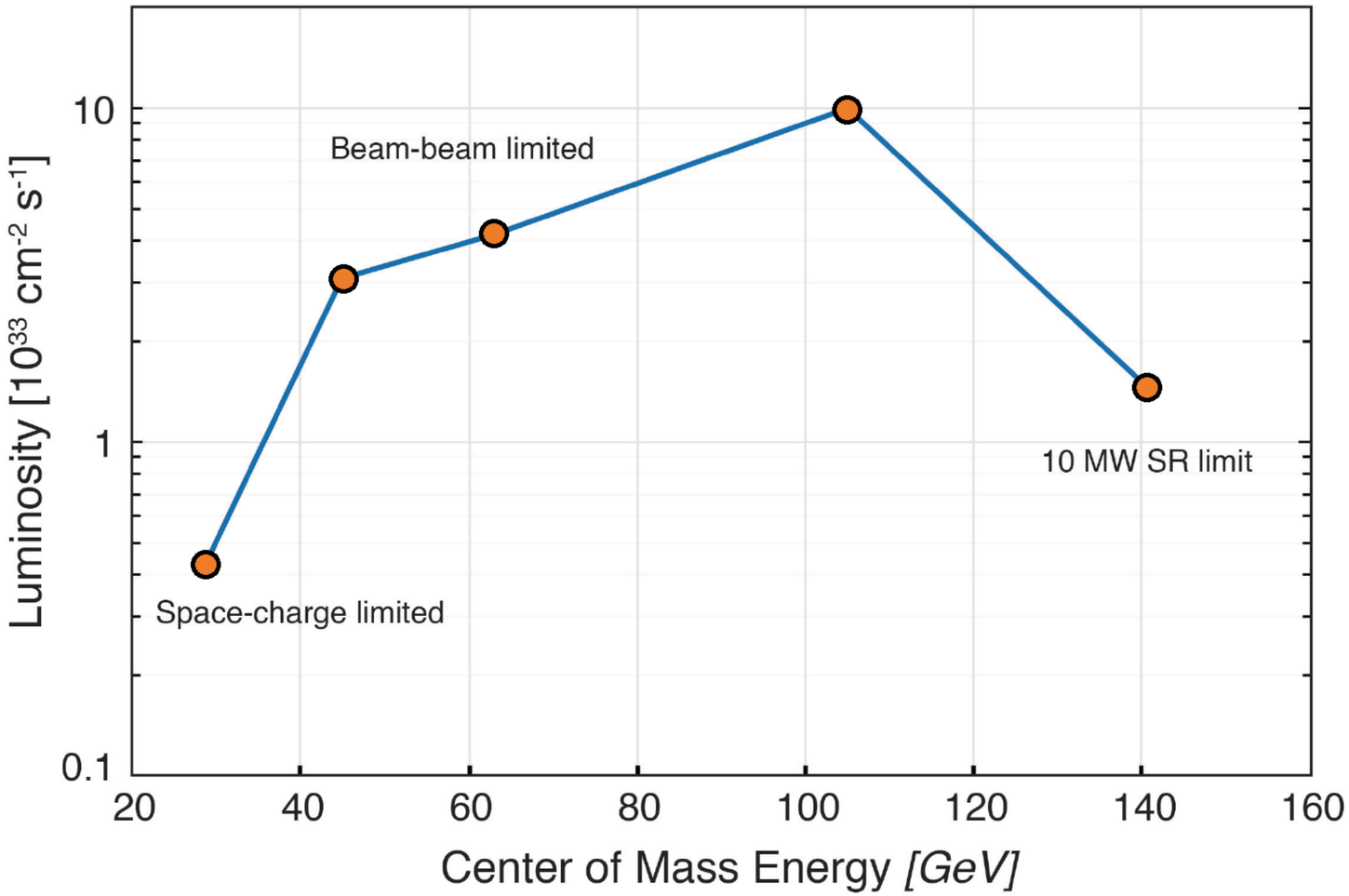

Luminosity for eA similar within factor 2–3

The electron-proton/ion collider (ePIC) detector

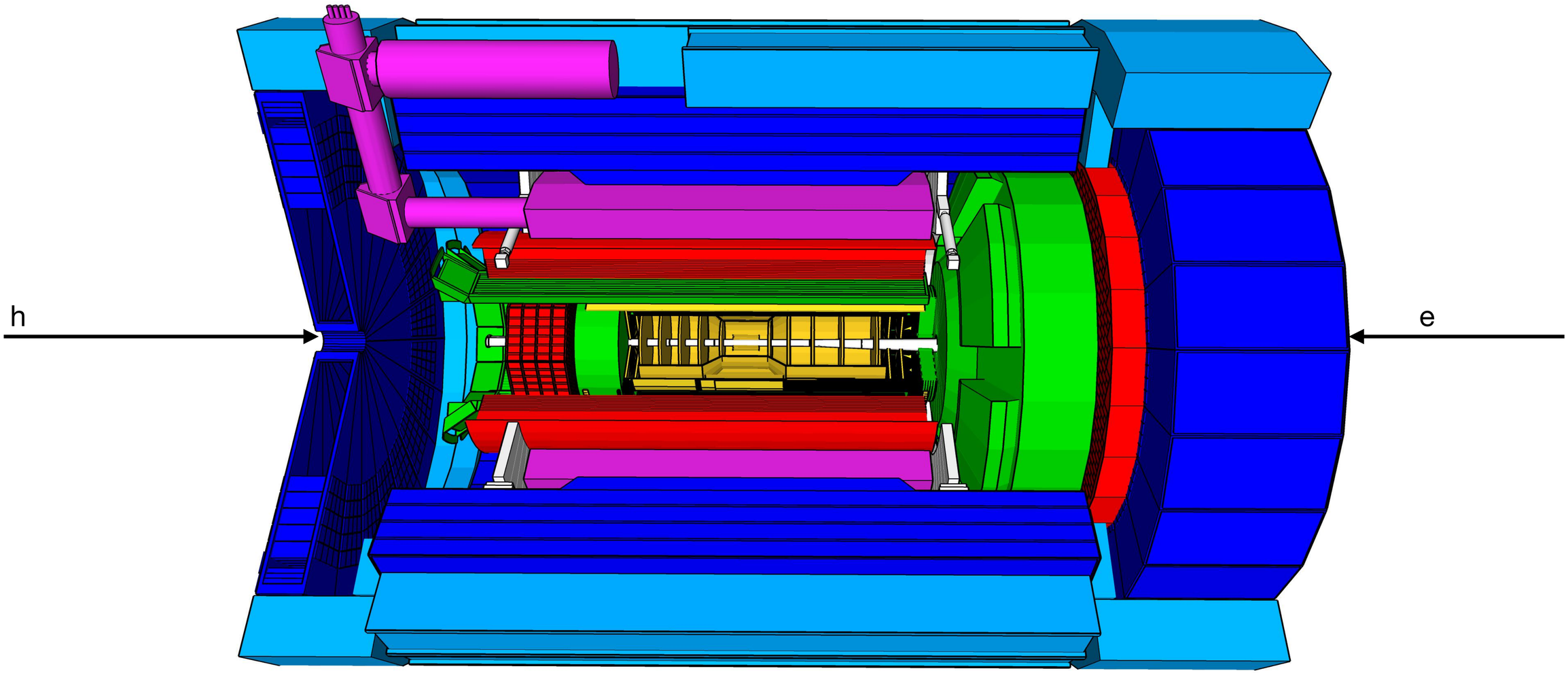

The electron-proton/ion collider (ePIC) detector

hermetic coverage:
$0^o \leq \phi \leq 360^o$
$2^o \leq \theta \leq 178^o \iff -4 < \eta < 4$

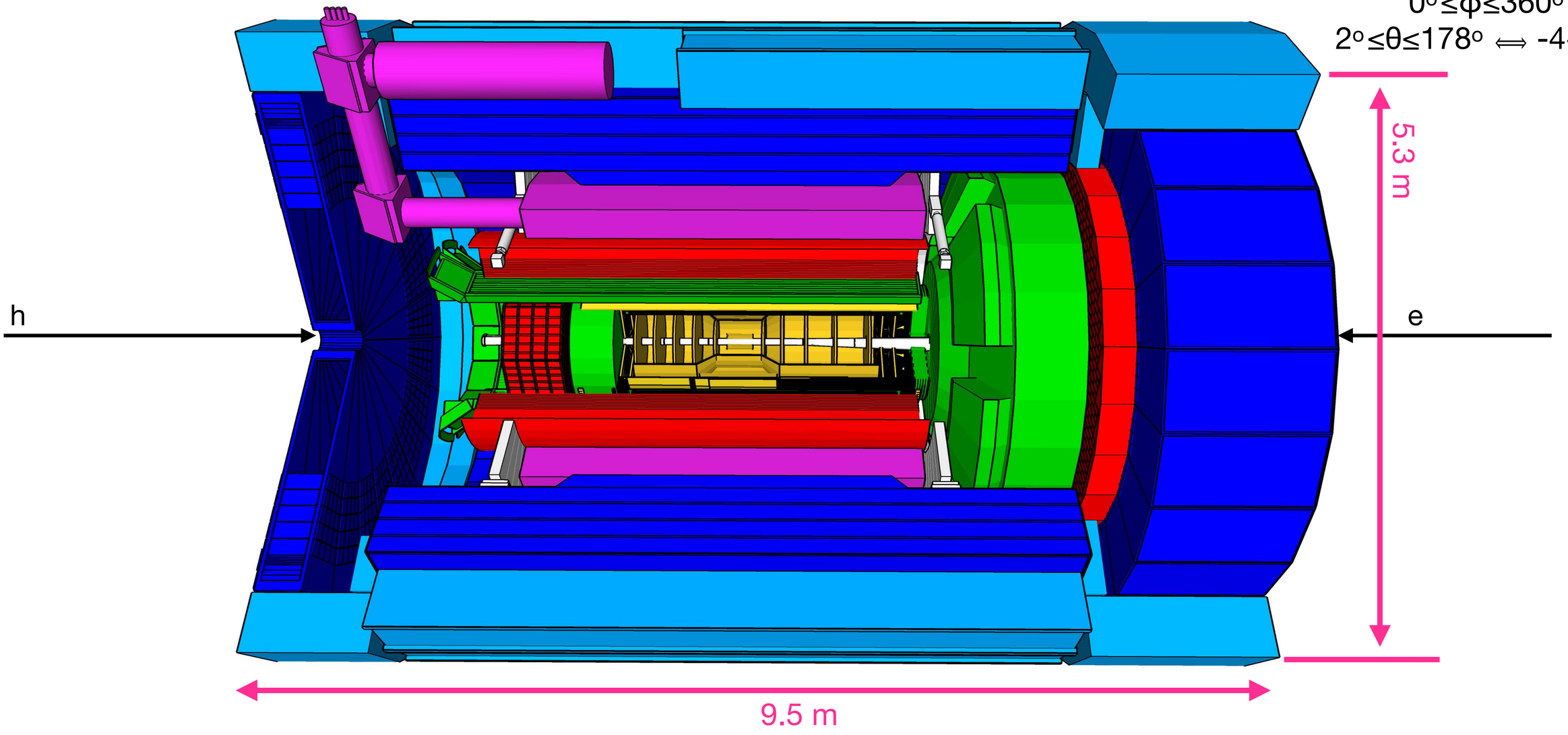

The electron-proton/ion collider (ePIC) detector

hermetic coverage:
$0^o \leq \phi \leq 360^o$
$2^o \leq \theta \leq 178^o \iff -4 < \eta < 4$

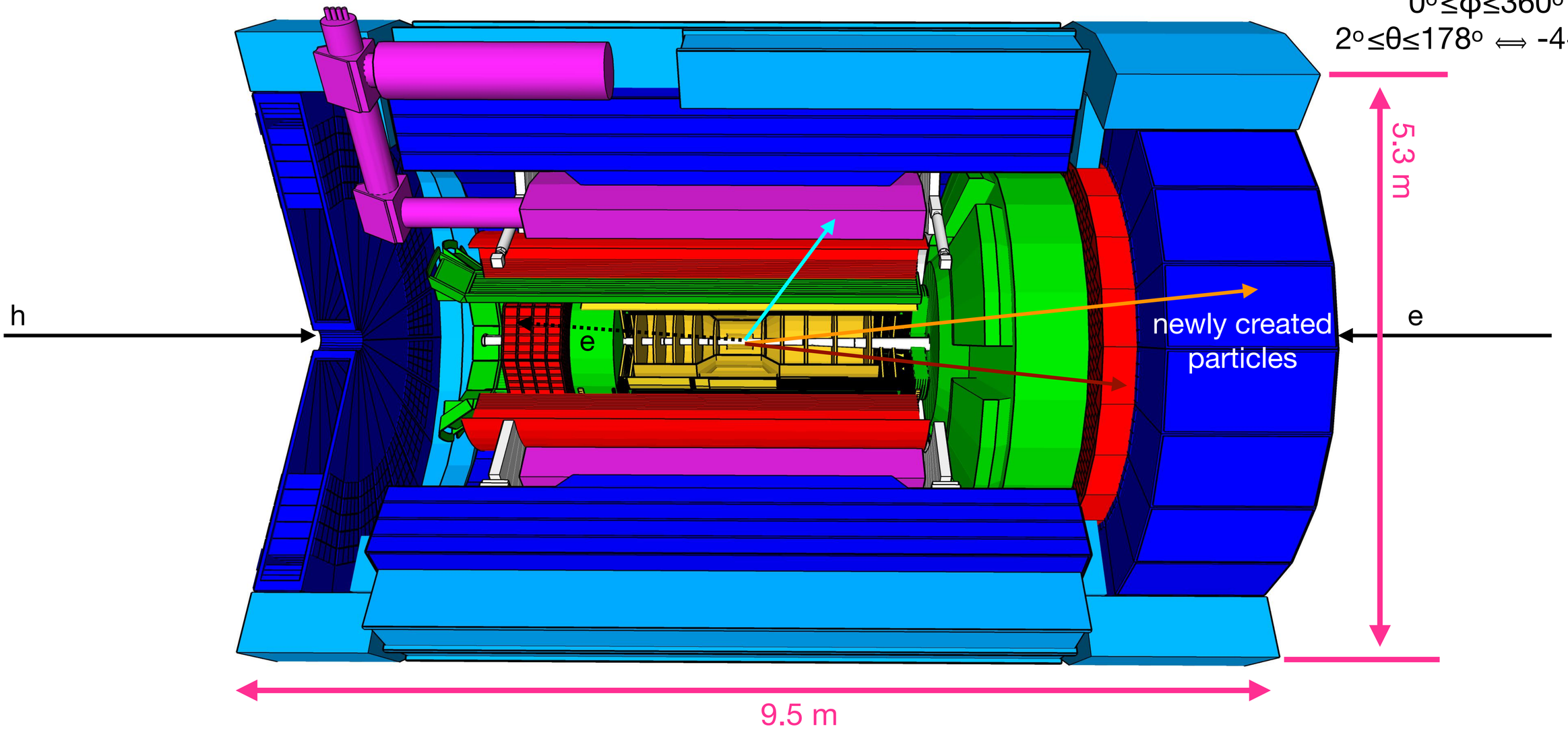

The electron-proton/ion collider (ePIC) detector

- **Tracking**
- **PID**
- **Electromagnetic calorimeter**
- **Hadronic calorimeter**

hermetic coverage:
$0^o \leq \phi \leq 360^o$
$2^o \leq \theta \leq 178^o \iff -4 < \eta < 4$

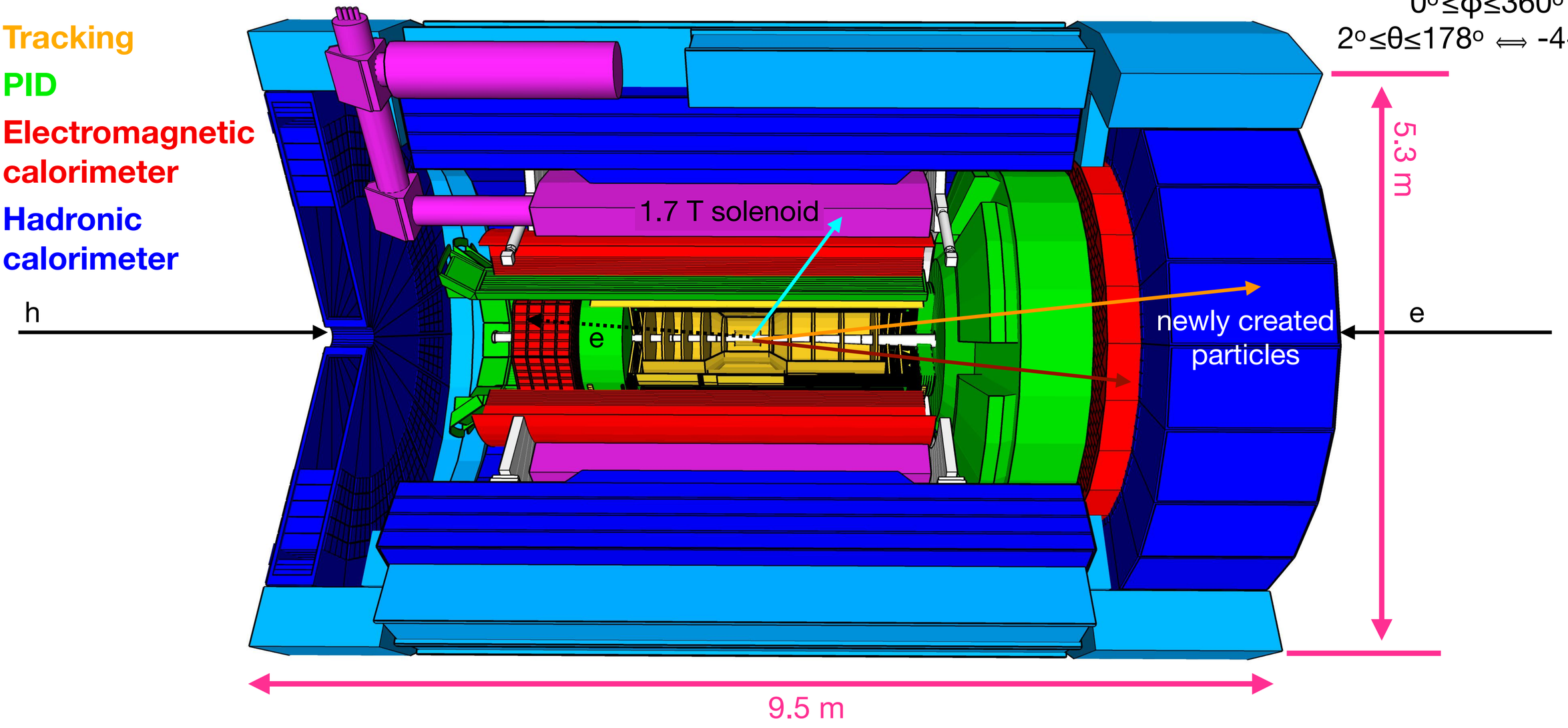

The electron-proton/ion collider (ePIC) detector

- **Tracking**
- **PID**
- **Electromagnetic calorimeter**
- **Hadronic calorimeter**

hermetic coverage:
$0^o \le \phi \le 360^o$
$2^o \le \theta \le 178^o \iff -4 < \eta < 4$

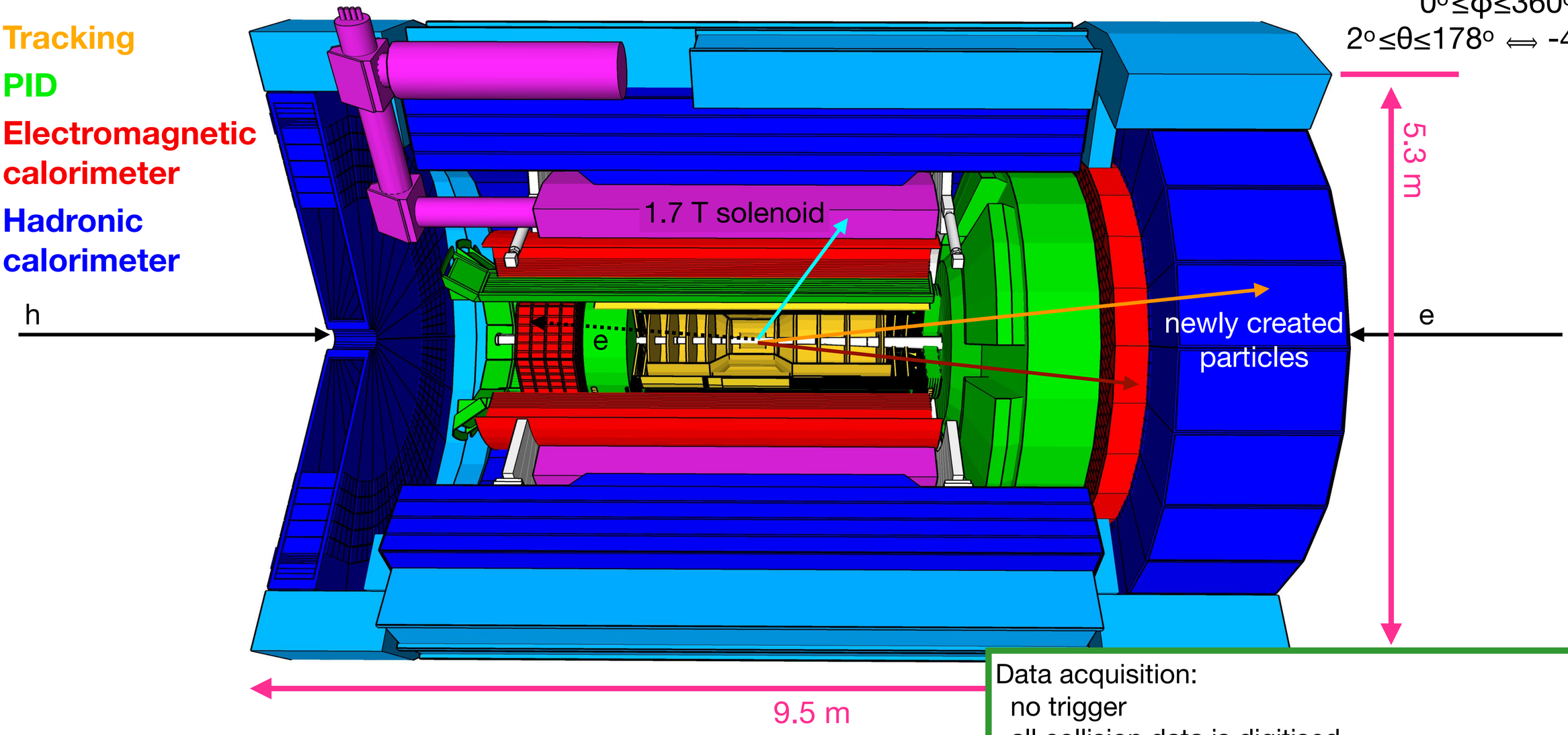

Data acquisition:
no trigger
all collision data is digitised
with strong zero-suppression at front-end electronics

Far backward/forward systems

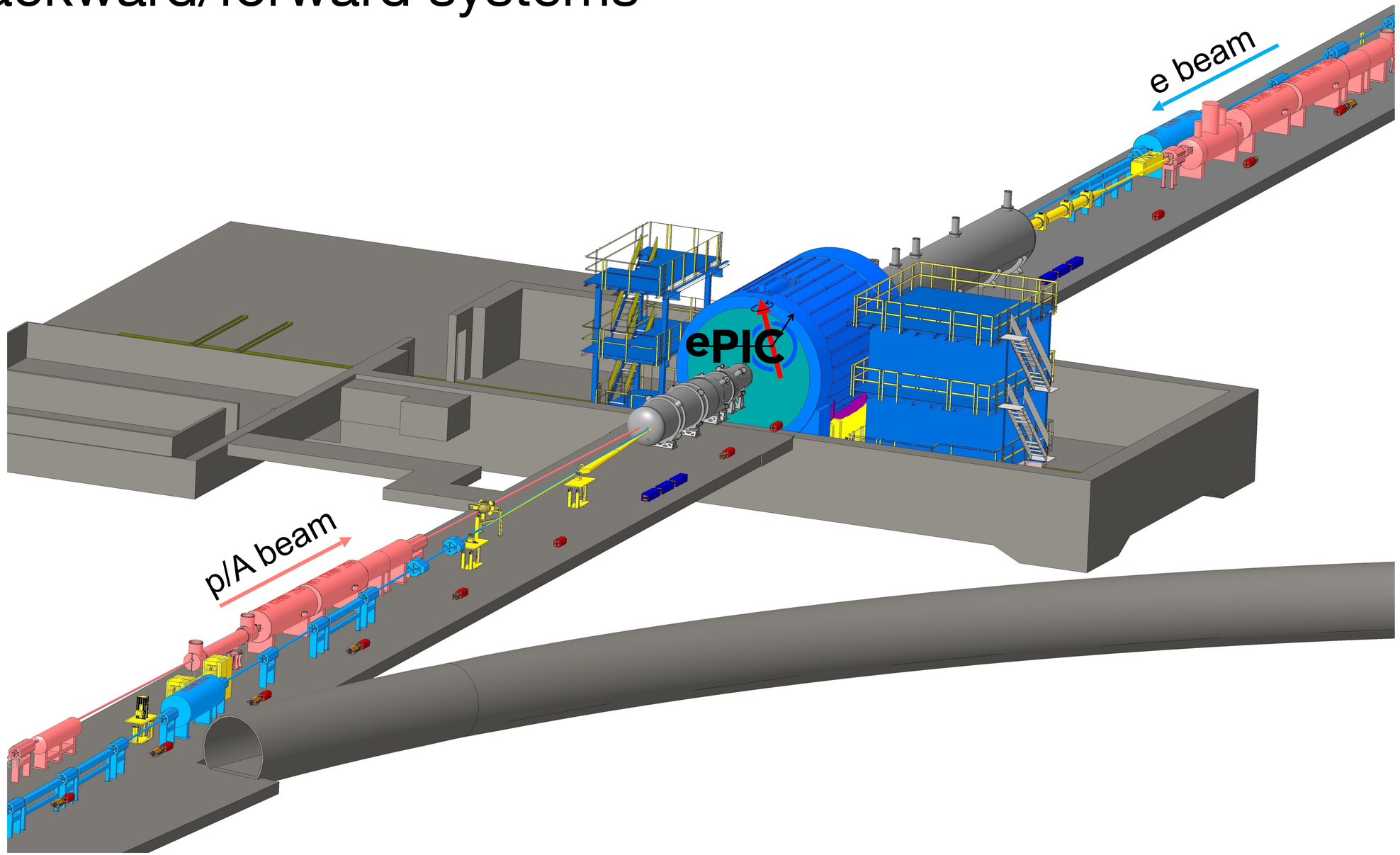

Far backward/forward systems

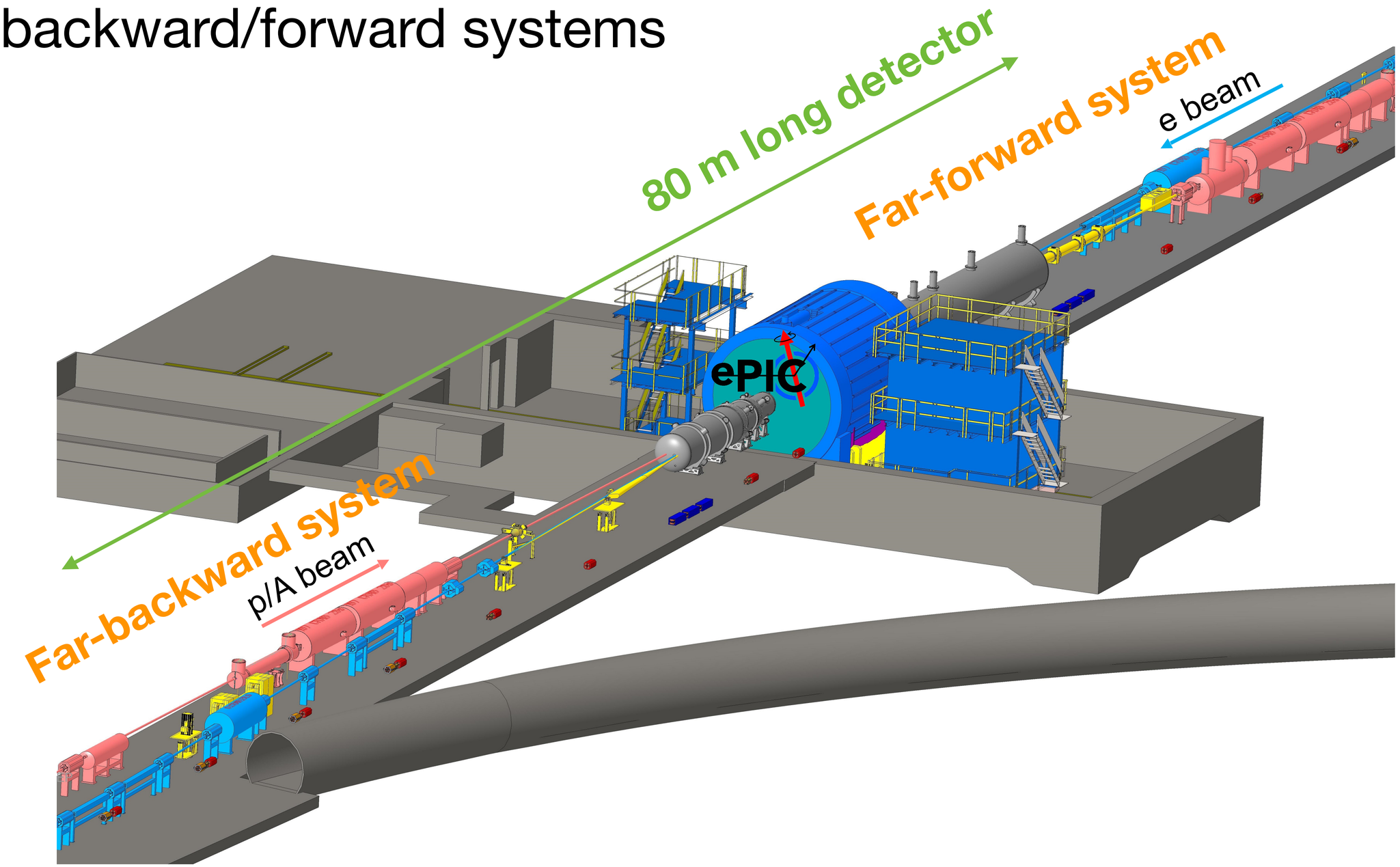

Far backward/forward systems

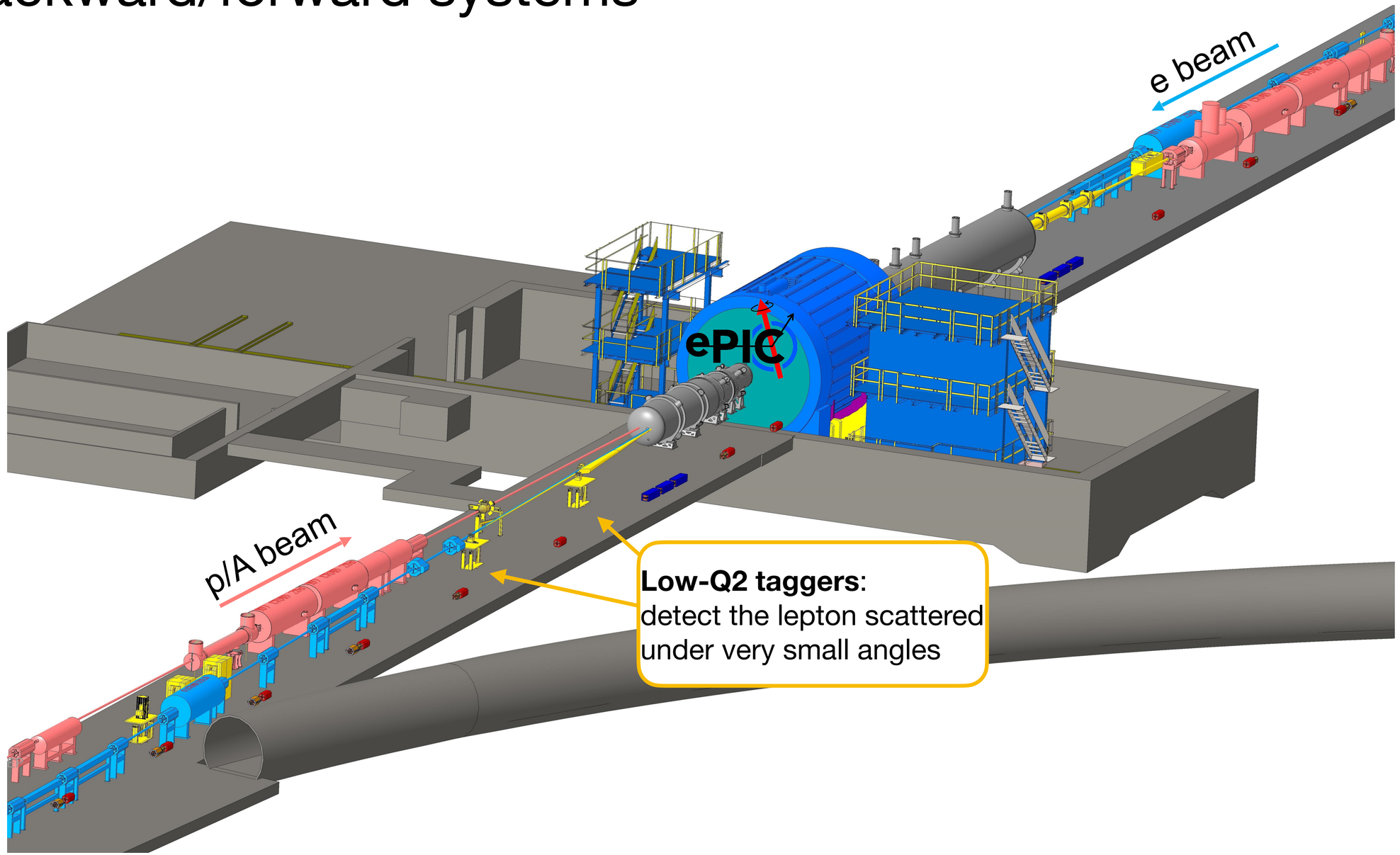

Far backward/forward systems

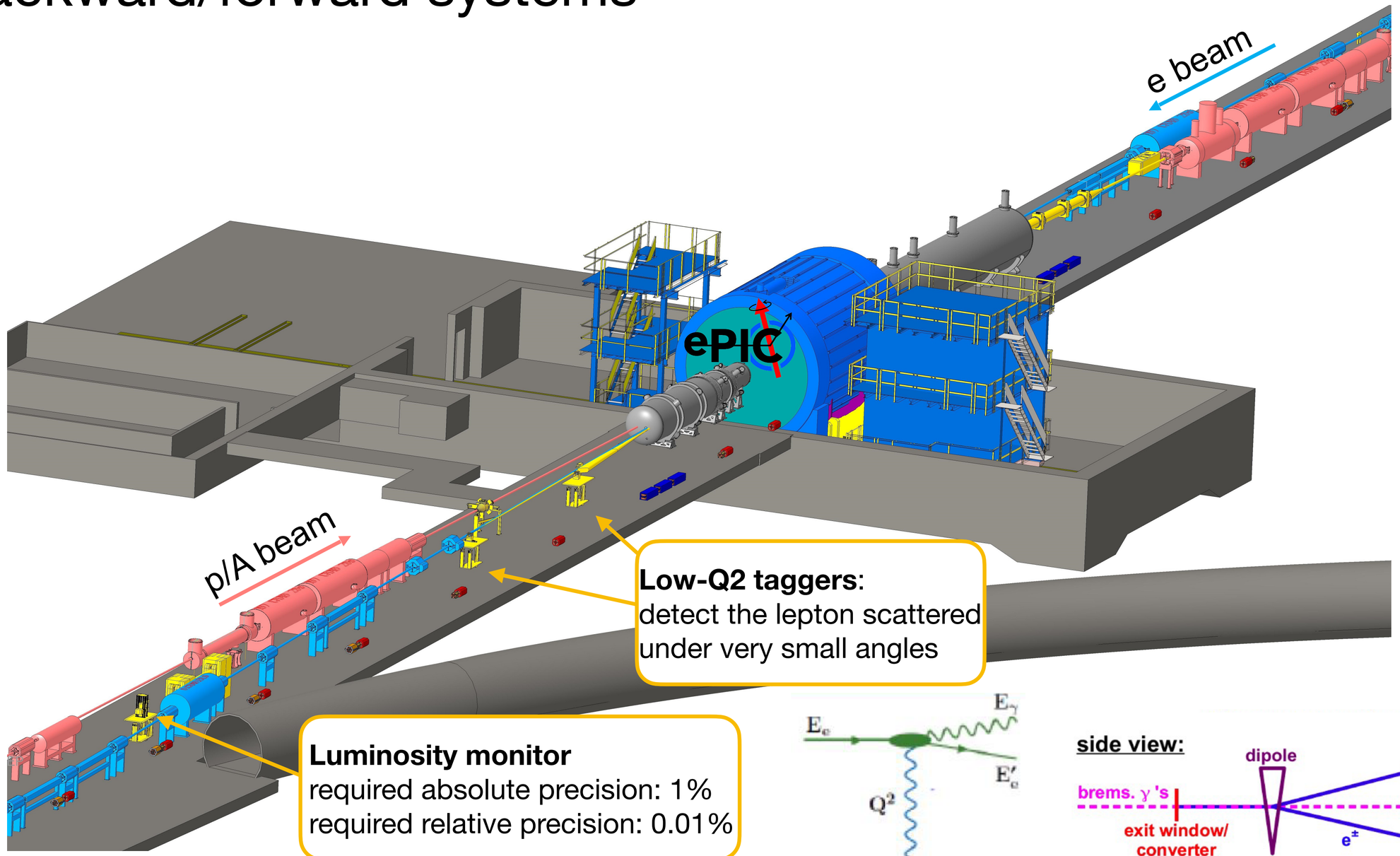

Low-Q2 taggers:
detect the lepton scattered under very small angles

Luminosity monitor
required absolute precision: 1%
required relative precision: 0.01%

Far backward/forward systems

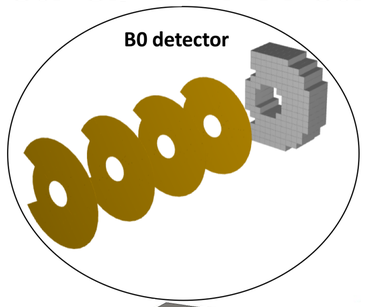

B0 system: trackers+electromagnetic calorimeters inside magnetic field to detect **protons and photons**

e beam

p/A beam

ePIC

Low-Q2 taggers:
detect the lepton scattered under very small angles

Luminosity monitor
required absolute precision: 1%
required relative precision: 0.01%

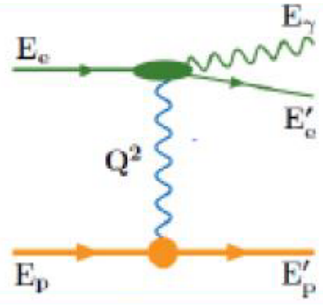

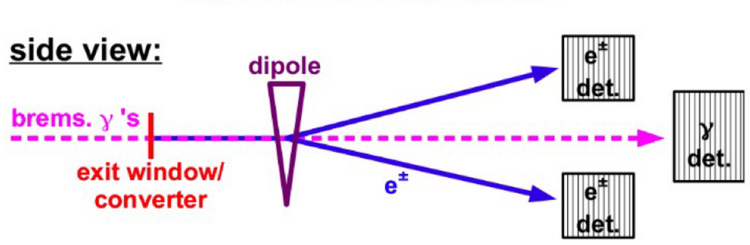

Far backward/forward systems

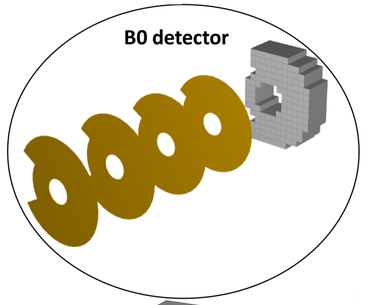

B0 system: trackers+electromagnetic calorimeters inside magnetic field to detect **protons and photons**

e beam

Roman pots and off-momentum detectors: reconstruct **far-forward protons** (and other charged particles+light ions)

ePIC

p/A beam

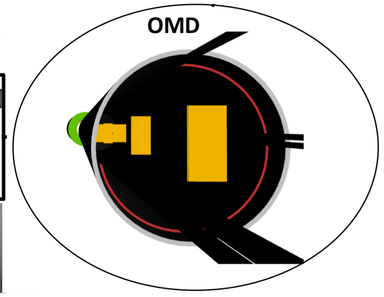

Low-Q2 taggers: detect the lepton scattered under very small angles

Luminosity monitor
required absolute precision: 1%
required relative precision: 0.01%

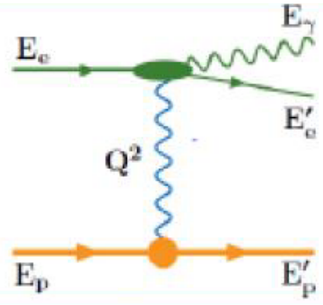

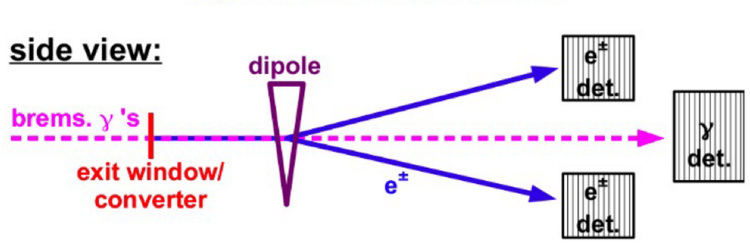

Far backward/forward systems

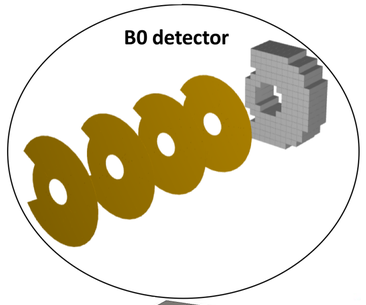

B0 system: trackers+electromagnetic calorimeters inside magnetic field to detect **protons and photons**

Zero-degree calorimeters: detection of **neutrons and photons**

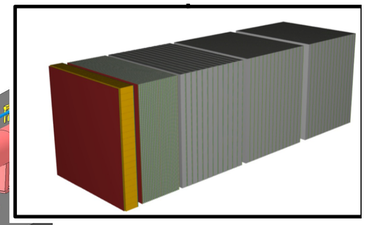

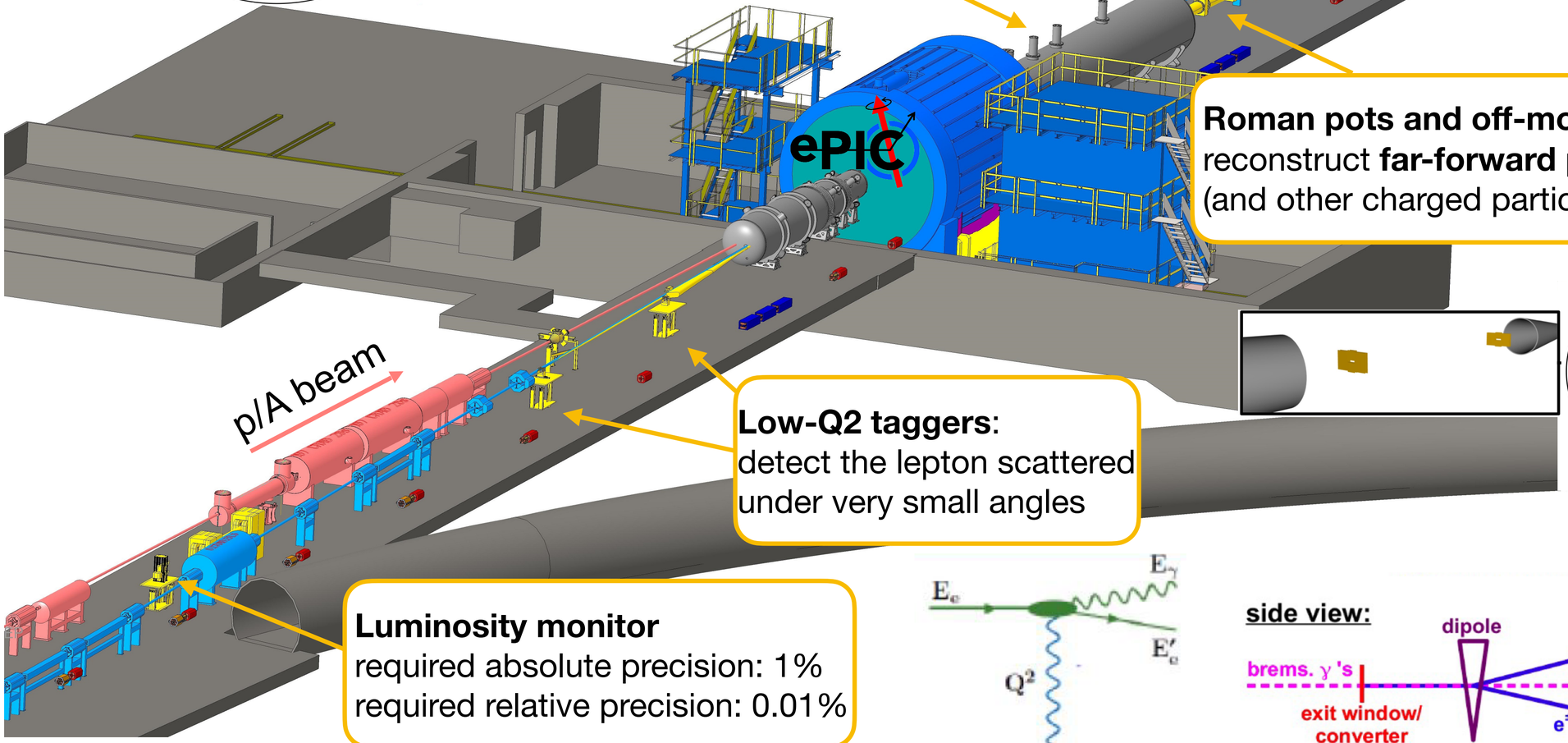

Roman pots and off-momentum detectors: reconstruct **far-forward protons** (and other charged particles+light ions)

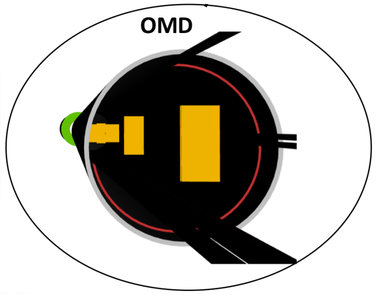

Low-Q2 taggers: detect the lepton scattered under very small angles

Luminosity monitor
required absolute precision: 1%
required relative precision: 0.01%

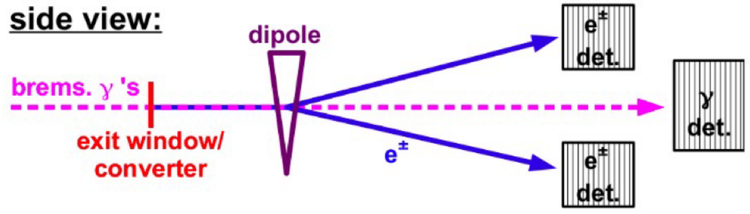

Timeline

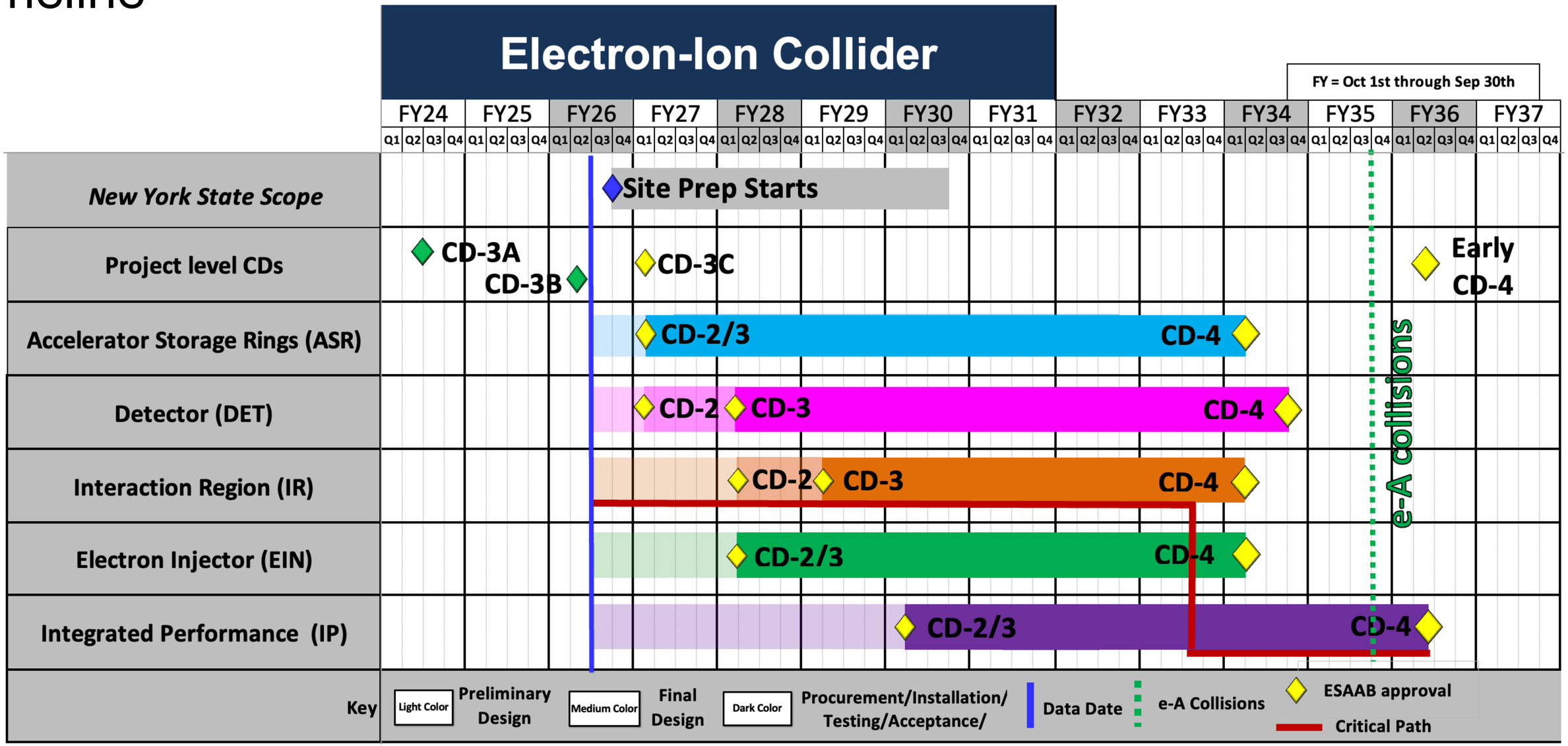
Electron-Ion Collider
FY = Oct 1st through Sep 30th
FY24 FY25 FY26 FY27 FY28 FY29 FY30 FY31 FY32 FY33 FY34 FY35 FY36 FY37
Q1 Q2 Q3 Q4
New York State Scope
Site Prep Starts
Project level CDs
CD-3A
CD-3B
CD-3C
Early CD-4
Accelerator Storage Rings (ASR)
CD-2/3
CD-4
Detector (DET)
CD-2
CD-3
CD-4
Interaction Region (IR)
CD-2
CD-3
CD-4
Electron Injector (EIN)
CD-2/3
CD-4
Integrated Performance (IP)
CD-2/3
CD-4
e-A collisions
Key
Light Color
Preliminary Design
Medium Color
Final Design
Dark Color
Procurement/Installation/ Testing/Acceptance/
Data Date
e-A Collisions
ESAAB approval
Critical Path

Kinematic coverage at the EIC

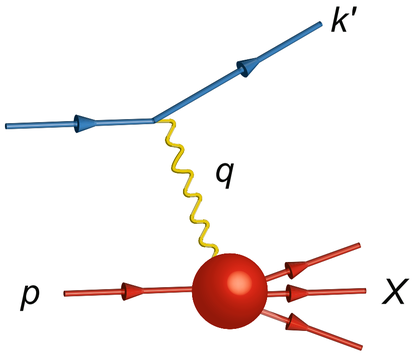

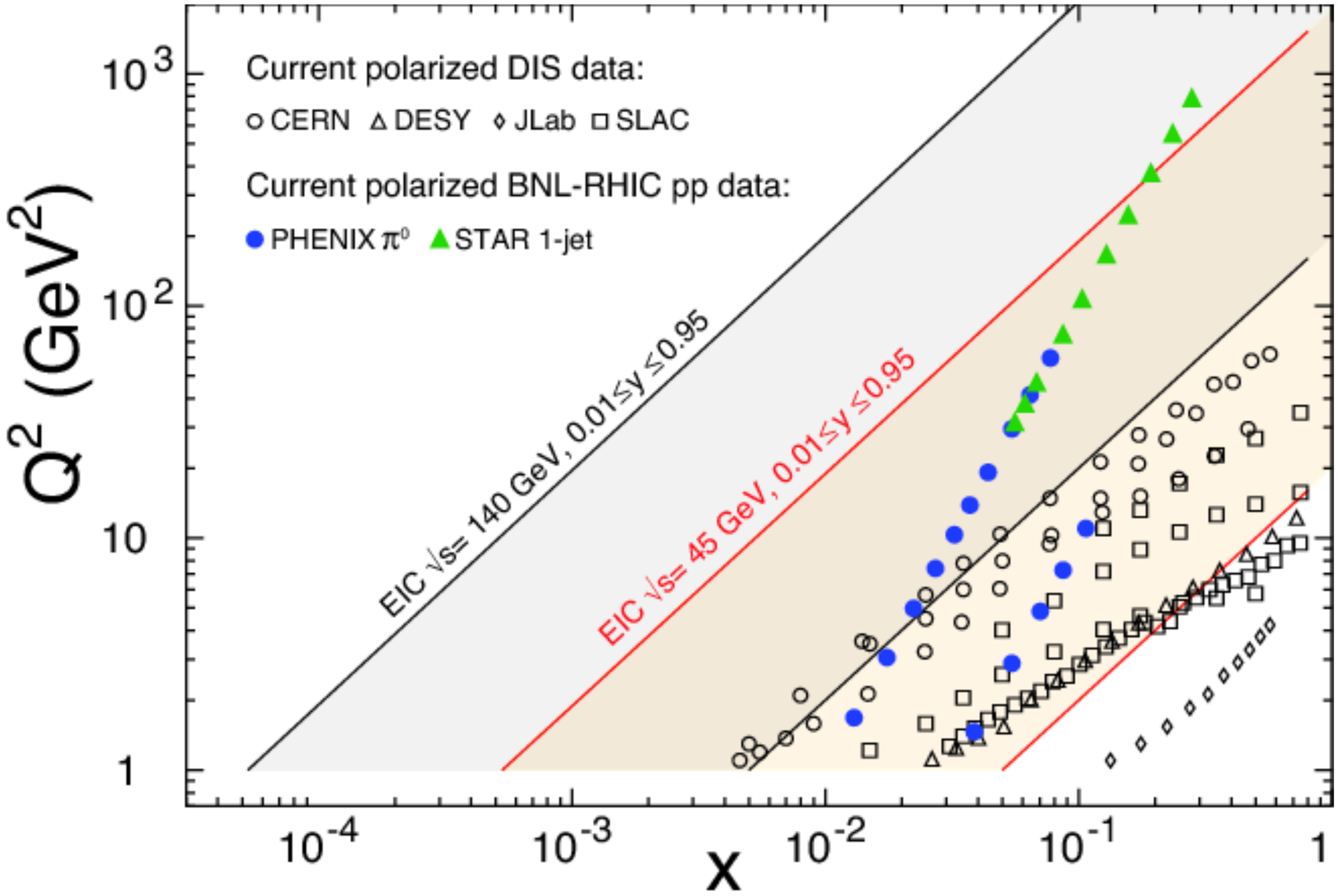

Gluon helicity distribution of the proton

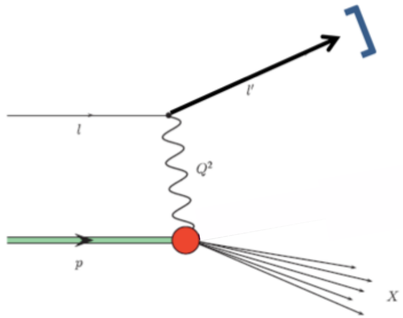

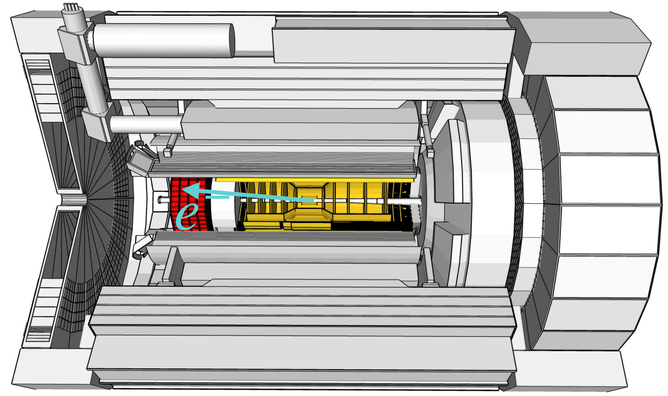

- High e^- purity needed:
  suppression of π contamination via EMCAL
- Precise track reconstruction needed:
  trackers and EMCAL

Gluon helicity distribution of the proton

g_1^p: world data

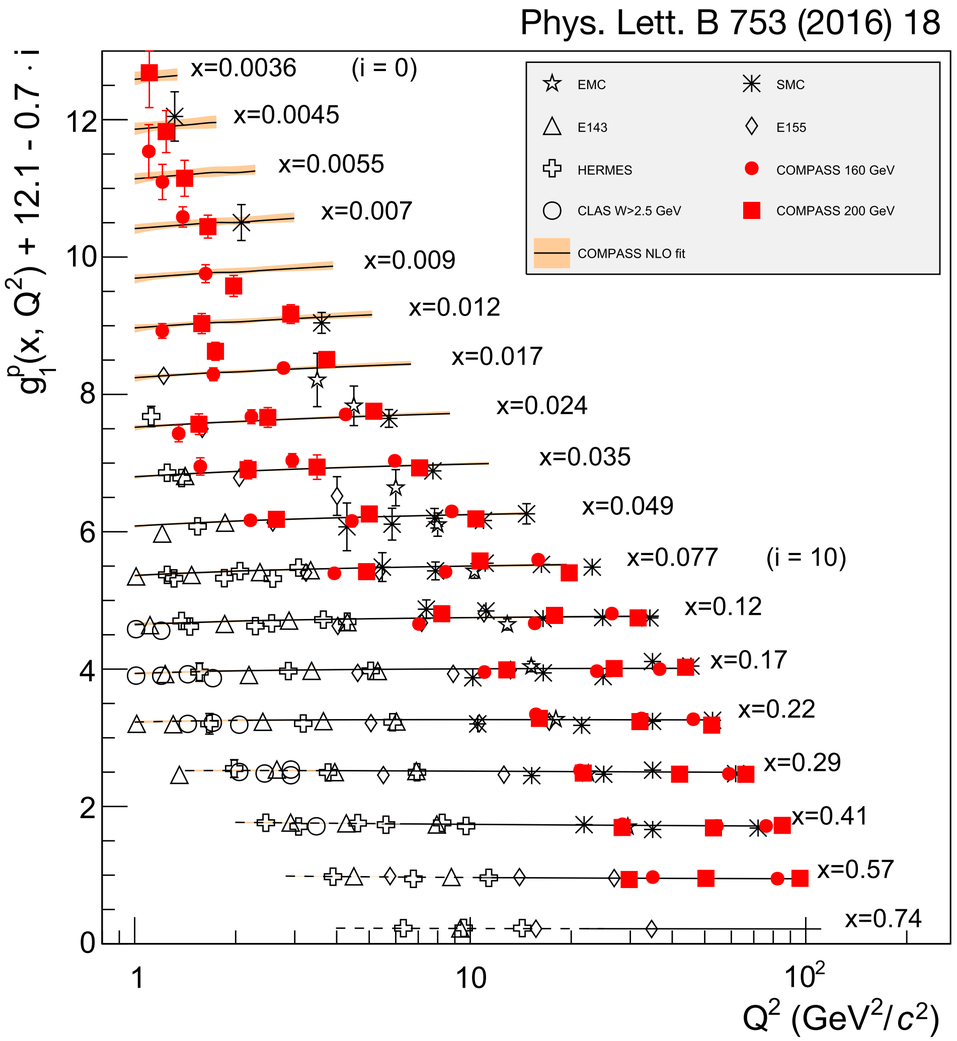

Gluon helicity distribution of the proton

g_1^p: world data

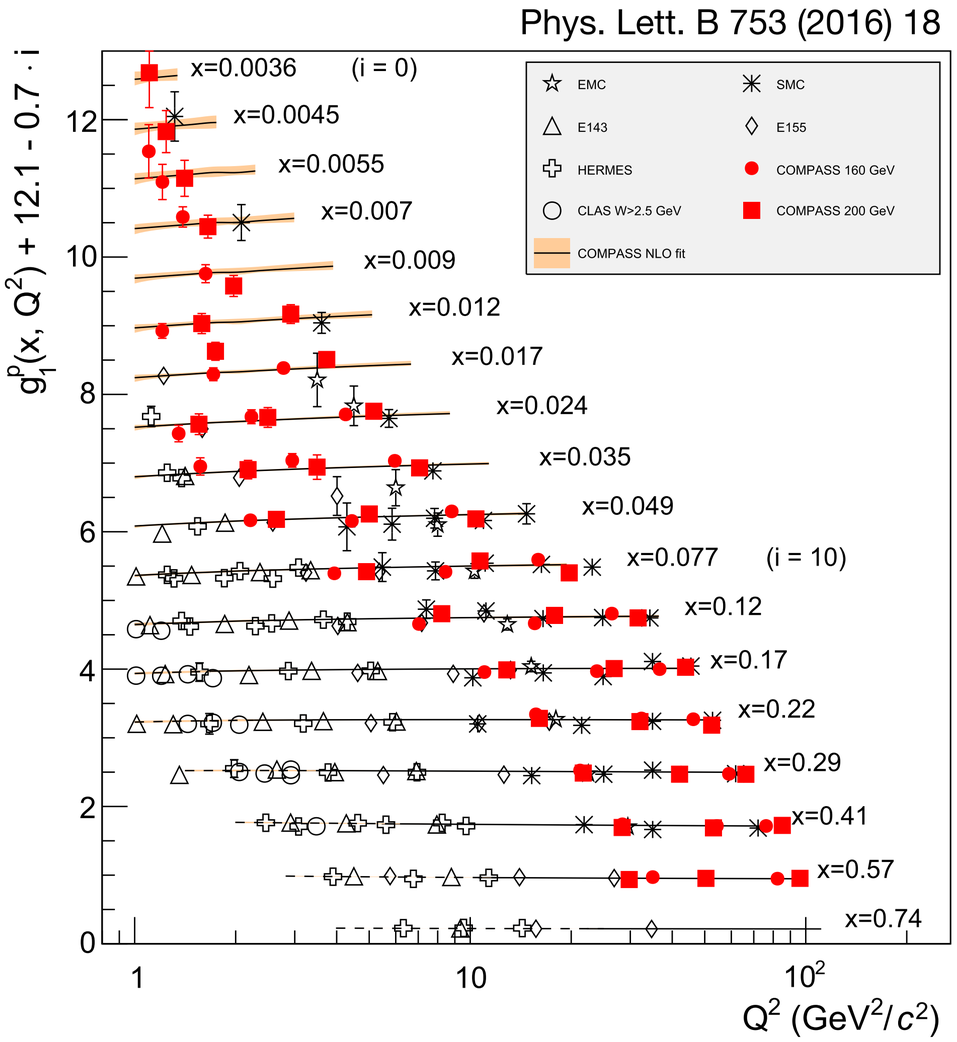

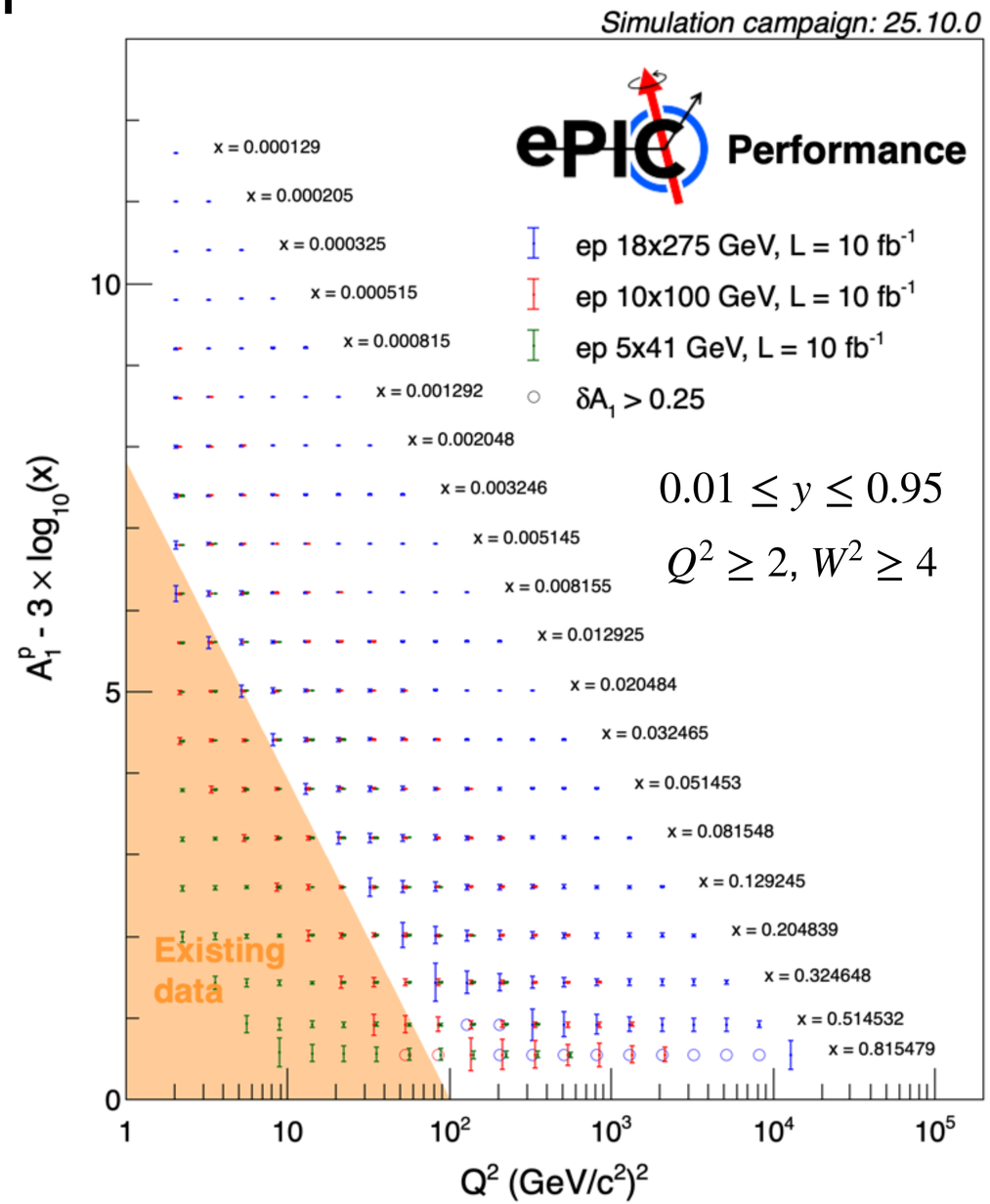

Gluon helicity distribution of the proton

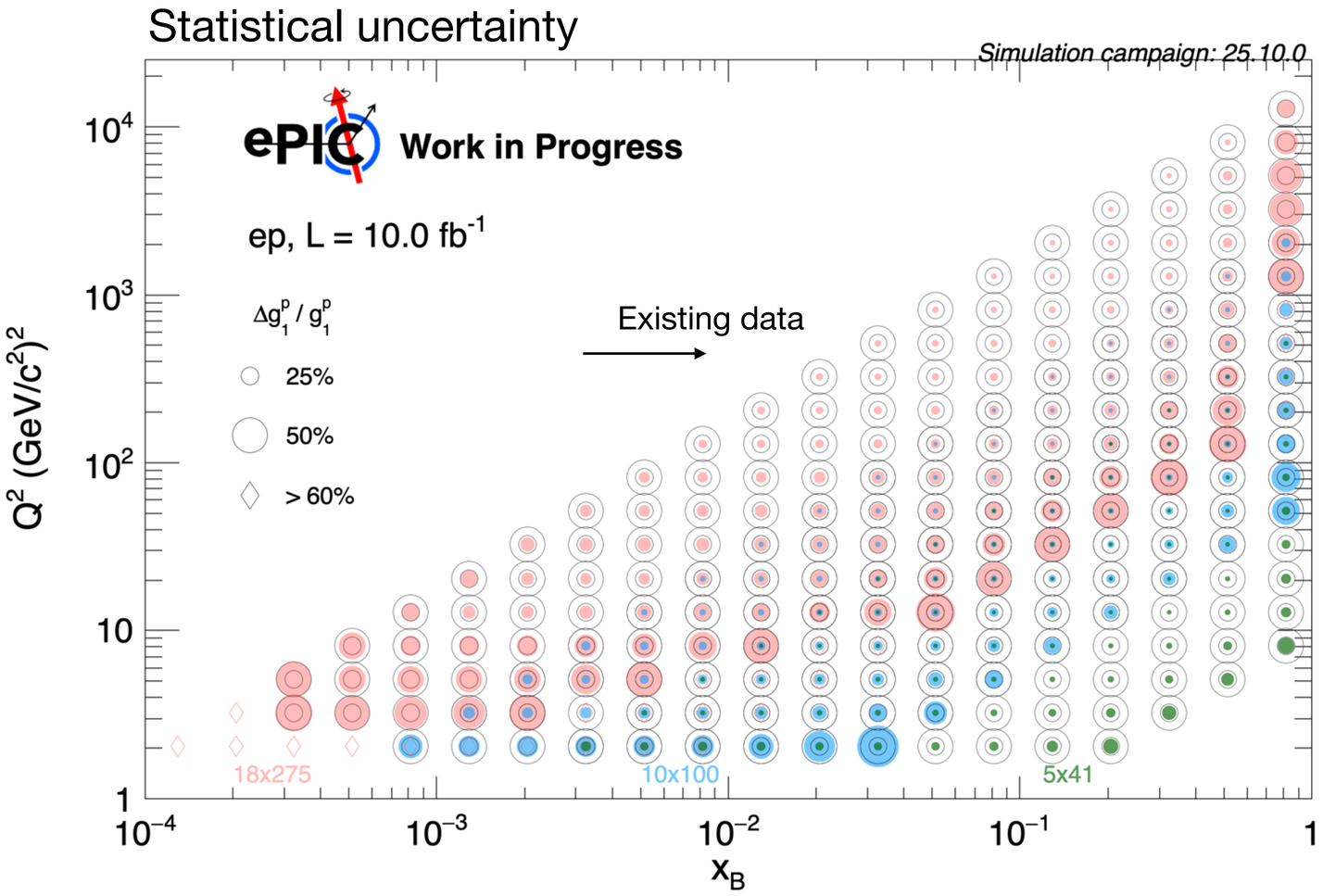

Gluon helicity distribution of the proton

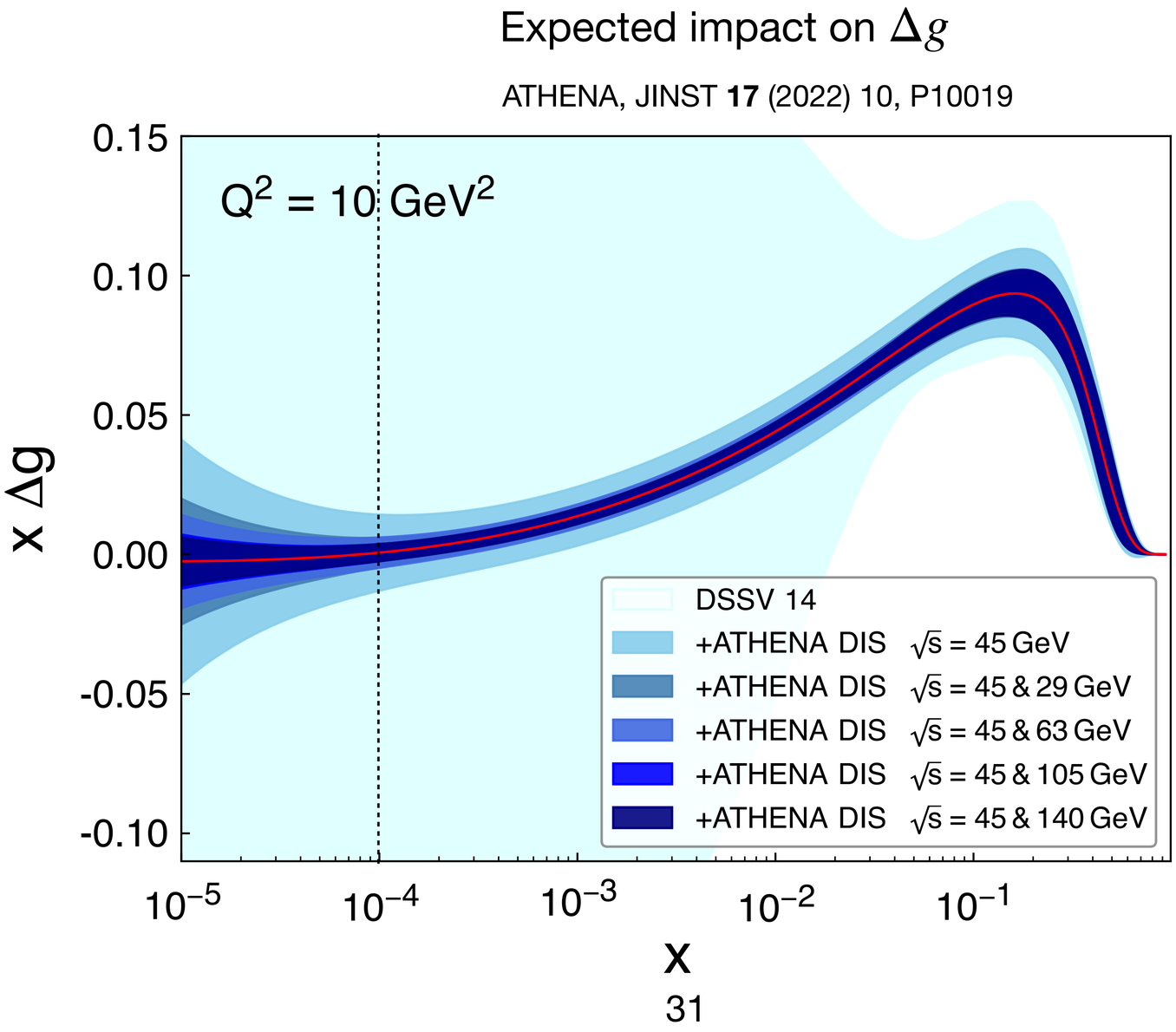

Gluon helicity distribution of the neutron

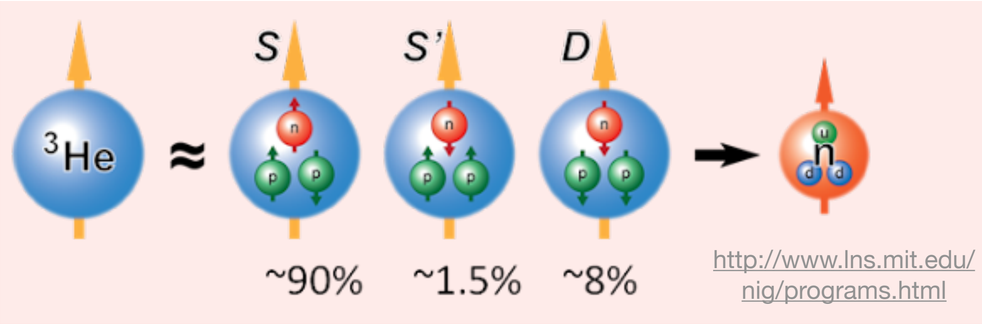

Gluon helicity distribution of the neutron

Access to spin structure of the neutron

inclusive DIS

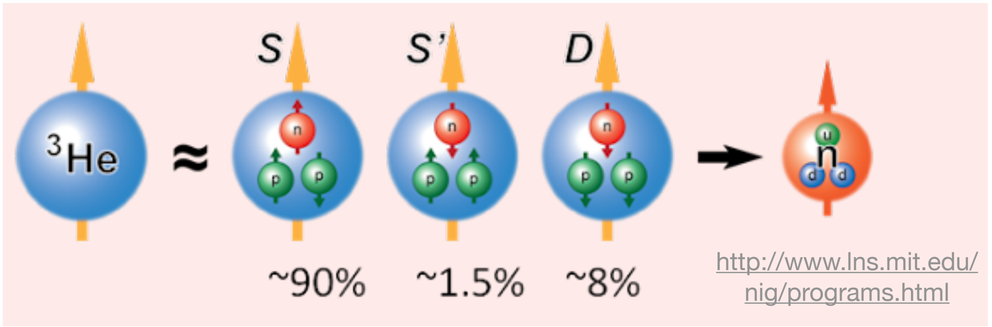

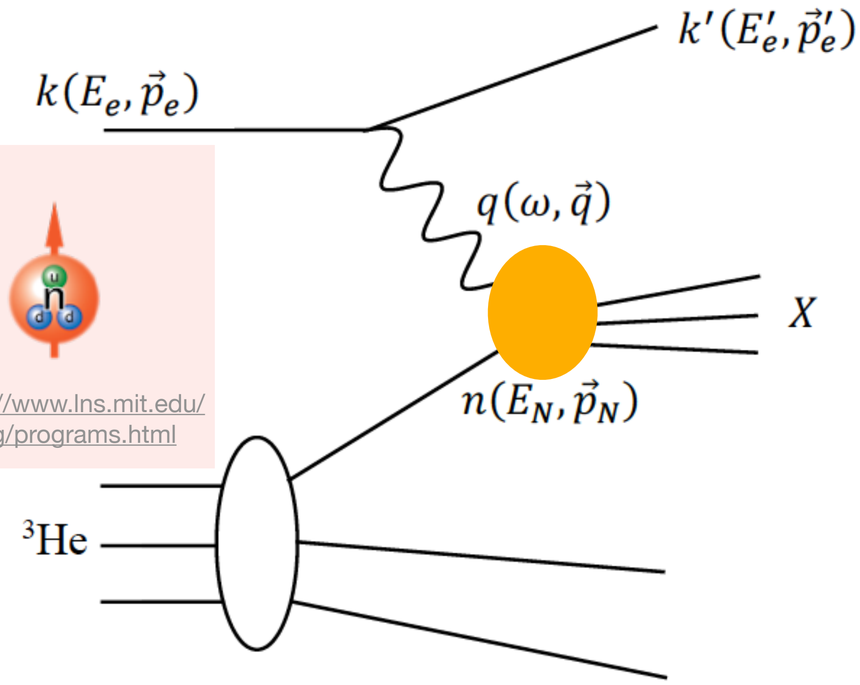

Gluon helicity distribution of the neutron

Access to spin structure of the neutron

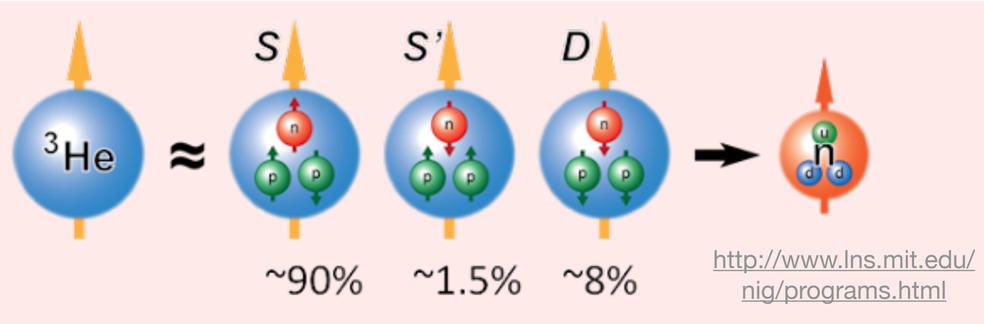

inclusive DIS

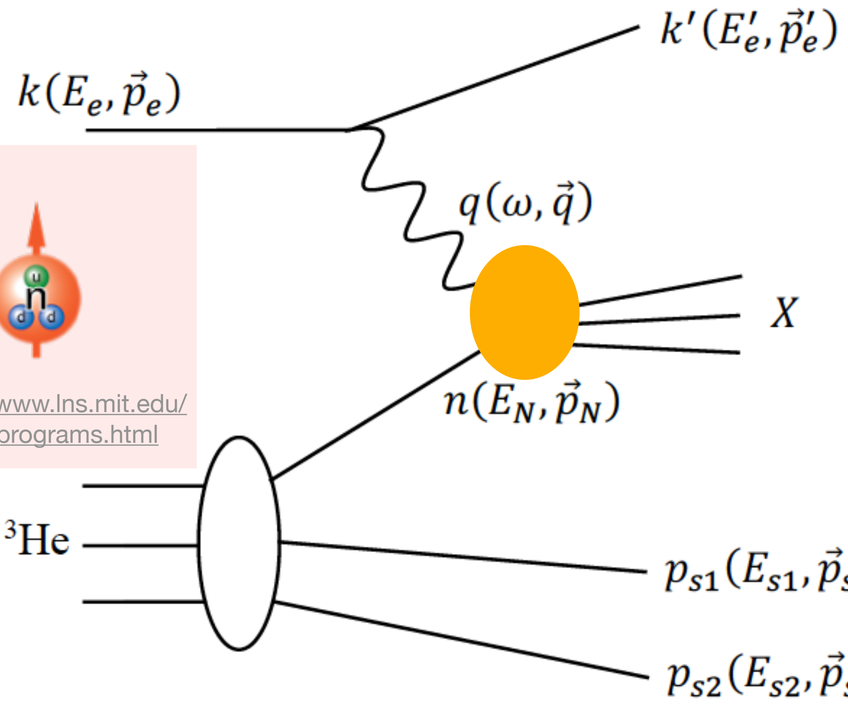

tagged DIS

double tagging of protons in far forward system

Gluon helicity distribution of the neutron

Access to spin structure of the neutron

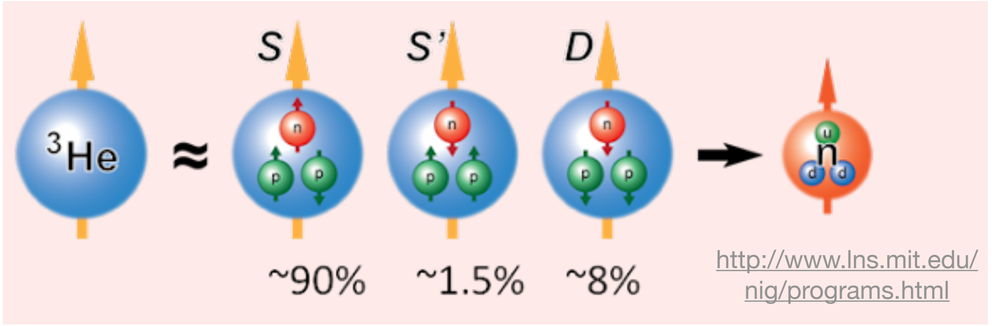

inclusive DIS

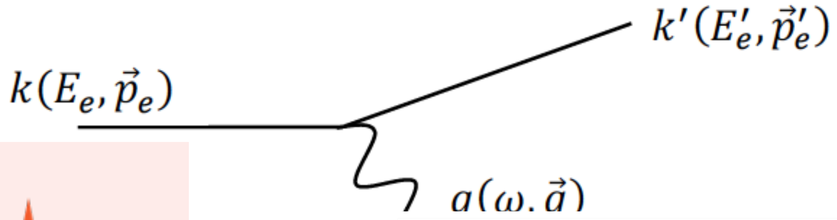

Tagging of protons
in far-forward system

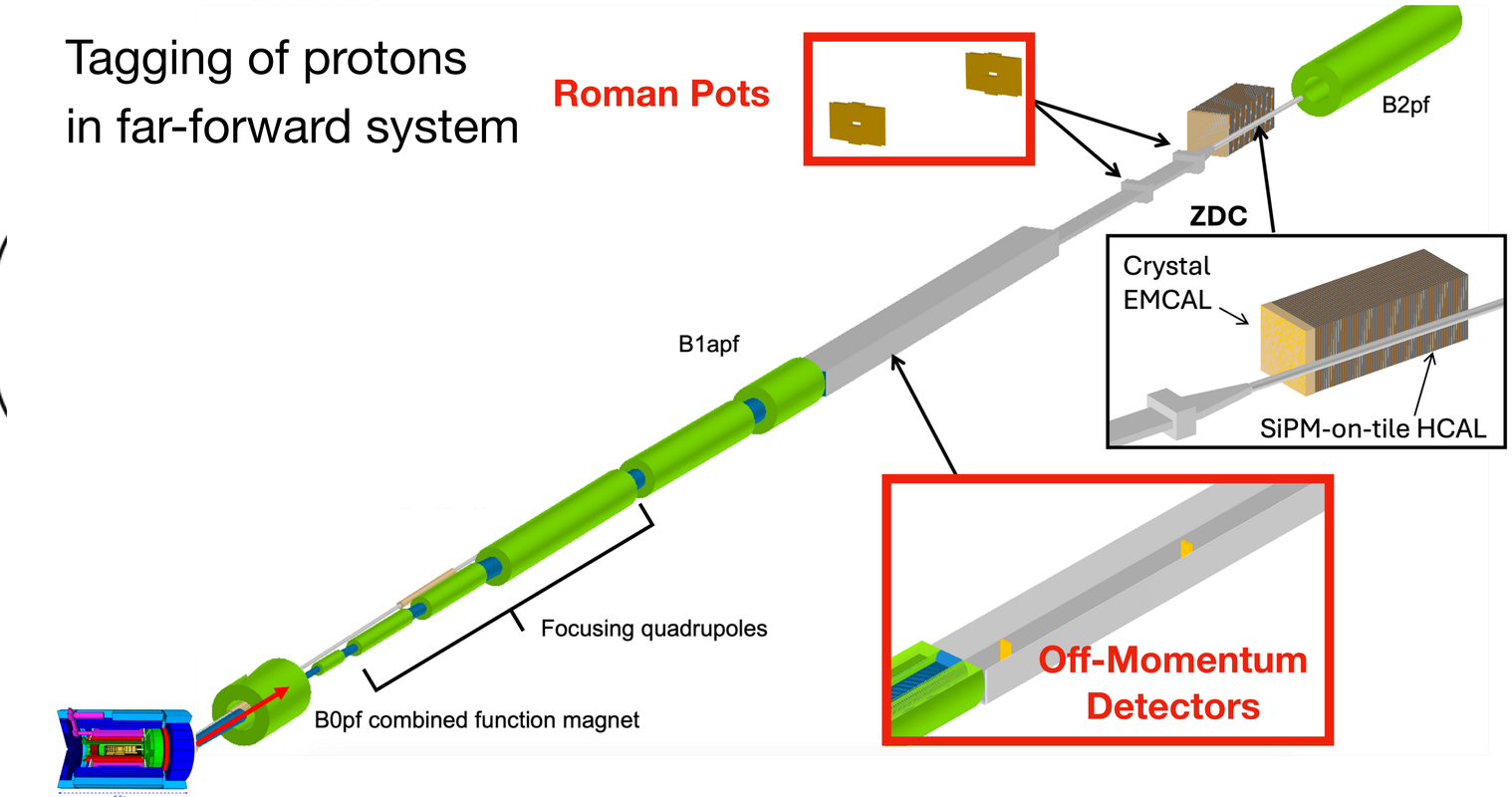

Gluon helicity distribution of the neutron

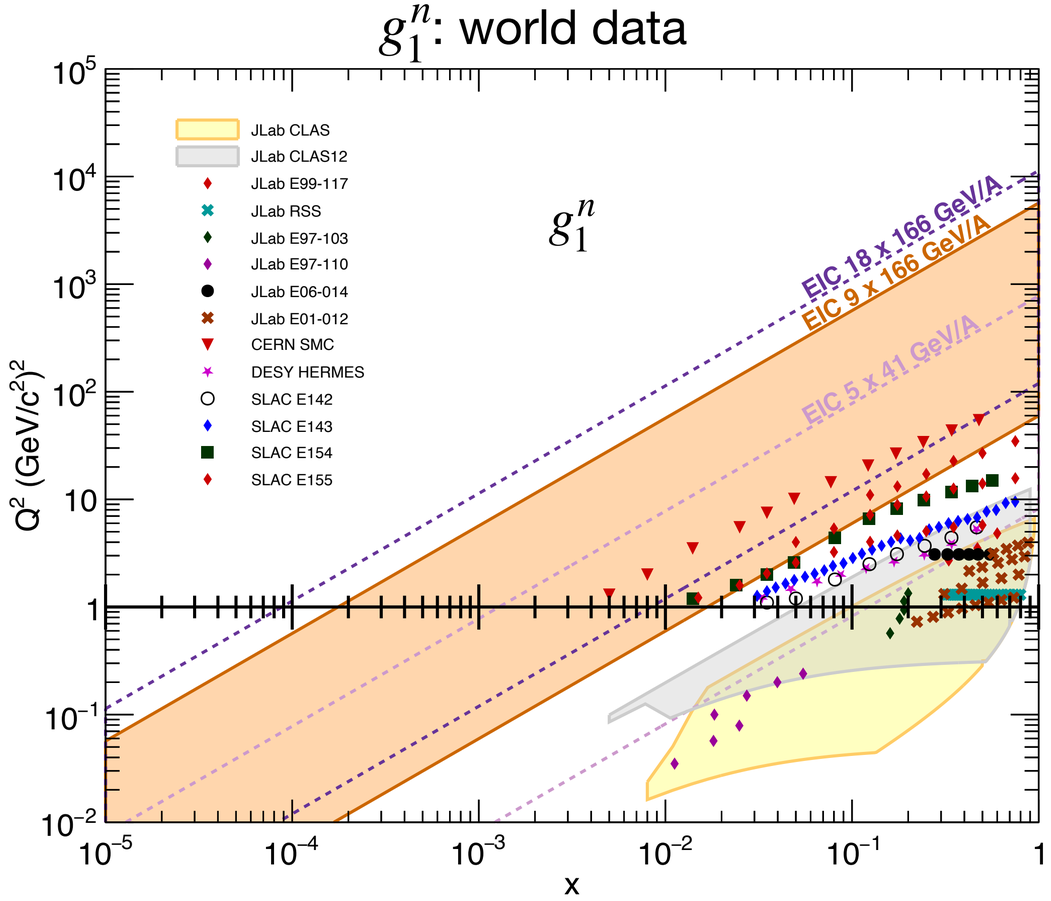

Gluon helicity distribution of the neutron

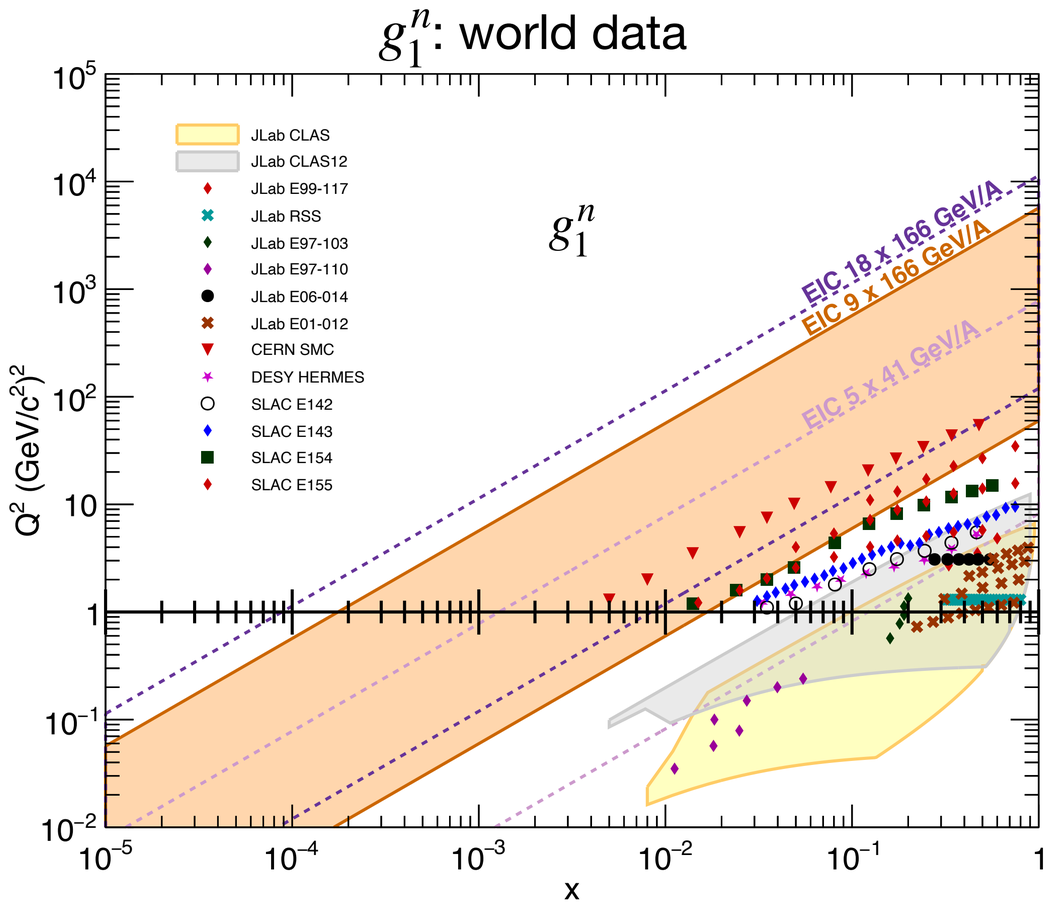

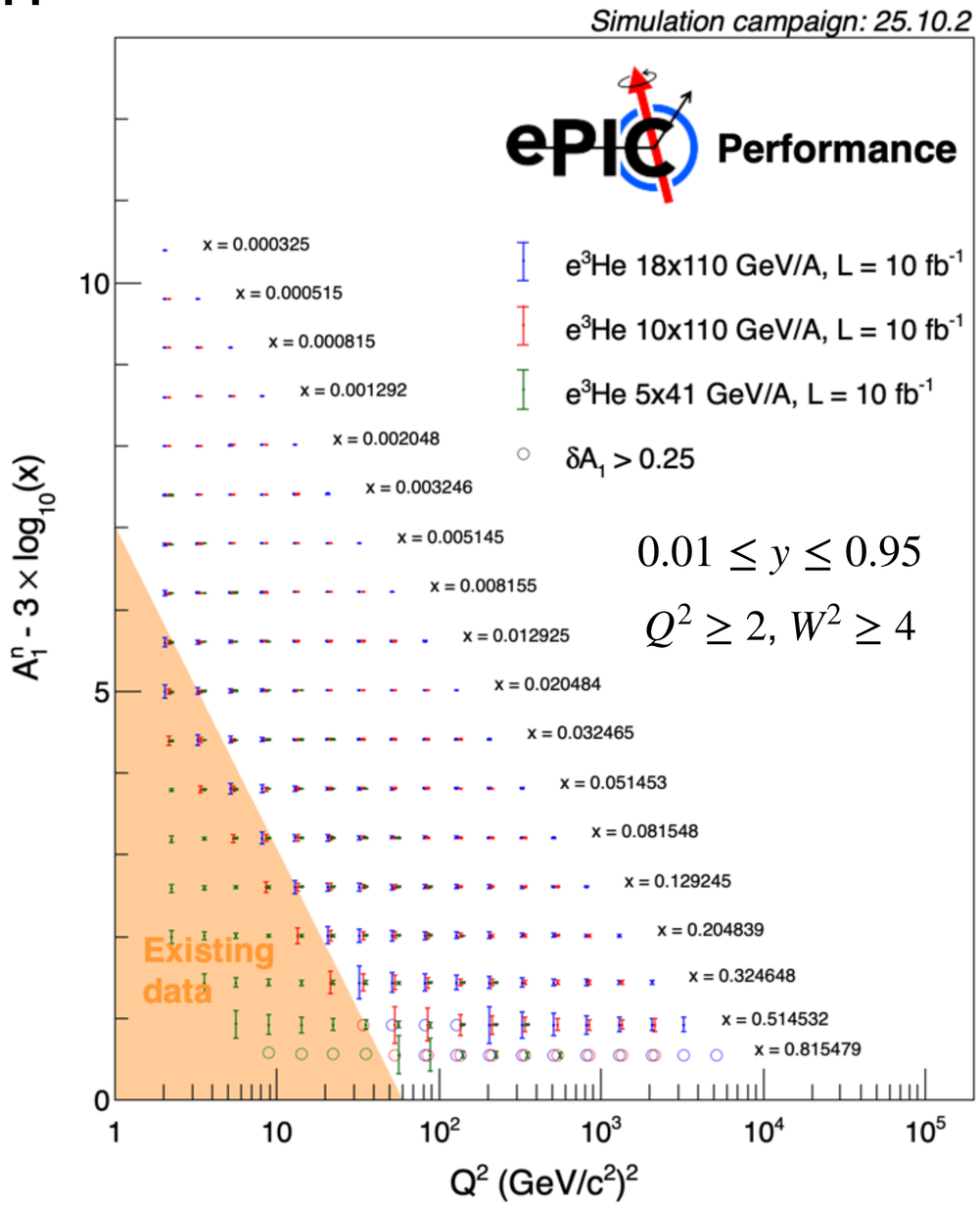

Gluon helicity distribution of the neutron

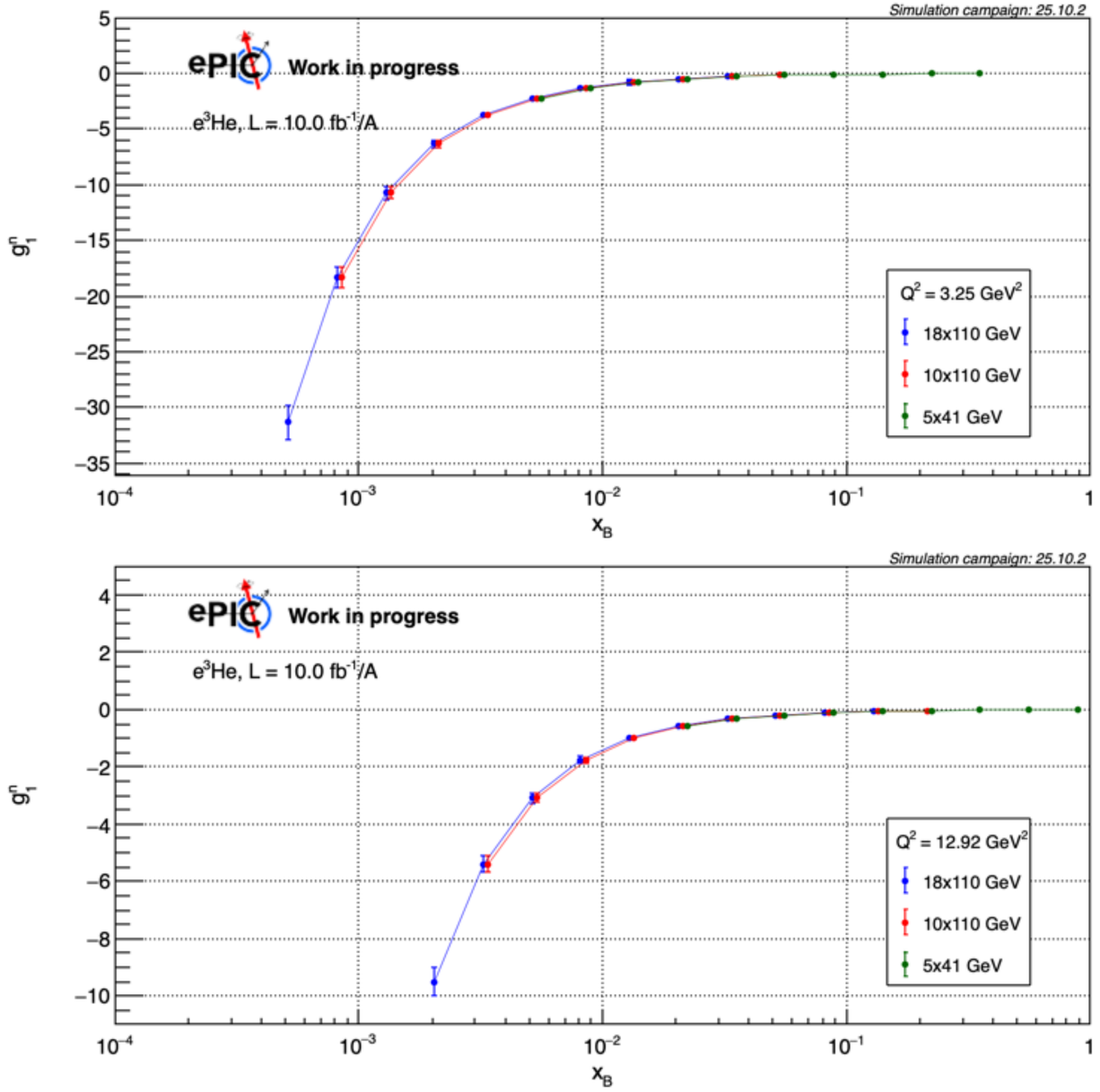

Quark helicity distributions of the proton

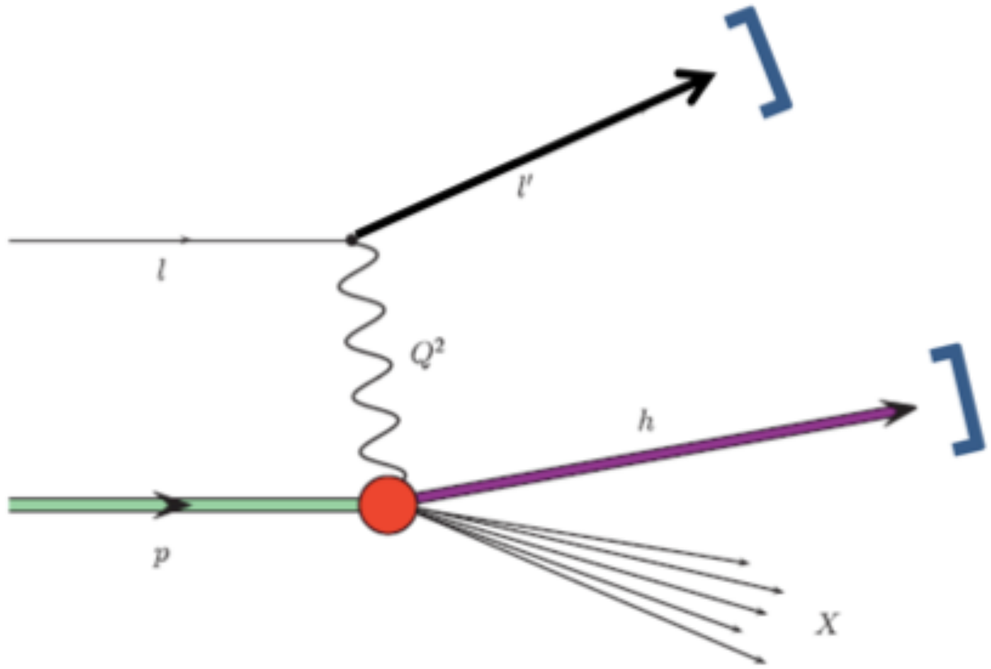

Quark helicity distributions of the proton

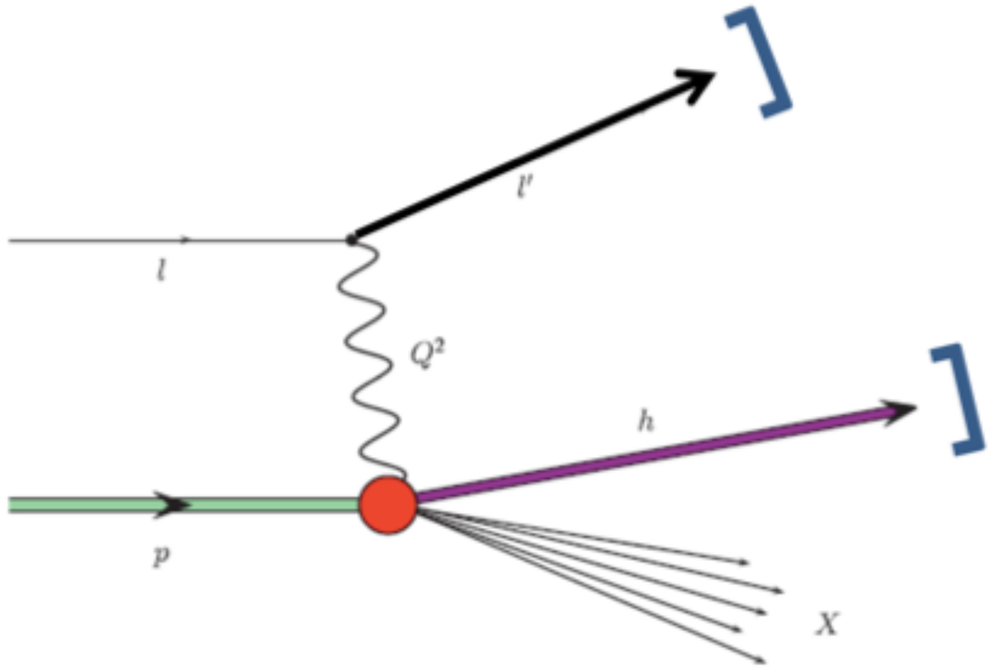

Hadron particle identification:
pions, kaons and protons

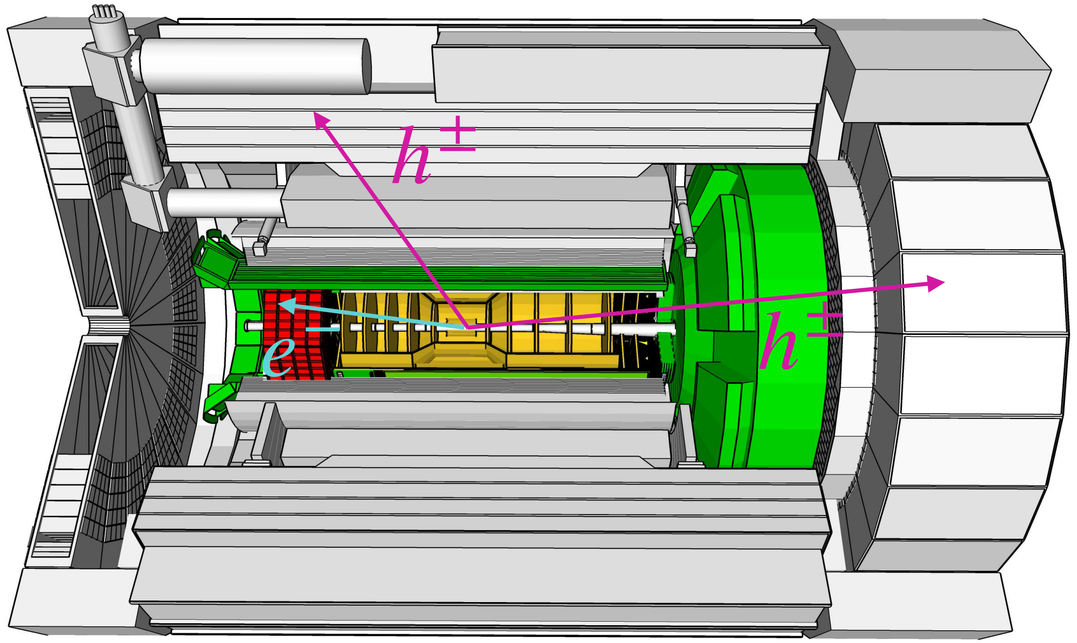

ePIC particle identification

Particle identification: Cherenkov detectors

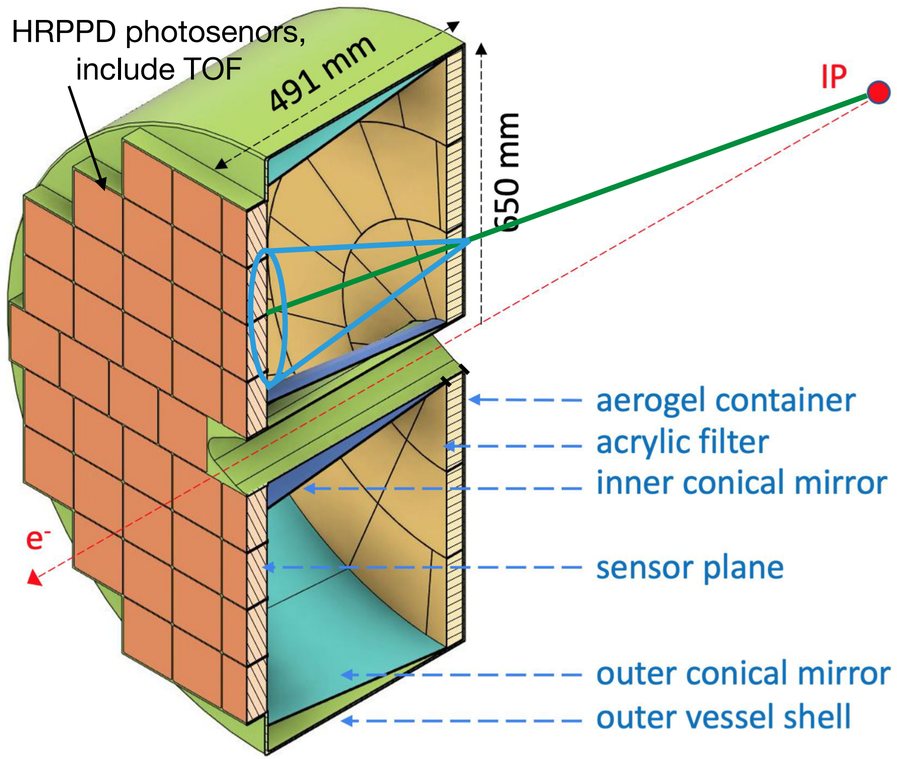

ePIC particle identification

Particle identification: Cherenkov detectors

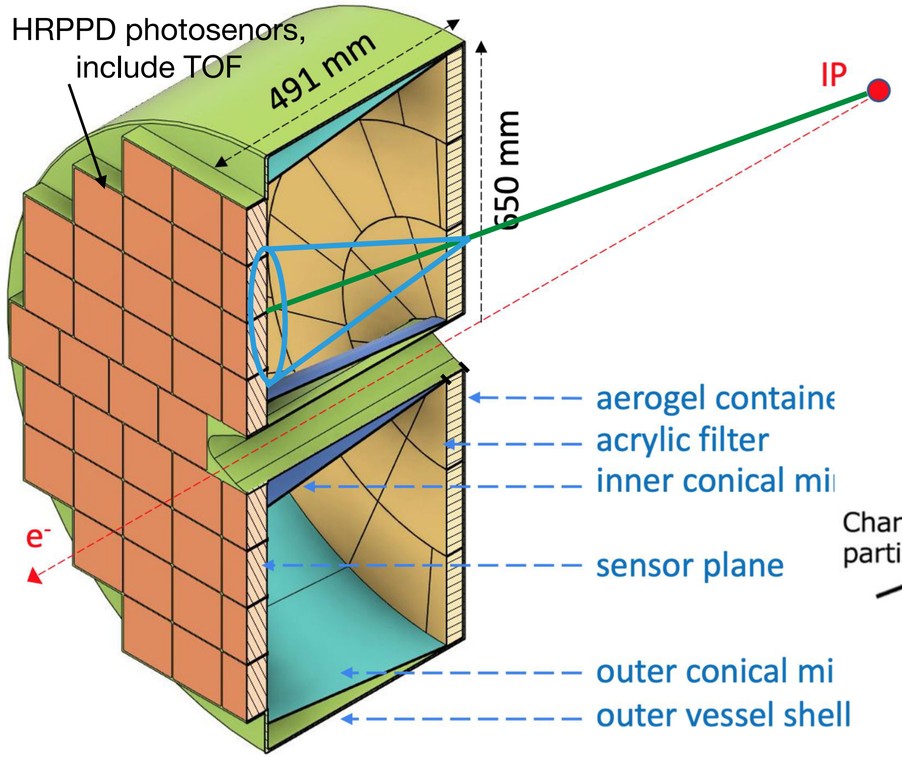

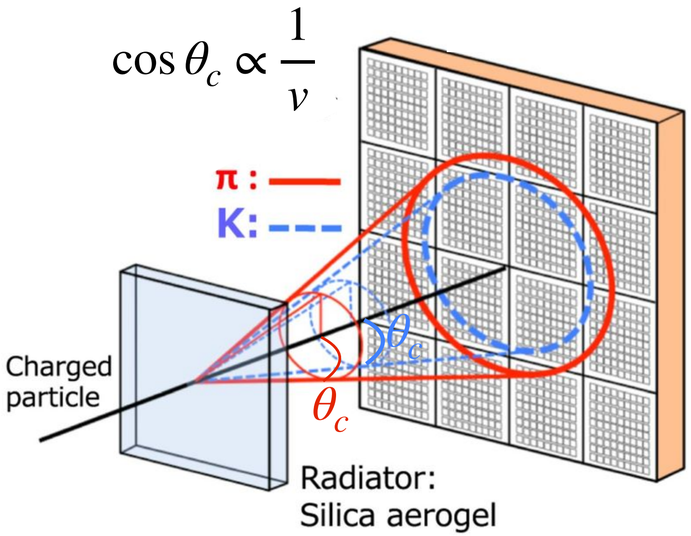

ePIC particle identification

Particle identification: Cherenkov detectors

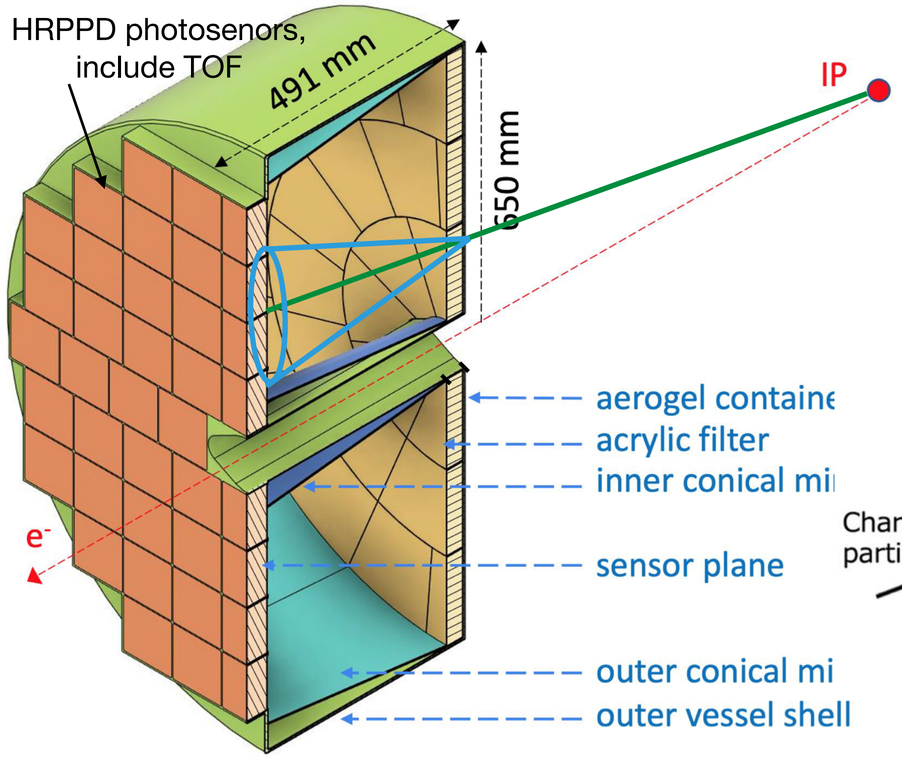

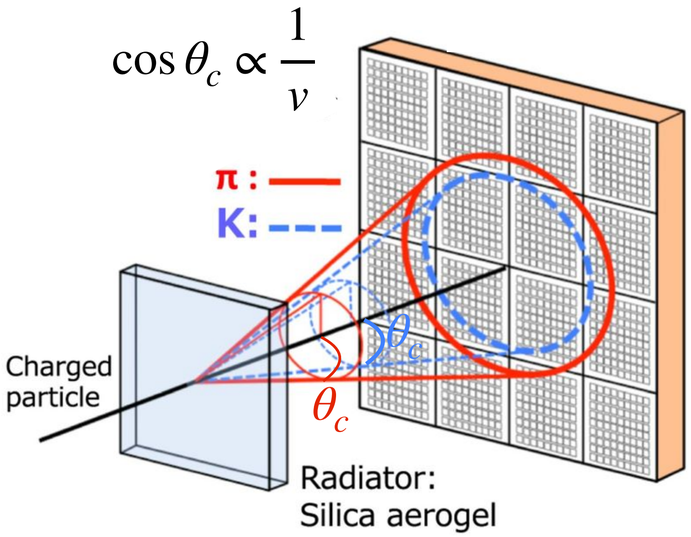

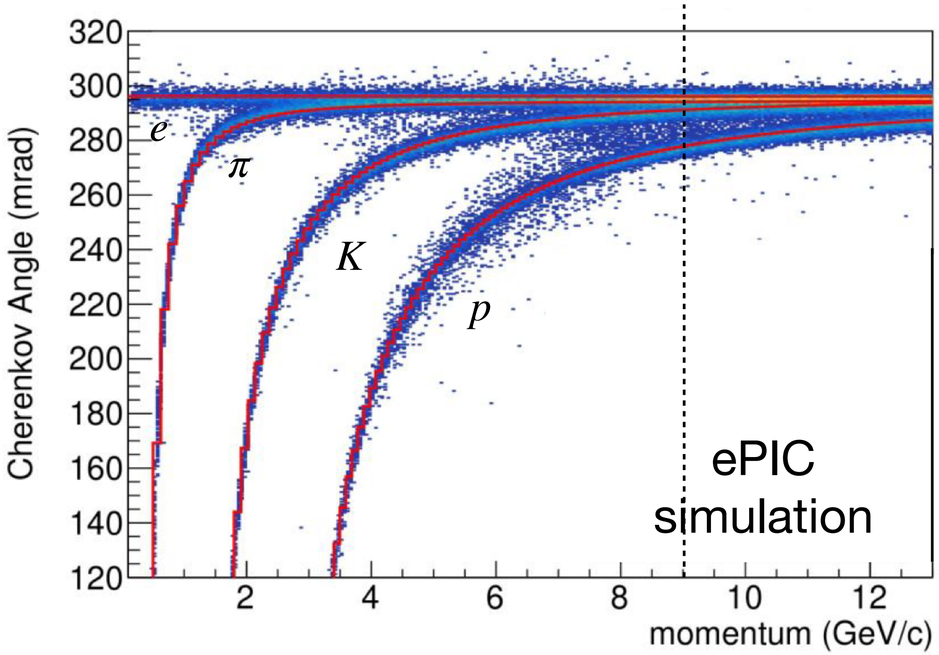

ePIC particle identification

AC-LGAD based TOF, for p < 0.5 – 3 GeV/c

$$v = \frac{L}{t_{stop} - t_{start}}$$

detectors based on
Cherenkov radiation
for 1 GeV/c<p<50 GeV/c

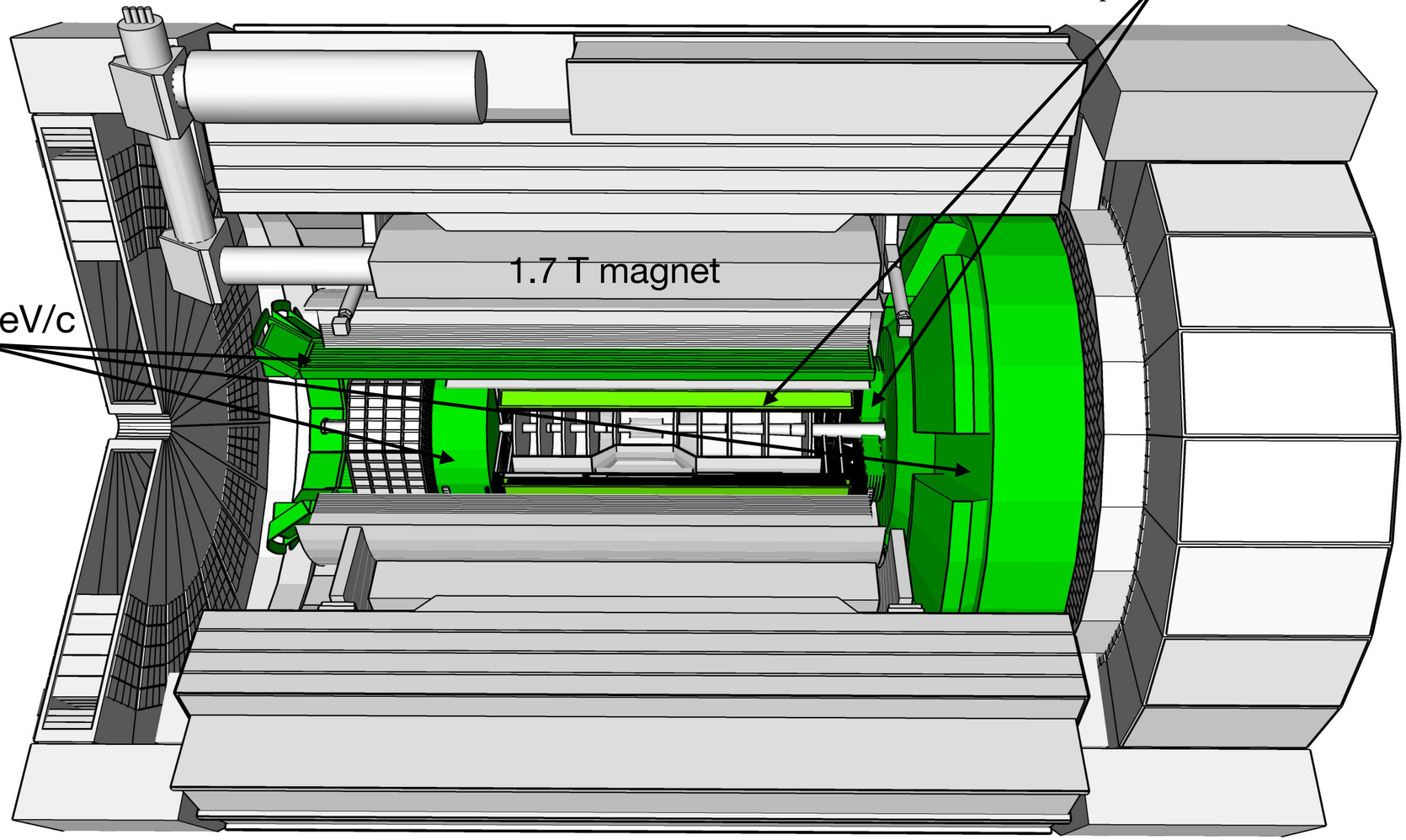

ePIC particle identification

Particle identification: time of flight

Barrel Region
- e/pi up to 0.5 GeV/c
- pi/K up to 1.9 GeV/c
- K/p up to 3.1 GeV/c

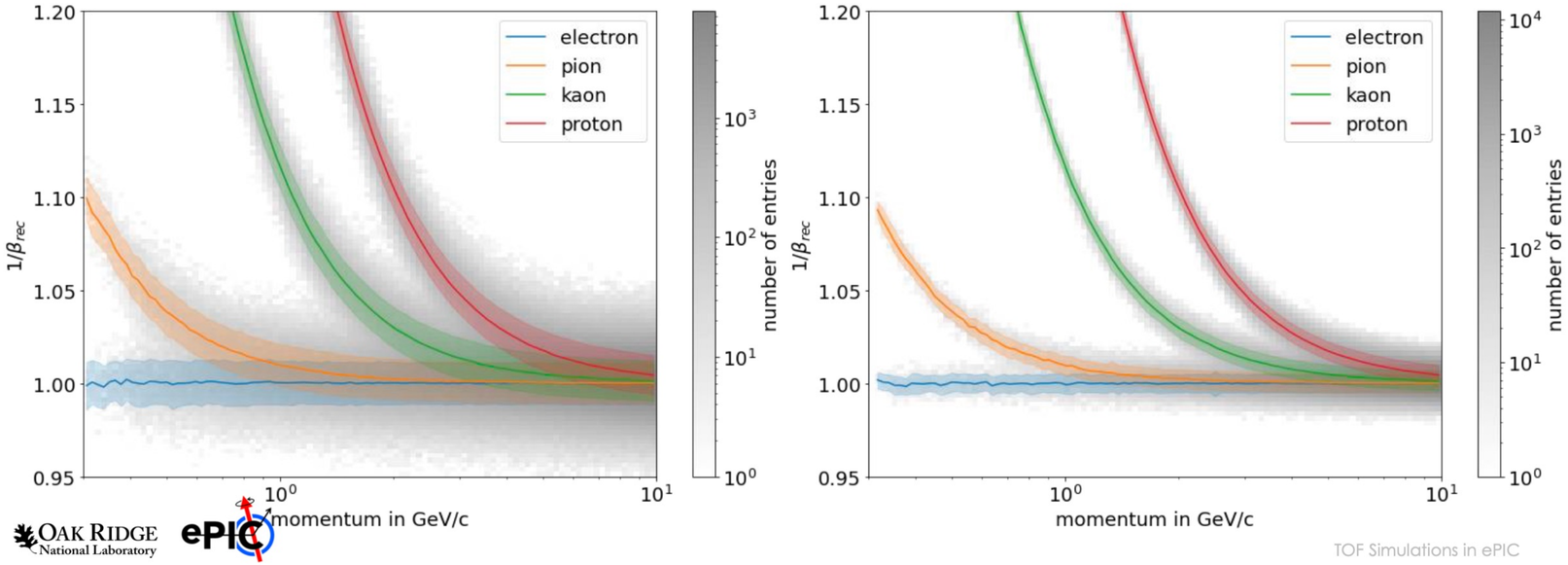

Endcap Region
- e/pi up to 0.8 GeV/c
- pi/K up to 2.7 GeV/c
- K/p up to 4.6 GeV/c

ePIC particle identification

Particle identification: coverage

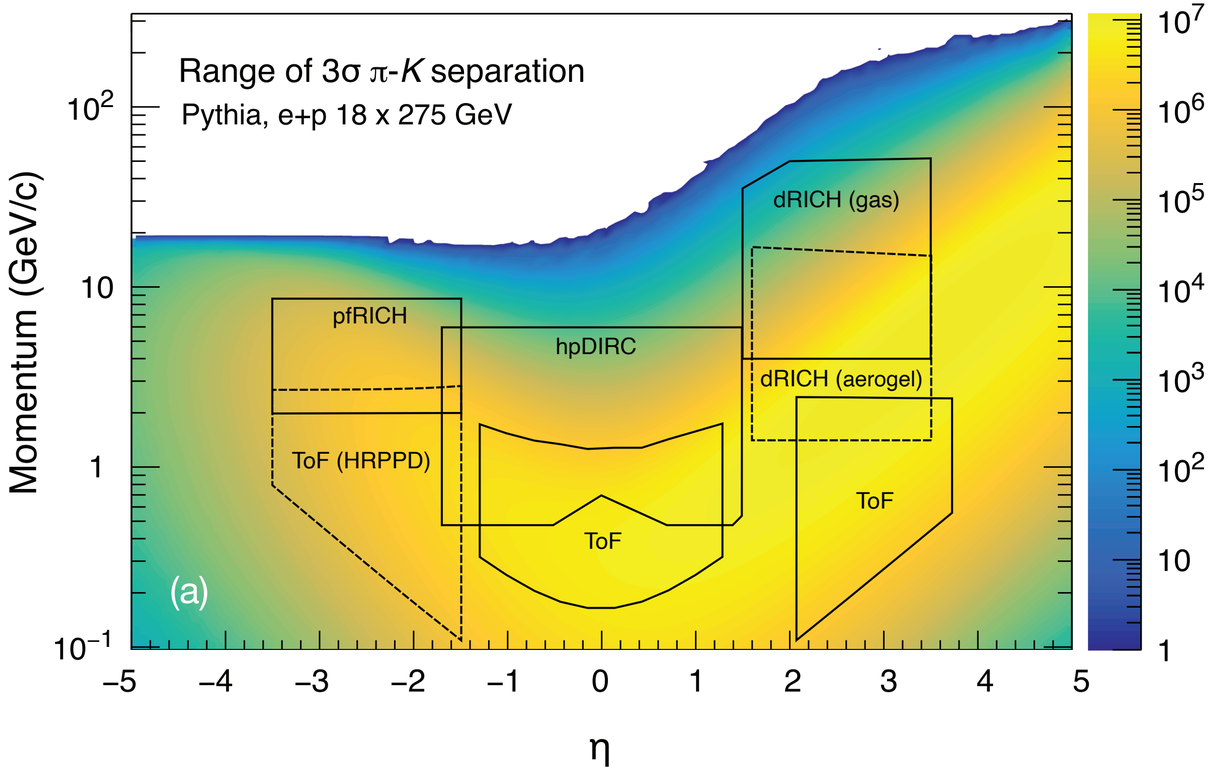

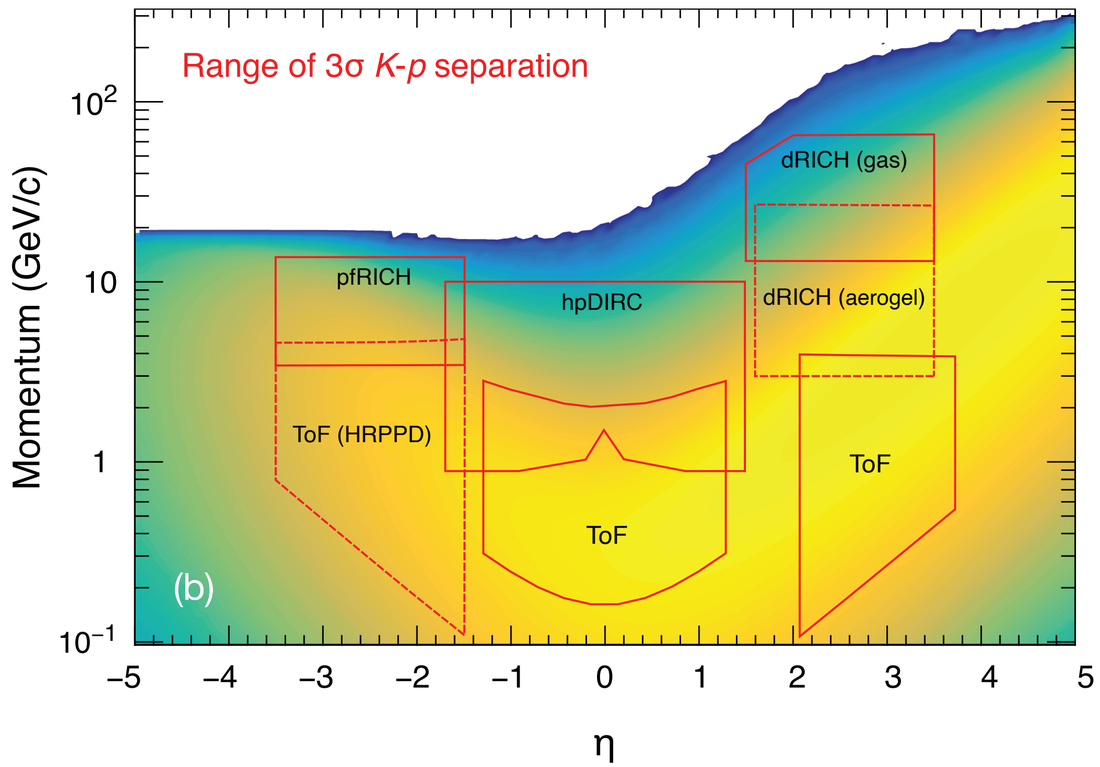

Quark helicity distributions of the proton

Kinematic coverage

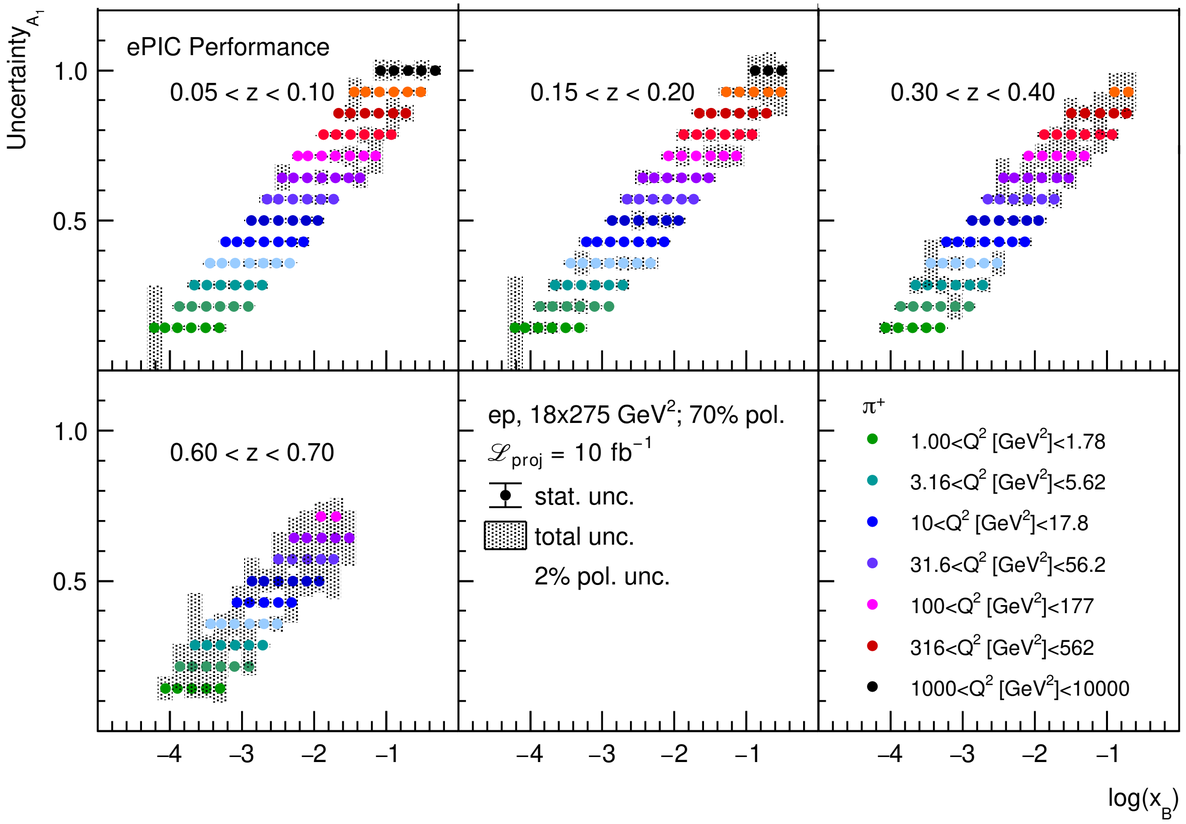

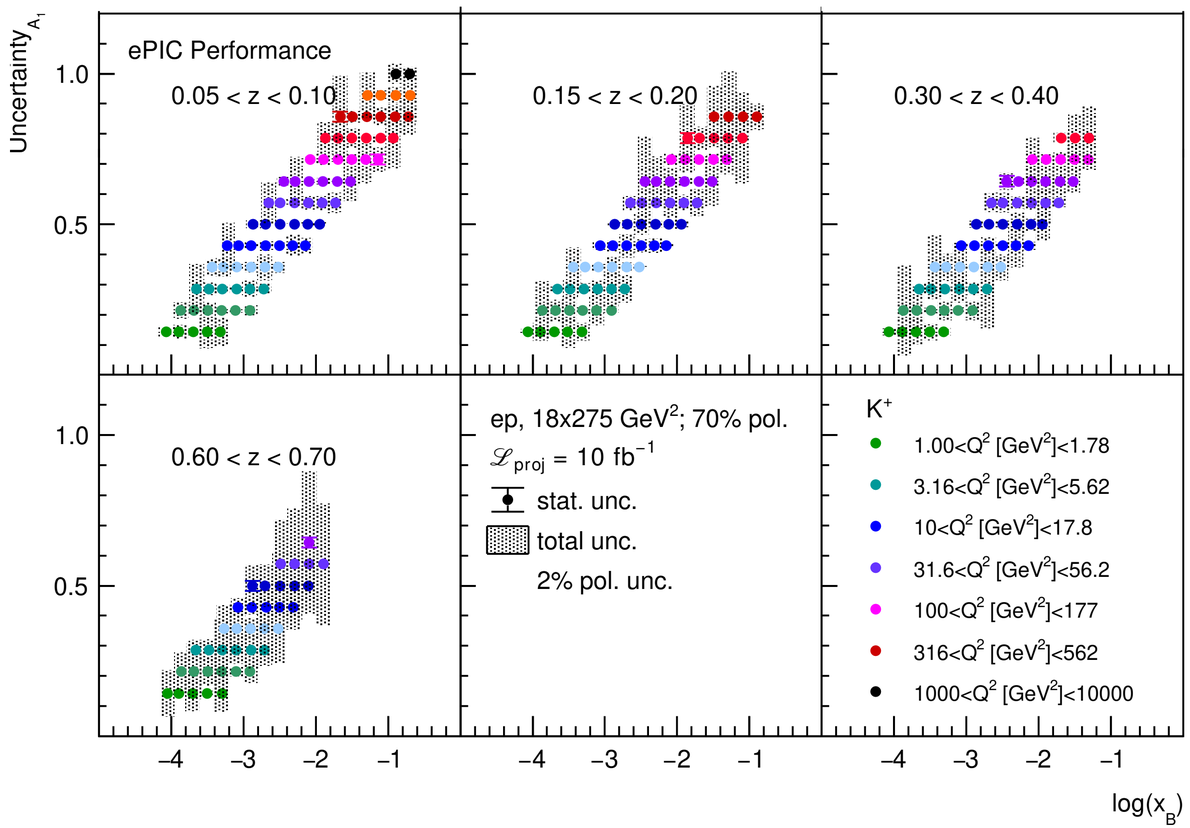

Quark helicity distributions of the proton

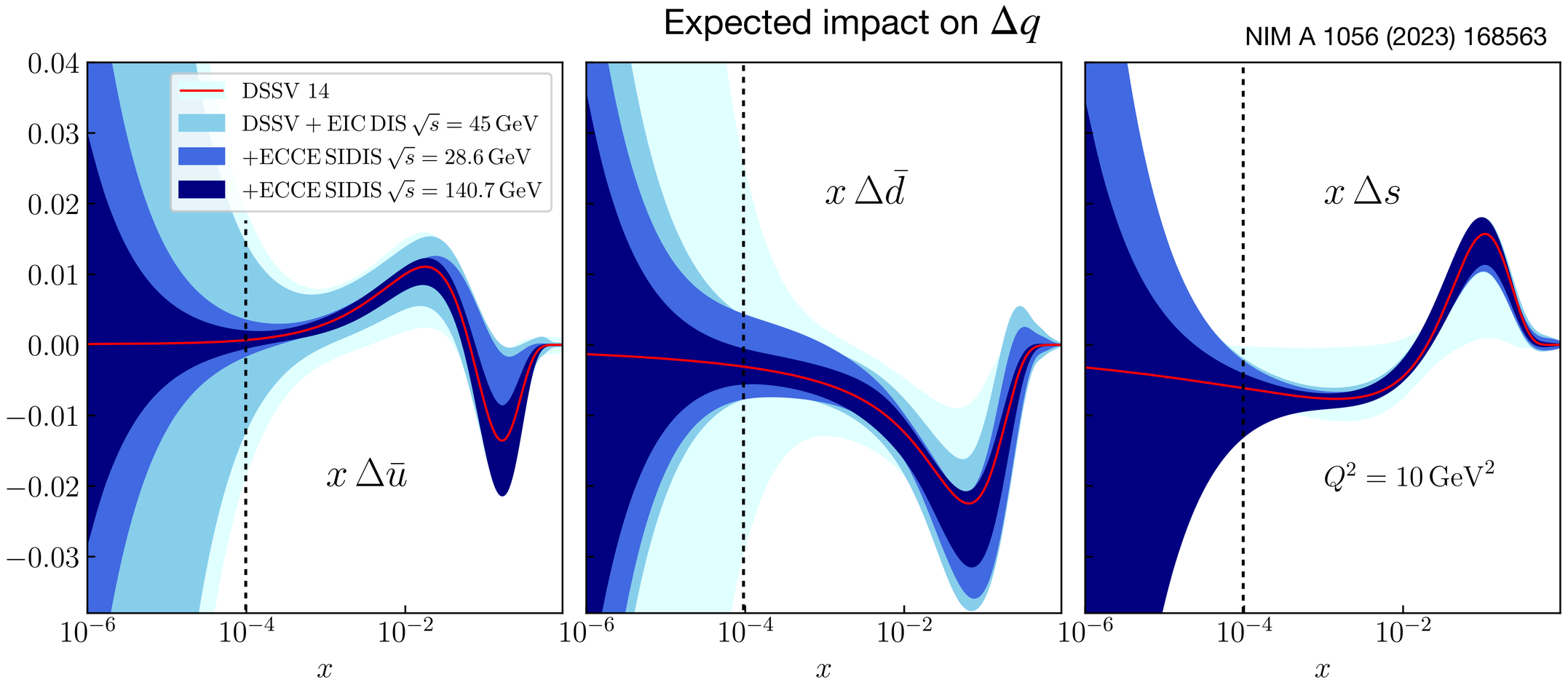

1D image

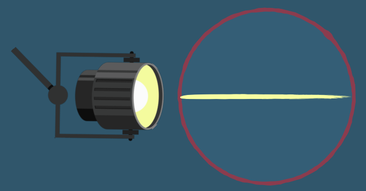

1D image

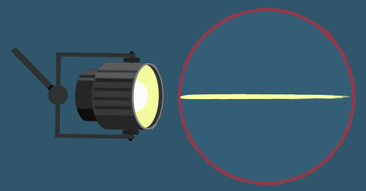

3D tomographies of the nucleon

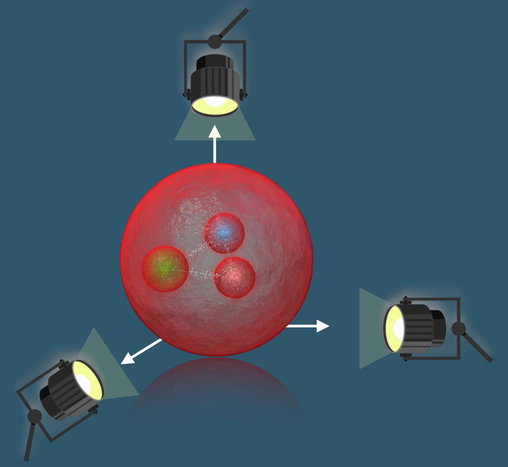

The various dimensions of the nucleon

Wigner distributions $W(x, \vec{k}_T, \vec{b}_\perp)$

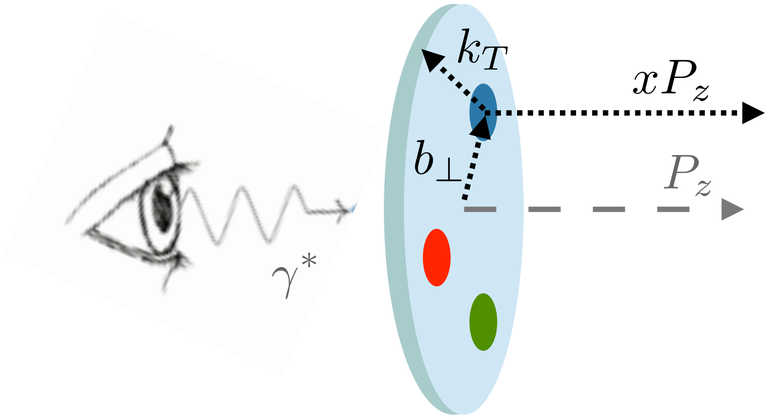

The various dimensions of the nucleon

Wigner distributions $W(x, \vec{k}_T, \vec{b}_\perp)$

$\int d^2\vec{b}_\perp$

transverse-momentum dependent (TMD) parton distribution functions (PDFs)

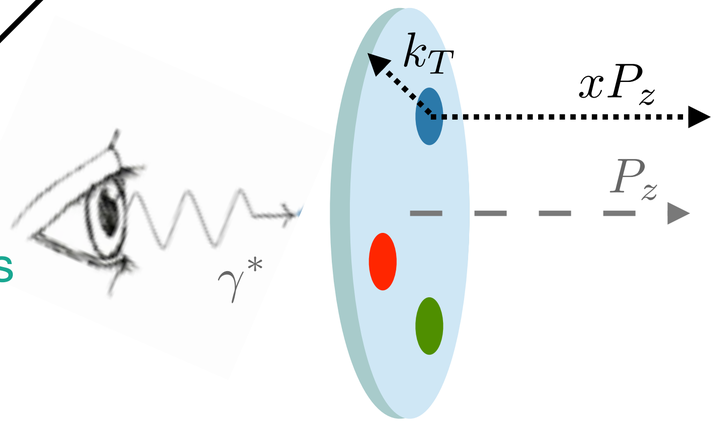

The various dimensions of the nucleon

Wigner distributions $W(x, \vec{k}_T, \vec{b}_\perp)$

$\int d^2\vec{b}_\perp$

transverse-momentum dependent (TMD) parton distribution functions (PDFs)

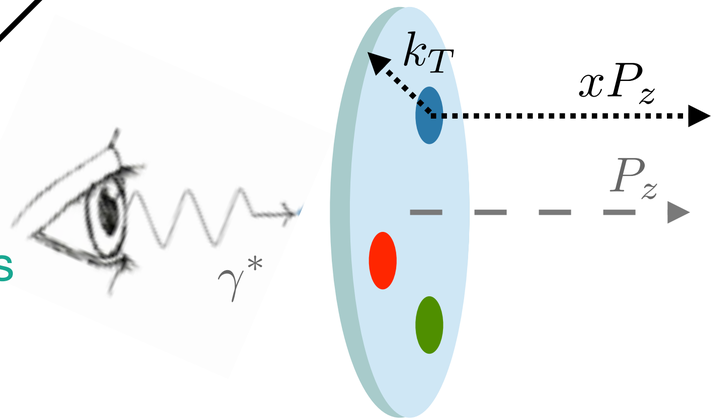

Semi-inclusive production

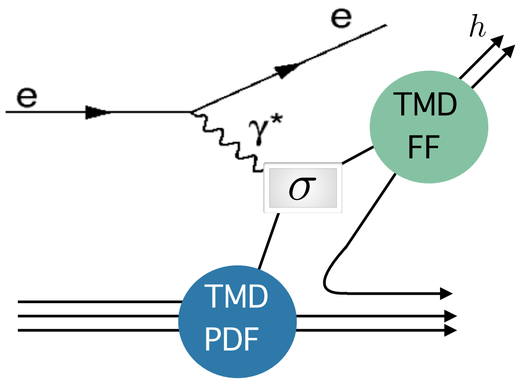

The various dimensions of the nucleon

Wigner distributions $W(x, \vec{k}_T, \vec{b}_\perp)$

$\int d^2\vec{b}_\perp$

transverse-momentum dependent (TMD) parton distribution functions (PDFs)

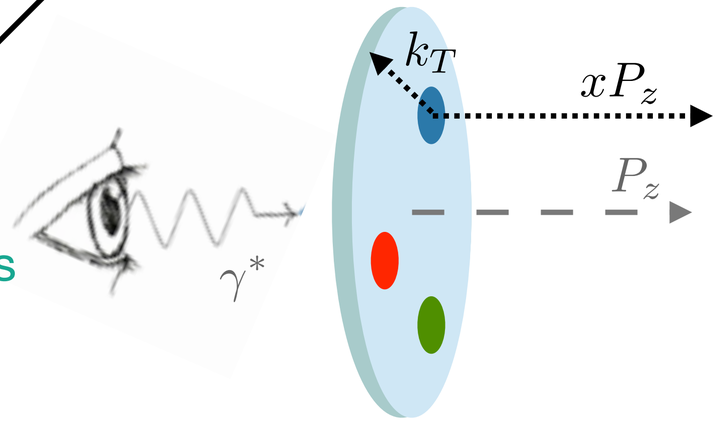

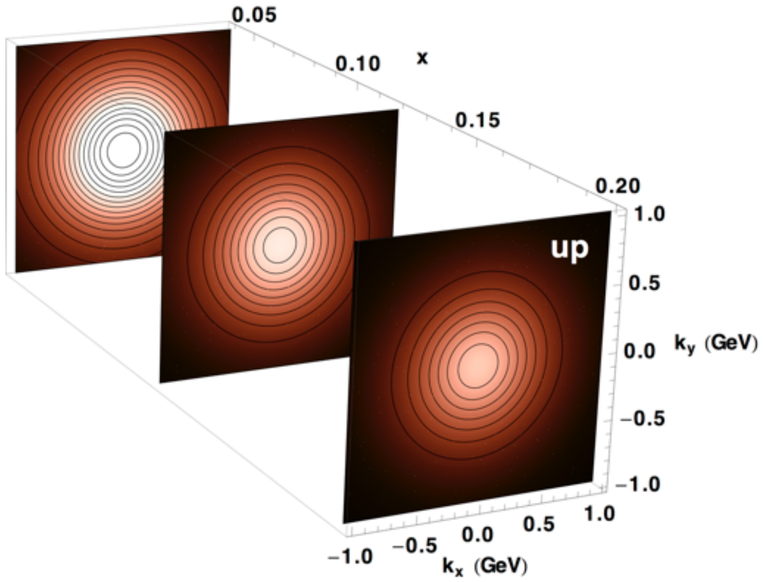

The various dimensions of the nucleon

Wigner distributions $W(x, \vec{k}_T, \vec{b}_\perp)$

$\int d^2\vec{b}_\perp$

transverse-momentum dependent (TMD) parton distribution functions (PDFs)

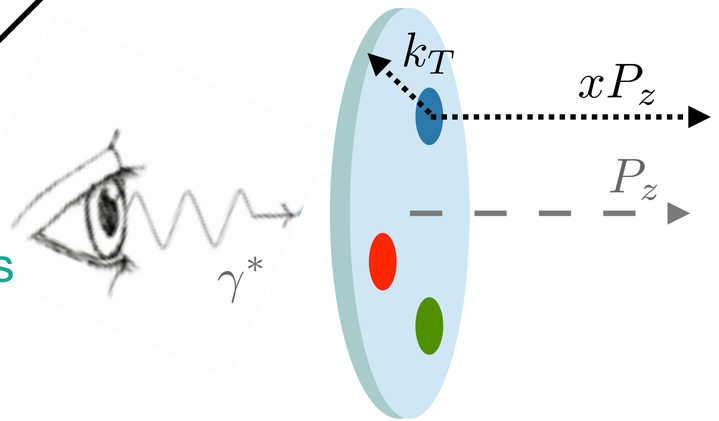

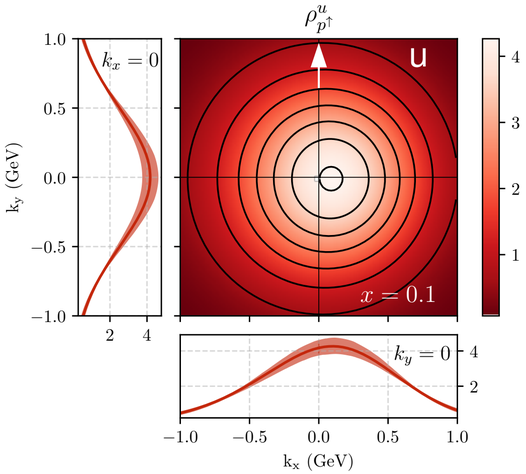

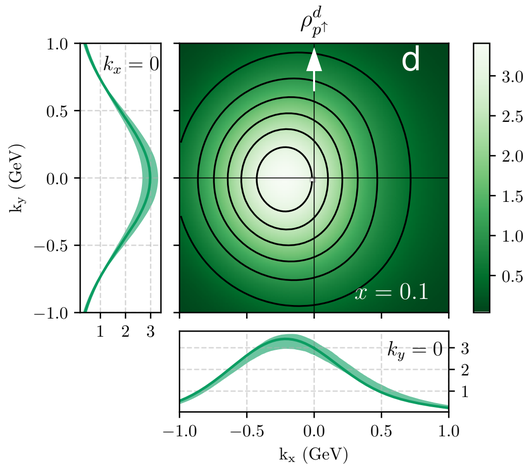

The various dimensions of the nucleon

Wigner distributions $W(x, \vec{k}_T, \vec{b}_\perp)$

$\int d^2\vec{b}_\perp$

$\int d^2\vec{k}_T$

transverse-momentum dependent (TMD) parton distribution functions (PDFs)

impact-parameter dependent PDFs

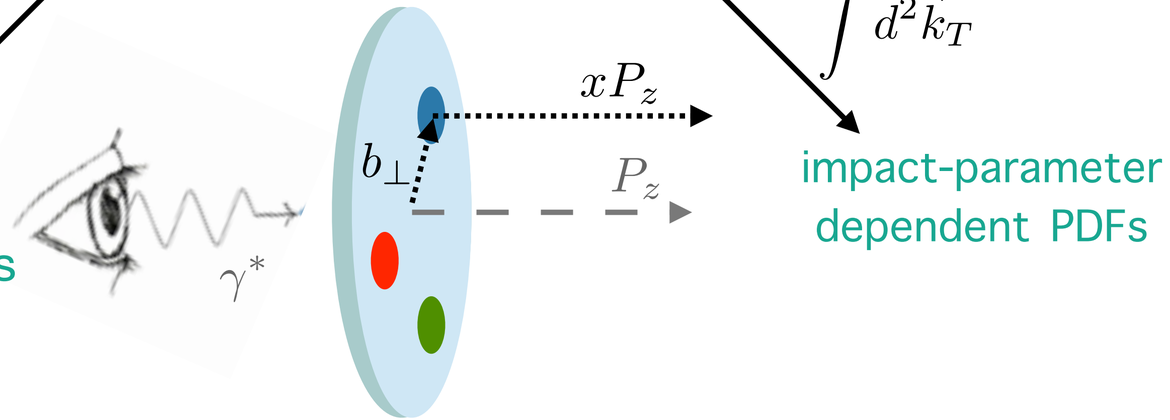

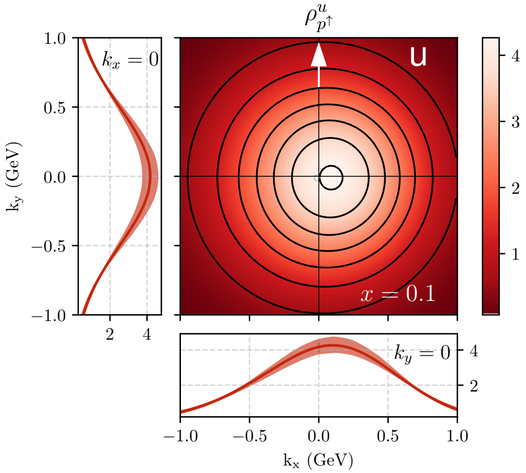

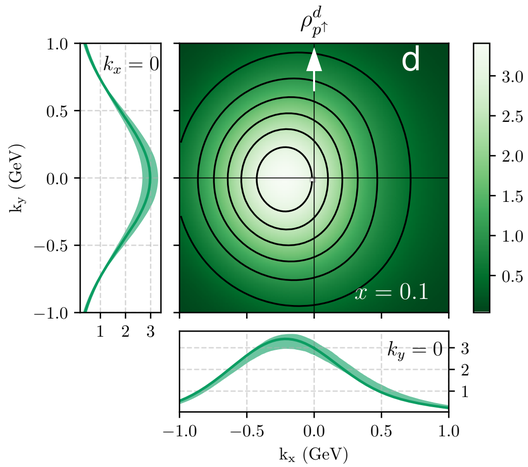

The various dimensions of the nucleon

Wigner distributions $W(x, \vec{k}_T, \vec{b}_\perp)$

$\int d^2\vec{b}_\perp$

$\int d^2\vec{k}_T$

transverse-momentum dependent (TMD) parton distribution functions (PDFs)

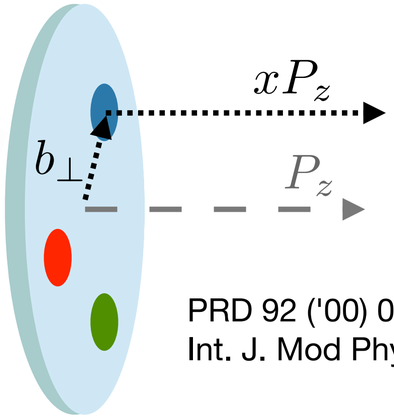

impact-parameter dependent PDFs

PRD 92 ('00) 071503
Int. J. Mod Phys. A 18 ('03) 173

Fourier transform

generalised parton distributions (GPDs)

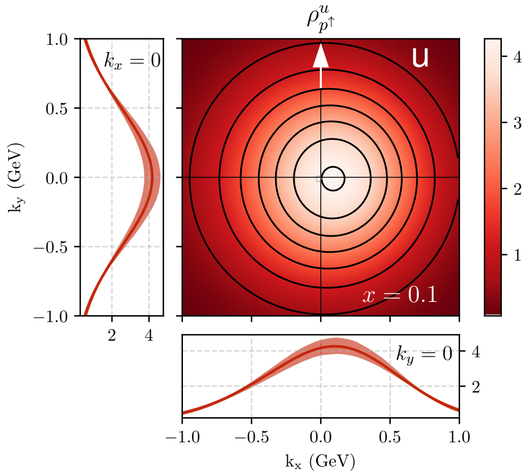

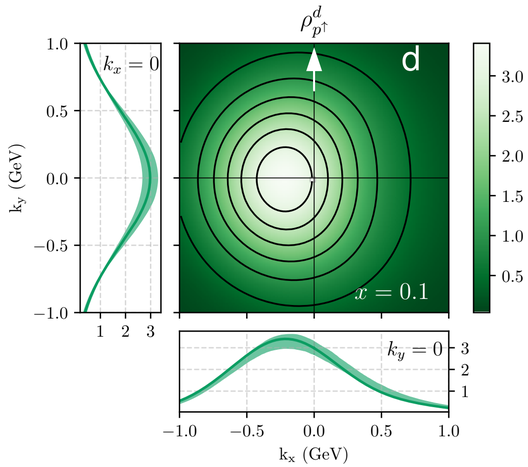

The various dimensions of the nucleon

Wigner distributions $W(x, \vec{k}_T, \vec{b}_\perp)$

$\int d^2\vec{b}_\perp$

$\int d^2\vec{k}_T$

transverse-momentum dependent (TMD) parton distribution functions (PDFs)

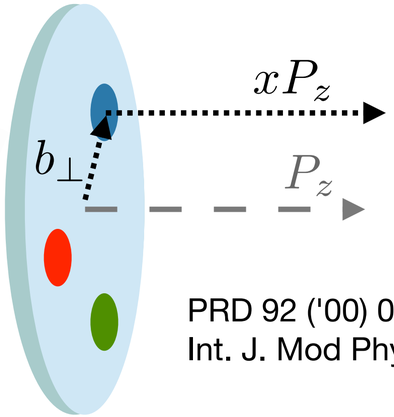

impact-parameter dependent PDFs

PRD 92 ('00) 071503
Int. J. Mod Phys. A 18 ('03) 173

Fourier transform

generalised parton distributions (GPDs)

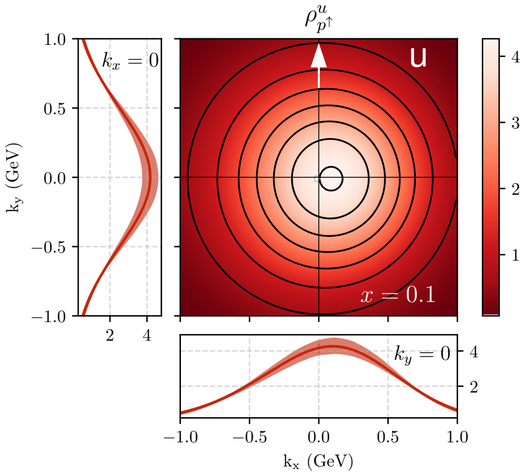

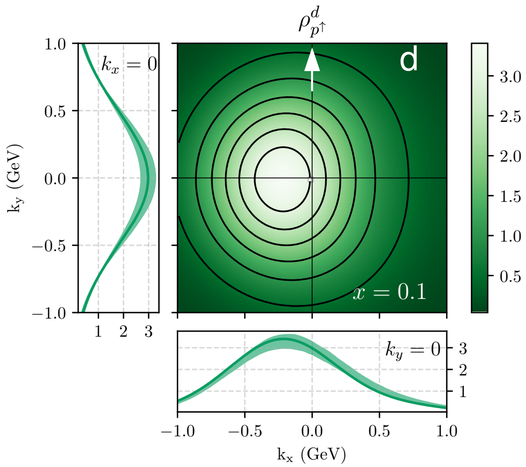

Exclusive production

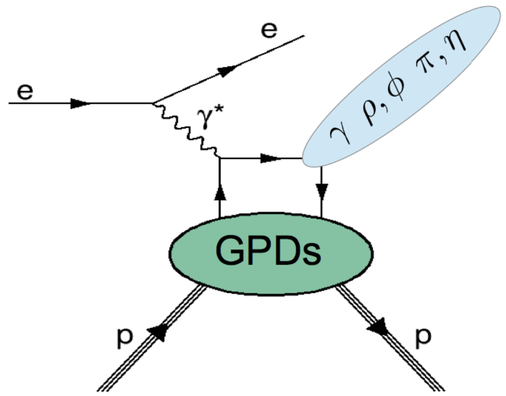

The various dimensions of the nucleon

Wigner distributions $W(x, \vec{k}_T, \vec{b}_\perp)$

$\int d^2\vec{b}_\perp$

$\int d^2\vec{k}_T$

transverse-momentum dependent (TMD) parton distribution functions (PDFs)

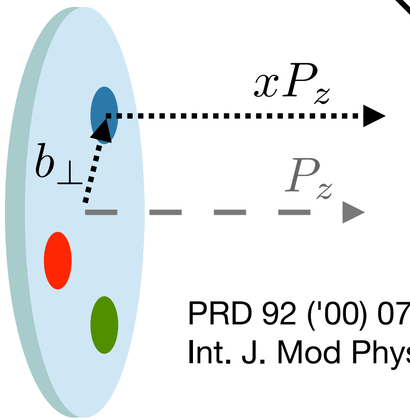

impact-parameter dependent PDFs

PRD 92 ('00) 071503
Int. J. Mod Phys. A 18 ('03) 173

Fourier transform

generalised parton distributions (GPDs)

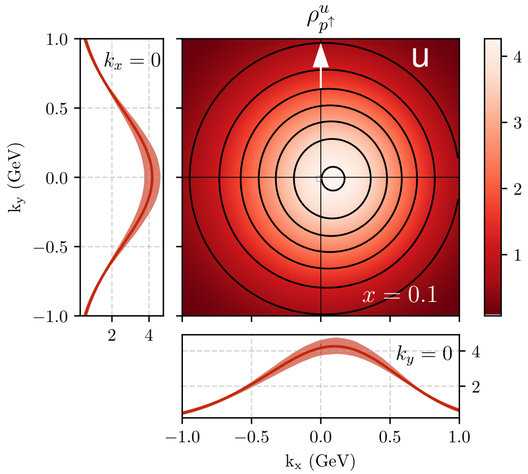

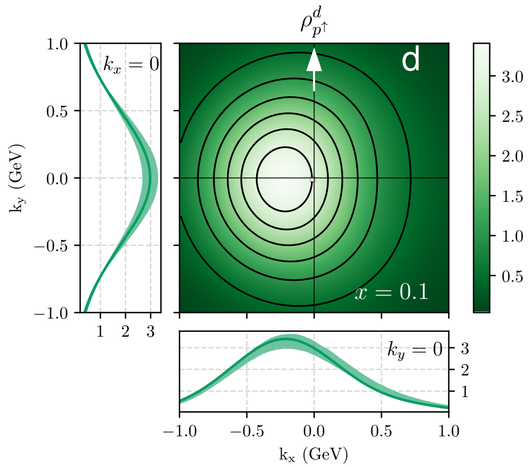

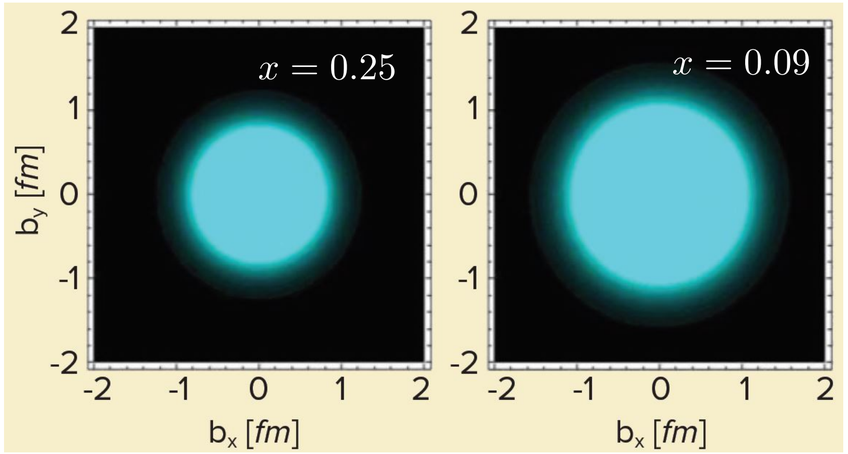

The various dimensions of the nucleon

Wigner distributions $W(x, \vec{k}_T, \vec{b}_\perp)$

$\int d^2\vec{b}_\perp$

$\int d^2\vec{k}_T$

transverse-momentum dependent (TMD) parton distribution functions (PDFs)

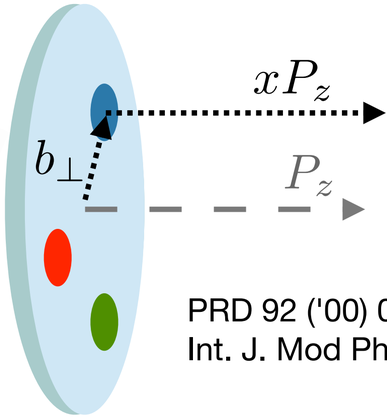

impact-parameter dependent PDFs

PRD 92 ('00) 071503
Int. J. Mod Phys. A 18 ('03) 173

Fourier transform

generalised parton distributions (GPDs)

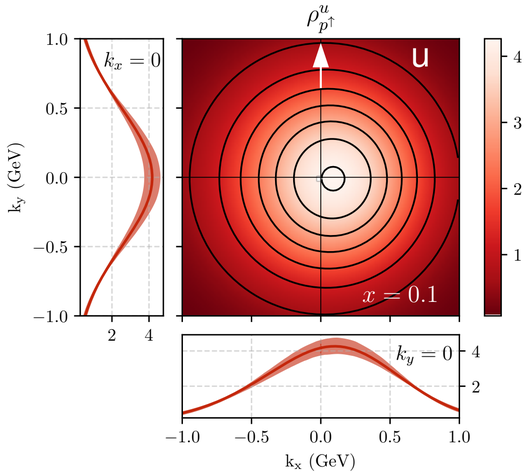

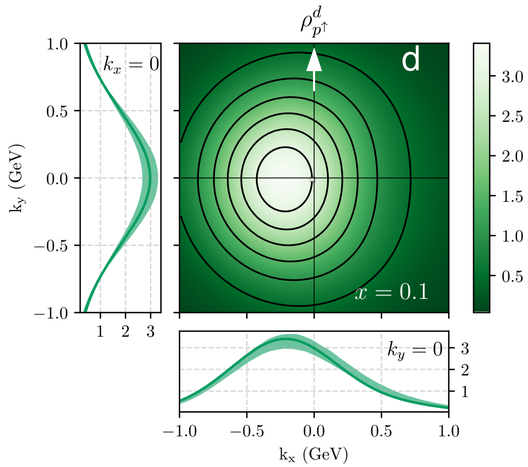

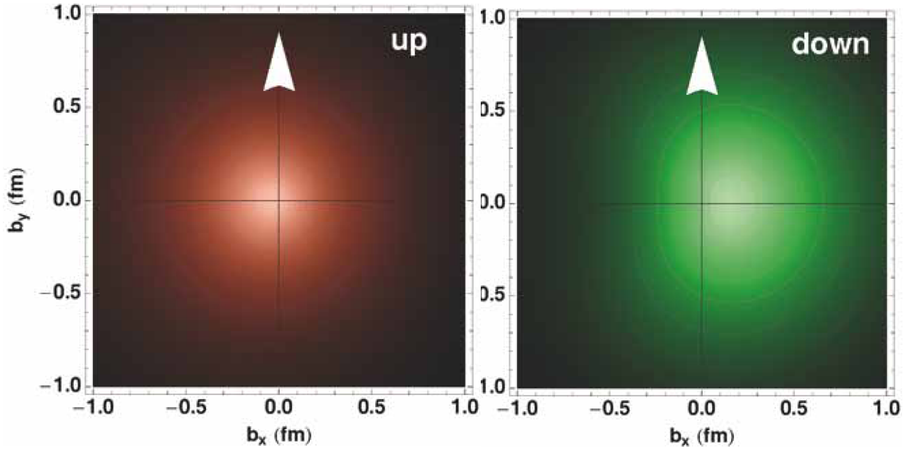

The various dimensions of the nucleon

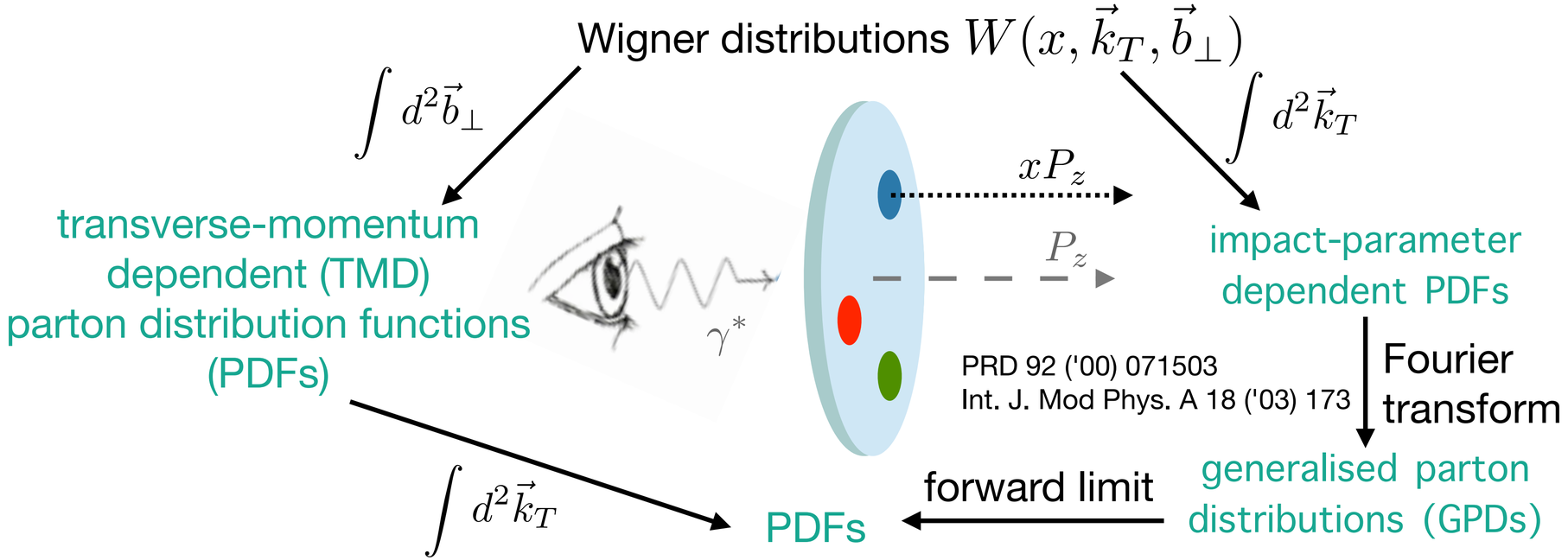

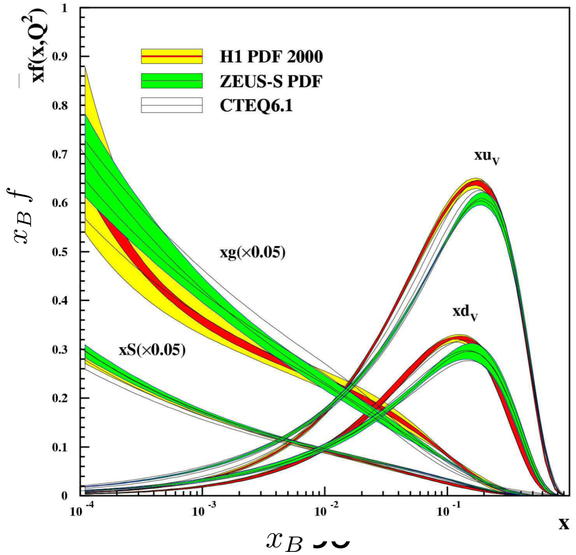

Transverse-momentum-dependent PDFs (TMD PDFs)

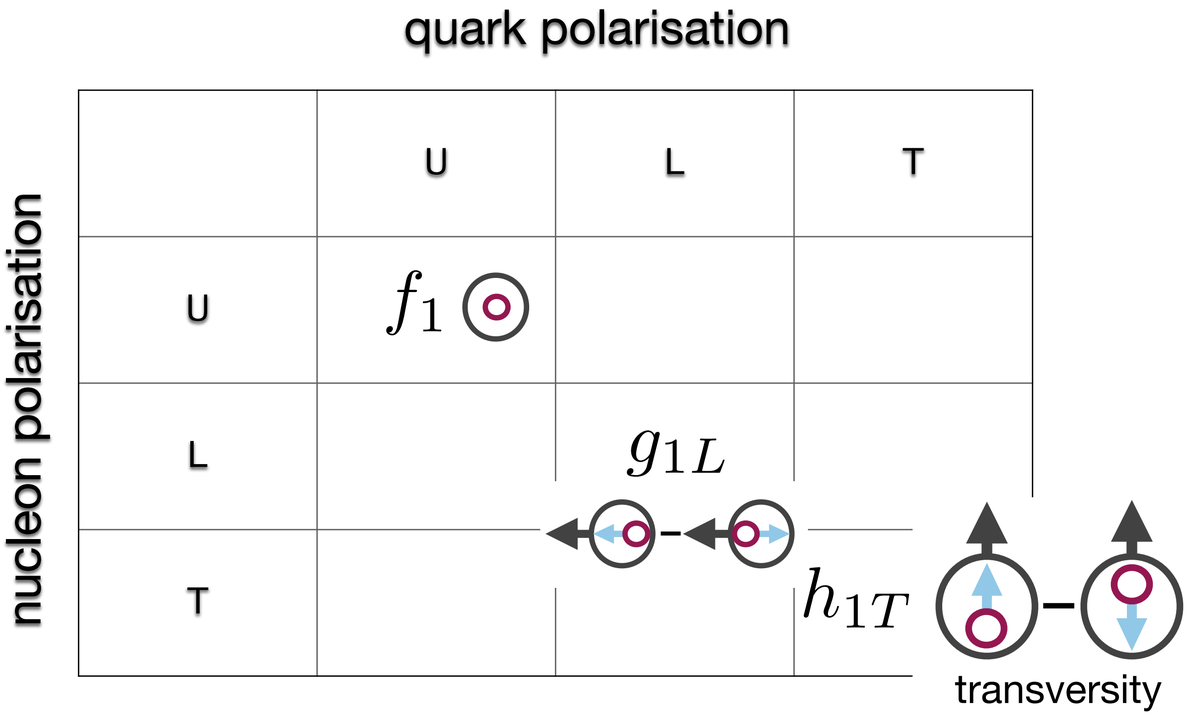

survive integration of parton transverse momentum

Transverse-momentum-dependent PDFs (TMD PDFs)

quark polarisation

nucleon polarisation	U	L	T
U	f_1		$h_1^\perp$
L		g_{1L}	$h_{1L}^\perp$
T	$f_{1T}^\perp$	$g_{1T}^\perp$	$h_{1T}\, h_{1T}^\perp$

Transverse-momentum-dependent PDFs (TMD PDFs)

quark polarisation

nucleon polarisation	U	L	T
U	f_1		$h_1^\perp$
L		g_{1L}	$h_{1L}^\perp$
T	$f_{1T}^\perp$	$g_{1T}^\perp$	$h_{1T}\, h_{1T}^\perp$

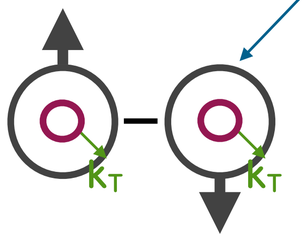

Transverse-momentum-dependent PDFs (TMD PDFs)

quark polarisation

nucleon polarisation	U	L	T
U	f_1		$h_1^\perp$
L		g_{1L}	$h_{1L}^\perp$
T	$f_{1T}^\perp$	$g_{1T}^\perp$	$h_{1T}\, h_{1T}^\perp$

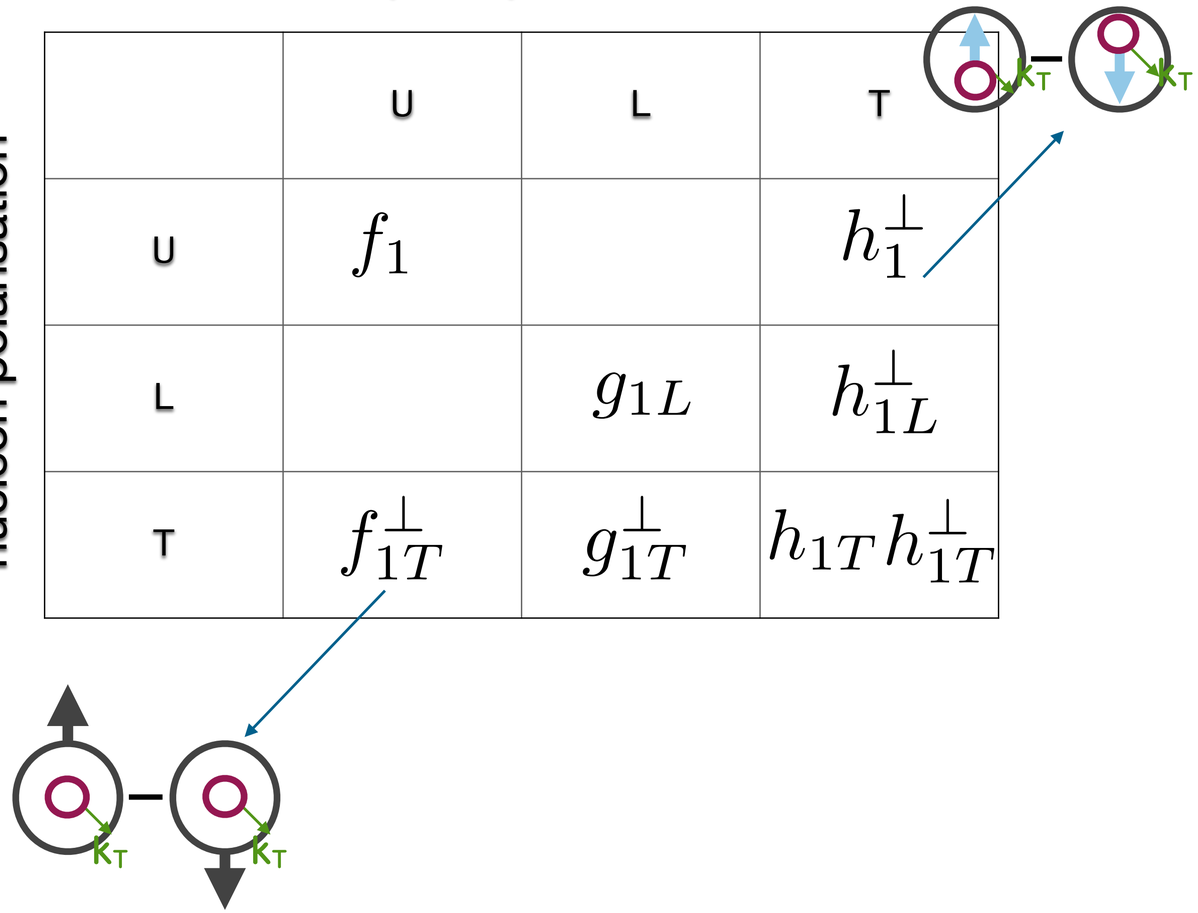

Transverse-momentum-dependent PDFs (TMD PDFs)

quark polarisation

nucleon polarisation	U	L	T
U	f_1		$h_1^\perp$
L		g_{1L}	$h_{1L}^\perp$
T	$f_{1T}^\perp$	$g_{1T}^\perp$	$h_{1T}\, h_{1T}^\perp$

Chiral odd

Transverse-momentum-dependent PDFs (TMD PDFs)

quark polarisation

nucleon polarisation	U	L	T
U	f_1		$h_1^\perp$
L		g_{1L}	$h_{1L}^\perp$
T	$f_{1T}^\perp$	$g_{1T}^\perp$	$h_{1T}\, h_{1T}^\perp$

Chiral odd

Naive T-odd

TMD PDFs: correlations

Unpolarized

Spin-spin correlations

Spin-momentum correlations

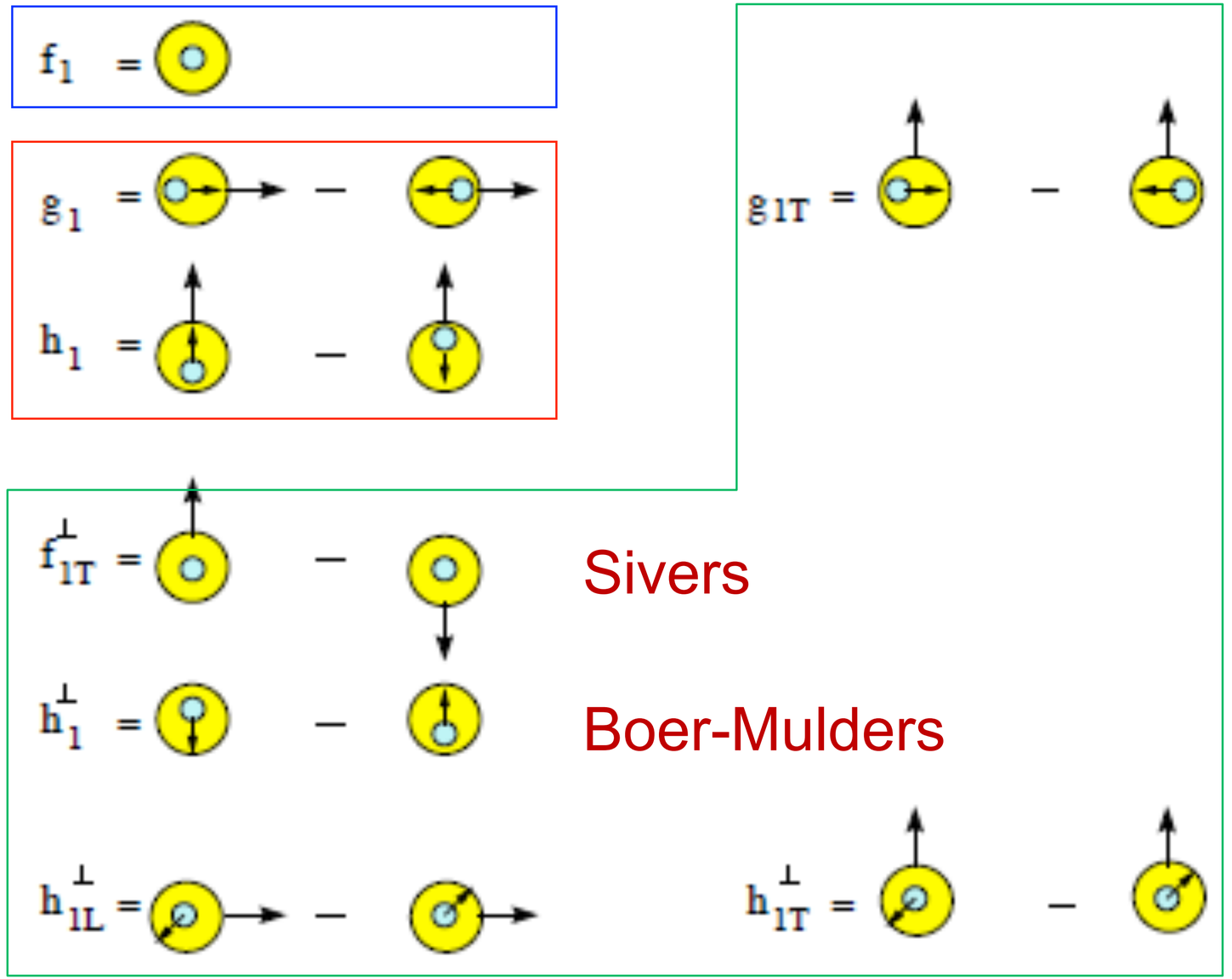

TMD semi-inclusive DIS

$$Q^2 = -q^2$$

$$x_B = \frac{Q^2}{2P \cdot q}$$

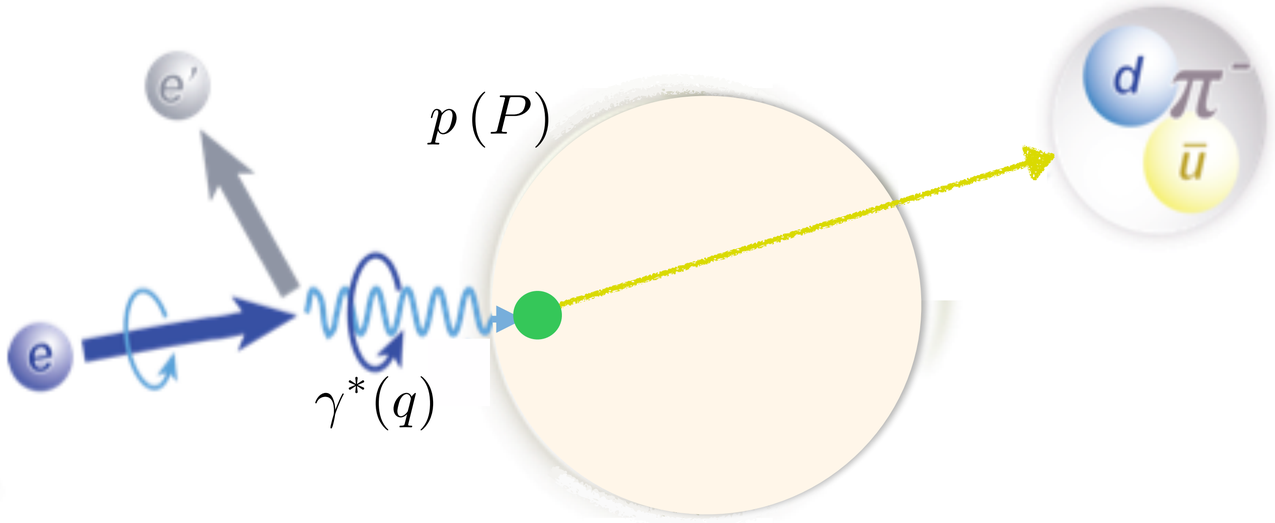

Highly virtual photon:
$Q^2 \gg 1$ GeV^2
provides hard
scale of process

TMD semi-inclusive DIS

$$Q^2 = -q^2$$

$$x_B = \frac{Q^2}{2P \cdot q}$$

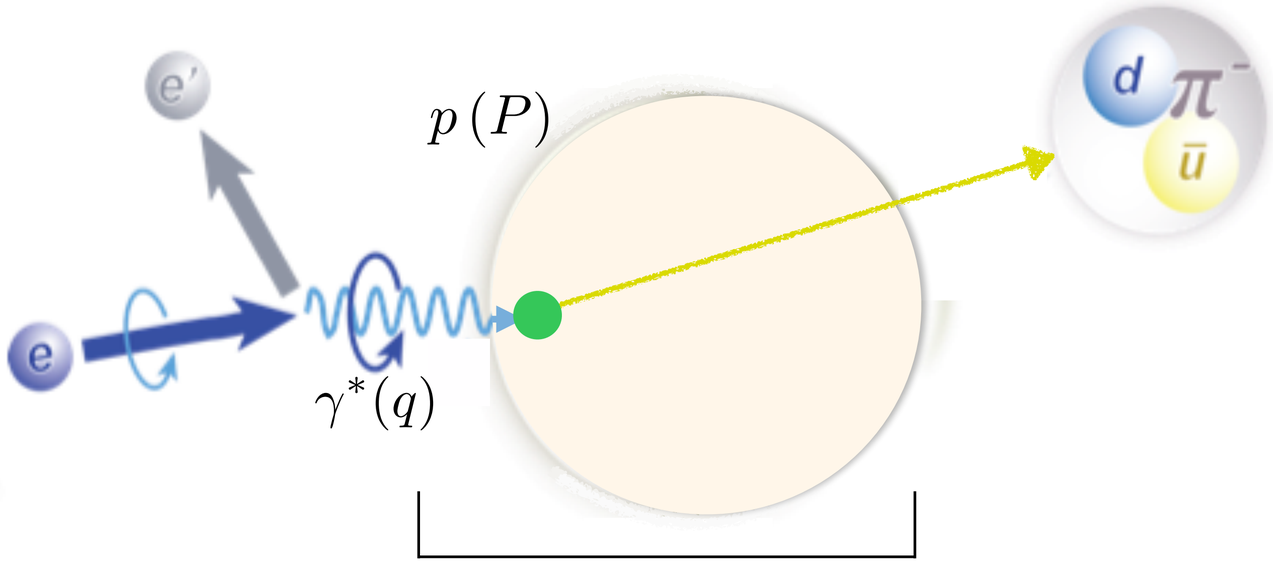

parton distribution function $PDF(x_B)$

Highly virtual photon:
$Q^2 \gg 1$ GeV^2
provides hard
scale of process

TMD semi-inclusive DIS

$$Q^2 = -q^2$$

$$x_B = \frac{Q^2}{2P \cdot q}$$

$$z \overset{\text{lab}}{=} \frac{E_h}{E_{\gamma *}}$$

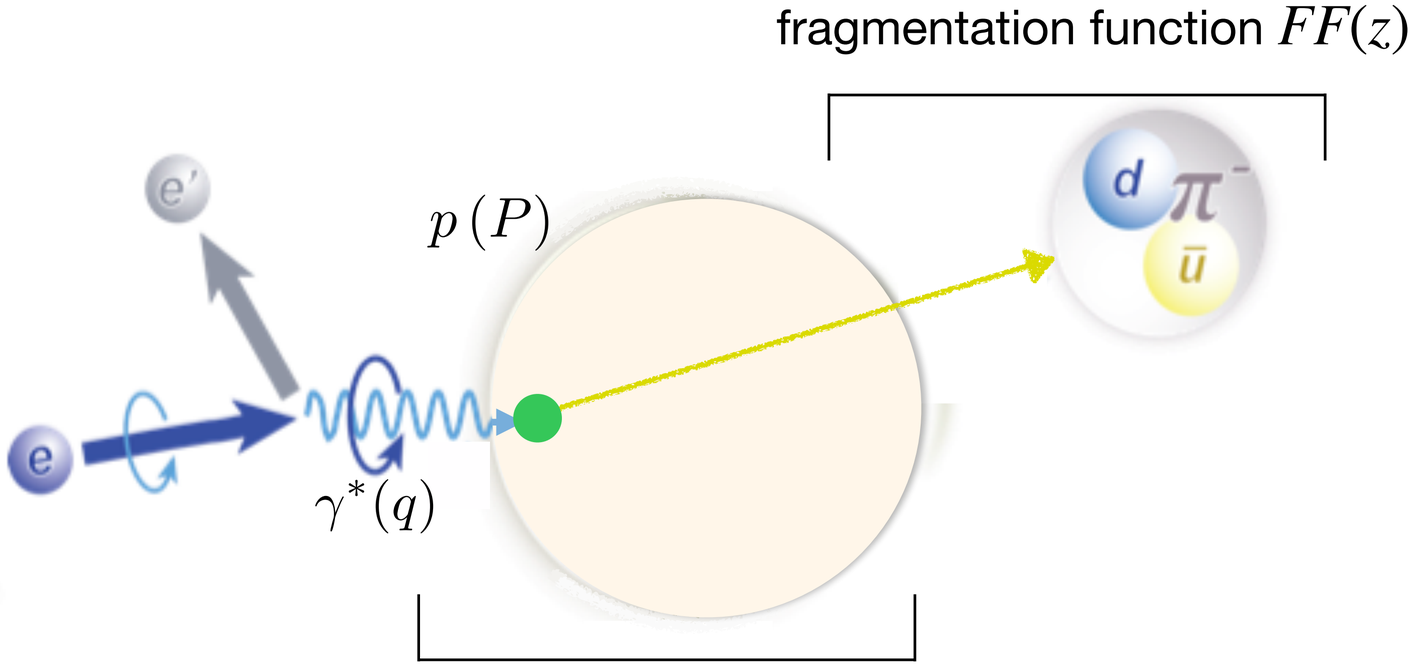

Highly virtual photon:
$Q^2 \gg 1$ GeV^2
provides hard
scale of process

TMD semi-inclusive DIS

$$Q^2 = -q^2$$

$$x_B = \frac{Q^2}{2P \cdot q}$$

$$z \overset{\text{lab}}{=} \frac{E_h}{E_{\gamma *}}$$

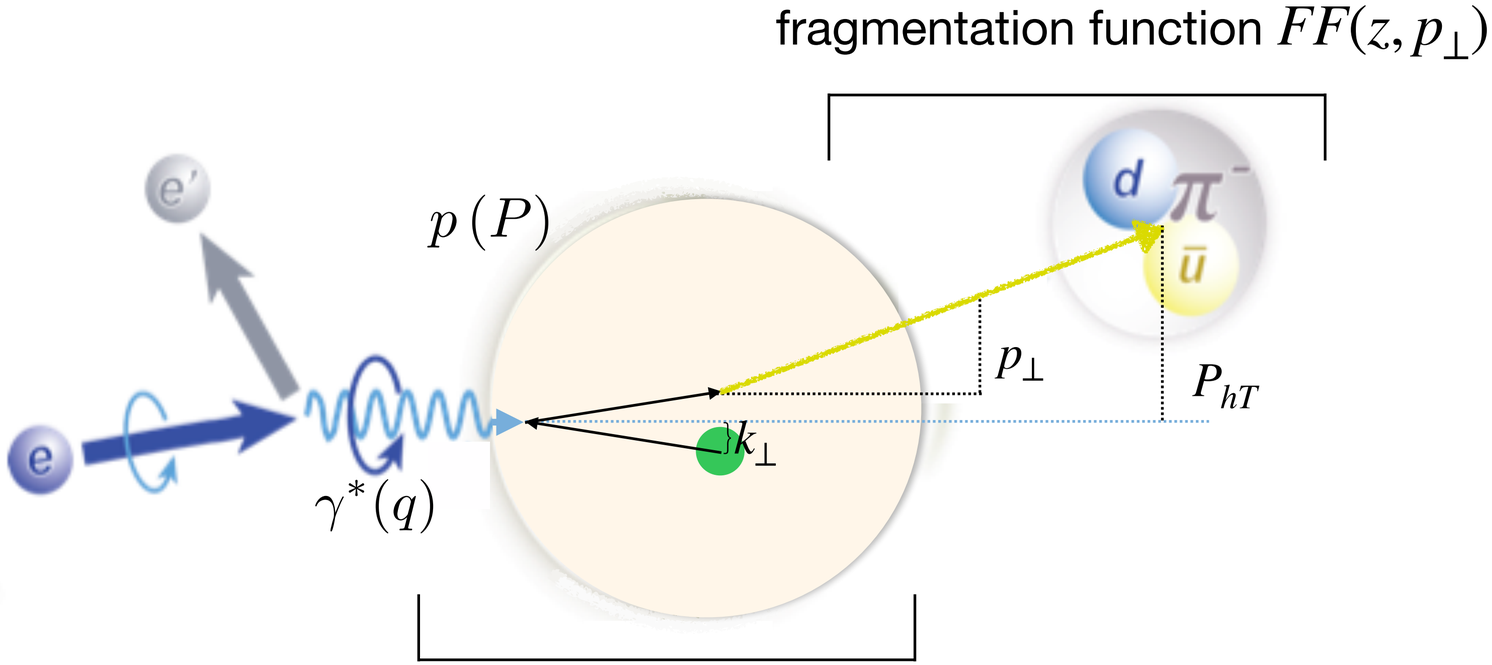

Highly virtual photon:
$Q^2 \gg 1$ GeV^2
provides hard
scale of process

TMD semi-inclusive DIS

$$Q^2 = -q^2$$

$$x_B = \frac{Q^2}{2P \cdot q}$$

$$z \overset{\text{lab}}{=} \frac{E_h}{E_{\gamma *}}$$

fragmentation function $FF(z, p_\perp, Q^2)$

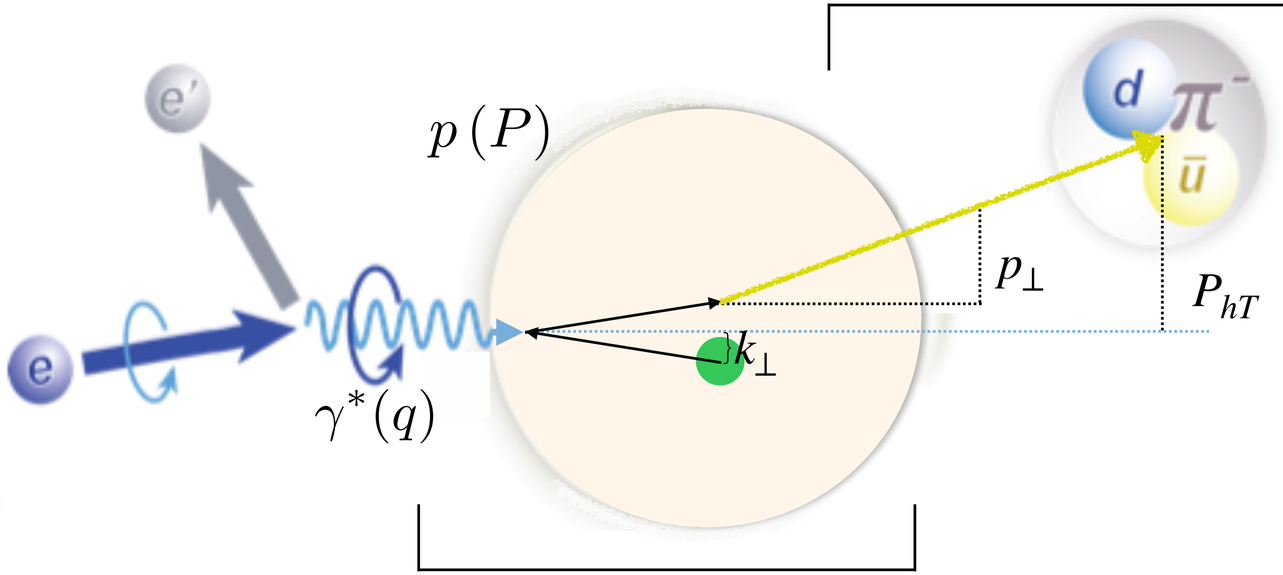

Transverse-momentum-dependent (TMD)
parton distribution function $PDF(x_B, k_\perp, Q^2)$

TMD evolution

Highly virtual photon:
$Q^2 \gg 1$ GeV^2
provides hard
scale of process

TMD semi-inclusive DIS

$$Q^2 = -q^2$$

$$x_B = \frac{Q^2}{2P \cdot q}$$

$$z \overset{\text{lab}}{=} \frac{E_h}{E_{\gamma *}}$$

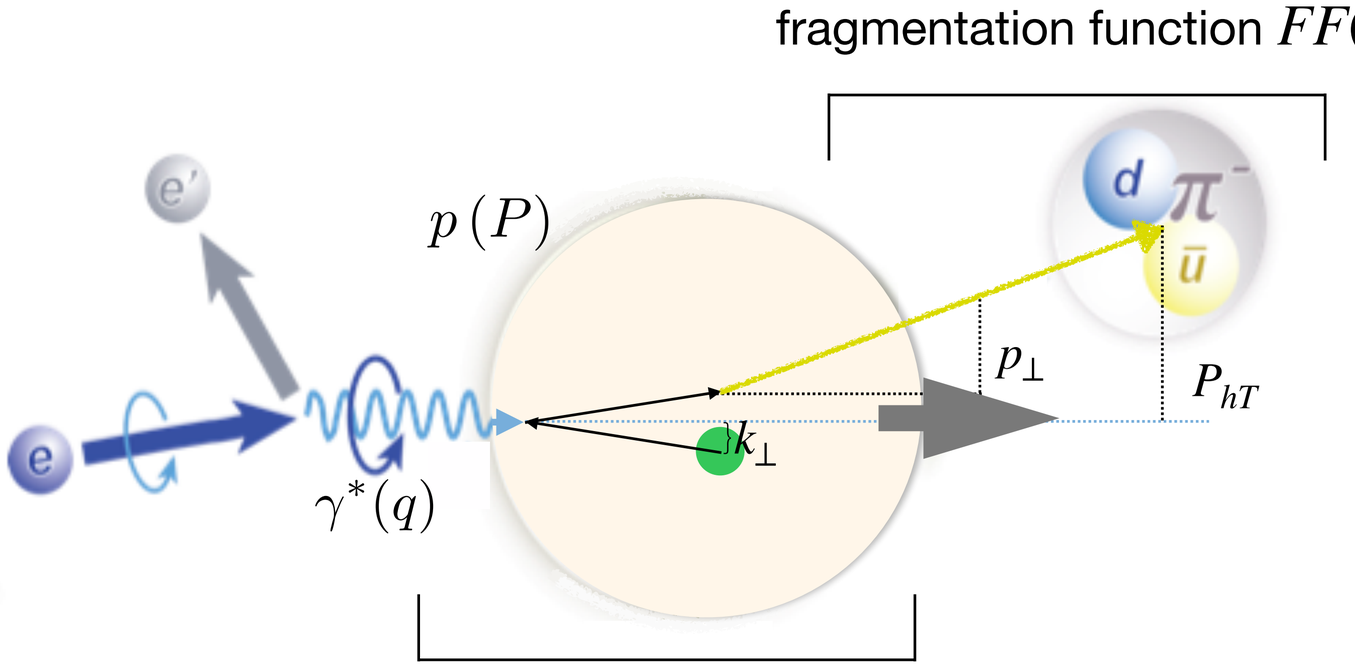

TMD evolution

Highly virtual photon:
$Q^2 \gg 1$ GeV^2
provides hard
scale of process

TMD semi-inclusive DIS

$$Q^2 = -q^2$$

$$x_B = \frac{Q^2}{2P \cdot q}$$

$$z \overset{\text{lab}}{=} \frac{E_h}{E_{\gamma *}}$$

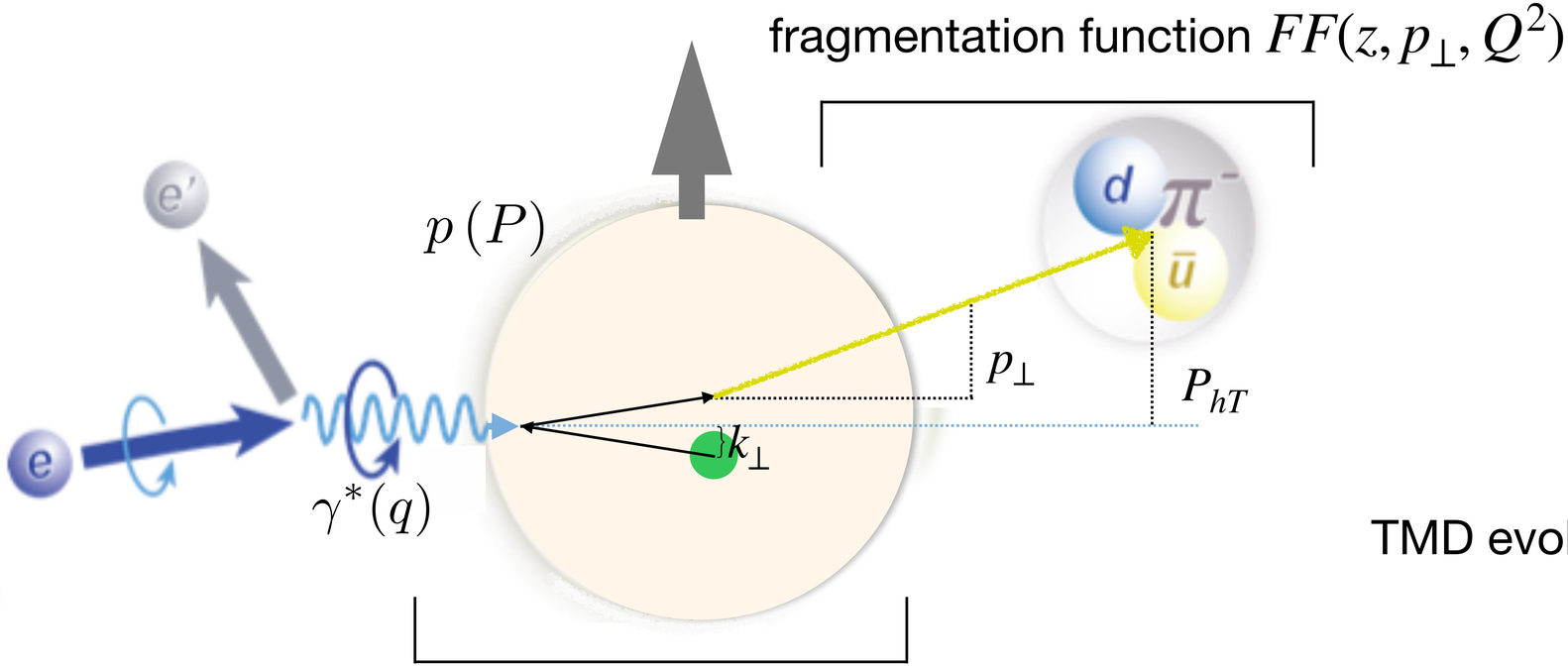

TMD evolution

Highly virtual photon:
$Q^2 \gg 1$ GeV^2
provides hard
scale of process

TMD semi-inclusive DIS

$$Q^2 = -q^2$$

$$x_B = \frac{Q^2}{2P \cdot q}$$

$$z \overset{\text{lab}}{=} \frac{E_h}{E_{\gamma *}}$$

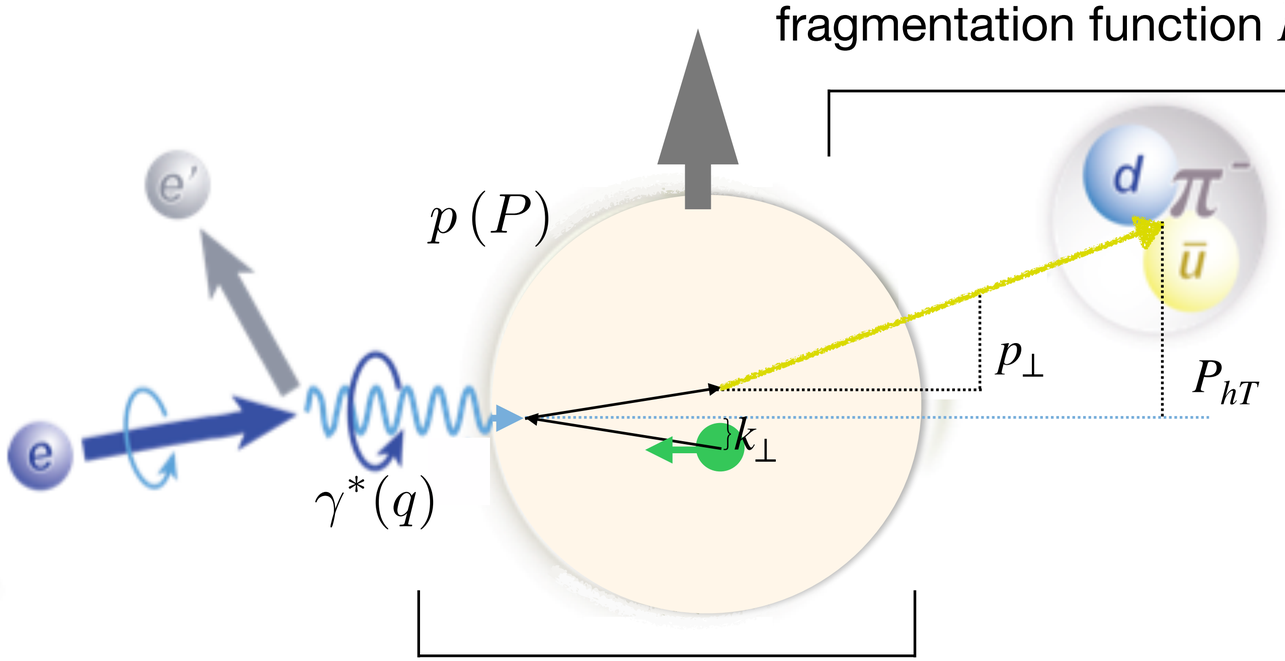

TMD evolution

Highly virtual photon:
$Q^2 \gg 1$ GeV^2
provides hard
scale of process

TMD semi-inclusive DIS

$$Q^2 = -q^2$$

$$x_B = \frac{Q^2}{2P \cdot q}$$

$$z \overset{\text{lab}}{=} \frac{E_h}{E_{\gamma *}}$$

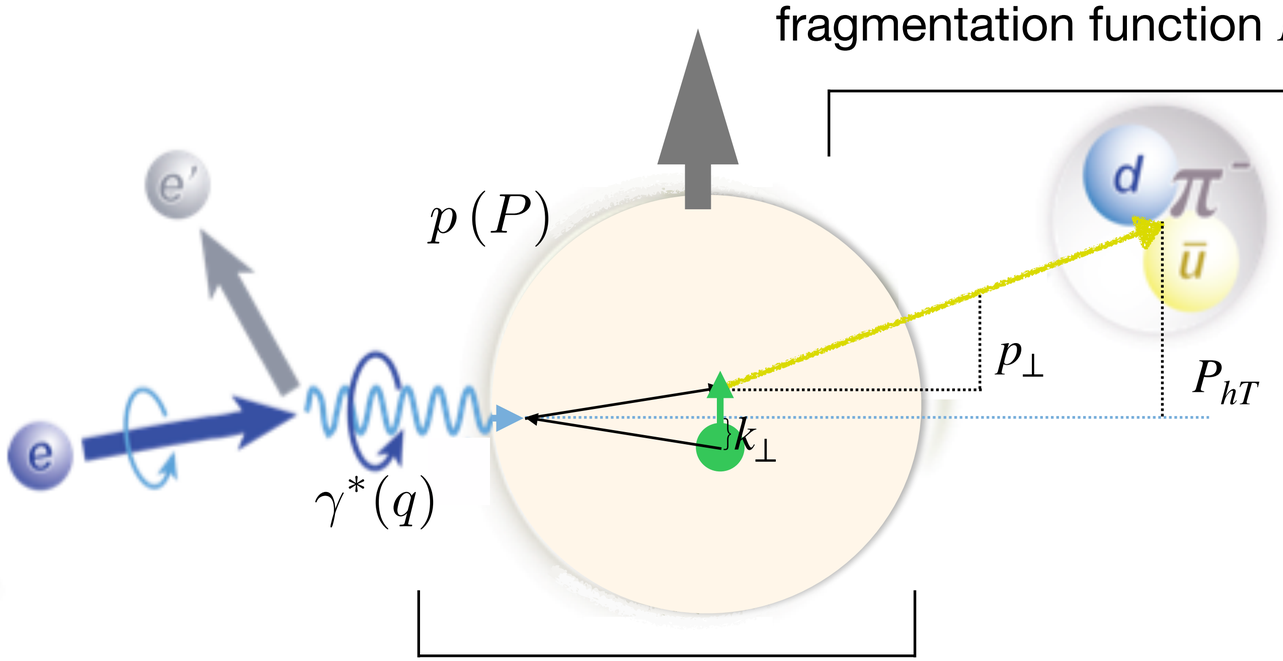

TMD evolution

Highly virtual photon:
$Q^2 \gg 1$ GeV^2
provides hard
scale of process

Semi-inclusive DIS cross section

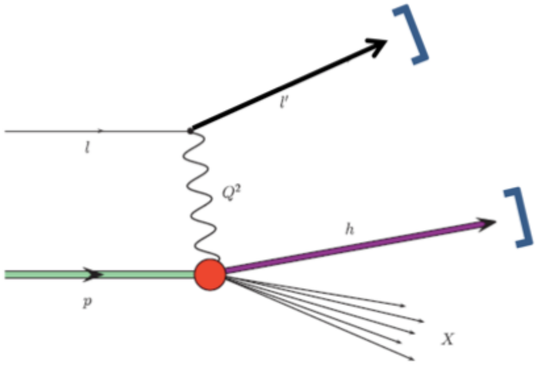

$$
\begin{aligned}
\sigma^h(\phi,\phi_S) &= \sigma^h_{UU}\Big\{1+2\langle\cos(\phi)\rangle^h_{UU}\,\cos(\phi)+2\langle\cos(2\phi)\rangle^h_{UU}\,\cos(2\phi)\\
&+ \lambda_l\,2\langle\sin(\phi)\rangle^h_{LU}\,\sin(\phi)\\
&+ S_L\Big[2\langle\sin(\phi)\rangle^h_{UL}\,\sin(\phi)+2\langle\sin(2\phi)\rangle^h_{UL}\,\sin(2\phi)\\
&+ \lambda_l\Big(2\langle\cos(0\phi)\rangle^h_{LL}\,\cos(0\phi)+2\langle\cos(\phi)\rangle^h_{LL}\,\cos(\phi)\Big)\Big]\\
&+ S_T\Big[2\langle\sin(\phi-\phi_S)\rangle^h_{UT}\,\sin(\phi-\phi_S)+2\langle\,\sin(\phi+\phi_S)\rangle^h_{UT}\,\sin(\phi+\phi_S)\\
&+ 2\langle\sin(3\phi-\phi_S)\rangle^h_{UT}\,\sin(3\phi-\phi_S)+2\langle\sin(\phi_S)\rangle^h_{UT}\,\sin(\phi_S)\\
&+ 2\langle\sin(2\phi-\phi_S)\rangle^h_{UT}\,\sin(2\phi-\phi_S)\\
&+ \lambda_l\Big(2\langle\cos(\phi-\phi_S)\rangle^h_{LT}\,\cos(\phi-\phi_S)\\
&+ 2\langle\cos(\phi_S)\rangle^h_{LT}\,\cos(\phi_S)+2\langle\cos(2\phi-\phi_S)\rangle^h_{LT}\,\cos(2\phi-\phi_S)\Big)\Big]\Big\}
\end{aligned}
$$

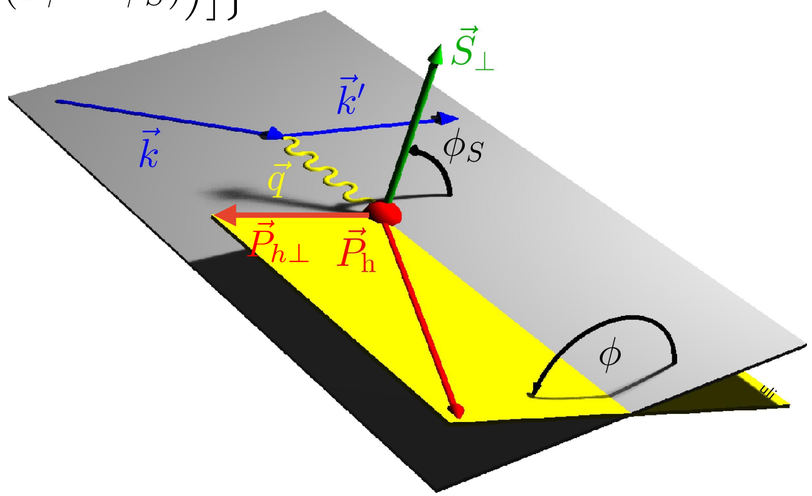

Semi-inclusive DIS cross section

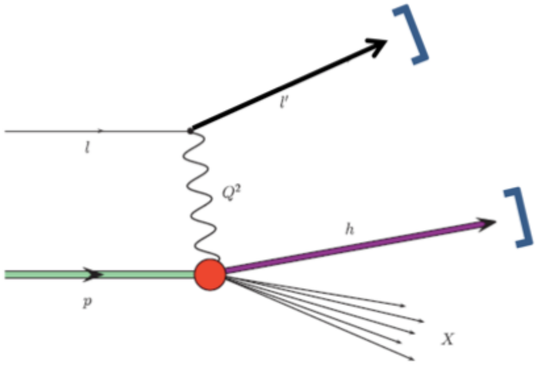

$$
\begin{aligned}
\sigma^h(\phi,\phi_S) &= \sigma^h_{UU}\Big\{1 + 2\langle\cos(\phi)\rangle^h_{UU}\,\cos(\phi) + 2\langle\cos(2\phi)\rangle^h_{UU}\,\cos(2\phi) \\
&+ \lambda_l\, 2\langle\sin(\phi)\rangle^h_{LU}\,\sin(\phi) \\
&+ S_L\Big[2\langle\sin(\phi)\rangle^h_{UL}\,\sin(\phi) + 2\langle\sin(2\phi)\rangle^h_{UL}\,\sin(2\phi) \\
&+ \lambda_l\Big(2\langle\cos(0\phi)\rangle^h_{LL}\,\cos(0\phi) + 2\langle\cos(\phi)\rangle^h_{LL}\,\cos(\phi)\Big)\Big] \\
&+ S_T\Big[2\langle\sin(\phi-\phi_S)\rangle^h_{UT}\,\sin(\phi-\phi_S) + 2\langle\sin(\phi+\phi_S)\rangle^h_{UT}\,\sin(\phi+\phi_S) \\
&+ 2\langle\sin(3\phi-\phi_S)\rangle^h_{UT}\,\sin(3\phi-\phi_S) + 2\langle\sin(\phi_S)\rangle^h_{UT}\,\sin(\phi_S) \\
&+ 2\langle\sin(2\phi-\phi_S)\rangle^h_{UT}\,\sin(2\phi-\phi_S) \\
&+ \lambda_l\Big(2\langle\cos(\phi-\phi_S)\rangle^h_{LT}\,\cos(\phi-\phi_S) \\
&+ 2\langle\cos(\phi_S)\rangle^h_{LT}\,\cos(\phi_S) + 2\langle\cos(2\phi-\phi_S)\rangle^h_{LT}\,\cos(2\phi-\phi_S)\Big)\Big]\Big\}
\end{aligned}
$$

longitudinal target polarisation

transverse target polarisation

beam polarisation

beam polarisation

target polarisation

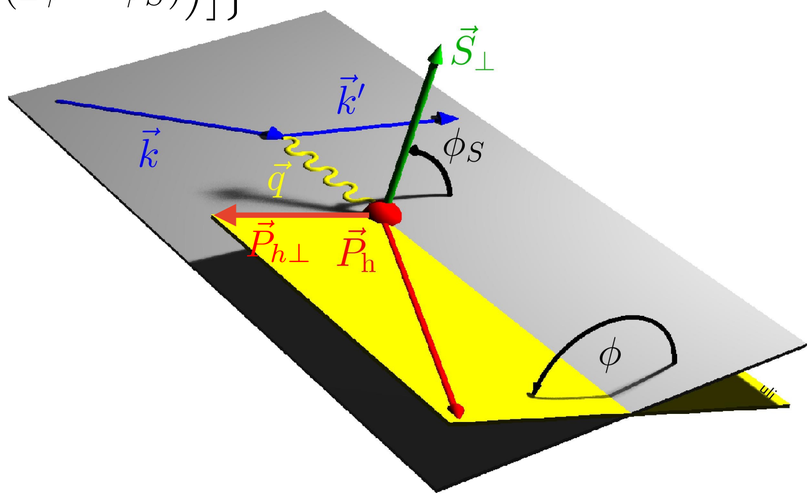

Semi-inclusive DIS cross section

$$
\begin{aligned}
\sigma^h(\phi,\phi_S) &= \sigma^h_{UU}\Big\{1 + 2\langle\cos(\phi)\rangle^h_{UU}\,\cos(\phi) + 2\langle\cos(2\phi)\rangle^h_{UU}\,\cos(2\phi) \\
&+ \lambda_l\, 2\langle\sin(\phi)\rangle^h_{LU}\,\sin(\phi) \\
&+ S_L\Big[2\langle\sin(\phi)\rangle^h_{UL}\,\sin(\phi) + 2\langle\sin(2\phi)\rangle^h_{UL}\,\sin(2\phi) \\
&+ \lambda_l\Big(2\langle\cos(0\phi)\rangle^h_{LL}\,\cos(0\phi) + 2\langle\cos(\phi)\rangle^h_{LL}\,\cos(\phi)\Big)\Big] \\
&+ S_T\Big[2\langle\sin(\phi-\phi_S)\rangle^h_{UT}\,\sin(\phi-\phi_S) + 2\langle\sin(\phi+\phi_S)\rangle^h_{UT}\,\sin(\phi+\phi_S) \\
&+ 2\langle\sin(3\phi-\phi_S)\rangle^h_{UT}\,\sin(3\phi-\phi_S) + 2\langle\sin(\phi_S)\rangle^h_{UT}\,\sin(\phi_S) \\
&+ 2\langle\sin(2\phi-\phi_S)\rangle^h_{UT}\,\sin(2\phi-\phi_S) \\
&+ \lambda_l\Big(2\langle\cos(\phi-\phi_S)\rangle^h_{LT}\,\cos(\phi-\phi_S) \\
&+ 2\langle\cos(\phi_S)\rangle^h_{LT}\,\cos(\phi_S) + 2\langle\cos(2\phi-\phi_S)\rangle^h_{LT}\,\cos(2\phi-\phi_S)\Big)\Big]\Big\}
\end{aligned}
$$

longitudinal target polarisation

transverse target polarisation

beam polarisation

leading twist

beam polarisation

target polarisation

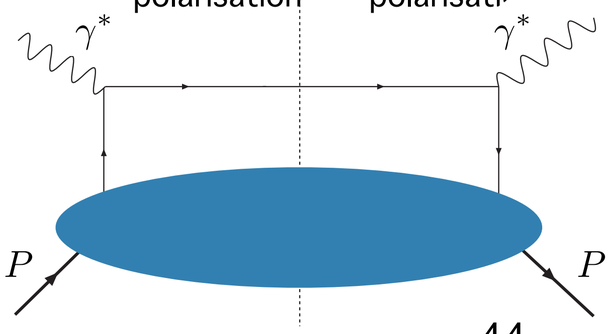

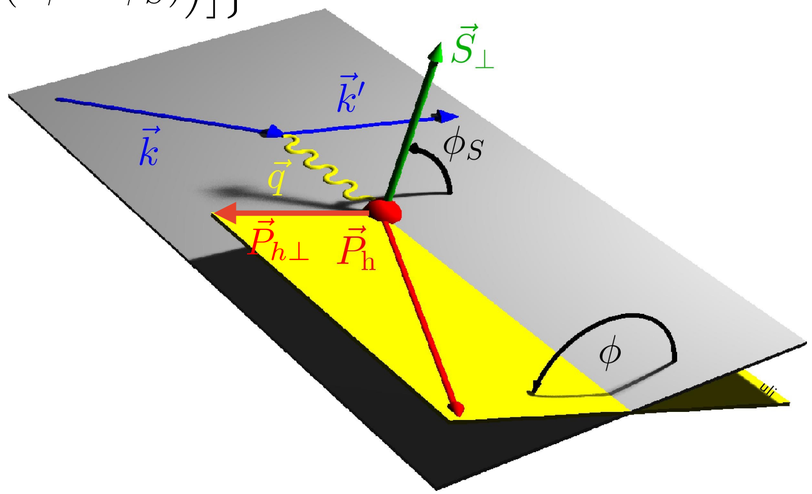

Semi-inclusive DIS cross section

$$
\begin{aligned}
\sigma^h(\phi,\phi_S) &= \sigma^h_{UU}\Big\{1 + 2\langle\cos(\phi)\rangle^h_{UU}\cos(\phi) + 2\langle\cos(2\phi)\rangle^h_{UU}\cos(2\phi) \\
&+ \lambda_l\, 2\langle\sin(\phi)\rangle^h_{LU}\sin(\phi) \\
&+ S_L\Big[2\langle\sin(\phi)\rangle^h_{UL}\sin(\phi) + 2\langle\sin(2\phi)\rangle^h_{UL}\sin(2\phi) \\
&+ \lambda_l\Big(2\langle\cos(0\phi)\rangle^h_{LL}\cos(0\phi) + 2\langle\cos(\phi)\rangle^h_{LL}\cos(\phi)\Big)\Big] \\
&+ S_T\Big[2\langle\sin(\phi-\phi_S)\rangle^h_{UT}\sin(\phi-\phi_S) + 2\langle\sin(\phi+\phi_S)\rangle^h_{UT}\sin(\phi+\phi_S) \\
&+ 2\langle\sin(3\phi-\phi_S)\rangle^h_{UT}\sin(3\phi-\phi_S) + 2\langle\sin(\phi_S)\rangle^h_{UT}\sin(\phi_S) \\
&+ 2\langle\sin(2\phi-\phi_S)\rangle^h_{UT}\sin(2\phi-\phi_S) \\
&+ \lambda_l\Big(2\langle\cos(\phi-\phi_S)\rangle^h_{LT}\cos(\phi-\phi_S) \\
&+ 2\langle\cos(\phi_S)\rangle^h_{LT}\cos(\phi_S) + 2\langle\cos(2\phi-\phi_S)\rangle^h_{LT}\cos(2\phi-\phi_S)\Big)\Big]\Big\}
\end{aligned}
$$

longitudinal target polarisation

transverse target polarisation

beam polarisation

sub-leading twist

beam polarisation

target polarisation

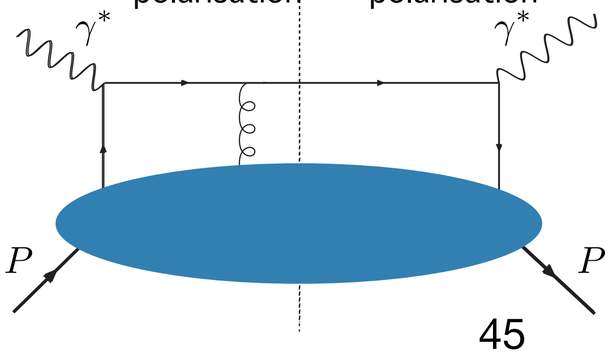

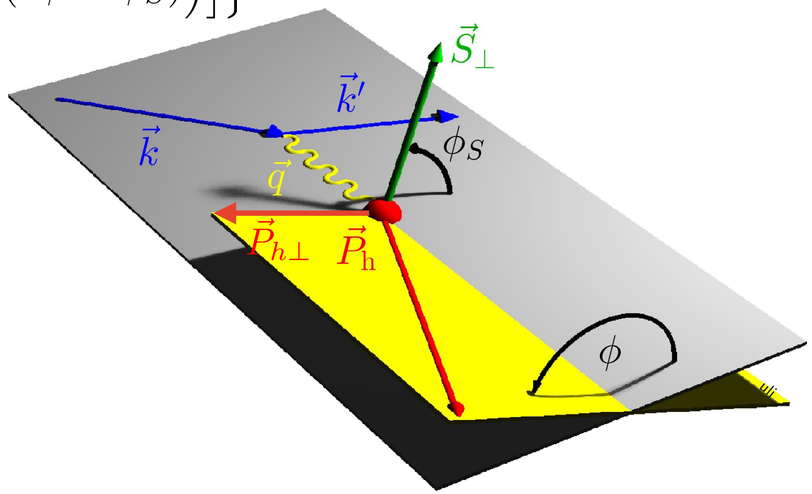

TMD PDFs and TMD fragmentation functions

Azimuthal amplitudes related to structure functions F_{XY} :

$$2\langle \sin(\phi + \phi_S)\rangle^h_{UT} = \epsilon\, F^{\sin(\phi+\phi_S)}_{UT}$$

TMD PDFs and TMD fragmentation functions

Azimuthal amplitudes related to structure functions F_{XY} :

$$2\langle \sin(\phi + \phi_S)\rangle^h_{UT} = \epsilon\, F^{\sin(\phi+\phi_S)}_{UT}$$

$$F_{XY} \propto \mathcal{C}\left[\text{TMD PDF}(x, k_\perp) \times \text{ TMD FF } (z, p_\perp)\right]$$

$$z \overset{\text{lab}}{=} \frac{E_h}{E_{\gamma *}}$$

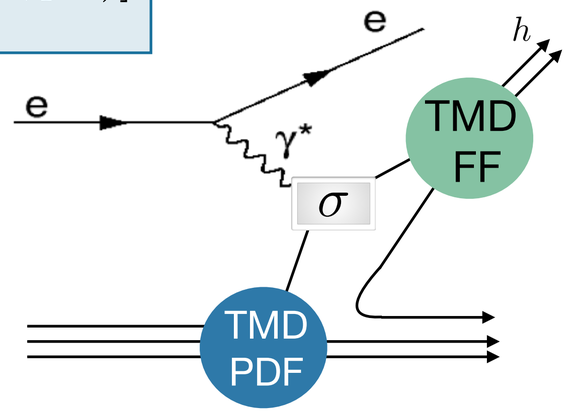

TMD PDFs and TMD fragmentation functions

Azimuthal amplitudes related to structure functions F_{XY} :

$$2\langle \sin(\phi + \phi_S)\rangle^h_{UT} = \epsilon\, F^{\sin(\phi+\phi_S)}_{UT}$$

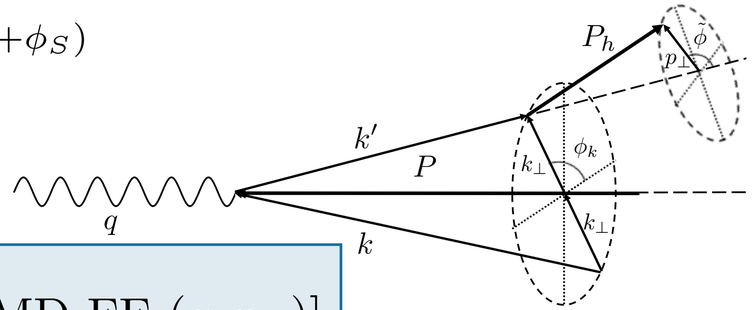

$$F_{XY} \propto \mathcal{C}\left[\text{TMD PDF}(x, k_\perp) \times \text{ TMD FF } (z, p_\perp)\right]$$

$$z \overset{\text{lab}}{=} \frac{E_h}{E_{\gamma *}}$$

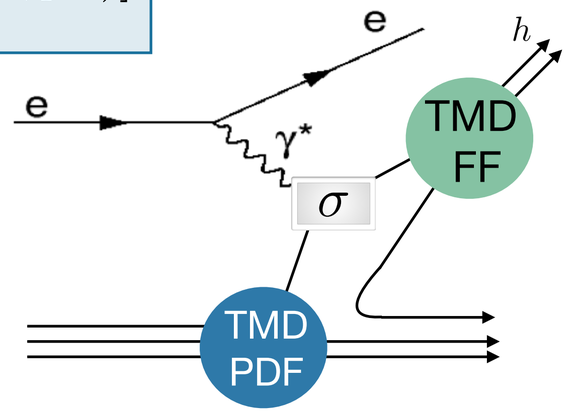

TMD PDFs and TMD fragmentation functions

Azimuthal amplitudes related to structure functions F_{XY} :

$$2\langle \sin(\phi + \phi_S)\rangle^h_{UT} = \epsilon\, F^{\sin(\phi+\phi_S)}_{UT}$$

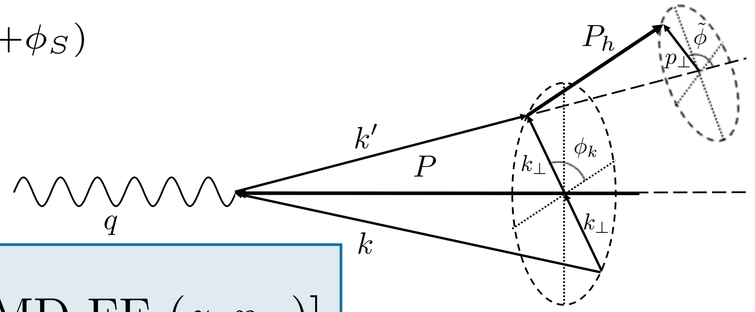

$$F_{XY} \propto \mathcal{C}\left[\text{TMD PDF}(x, k_\perp) \times \text{ TMD FF } (z, p_\perp)\right]$$

$$z \overset{\text{lab}}{=} \frac{E_h}{E_{\gamma *}}$$

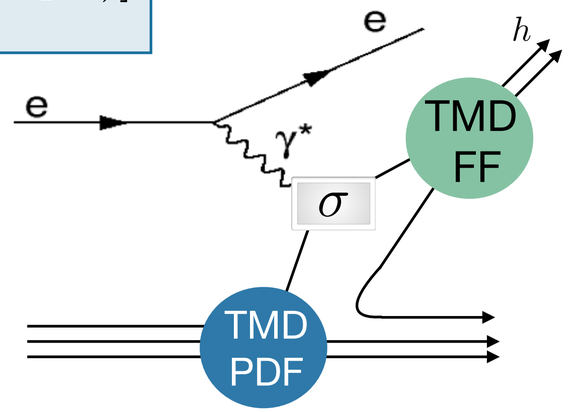

quark polarisation

nucleon polarisation

	U	L	T
U	f_1		$h_1^\perp$
L		g_{1L}	$h_{1L}^\perp$
T	$f_{1T}^\perp$	$g_{1T}^\perp$	$h_{1T}\, h_{1T}^\perp$

TMD PDFs and TMD fragmentation functions

Azimuthal amplitudes related to structure functions F_{XY} :

$$2\langle \sin(\phi+\phi_S)\rangle^h_{UT} = \epsilon\, F^{\sin(\phi+\phi_S)}_{UT}$$

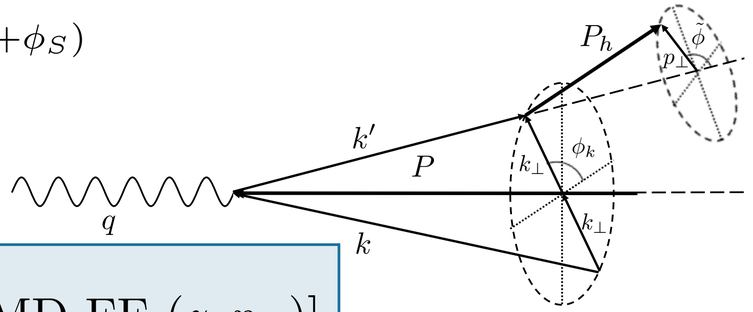

$$F_{XY} \propto \mathcal{C}\left[\text{TMD PDF}(x,k_\perp) \times \text{ TMD FF } (z,p_\perp)\right]$$

$$z \overset{\text{lab}}{=} \frac{E_h}{E_{\gamma*}}$$

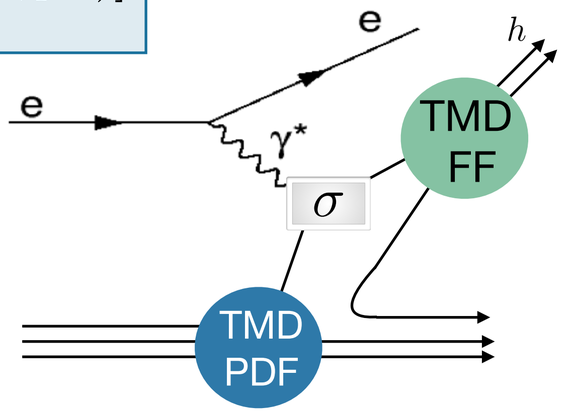

quark polarisation

nucleon polarisation

	U	L	T
U	f_1		$h_1^\perp$
L		g_{1L}	$h_{1L}^\perp$
T	$f_{1T}^\perp$	$g_{1T}^\perp$	$h_{1T}\, h_{1T}^\perp$

quark polarisation

hadron polarisation

	U	L	T
U	D_1		$H_1^\perp$

TMD PDFs and TMD fragmentation functions

Azimuthal amplitudes related to structure functions F_{XY} :

$$2\langle \sin(\phi + \phi_S)\rangle^h_{UT} = \epsilon\, F^{\sin(\phi+\phi_S)}_{UT}$$

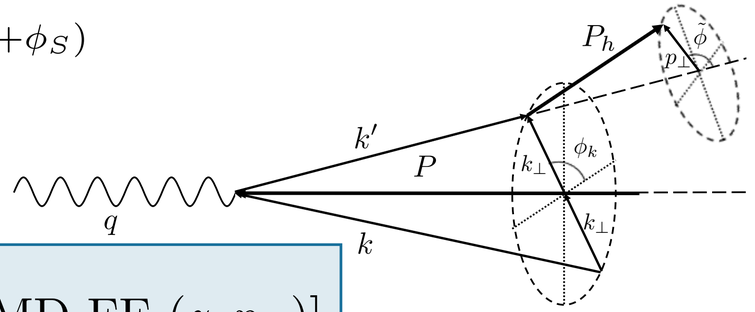

$$F_{XY} \propto \mathcal{C}\left[\text{TMD PDF}(x, k_\perp) \times \text{ TMD FF } (z, p_\perp)\right]$$

$$z \overset{\text{lab}}{=} \frac{E_h}{E_{\gamma *}}$$

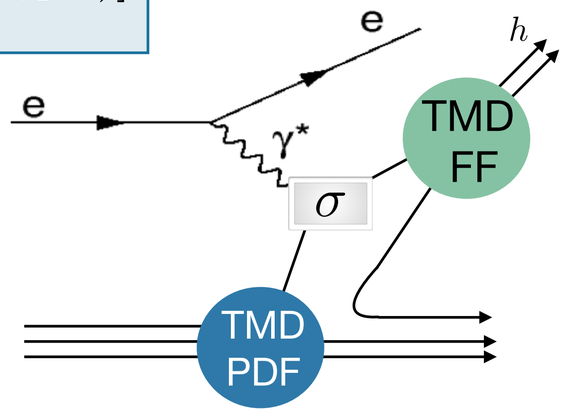

quark polarisation

nucleon polarisation

	U	L	T
U	f_1		$h_1^\perp$
L		g_{1L}	$h_{1L}^\perp$
T	$f_{1T}^\perp$	$g_{1T}^\perp$	$h_{1T}\, h_{1T}^\perp$

quark polarisation

hadron polarisation

	U	L	T
U	D_1		$H_1^\perp$

Chiral odd

TMD PDFs and TMD fragmentation functions

Azimuthal amplitudes related to structure functions F_{XY} :

$$2\langle \sin(\phi+\phi_S)\rangle^h_{UT} = \epsilon\, F^{\sin(\phi+\phi_S)}_{UT}$$

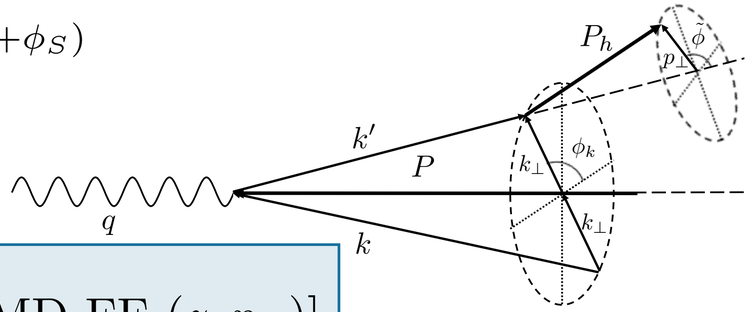

$$F_{XY} \propto \mathcal{C}\left[\text{TMD PDF}(x,k_\perp) \times \text{ TMD FF } (z,p_\perp)\right]$$

$$z \overset{\text{lab}}{=} \frac{E_h}{E_{\gamma *}}$$

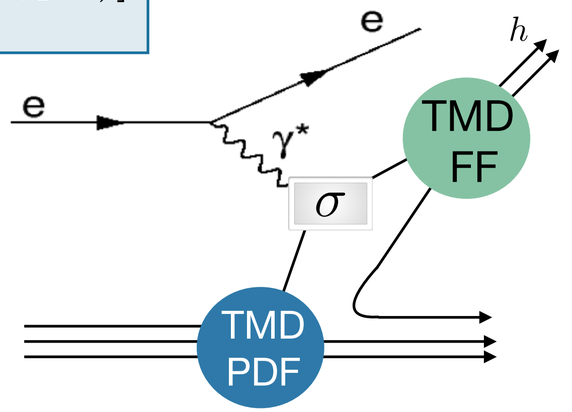

quark polarisation

nucleon polarisation

	U	L	T
U	f_1		$h_1^\perp$
L		g_{1L}	$h_{1L}^\perp$
T	$f_{1T}^\perp$	$g_{1T}^\perp$	$h_{1T}\, h_{1T}^\perp$

quark polarisation

hadron polarisation

	U	L	T
U	D_1		$H_1^\perp$

Chiral odd

Naive T-odd

TMD PDFs and TMD fragmentation functions

Azimuthal amplitudes related to structure functions F_{XY} :

$$2\langle \sin(\phi+\phi_S)\rangle^h_{UT} = \epsilon\, F^{\sin(\phi+\phi_S)}_{UT}$$

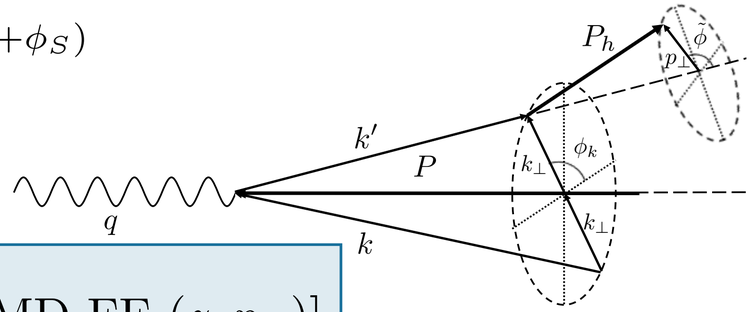

$$F_{XY} \propto \mathcal{C}\left[\text{TMD PDF}(x,k_\perp) \times \text{ TMD FF } (z,p_\perp)\right]$$

$$z \overset{\text{lab}}{=} \frac{E_h}{E_{\gamma*}}$$

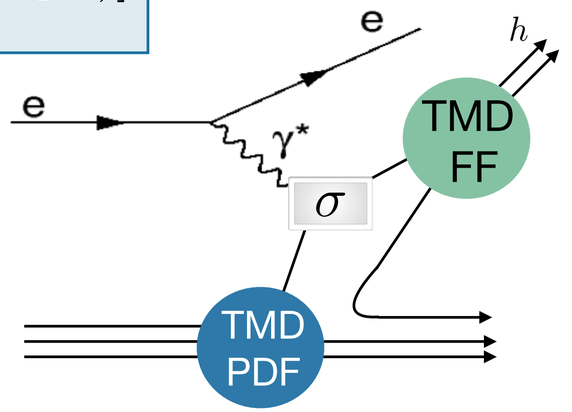

quark polarisation

nucleon polarisation

	U	L	T
U	f_1		$h_1^\perp$
L		g_{1L}	$h_{1L}^\perp$
T	$f_{1T}^\perp$	$g_{1T}^\perp$	$h_{1T}\, h_{1T}^\perp$

quark polarisation

hadron polarisation

	U	L	T
U	D_1		$H_1^\perp$

Chiral odd

Naive T-odd

TMD PDFs and TMD fragmentation functions

Azimuthal amplitudes related to structure functions F_{XY} :

$$2\langle \sin(\phi+\phi_S)\rangle^h_{UT} = \epsilon\, F^{\sin(\phi+\phi_S)}_{UT}$$

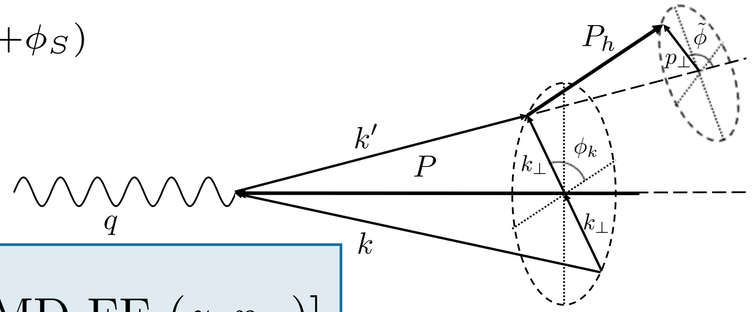

$$F_{XY} \propto \mathcal{C}\left[\text{TMD PDF}(x,k_\perp) \times \text{ TMD FF } (z,p_\perp)\right]$$

$$z \overset{\text{lab}}{=} \frac{E_h}{E_{\gamma*}}$$

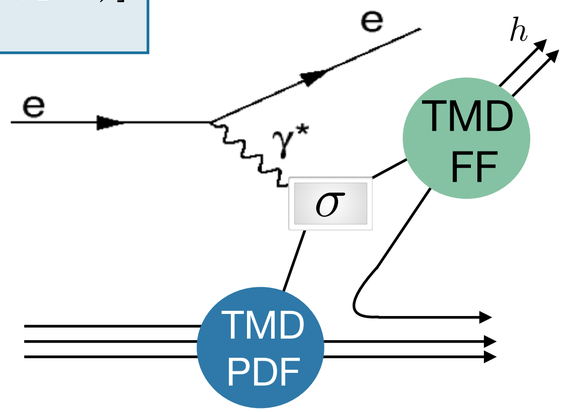

quark polarisation

nucleon polarisation

	U	L	T
U	f_1		$h_1^\perp$
L		g_{1L}	$h_{1L}^\perp$
T	$f_{1T}^\perp$	$g_{1T}^\perp$	$h_{1T}\, h_{1T}^\perp$

quark polarisation

hadron polarisation

	U	L	T
U	D_1		$H_1^\perp$

Chiral odd

Naive T-odd

TMD FFs

Unpolarized

Spin-spin correlations

Spin-momentum correlations

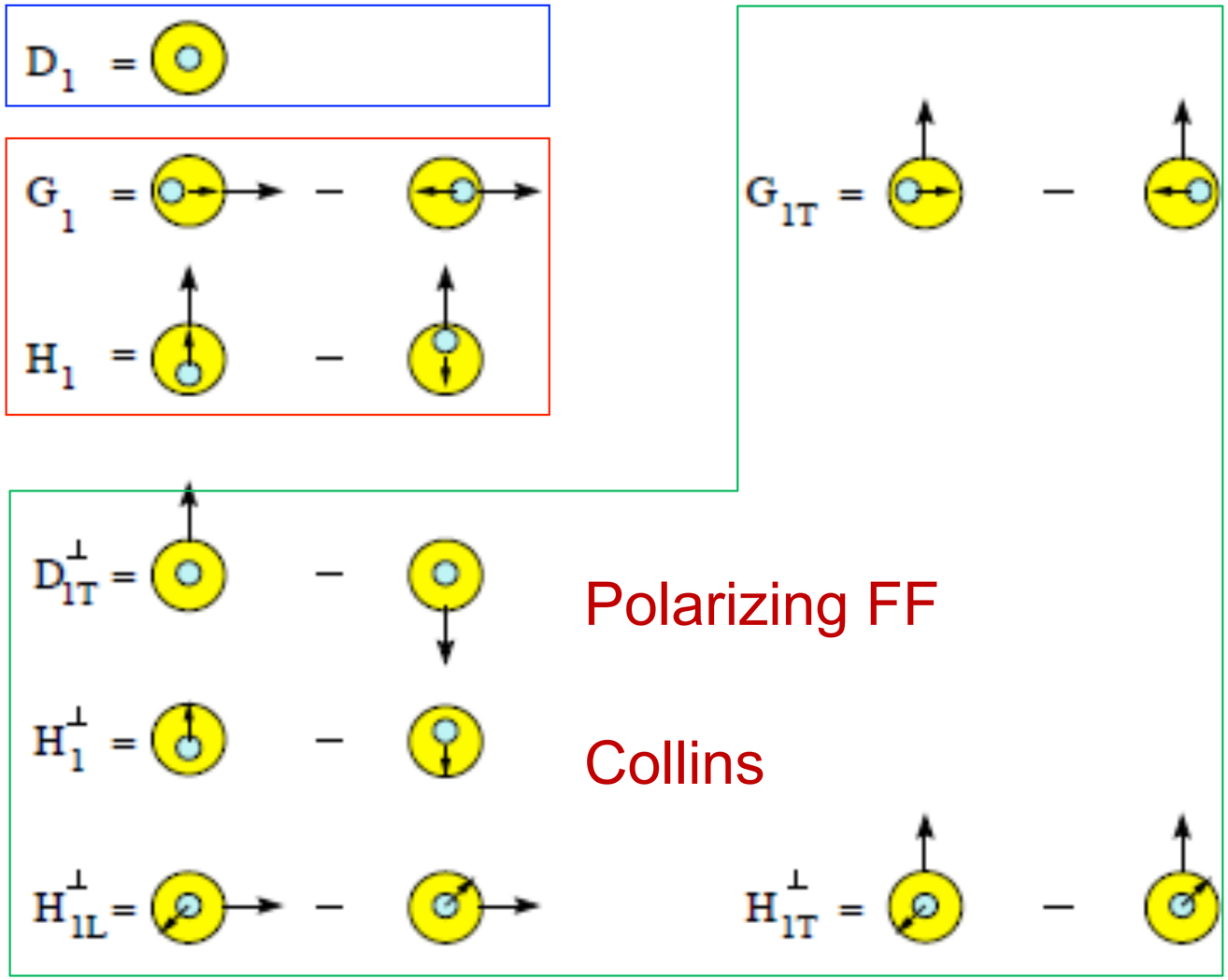

Fragmentation

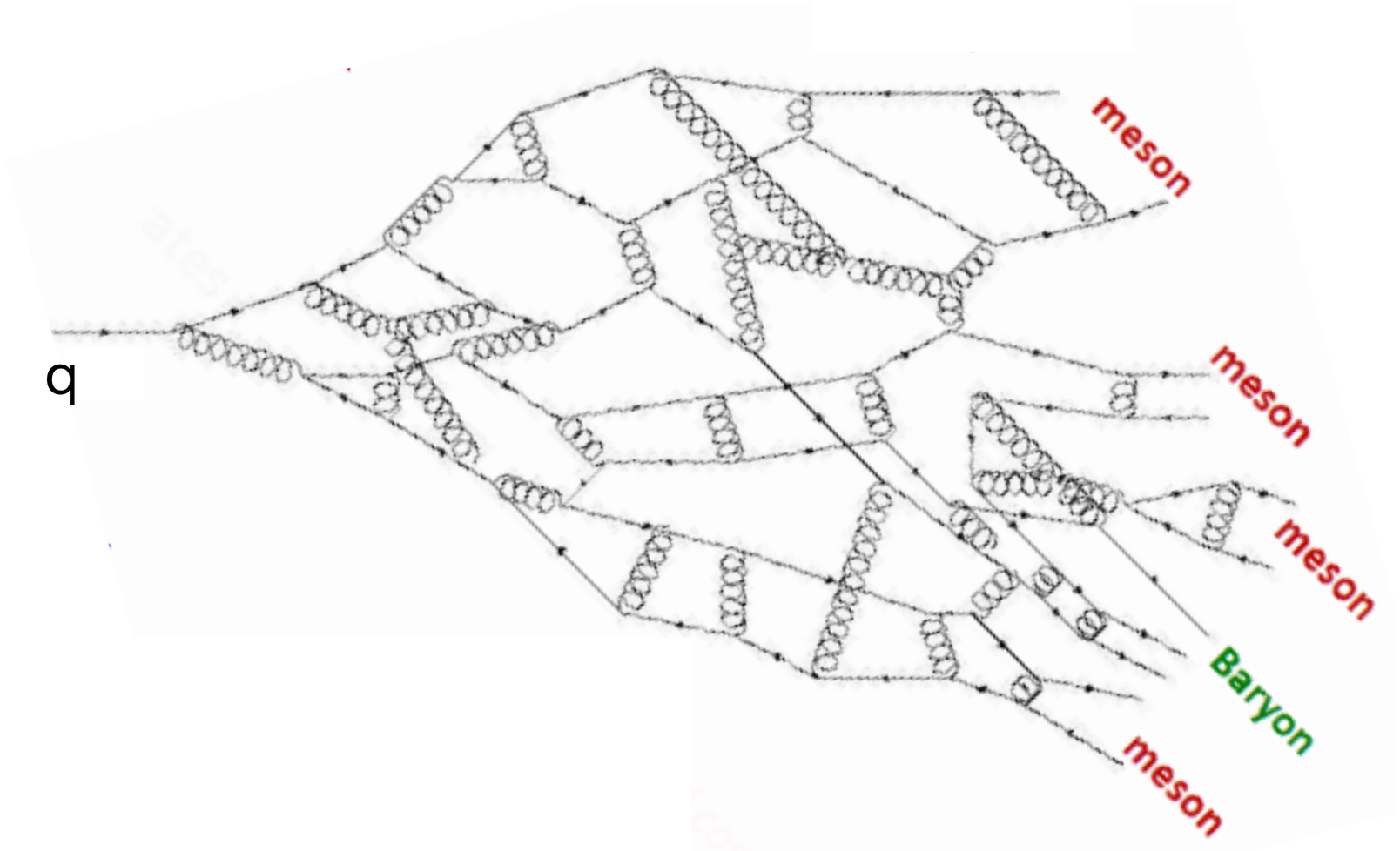

TMDs: factorisation and universality

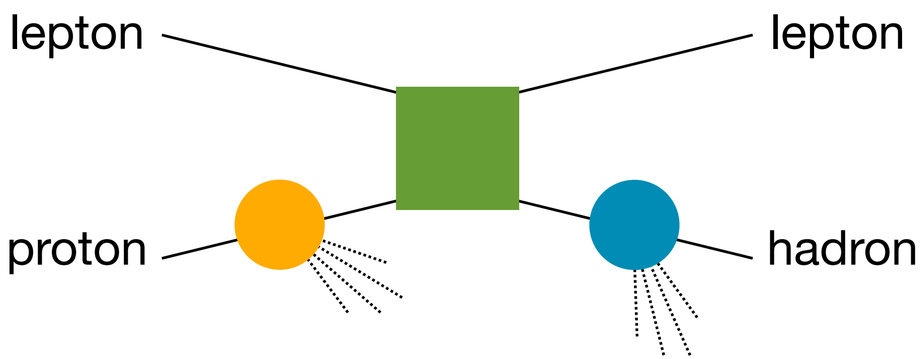

semi-inclusive DIS

Adapted from A. Bacchetta

TMDs: factorisation and universality

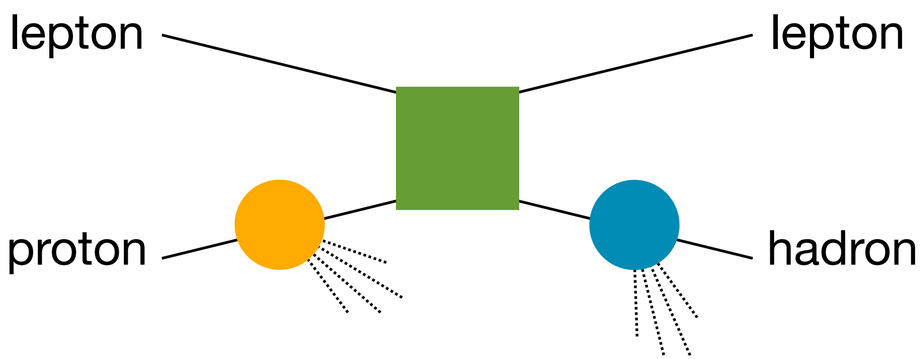

semi-inclusive DIS

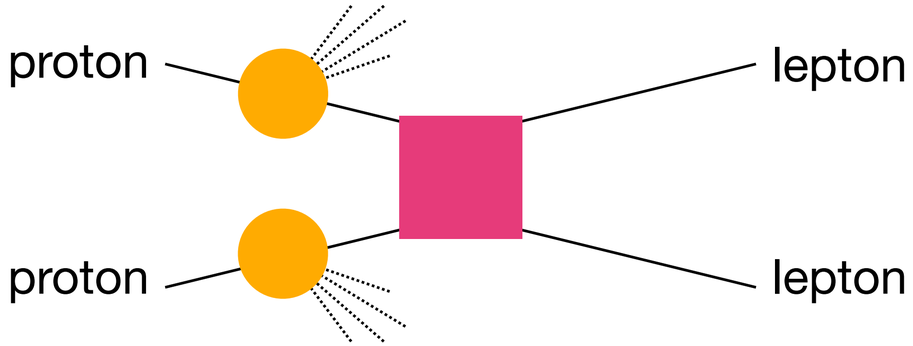

Drell-Yan

Adapted from A. Bacchetta

TMDs: factorisation and universality

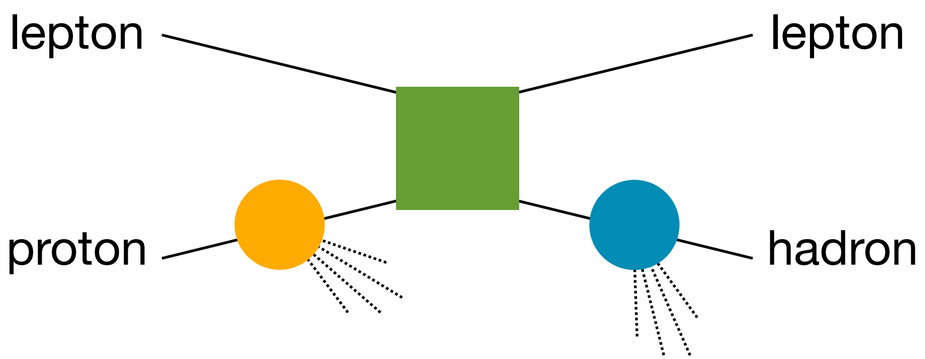

semi-inclusive DIS

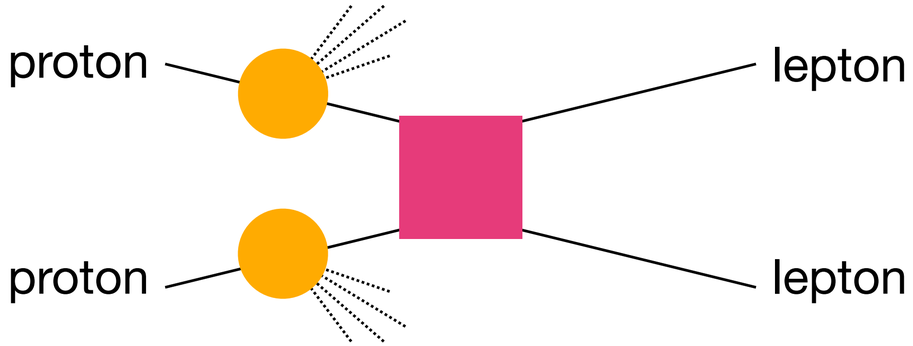

Drell-Yan

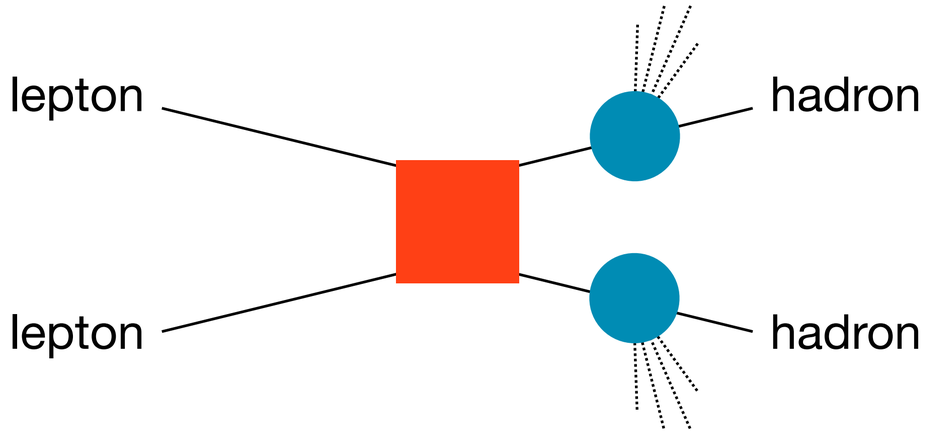

e^+e^- annihilation

Adapted from A. Bacchetta

TMDs: factorisation and universality

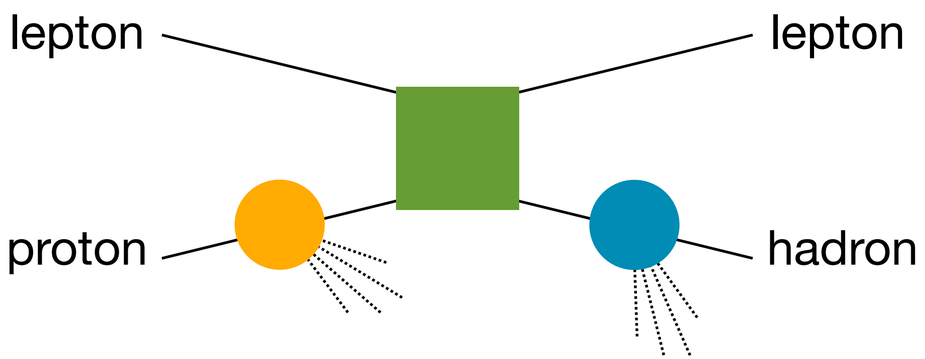

semi-inclusive DIS

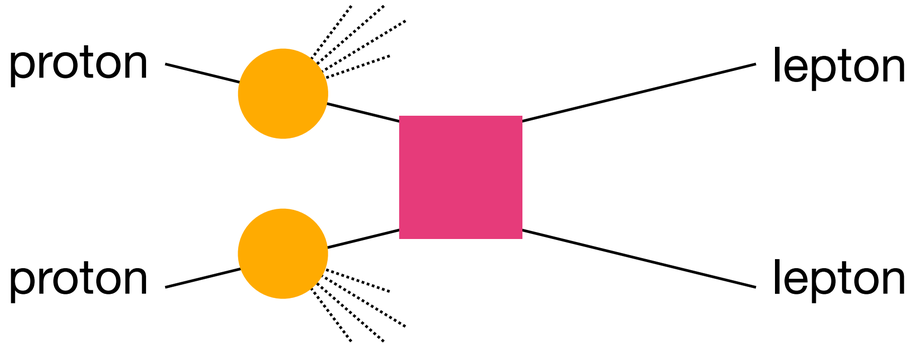

Drell-Yan

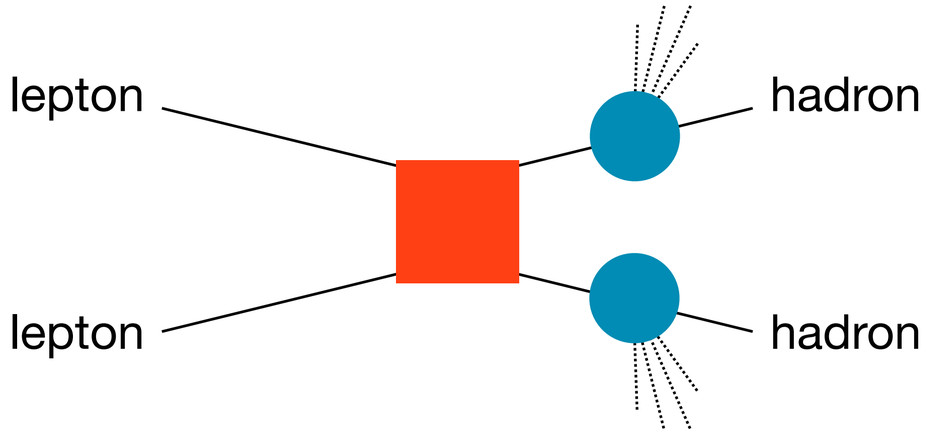

e^+e^- annihilation

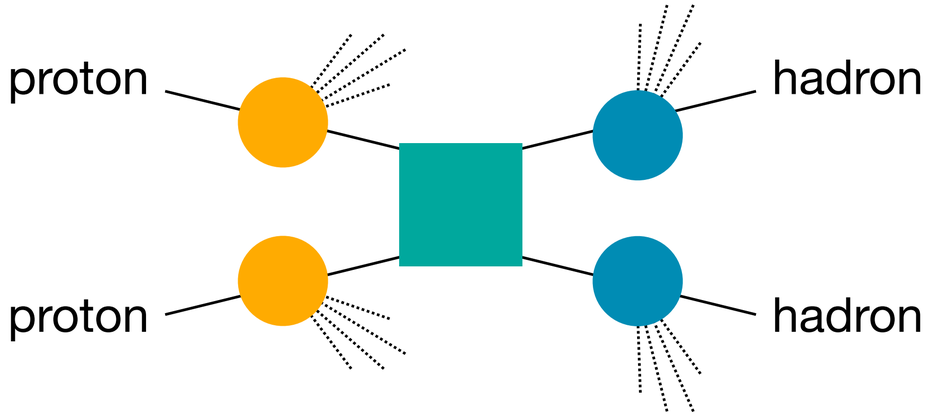

inclusive hadron production in pp collisions

Adapted from A. Bacchetta

TMDs: factorisation and universality

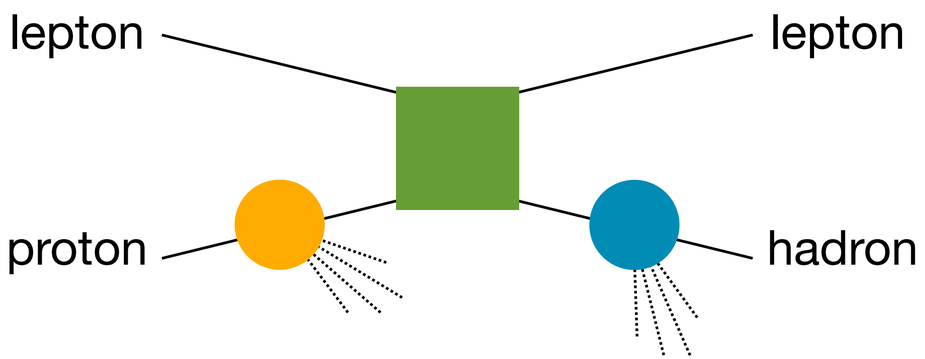

semi-inclusive DIS

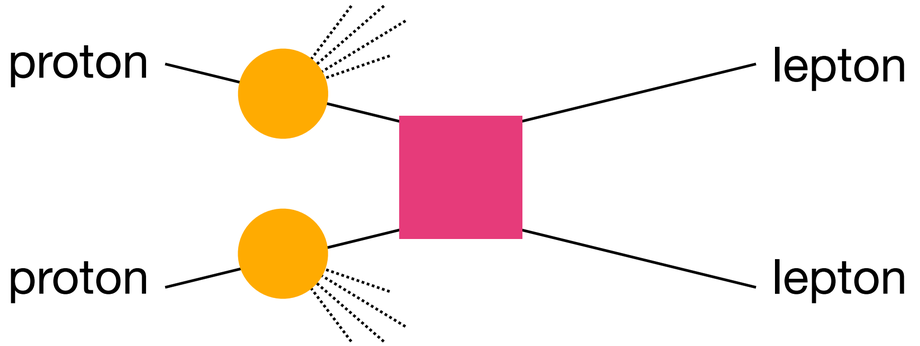

Drell-Yan

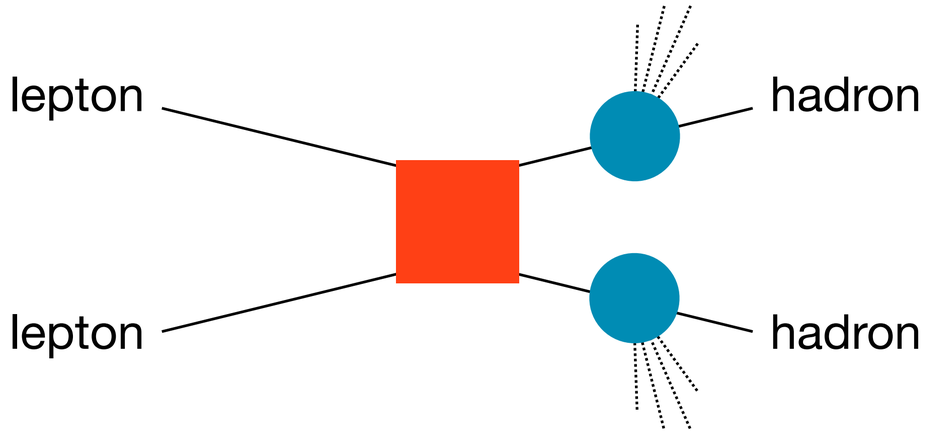

e^+e^- annihilation

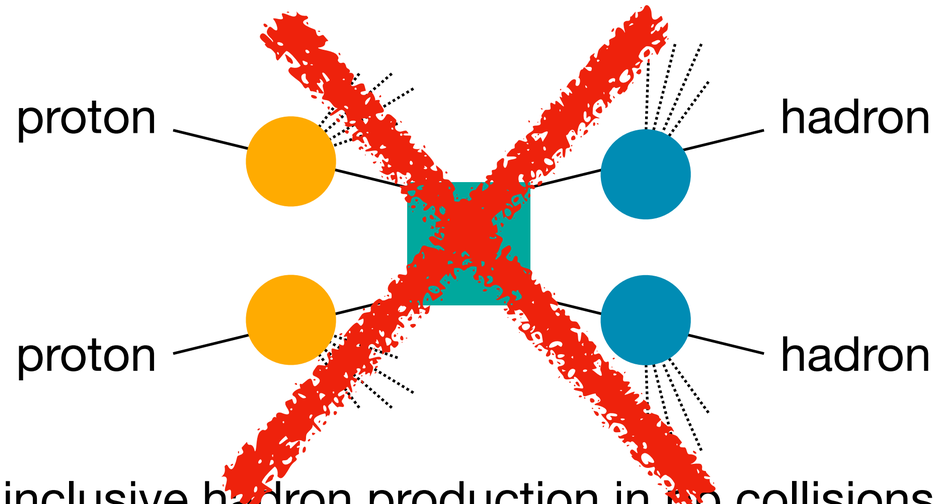

inclusive hadron production in pp collisions

Adapted from A. Bacchetta

Validity of TMD description

2 characteristic scales:
small P_{hT} and large Q^2

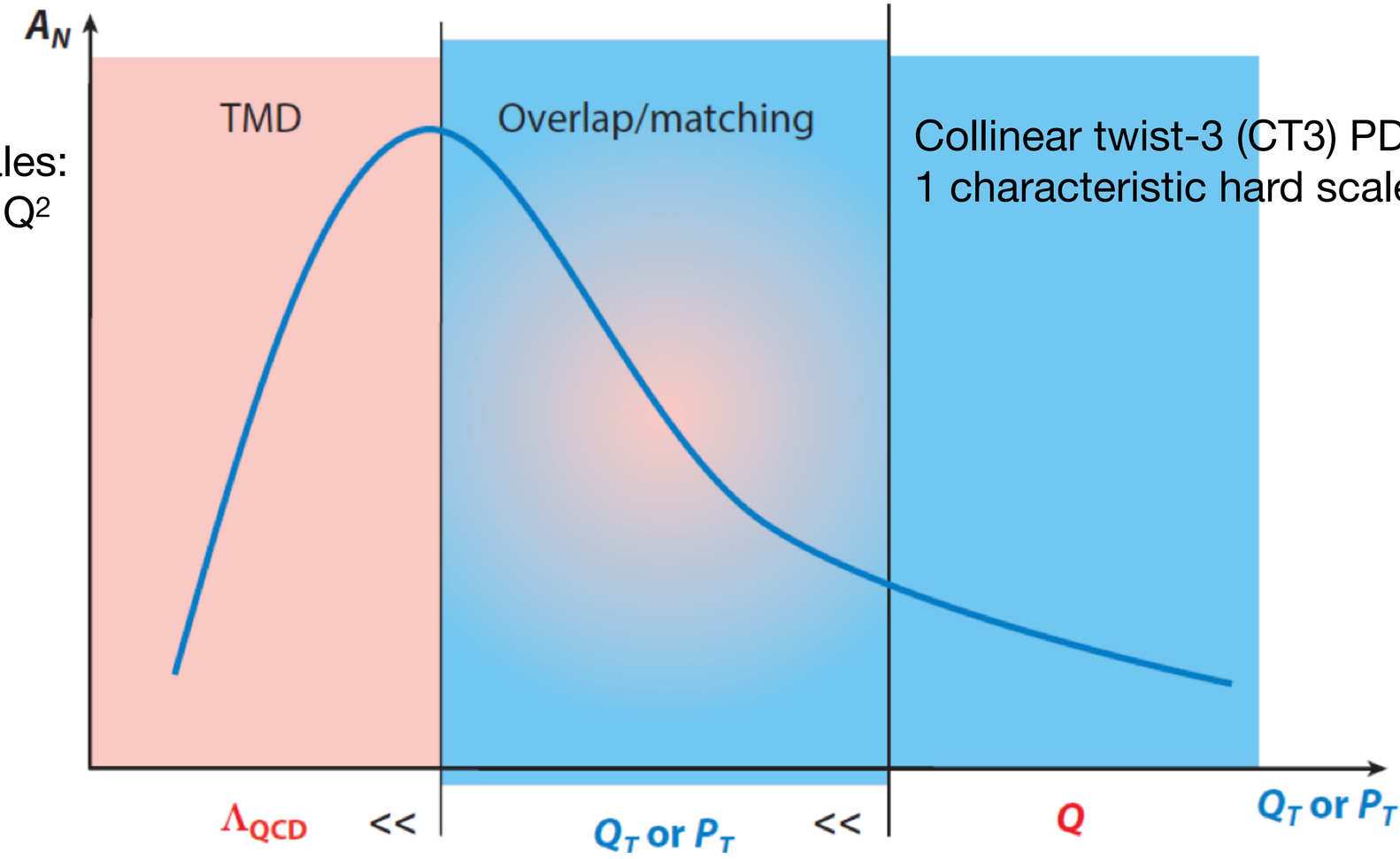

Collinear twist-3 (CT3) PDFs.
1 characteristic hard scale, e.g., P_{hT}

Consistent results for TMD
and CT3 in overlap region

Experiments investigating TMD PDFs and TMD FFs

Access to transversity in semi-inclusive DIS: Collins amplitude

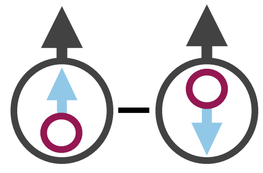

$$\mathscr{C}\left[h_{1T}^{q} \times H_{1}^{\perp,q}\right]$$

$$A_{UT} = \frac{1}{\langle \left| S_T \right| \rangle} \frac{N^{\uparrow}(\phi, \phi_S) - N^{\downarrow}(\phi, \phi_S)}{N^{\uparrow}(\phi, \phi_S) + N^{\downarrow}(\phi, \phi_S)}$$

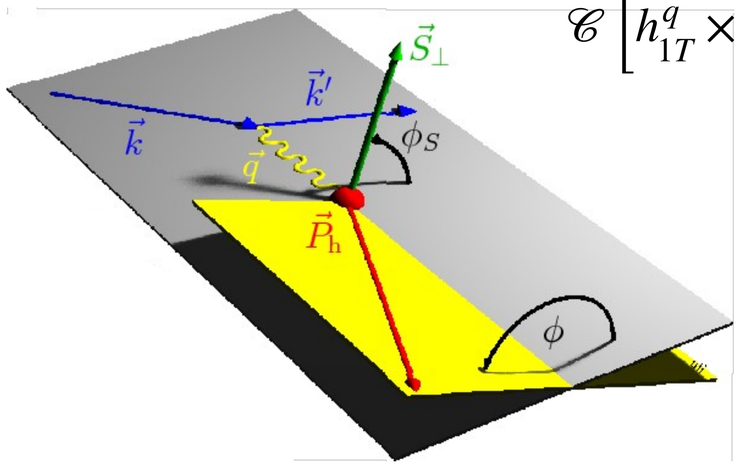

Access to transversity in semi-inclusive DIS: Collins amplitude

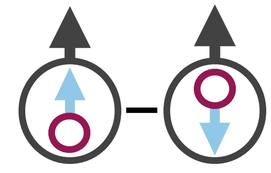

$$\mathscr{C}\left[h_{1T}^{q} \times H_{1}^{\perp,q}\right]$$

$$A_{UT} = \frac{1}{\langle |S_T| \rangle} \frac{N^{\uparrow}(\phi,\phi_S) - N^{\downarrow}(\phi,\phi_S)}{N^{\uparrow}(\phi,\phi_S) + N^{\downarrow}(\phi,\phi_S)}$$

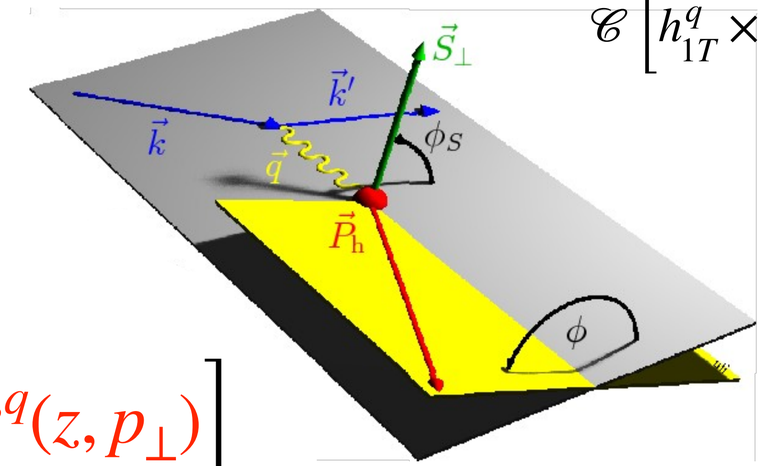

$$\sim \sin(\phi + \phi_S) \sum_q e_q^2 \, C\left[h_{1T}^{q}(x,k_\perp) \times H_1^{\perp,q}(z,p_\perp)\right]$$

Access to transversity in semi-inclusive DIS: Collins amplitude

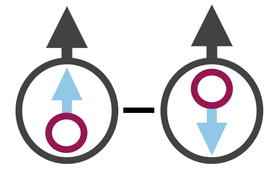

$$\mathscr{C}\left[h_{1T}^{q} \times H_{1}^{\perp,q}\right]$$

$$A_{UT} = \frac{1}{\langle |S_T| \rangle} \frac{N^{\uparrow}(\phi,\phi_S) - N^{\downarrow}(\phi,\phi_S)}{N^{\uparrow}(\phi,\phi_S) + N^{\downarrow}(\phi,\phi_S)}$$

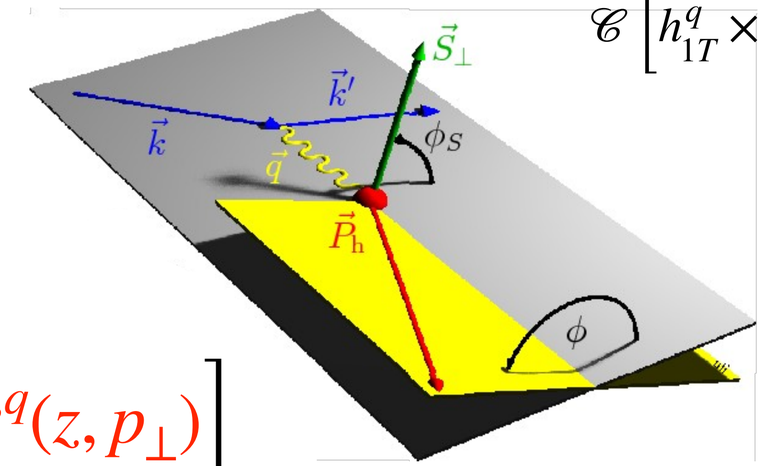

$$\sim \sin(\phi + \phi_S) \sum_q e_q^2 C\left[h_{1T}^{q}(x,k_\perp) \times H_1^{\perp,q}(z,p_\perp)\right]$$

Access to transversity in semi-inclusive DIS: Collins amplitude

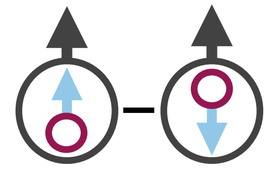

$$A_{UT} = \frac{1}{\langle |S_T| \rangle} \frac{N^{\uparrow}(\phi,\phi_S) - N^{\downarrow}(\phi,\phi_S)}{N^{\uparrow}(\phi,\phi_S) + N^{\downarrow}(\phi,\phi_S)}$$

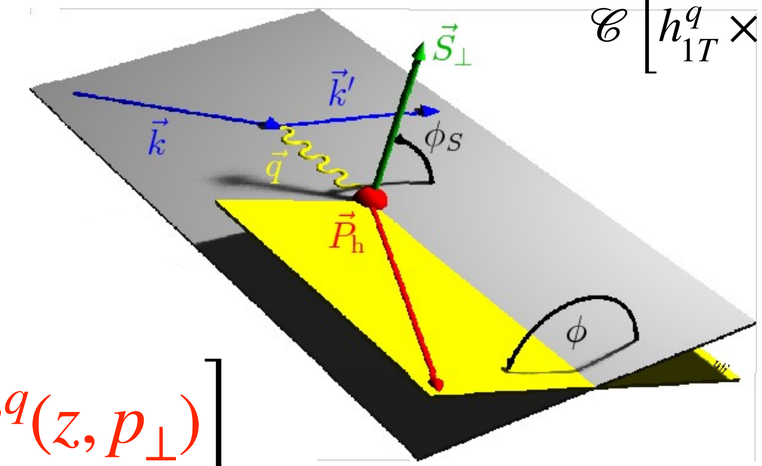

$$\sim \sin(\phi + \phi_S) \sum_q e_q^2 C\left[h_{1T}^{q}(x,k_\perp) \times H_1^{\perp,q}(z,p_\perp)\right]$$

$h_{1T}^{q}(x,k_\perp)$: transversity

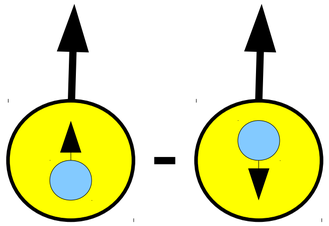

$H_1^{\perp,q}(z,p_\perp)$: Collins fragmentation function

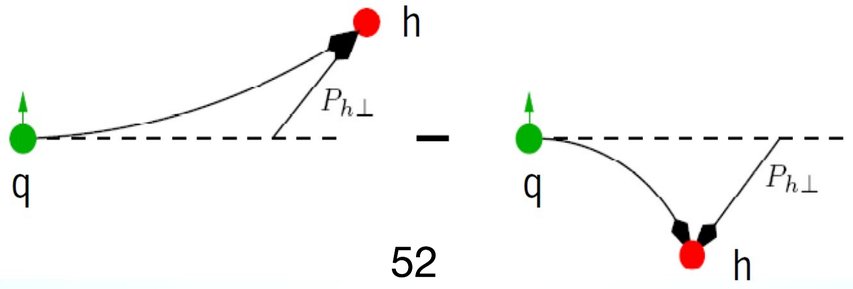

Collins amplitudes

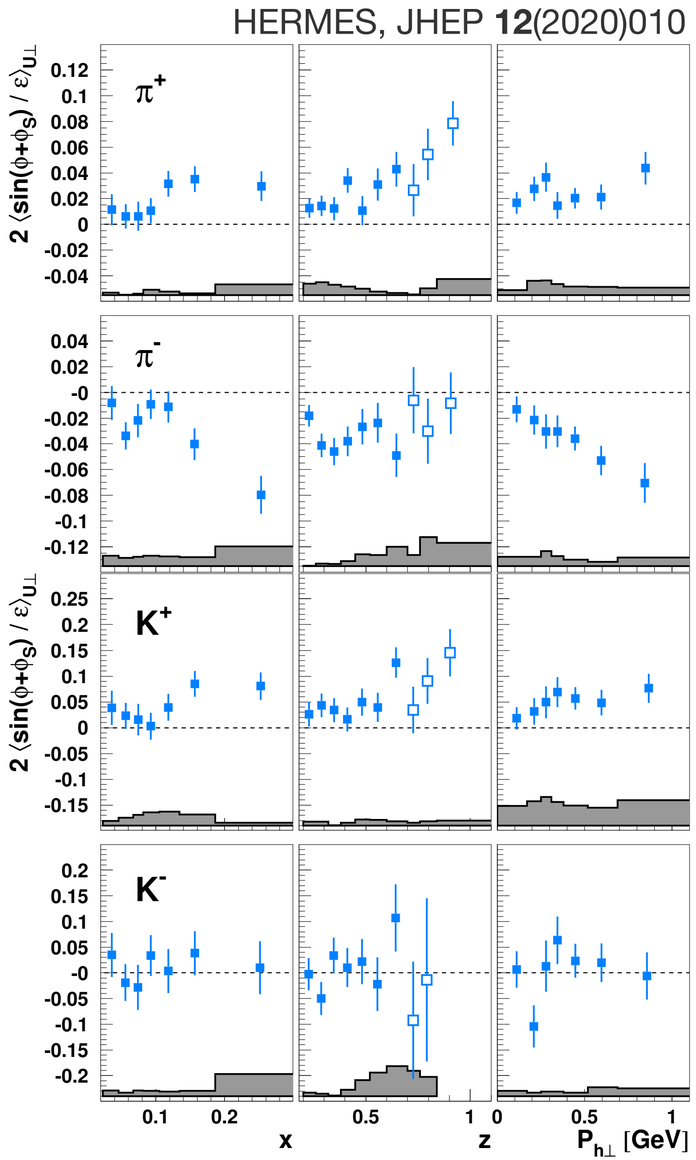

- Oppositely signed amplitudes for π^+ and π^-:

$$H_1^{\perp,u\to\pi^+} \approx -H_1^{\perp,u\to\pi^-}$$

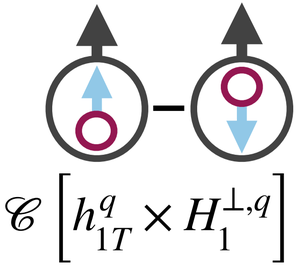

Artru model

X. Artru et al., Z. Phys. C**73** (1997) 527

polarisation component in lepton scattering plane reversed by photoabsorption:

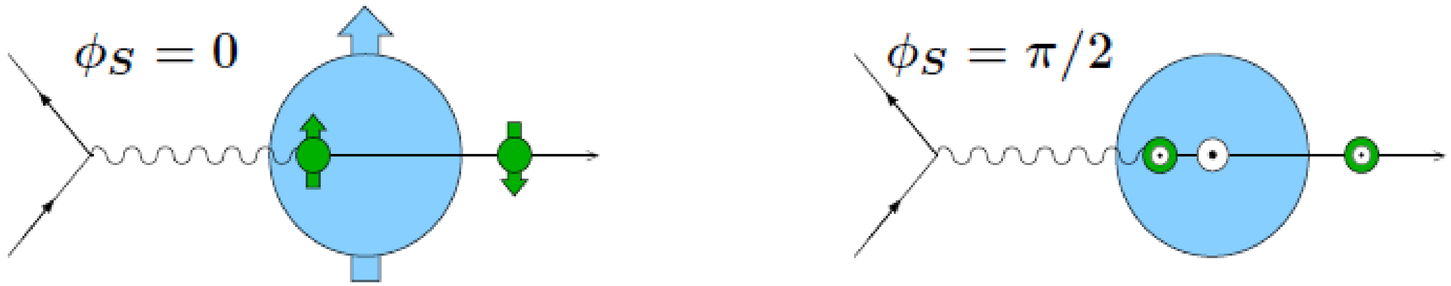

string break, quark-antiquark pair with vacuum numbers:

orbital angular momentum creates transverse momentum:

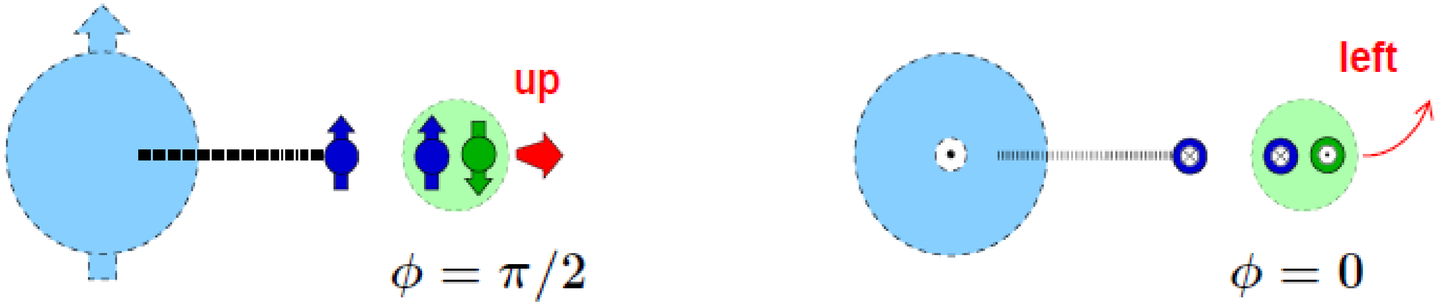

Courtesy U. Elschenbroich

Collins amplitudes

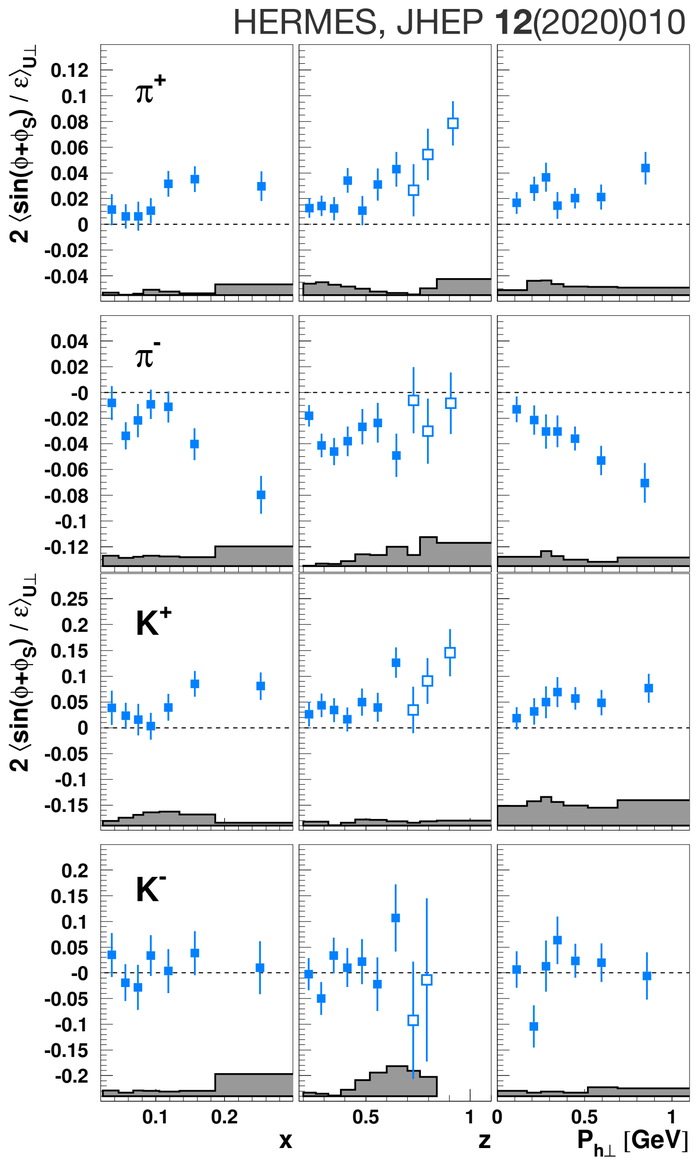

- Oppositely signed amplitudes for π^+ and π^-:

$$H_1^{\perp,u\to\pi^+} \approx -H_1^{\perp,u\to\pi^-}$$

- Amplitudes for K^+ larger than for π^+:

$$H_1^{\perp,u\to K^+} > H_1^{\perp,u\to\pi^+}$$

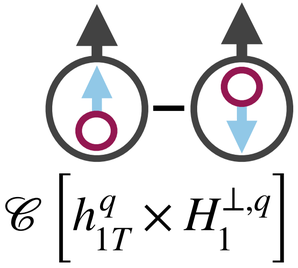

Collins amplitudes

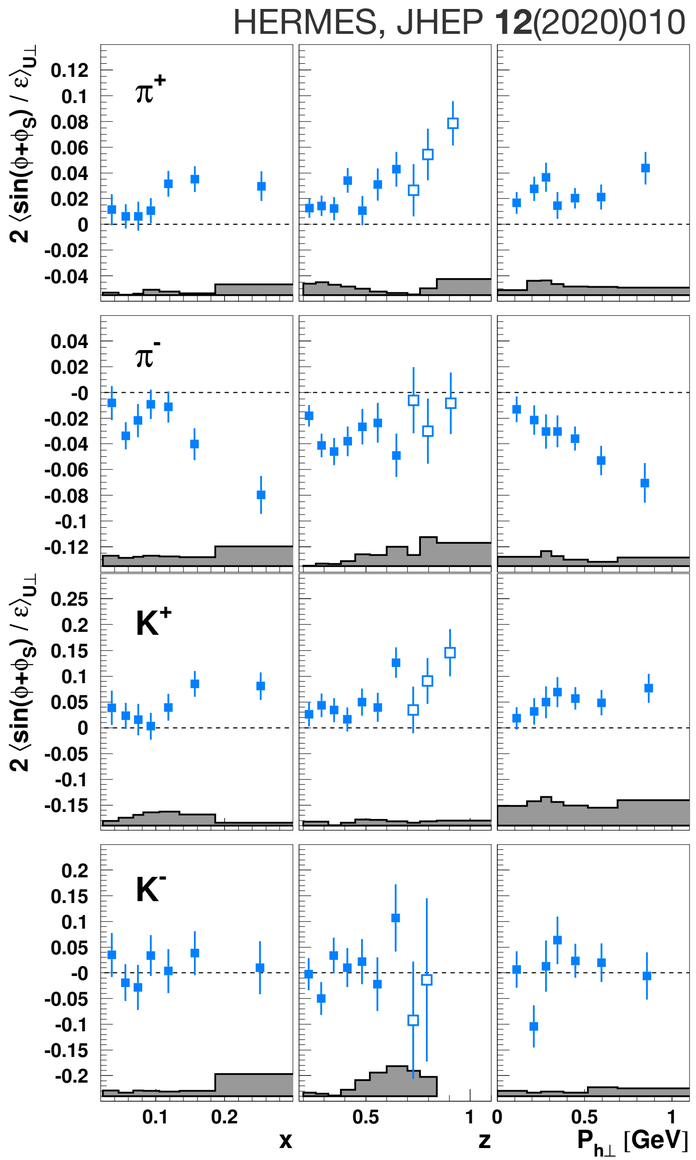

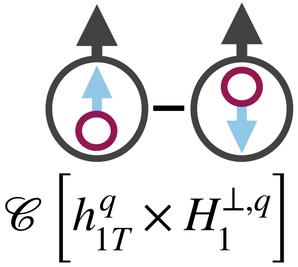

- Oppositely signed amplitudes for π^+ and π^-:

$$H_1^{\perp,u\to\pi^+} \approx -H_1^{\perp,u\to\pi^-}$$

- Amplitudes for K^+ larger than for π^+:

$$H_1^{\perp,u\to K^+} > H_1^{\perp,u\to\pi^+}$$

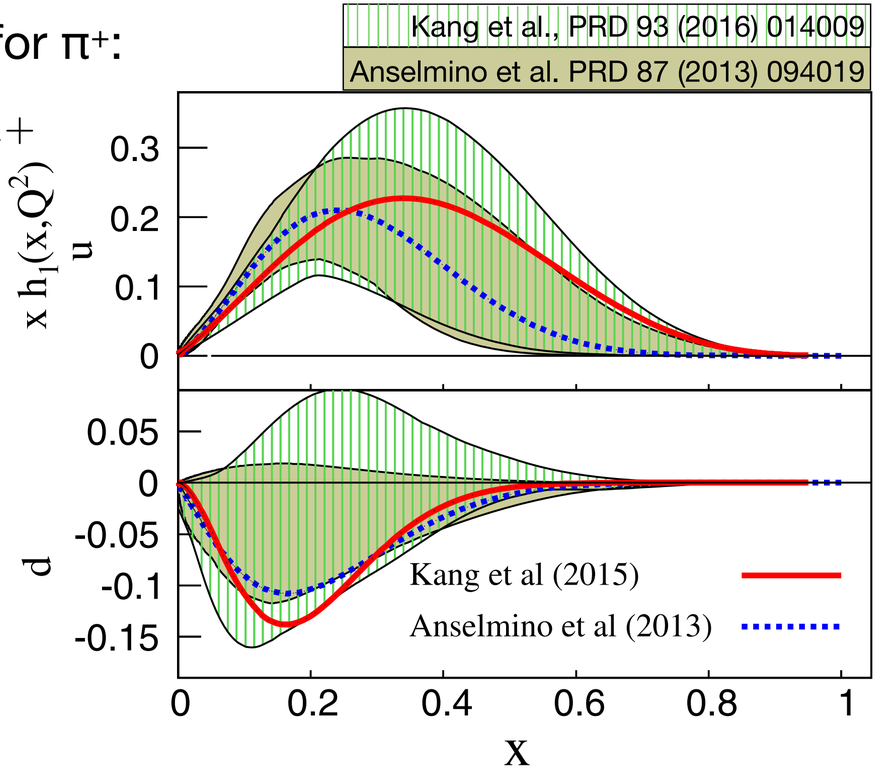

data from Belle, Babar, COMPASS, HERMES, Jefferson Lab Hall A

Access to Sivers in semi-inclusive DIS

$$A_{UT} = \frac{1}{\langle \left| S_T \right| \rangle} \frac{N^{\uparrow}(\phi, \phi_S) - N^{\downarrow}(\phi, \phi_S)}{N^{\uparrow}(\phi, \phi_S) + N^{\downarrow}(\phi, \phi_S)}$$

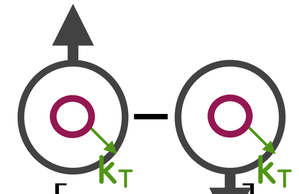

$$\mathscr{C}\left[f_{1T}^{\perp,q} \times D_1^q\right]$$

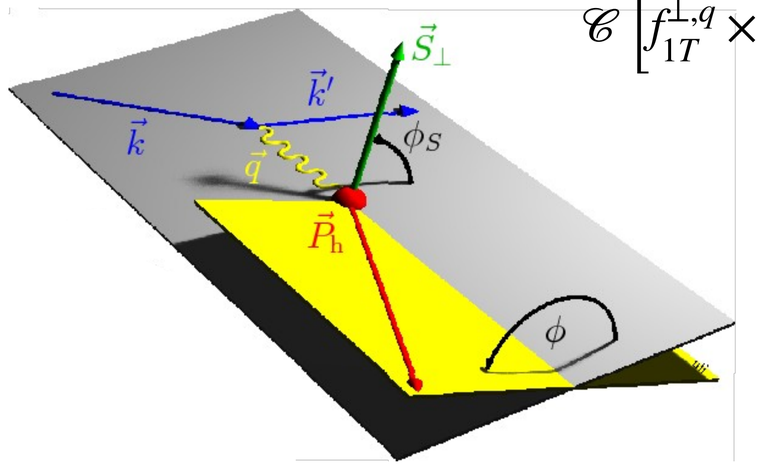

Access to Sivers in semi-inclusive DIS

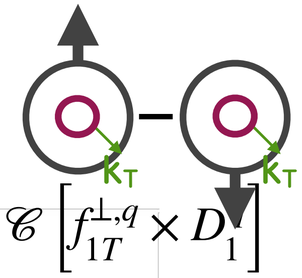

$$A_{UT} = \frac{1}{\langle |S_T| \rangle} \frac{N^{\uparrow}(\phi,\phi_S) - N^{\downarrow}(\phi,\phi_S)}{N^{\uparrow}(\phi,\phi_S) + N^{\downarrow}(\phi,\phi_S)}$$

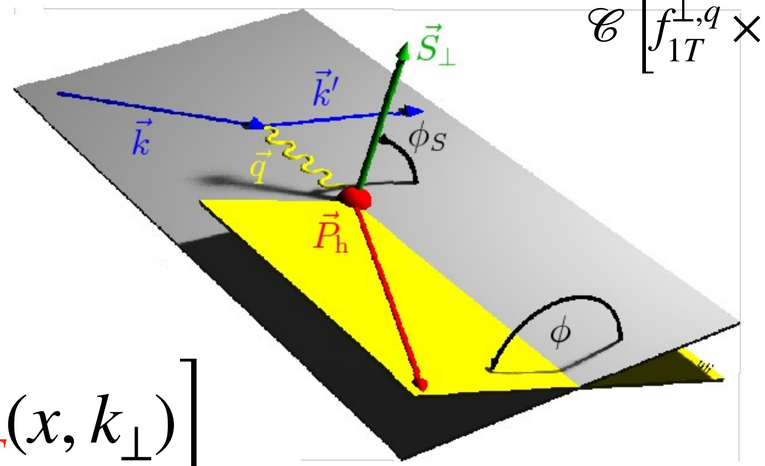

$$\sim \sin(\phi - \phi_S) \sum_q e_q^2 \, C\left[f_{1T}^{\perp,q}(x,k_\perp) \times D_{1T}^q(x,k_\perp)\right]$$

Access to Sivers in semi-inclusive DIS

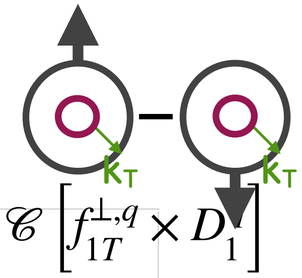

$$A_{UT} = \frac{1}{\langle |S_T| \rangle} \frac{N^{\uparrow}(\phi, \phi_S) - N^{\downarrow}(\phi, \phi_S)}{N^{\uparrow}(\phi, \phi_S) + N^{\downarrow}(\phi, \phi_S)}$$

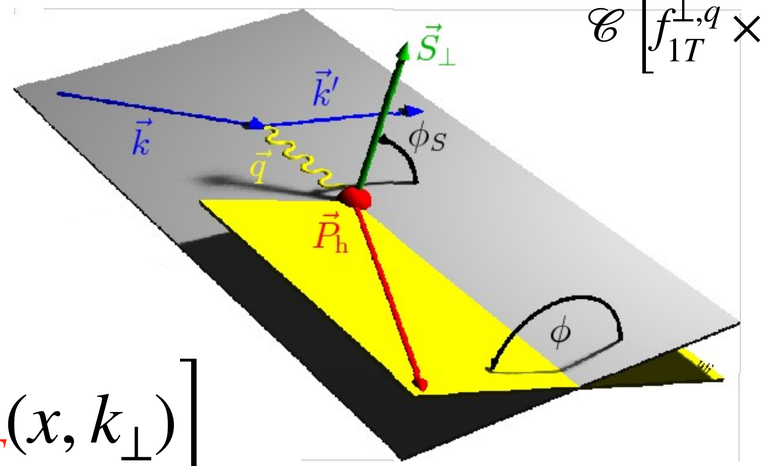

$$\sim \sin(\phi - \phi_S) \sum_q e_q^2 C\left[f_{1T}^{\perp,q}(x, k_\perp) \times D_{1T}^q(x, k_\perp)\right]$$

Access to Sivers in semi-inclusive DIS

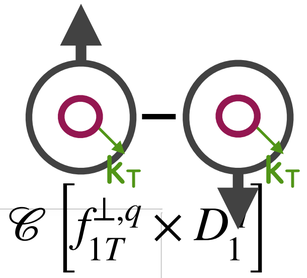

$$A_{UT} = \frac{1}{\langle |S_T| \rangle} \frac{N^{\uparrow}(\phi, \phi_S) - N^{\downarrow}(\phi, \phi_S)}{N^{\uparrow}(\phi, \phi_S) + N^{\downarrow}(\phi, \phi_S)}$$

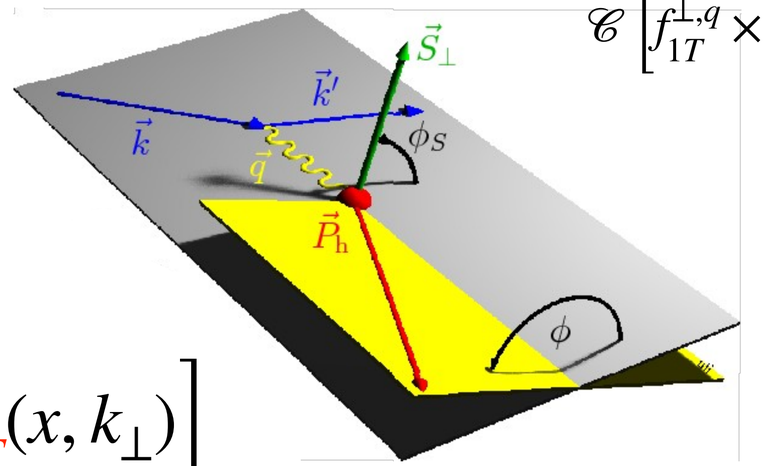

$$\sim \sin(\phi - \phi_S) \sum_q e_q^2 C\left[f_{1T}^{\perp,q}(x, k_\perp) \times D_{1T}^q(x, k_\perp)\right]$$

- Sivers function:
  - requires non-zero orbital angular momentum
  - final-state interactions ⟶ azimuthal asymmetries

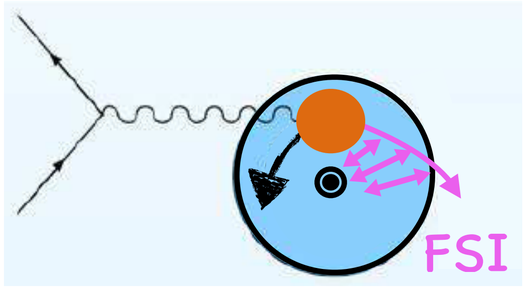

Sivers amplitudes

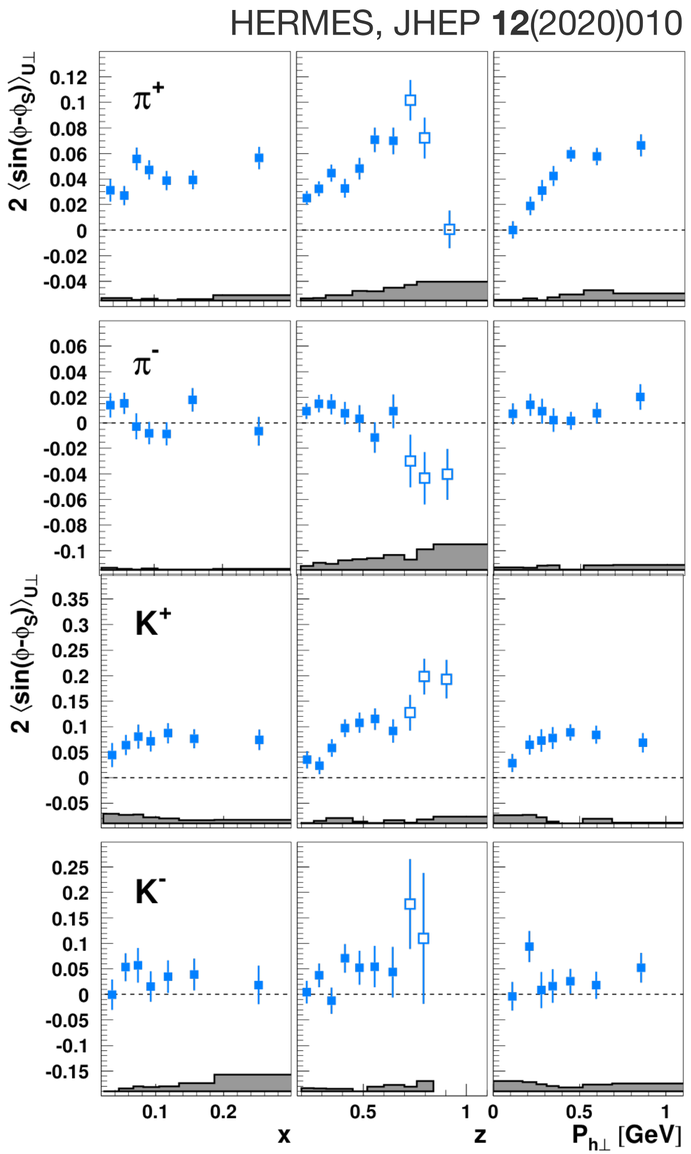

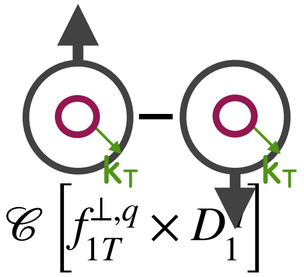

Sivers amplitudes

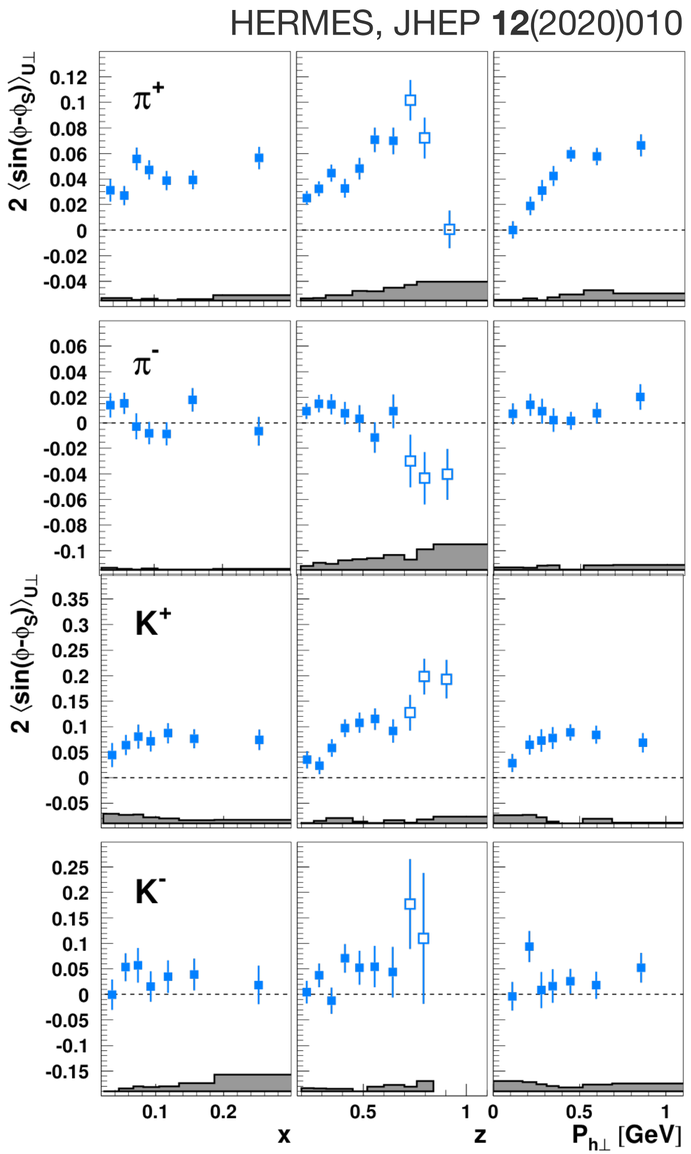

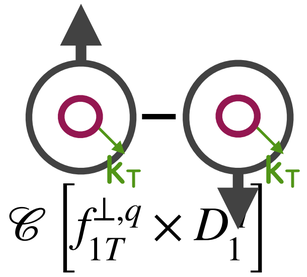

- π^+:
  - positive -> non-zero orbital angular momentum
- π^-:
  - consistent with zero → u and d quark cancelation

Sivers amplitudes

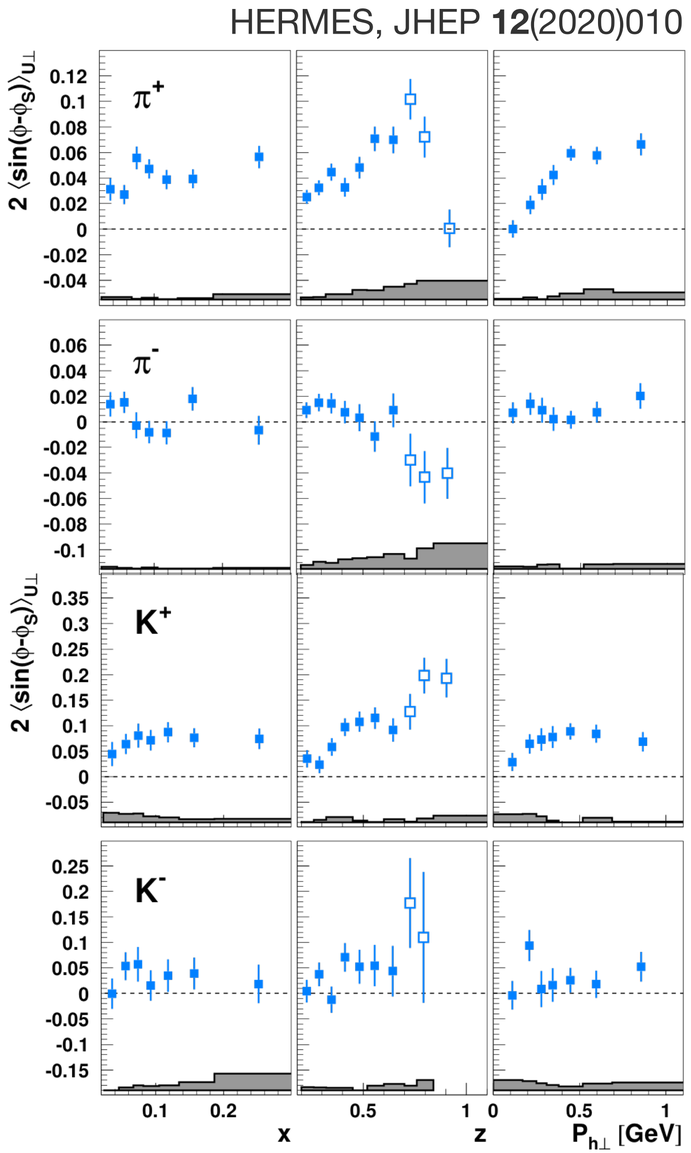

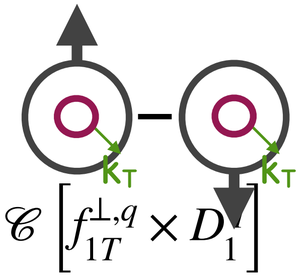

- π^+:
  - positive -> non-zero orbital angular momentum
- π^-:
  - consistent with zero → u and d quark cancelation
- Sivers function:
  - requires non-zero orbital angular momentum
  - final-state interactions ⟶ azimuthal asymmetries

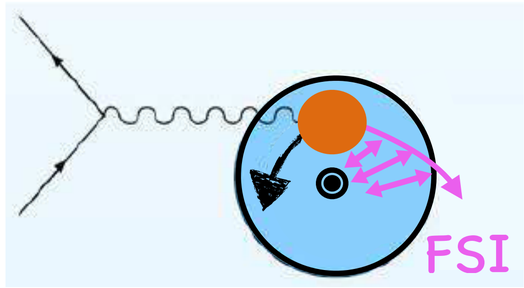

Sivers function

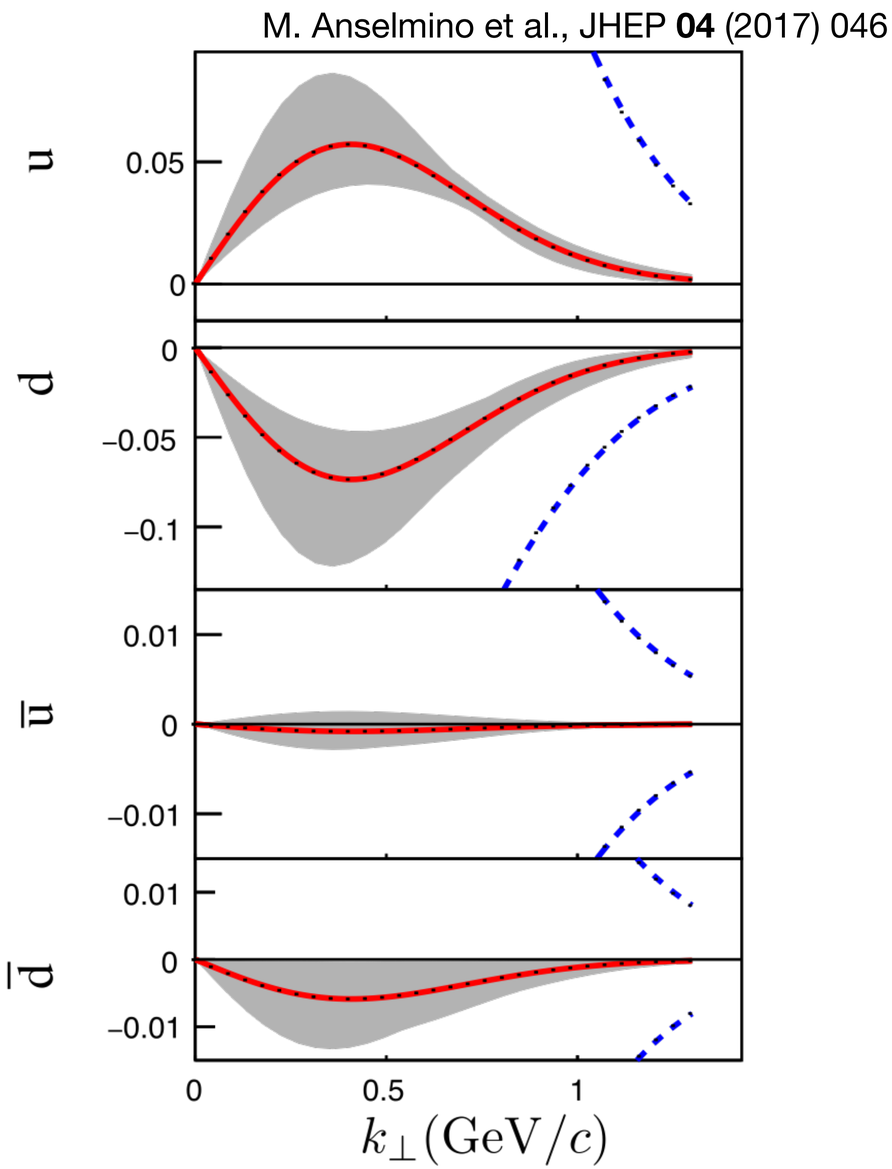

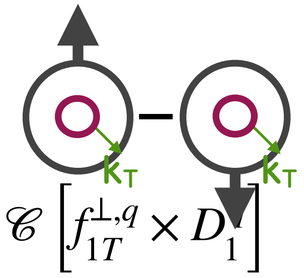

$x\, f_1(x, k_T, S_T)$

A. Accardi et al., Eur. Phys. J. A **52** (2016) 268

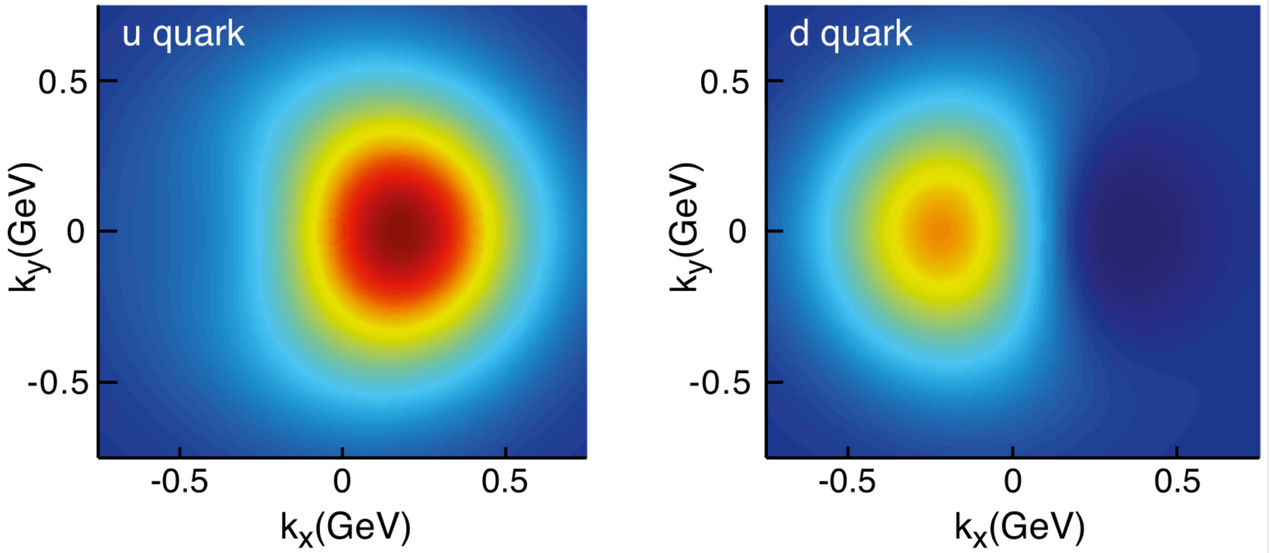

nucleon polarised along $\hat{y}$

Sivers: predicted sign change

J. C. Collins, Phys. Lett. B 536 (2002) 43

$$\Phi_{ij}(p,P,S) = \frac{1}{(2\pi)^4}\int d^4\xi\; e^{ip\cdot\xi}\left\langle P,S\right|\bar{\psi}_j(0)\,U_{[0,\xi]}\,\psi_i(\xi)\left|P,S\right\rangle$$

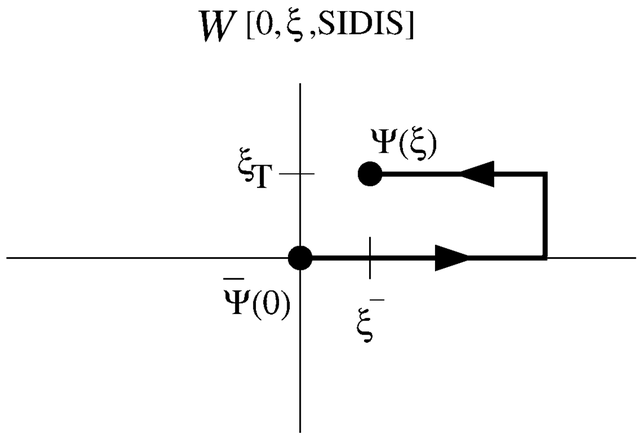

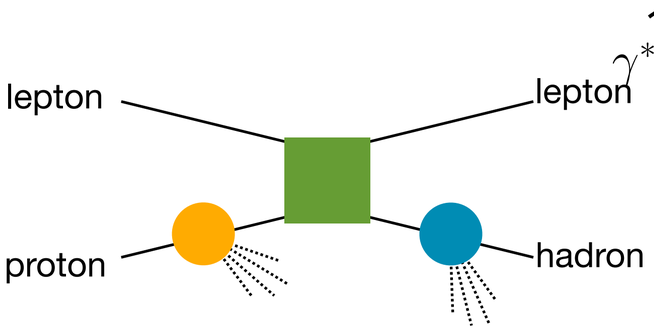

semi-inclusive DIS

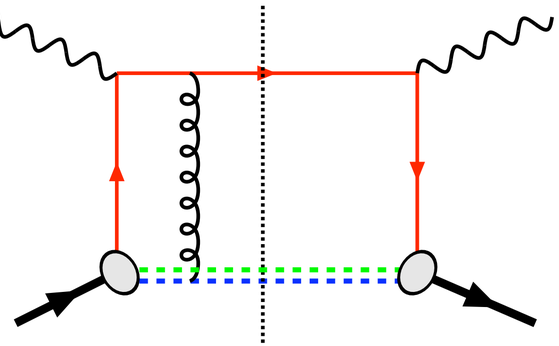

r (gb)

attractive

Sivers: predicted sign change

$$\Phi_{ij}(p,P,S) = \frac{1}{(2\pi)^4}\int d^4\xi\; e^{ip\cdot\xi}\left\langle P,S\right|\bar{\psi}_j(0)\,U_{[0,\xi]}\,\psi_i(\xi)\left|P,S\right\rangle$$

J. C. Collins, Phys. Lett. B 536 (2002) 43

$W_{[0,\xi,\mathrm{SIDIS}]}$

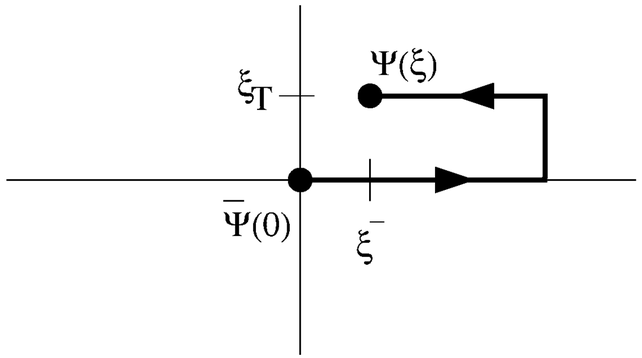

$U_{\xi,\mathrm{DY}]}$

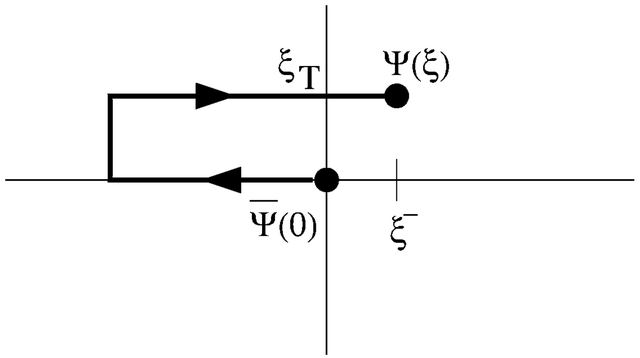

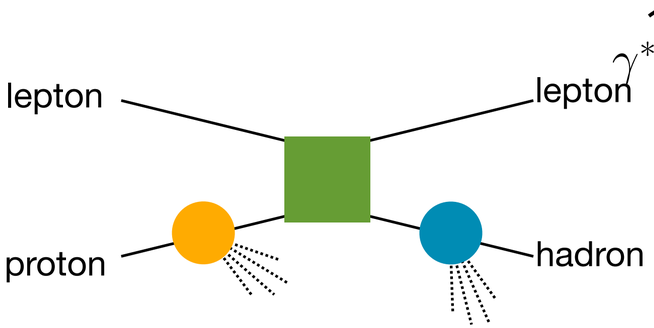

semi-inclusive DIS

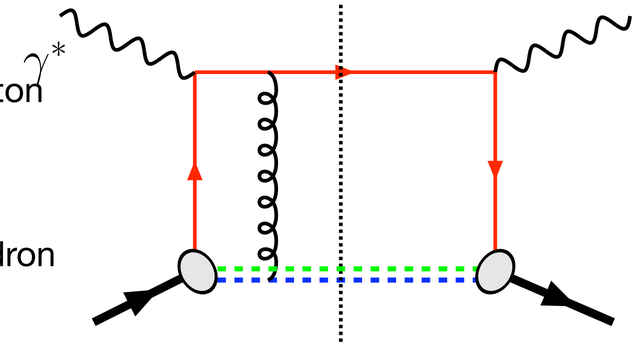

r (gb)

attractive

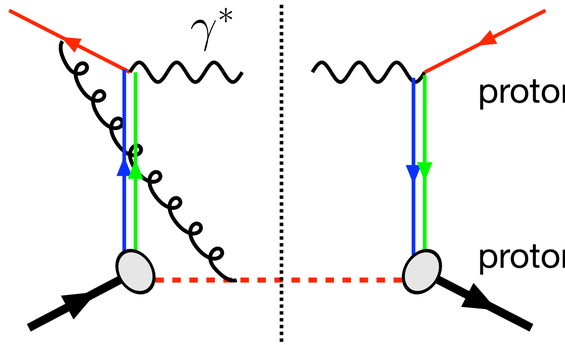

r r

repulsive

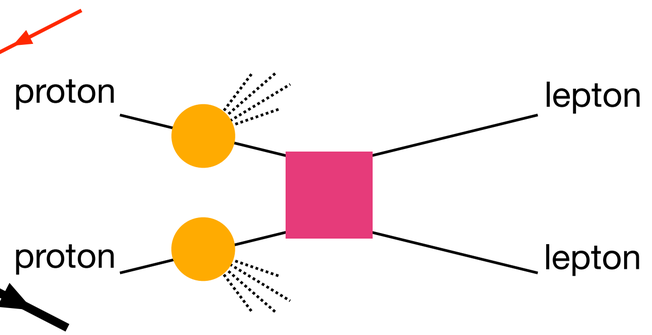

Drell-Yan

Sivers: predicted sign change

$$\Phi_{ij}(p,P,S) = \frac{1}{(2\pi)^4}\int d^4\xi\; e^{ip\cdot\xi}\left\langle P,S\right|\bar{\psi}_j(0)\,U_{[0,\xi]}\,\psi_i(\xi)\left|P,S\right\rangle$$

J. C. Collins, Phys. Lett. B 536 (2002) 43

$W_{[0,\xi,\mathrm{SIDIS}]}$

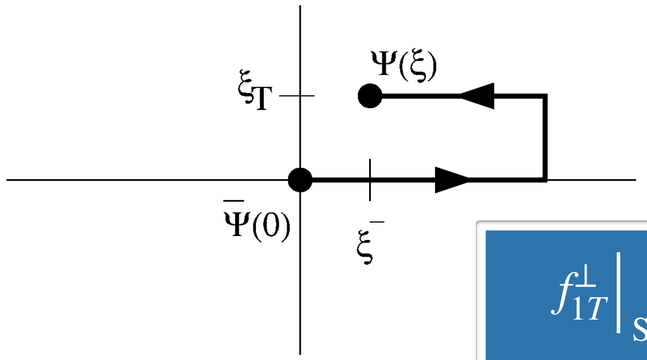

$U_{\xi,\mathrm{DY}]}$

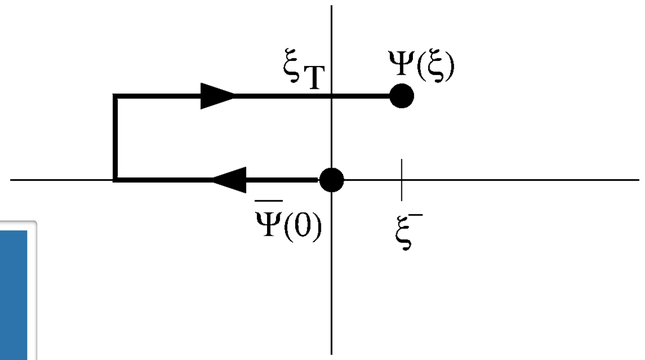

$$f_{1T}^{\perp}\Big|_{\mathrm{SIDIS}} = -f_{1T}^{\perp}\Big|_{\mathrm{DY}}$$

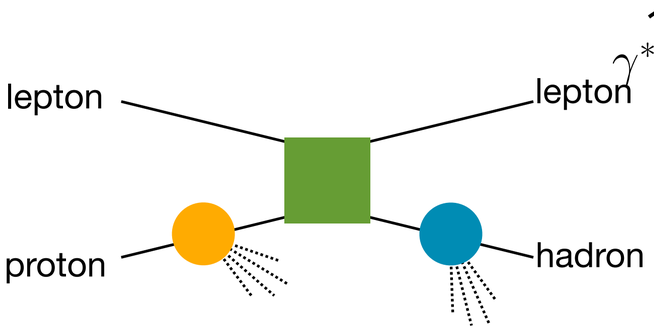

semi-inclusive DIS

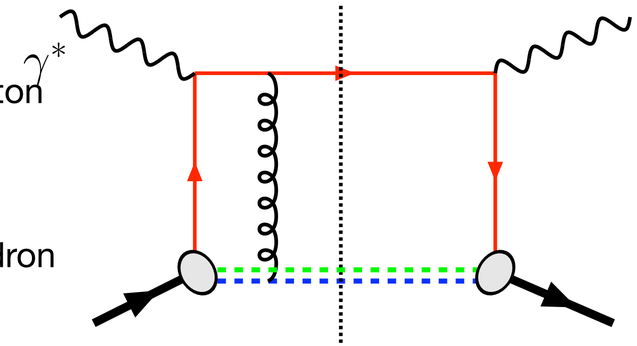

r (gb)

attractive

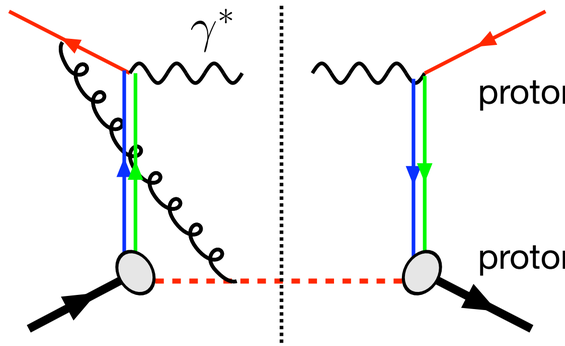

r r

repulsive

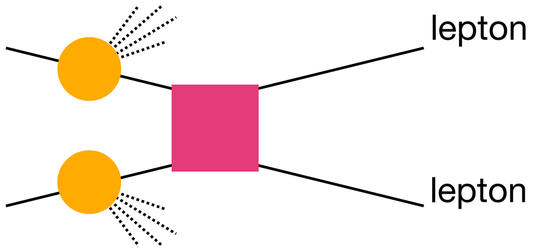

Drell-Yan

Experimental access to Sivers in Drell Yan

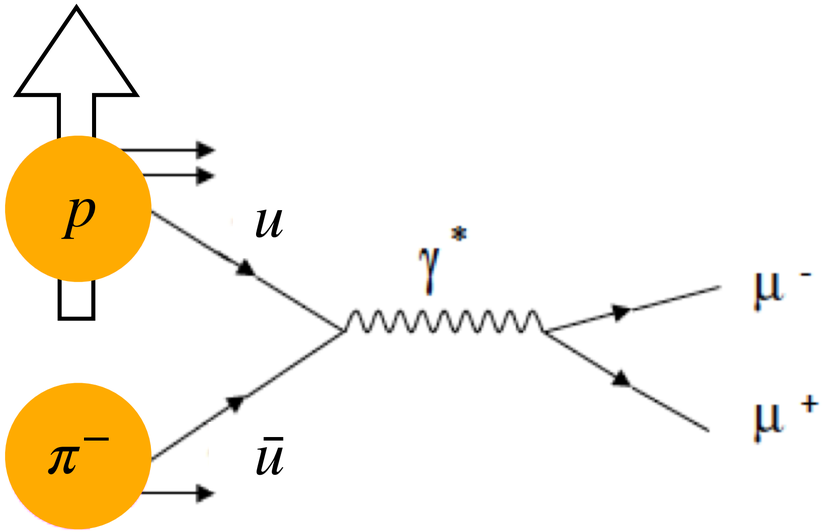

Experimental access to Sivers in Drell Yan

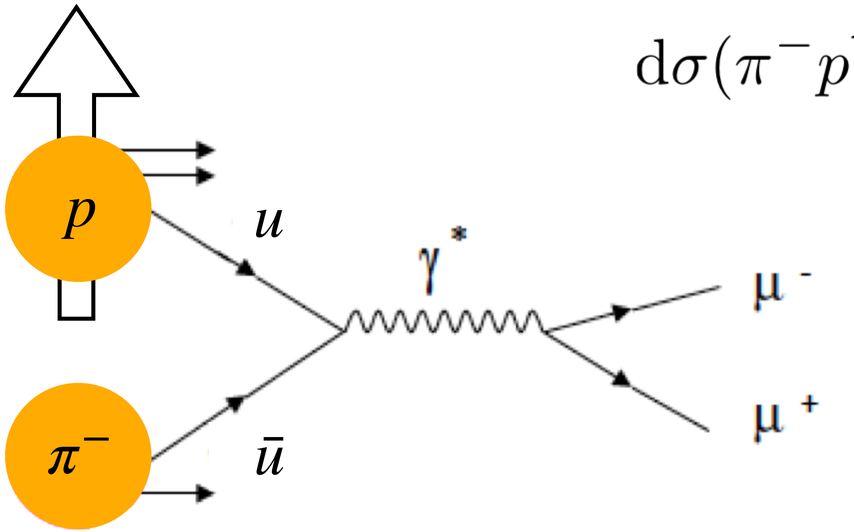

$$\mathrm{d}\sigma(\pi^- p^\uparrow \to \mu^+\mu^- X) \sim 1 + \overline{h}_1^\perp \otimes h_1^\perp \cos(2\phi)$$
$$+|S_T|\ \ \overline{f}_1 \otimes \overline{f}_{1T}^\perp \sin\phi_S$$
$$+|S_T|\ \ \overline{h}_1^\perp \otimes h_{1T}^\perp \sin(2\phi+\phi_S)$$
$$+|S_T|\ \ \overline{h}_1^\perp \otimes h_{1T} \sin(2\phi-\phi_S)$$

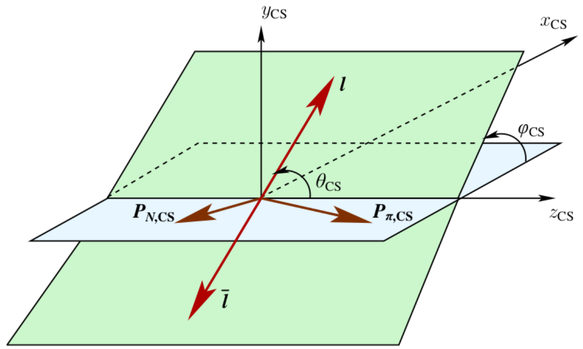

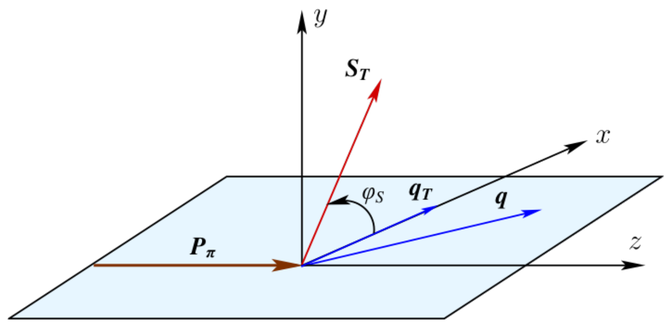

Experimental access to Sivers in Drell Yan

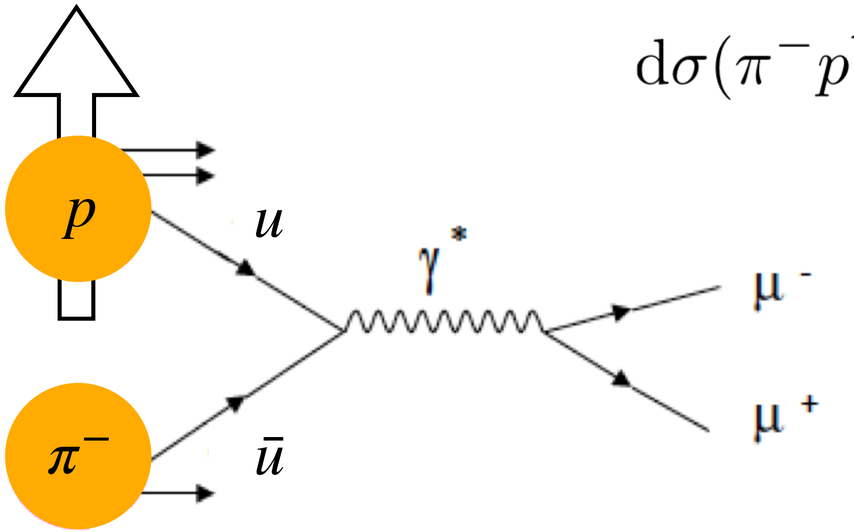

$$\mathrm{d}\sigma(\pi^- p^\uparrow \to \mu^+\mu^- X) \sim 1 + \overline{h}_1^\perp \otimes h_1^\perp \cos(2\phi)$$
$$+|S_T|\ \ \overline{f}_1 \otimes \overline{f}_{1T}^\perp \sin\phi_S$$
$$+|S_T|\ \overline{h}_1^\perp \otimes h_{1T}^\perp \sin(2\phi+\phi_S)$$
$$+|S_T|\ \underbrace{\overline{h}_1^\perp}_{\pi^-} \otimes \underbrace{h_{1T}}_{p} \sin(2\phi-\phi_S)$$

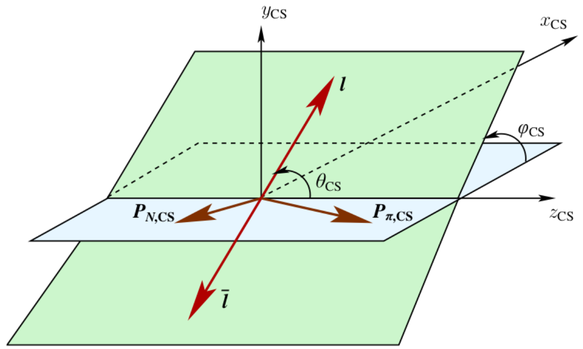

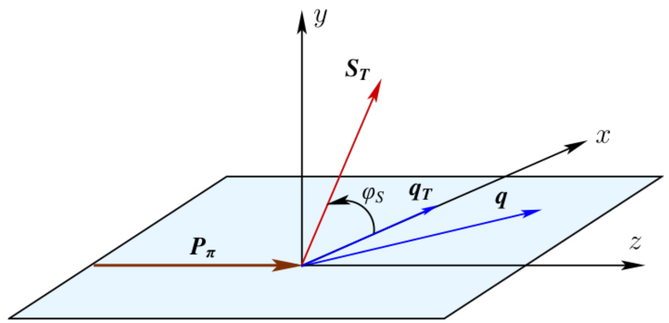

Experimental access to Sivers in Drell Yan

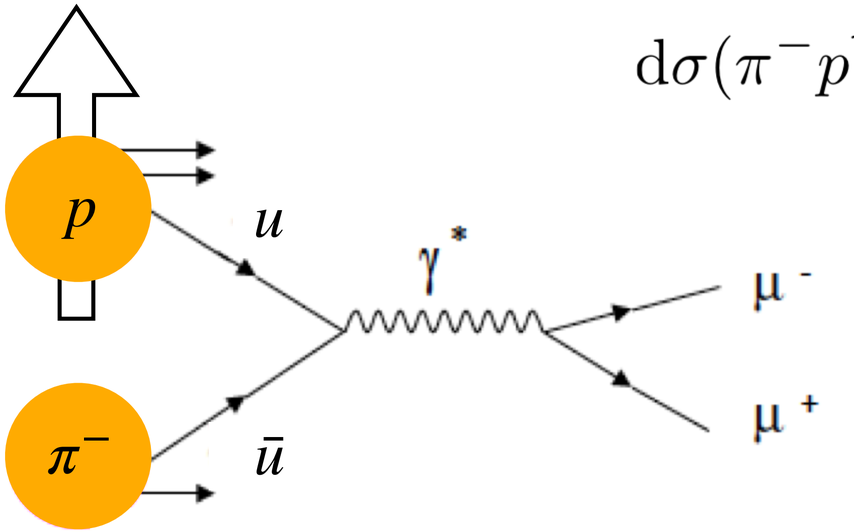

$$\mathrm{d}\sigma(\pi^- p^\uparrow \to \mu^+\mu^- X) \sim 1 + \overline{h}_1^\perp \otimes h_1^\perp \cos(2\phi)$$
$$+|S_T|\ \ \overline{f}_1 \otimes f_{1T}^\perp \sin\phi_S$$
$$+|S_T|\ \overline{h}_1^\perp \otimes h_{1T}^\perp \sin(2\phi+\phi_S)$$
$$+|S_T|\ \underbrace{\overline{h}_1^\perp}_{\pi^-} \otimes \underbrace{h_{1T}}_{p} \sin(2\phi-\phi_S)$$

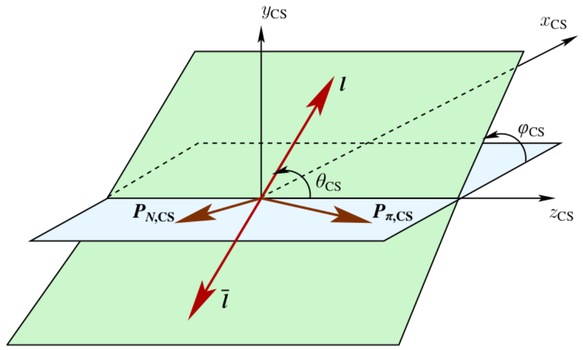

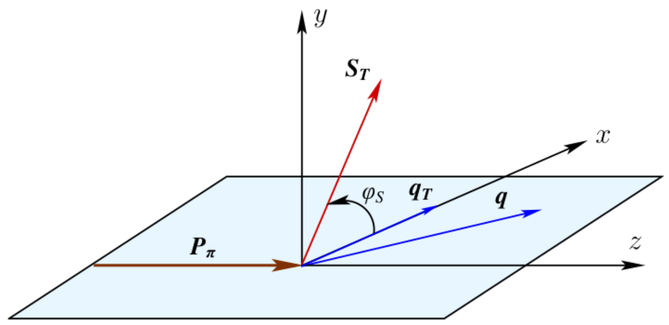

Investigation of the Sivers sign change in $p^{\uparrow}\pi$ collisions

M. Anselmino et al., JHEP **04** (2017) 046

M. G. Echevarria et al. PRD **89** (2014)074013

P. Sun, F. Yuan, PRD **88** (2013) 114012

COMPASS, PRL **119** (2017) 112002

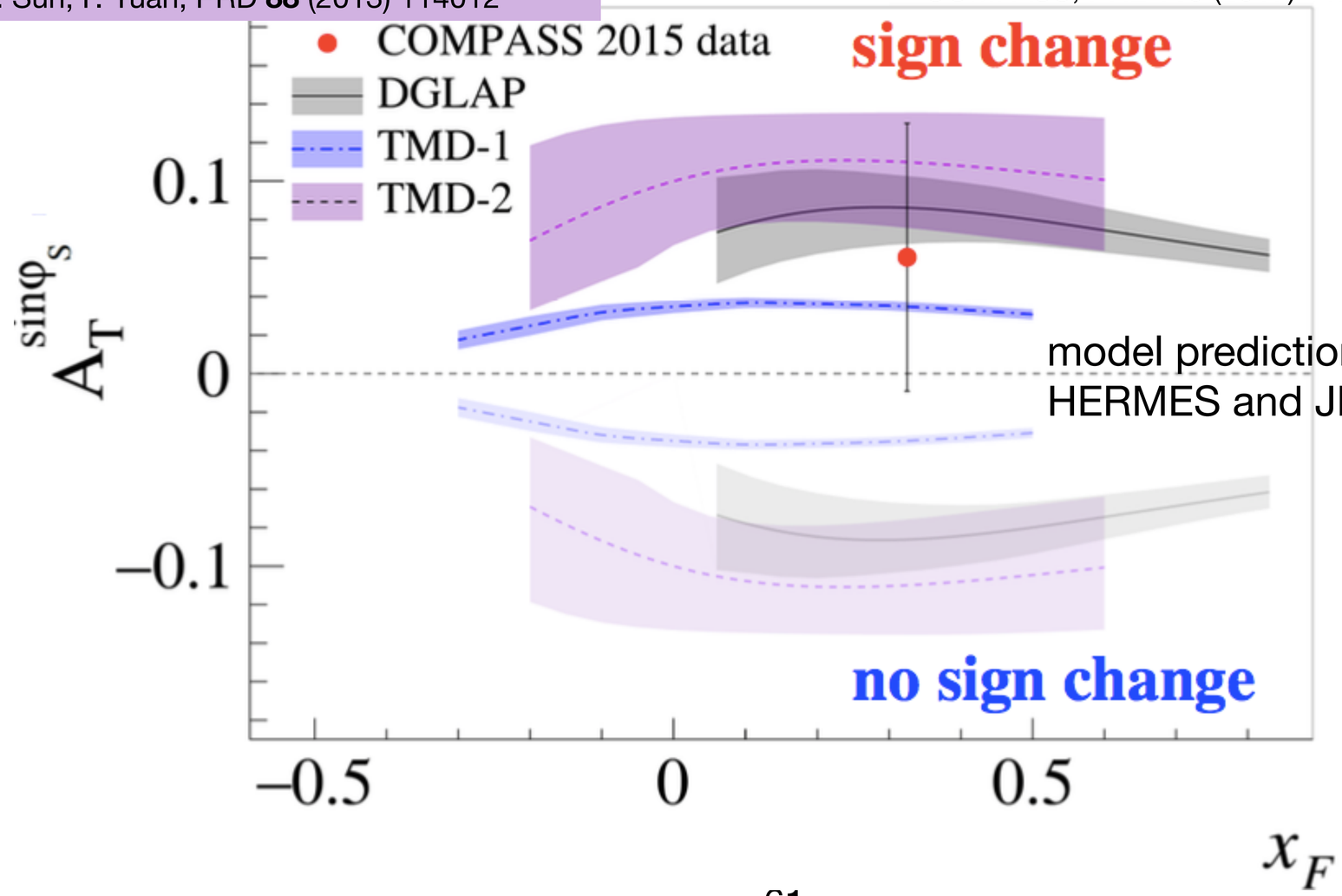

model predictions based on COMPASS, HERMES and JLab semi-inclusive DIS data

Investigation of the Sivers sign change in $p^{\uparrow}p$ collisions

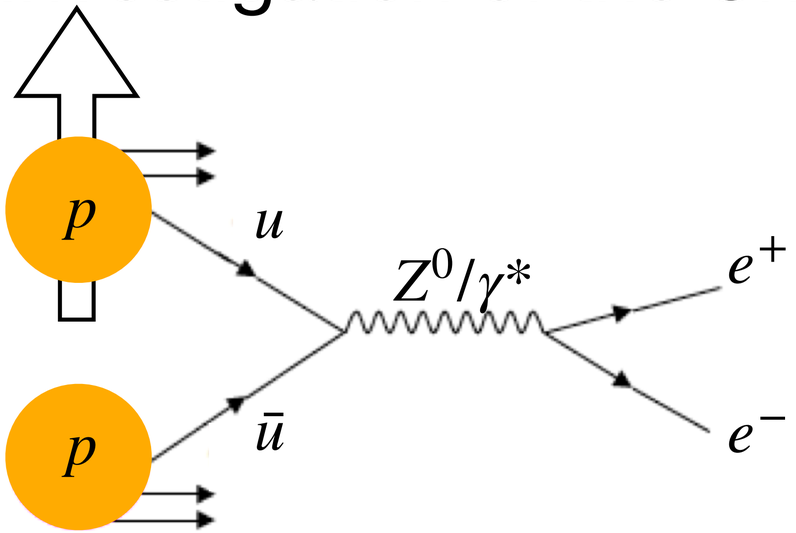

arXiv:2308.15496v1

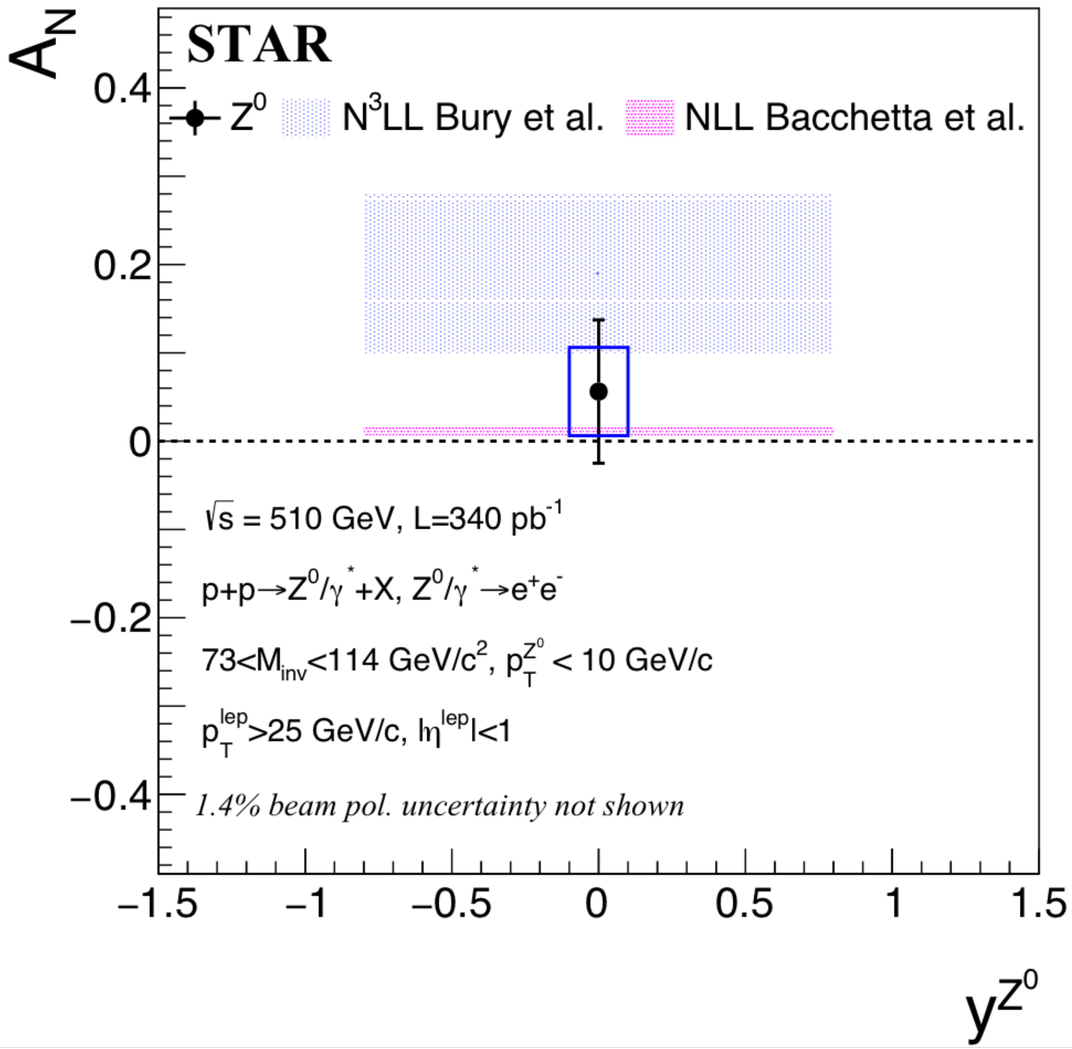

Investigation of the Sivers sign change in $p^{\uparrow}p$ collisions

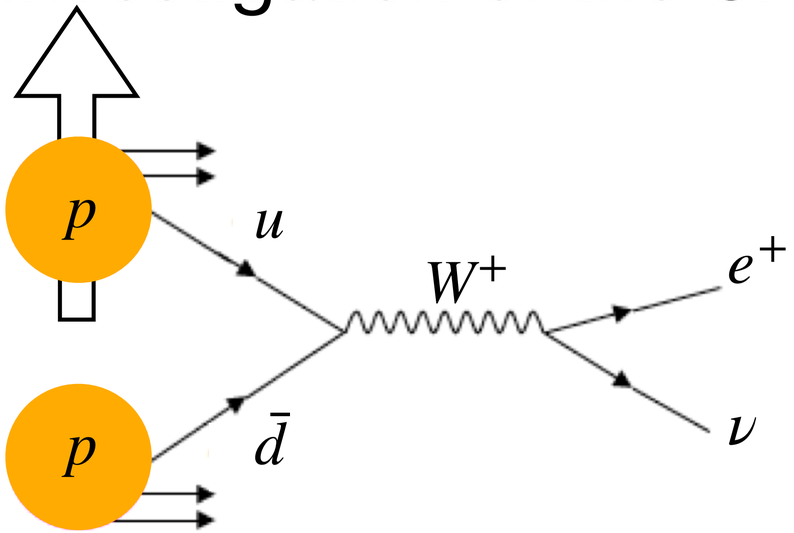

PRL **116** (2016) 132301

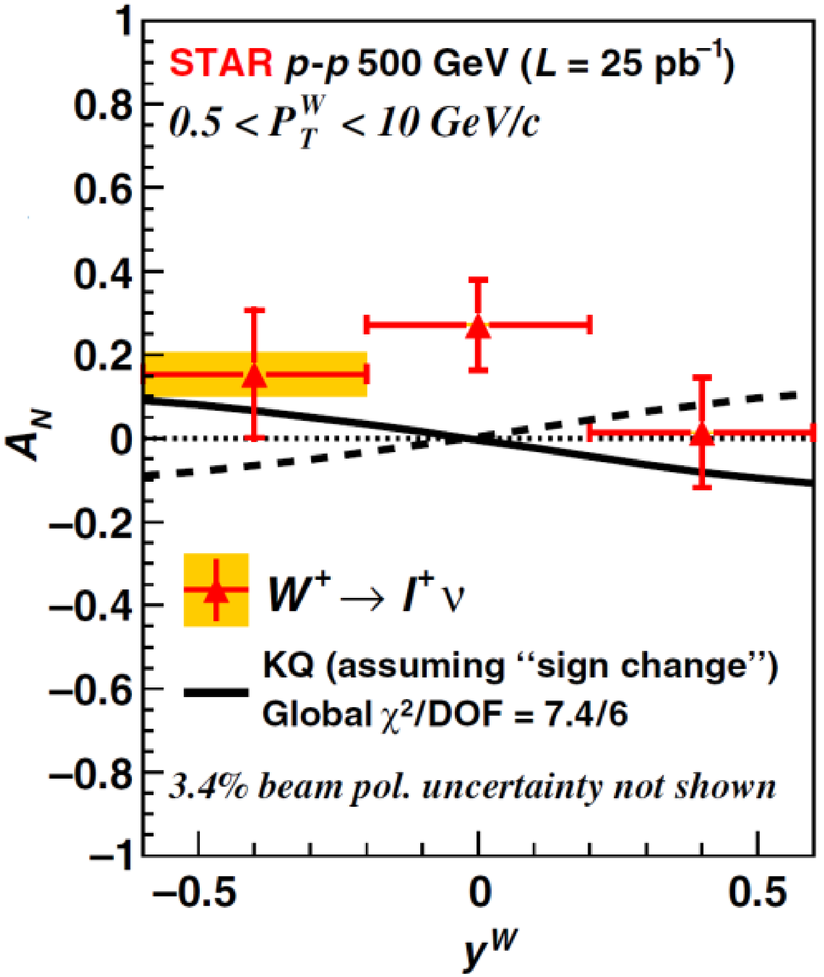

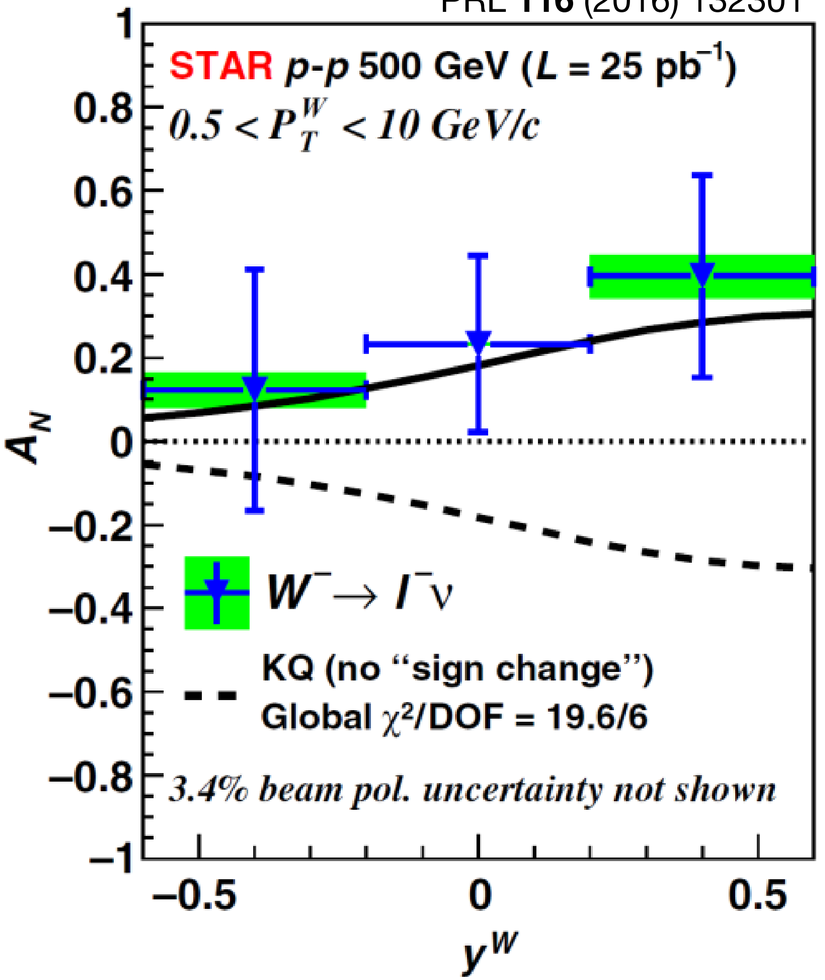

$$x_{1,2} = \frac{Q}{\sqrt{s}} e^{\pm y}$$

Boer-Mulders TMD PDF

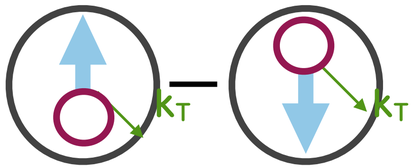

$$\mathscr{C}\left[h_1^{\perp,q} \times H_1^{\perp,q}\right]$$

Distribution of transversely polarised quarks in an unpolarised nucleon

Boer-Mulders TMD PDF

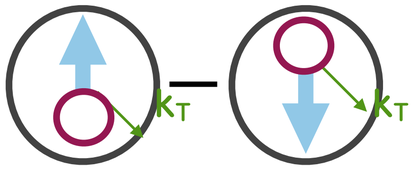

$$\mathscr{C}\left[h_1^{\perp,q} \times H_1^{\perp,q}\right]$$

Distribution of transversely polarised quarks in an unpolarised nucleon

spin physics with unpolarised hadrons!

Boer-Mulders TMD PDF

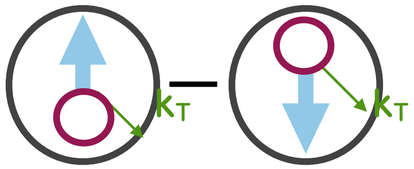

$$\mathscr{C}\left[h_1^{\perp,q} \times H_1^{\perp,q}\right]$$

Distribution of transversely polarised quarks in an unpolarised nucleon

spin physics with unpolarised hadrons!

access at unpolarised facilities, such as the LHC!

Boer-Mulders TMD PDF

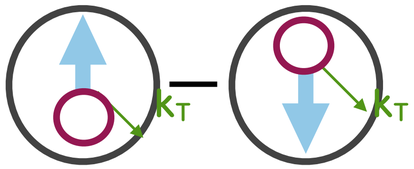

$$\mathscr{C}\left[h_1^{\perp,q} \times H_1^{\perp,q}\right]$$

Distribution of transversely polarised quarks in an unpolarised nucleon

spin physics with unpolarised hadrons!

access at unpolarised facilities, such as the LHC!

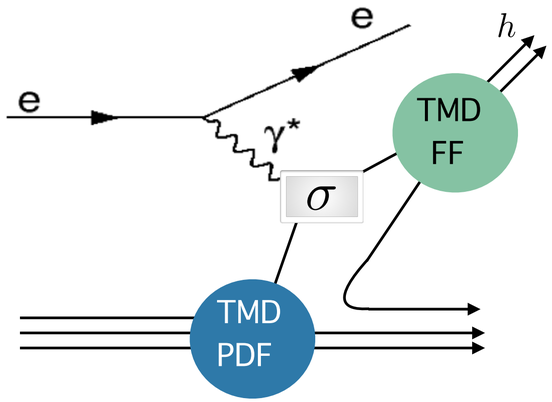

ep collisions: semi-inclusive DIS

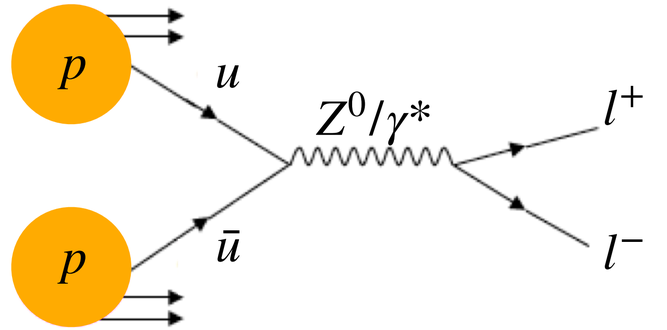

hh collsisions: Drell-Yan

Boer-Mulders TMD PDF

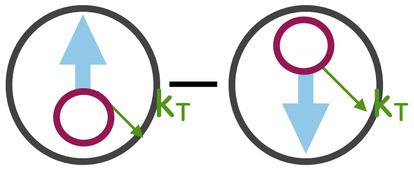

$$\mathscr{C}\left[h_1^{\perp,q} \times H_1^{\perp,q}\right]$$

Distribution of transversely polarised quarks in an unpolarised nucleon

spin physics with unpolarised hadrons!

access at unpolarised facilities, such as the LHC!

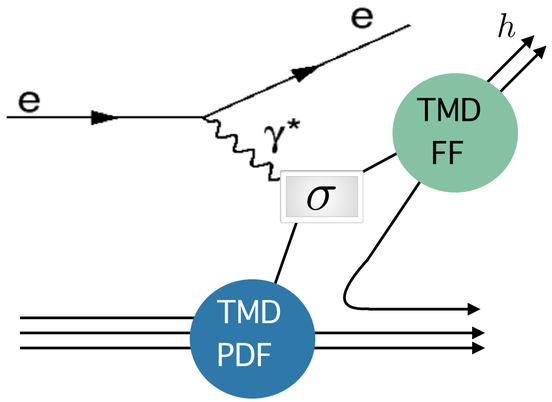

ep collisions: semi-inclusive DIS

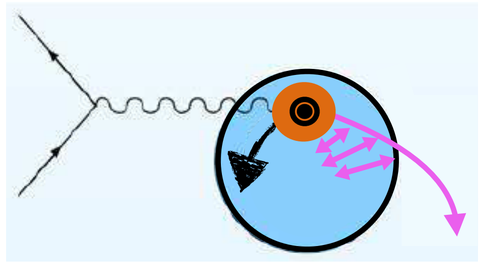

FSI vs. ISI → sign change

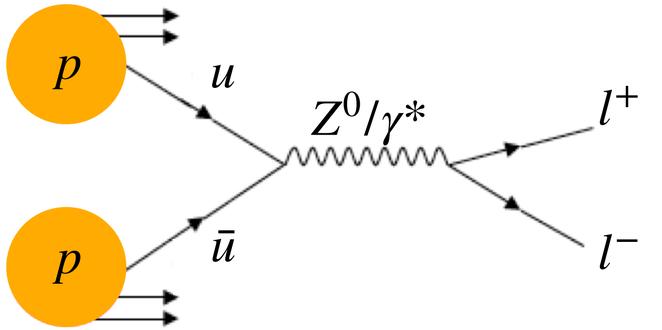

hh collsisions: Drell-Yan

Boer-Mulders TMD PDF in semi-inclusive DIS

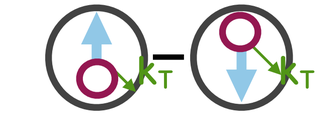

$$\mathscr{C}\left[h_1^{\perp,q} \times H_1^{\perp,q}\right]$$

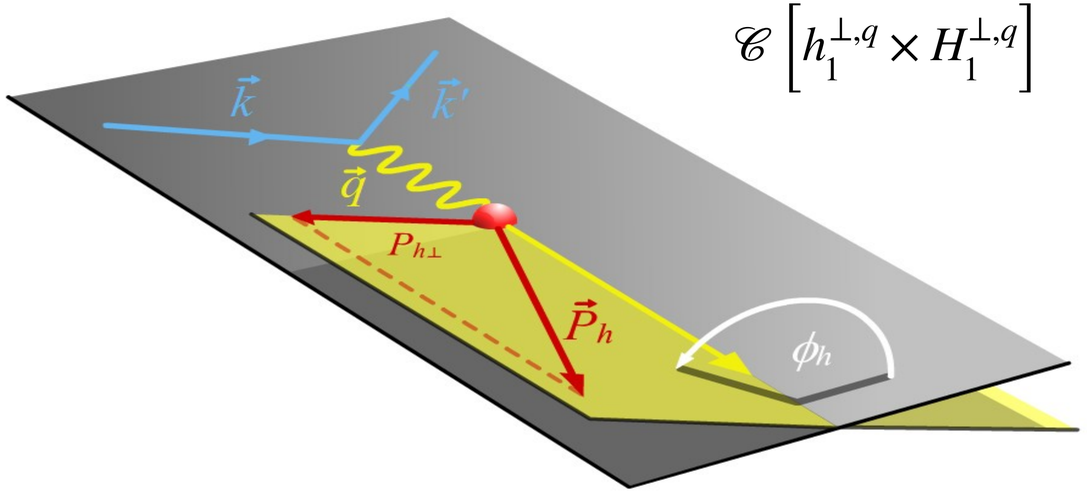

$$\sigma \sim \cos(2\phi_h) \sum_q e_q^2 \, C\left[\, h_1^q(x, k_\perp) \times H_1^{\perp,q}(z, p_\perp)\right]$$

$h_1^q(x, k_\perp)$: Boer Mulders 

$H_1^{\perp,q}(z, p_\perp)$: Collins fragmentation function

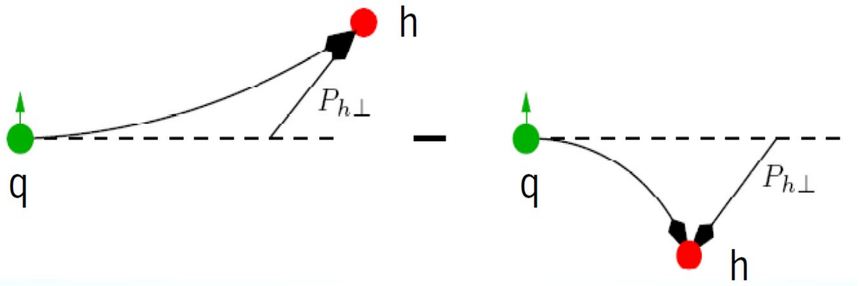

Boer-Mulders modulation: experimental access

$$\mathscr{C}\left[h_1^{\perp,q} \times H_1^{\perp,q}\right]$$

Measurement in ep: $\langle \cos(2\phi_h) \rangle_{Born}(j)$ $\langle \cos(2\phi_h) \rangle_{meas}(i)$

Boer-Mulders modulation: experimental access

$$\mathscr{C}\left[h_1^{\perp,q} \times H_1^{\perp,q}\right]$$

Measurement in ep: $\langle \cos(2\phi_h) \rangle_{Born}(j)$ $\langle \cos(2\phi_h) \rangle_{meas}(i)$

- QED radiate effects

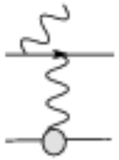

Boer-Mulders modulation: experimental access

$$\mathscr{C}\left[h_1^{\perp,q} \times H_1^{\perp,q}\right]$$

Measurement in ep: $\langle \cos(2\phi_h) \rangle_{Born}(j)$ $\langle \cos(2\phi_h) \rangle_{meas}(i)$

- QED radiate effects 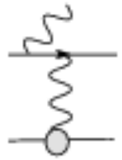
- limited geometric and kinematic acceptance of detector

Boer-Mulders modulation: experimental access

$$\mathscr{C}\left[h_1^{\perp,q} \times H_1^{\perp,q}\right]$$

Measurement in ep: $\langle \cos(2\phi_h) \rangle_{Born}(j)$ $\langle \cos(2\phi_h) \rangle_{meas}(i)$

- QED radiate effects

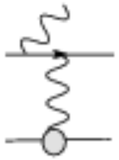

- limited geometric and kinematic acceptance of detector
- limited detector resolution

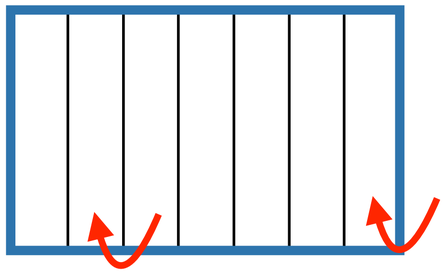

Boer-Mulders modulation: experimental access

$$\mathscr{C}\left[h_1^{\perp,q} \times H_1^{\perp,q}\right]$$

Measurement in ep: $\langle \cos(2\phi_h) \rangle_{Born}(j)$ $\langle \cos(2\phi_h) \rangle_{meas}(i)$

- QED radiate effects

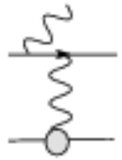

- limited geometric and kinematic acceptance of detector
- limited detector resolution

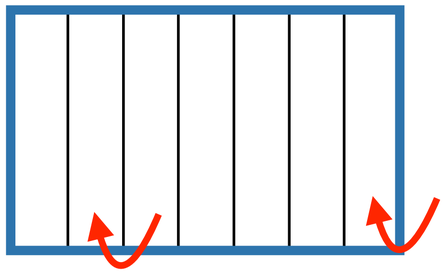

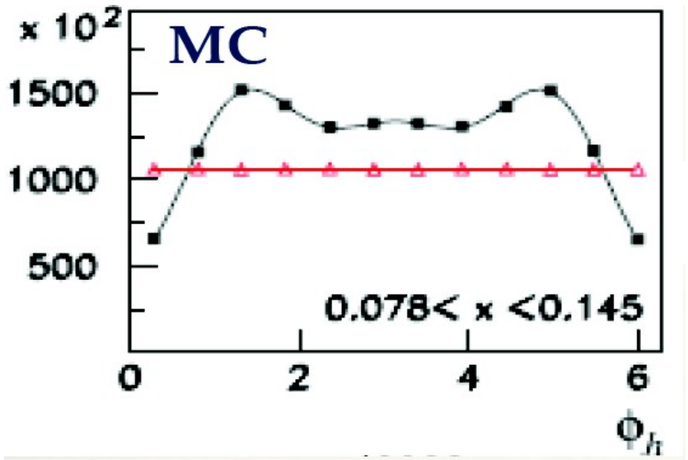

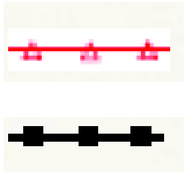

generated in 4π

inside acceptance

Boer-Mulders modulation: experimental access

$$\mathscr{C}\left[h_1^{\perp,q} \times H_1^{\perp,q}\right]$$

Measurement in ep:

Fully differential analysis

Unfolding in 400 x 12 bins

BINNING 400 kinematic bins x 12 ϕ-bins							
Variable	Bin limits						#
x	0.023	0.042	0.078	0.145	0.27	1	5
y	0.3	0.45	0.6	0.7	0.85		4
z	0.2	0.3	0.45	0.6	0.75	1	5
P_{hT}	0.05	0.2	0.35	0.5	0.75		4

tector

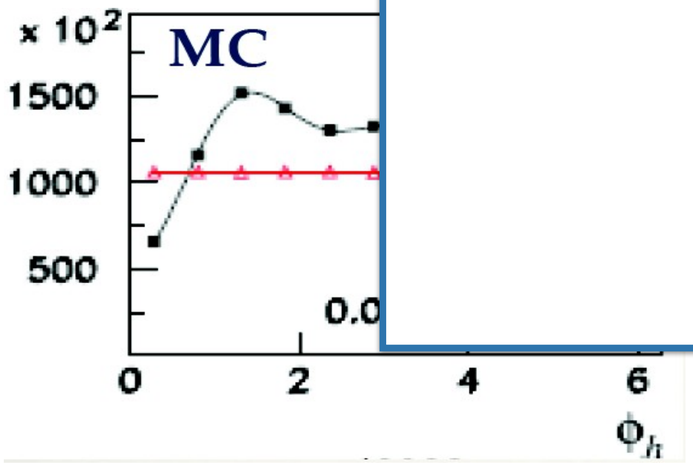

Boer-Mulders modulations

$$\mathscr{C}\left[h_1^{\perp,q} \times H_1^{\perp,q}\right]$$

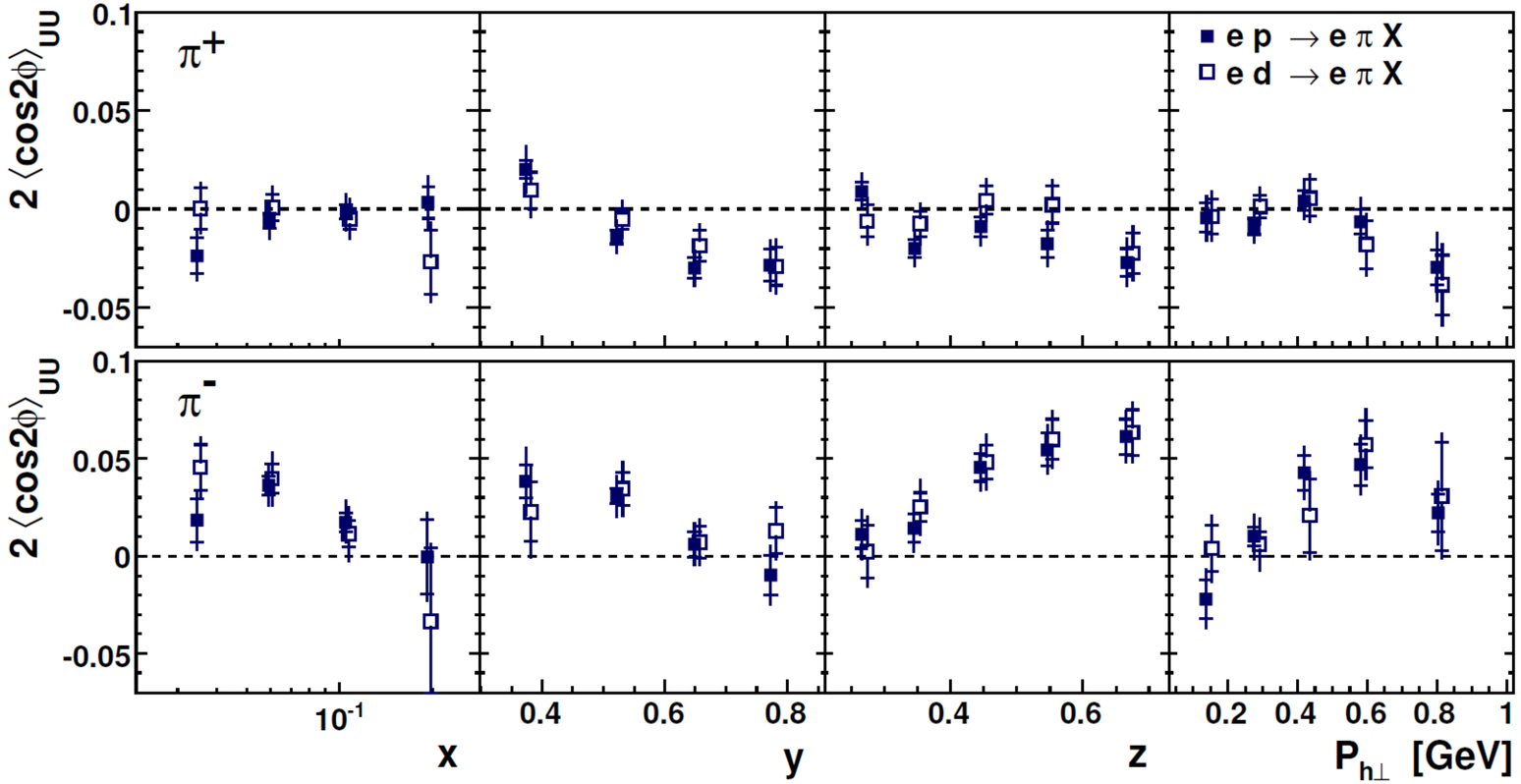

H–D comparison: $h_1^{\perp,u} \approx h_1^{\perp,d}$

Negative for π^+; positive for π^- $\rightarrow H_1^{\perp,u\rightarrow\pi^+} \approx -H_1^{\perp,u\rightarrow\pi^-}$

Study of quark TMD PDFs at the LHC

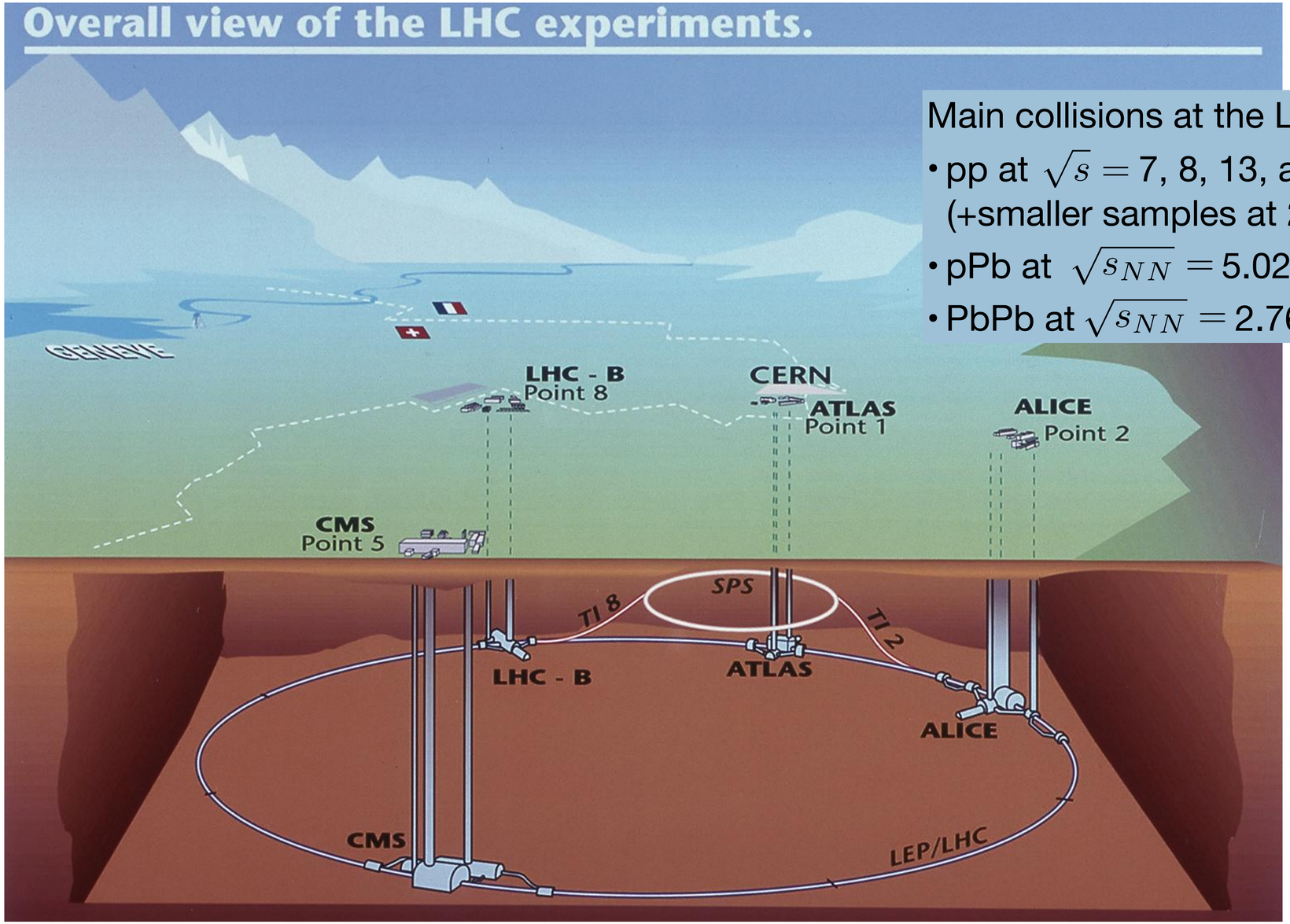

Main collisions at the LHC:

- pp at $\sqrt{s} = 7$, 8, 13, and 14 TeV (+smaller samples at 2.76 and 5.02 TeV)
- pPb at $\sqrt{s_{NN}} = 5.02$, 8.20, 8.80 TeV
- PbPb at $\sqrt{s_{NN}} = 2.76$, 5.02, 5.44 TeV

Study of quark TMD PDFs at the LHC

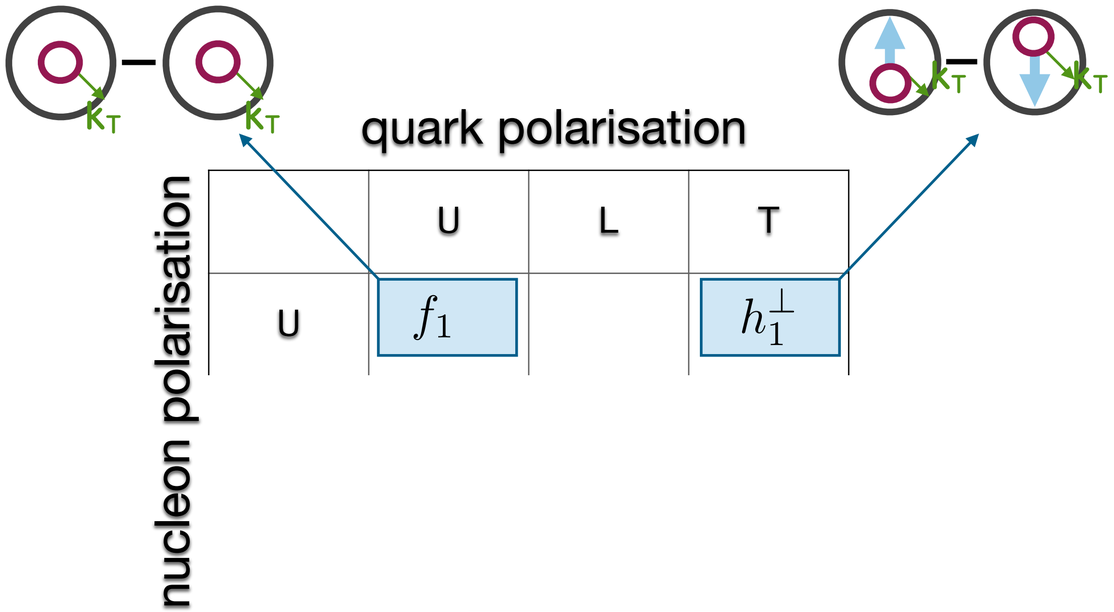

Main collisions at the LHC:

- pp at $\sqrt{s} = 7$, 8, 13, and 14 TeV (+smaller samples at 2.76 and 5.02 TeV)
- pPb at $\sqrt{s_{NN}} = 5.02$, 8.20, 8.80 TeV
- PbPb at $\sqrt{s_{NN}} = 2.76$, 5.02, 5.44 TeV

Study of spin-independent quark TMD PDFs at the LHC

Coverage Drell-Yan

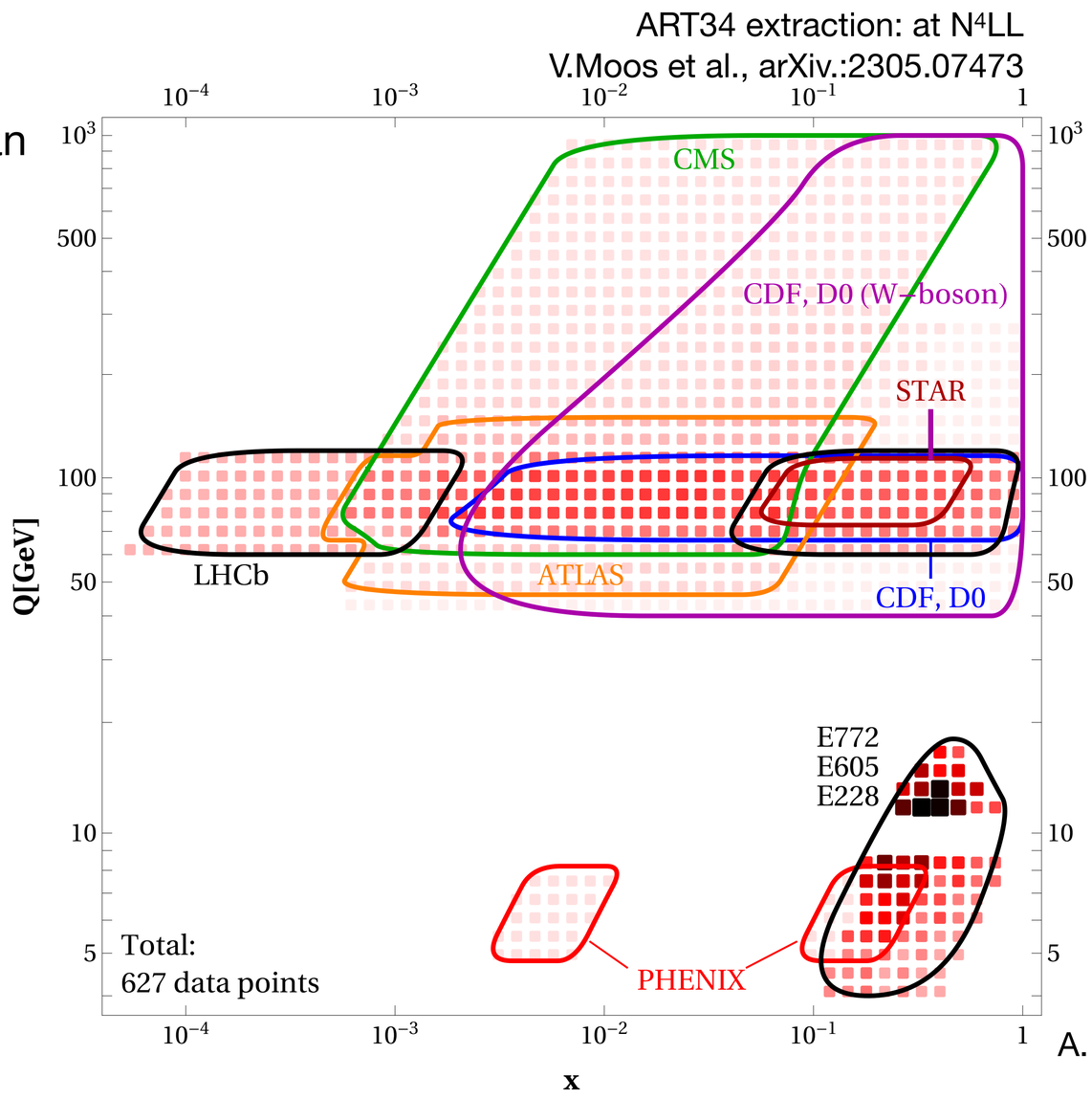

A. Vladimirov

Study of spin-independent quark TMD PDFs at the LHC

Coverage Drell-Yan

ART34 extraction: at N⁴LL
V.Moos et al., arXiv.:2305.07473

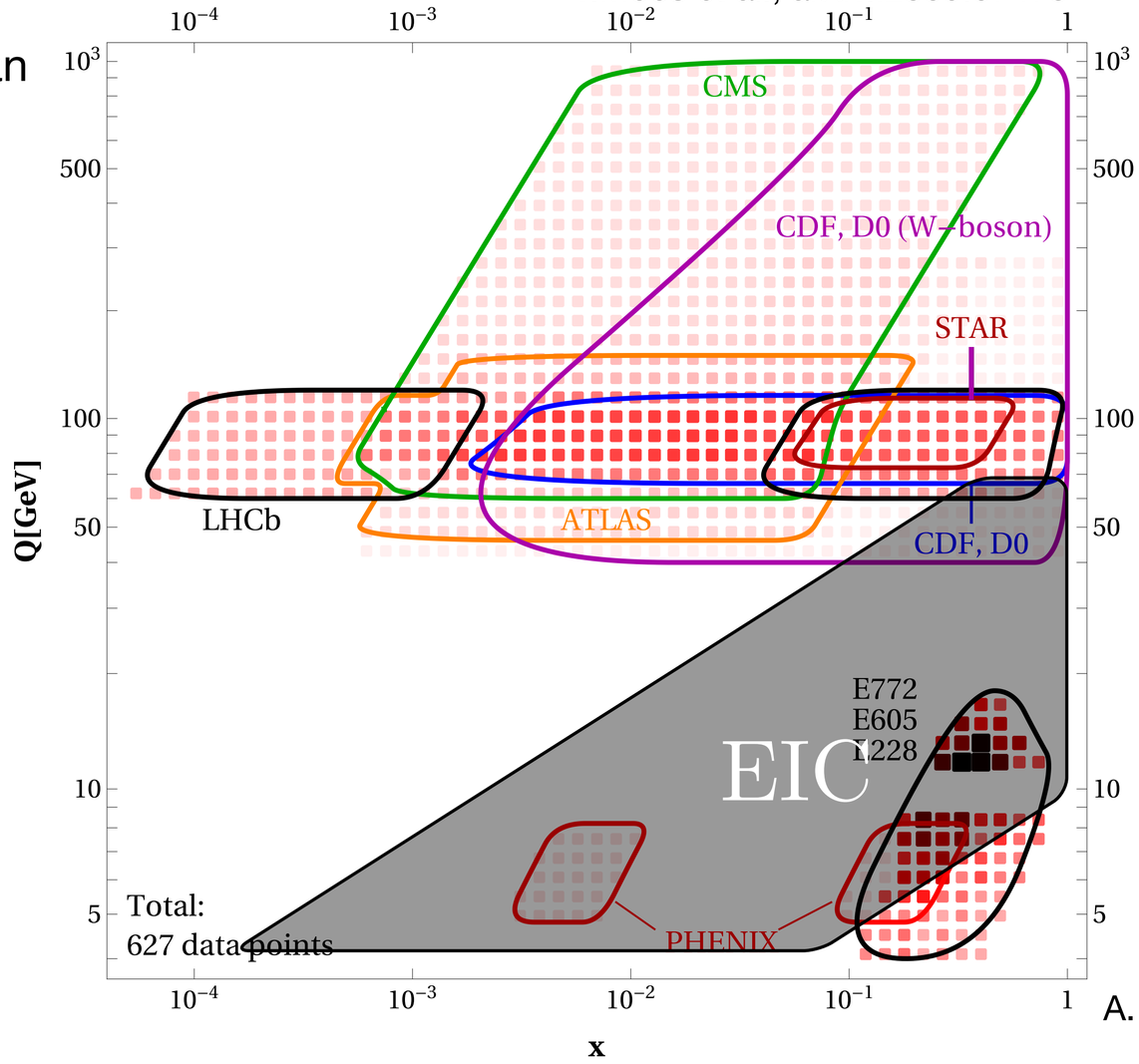

A. Vladimirov

Study of spin-independent quark TMD PDFs at the LHC

ART34 extraction: at N⁴LL
V.Moos et al., arXiv.:2305.07473

Coverage Drell-Yan

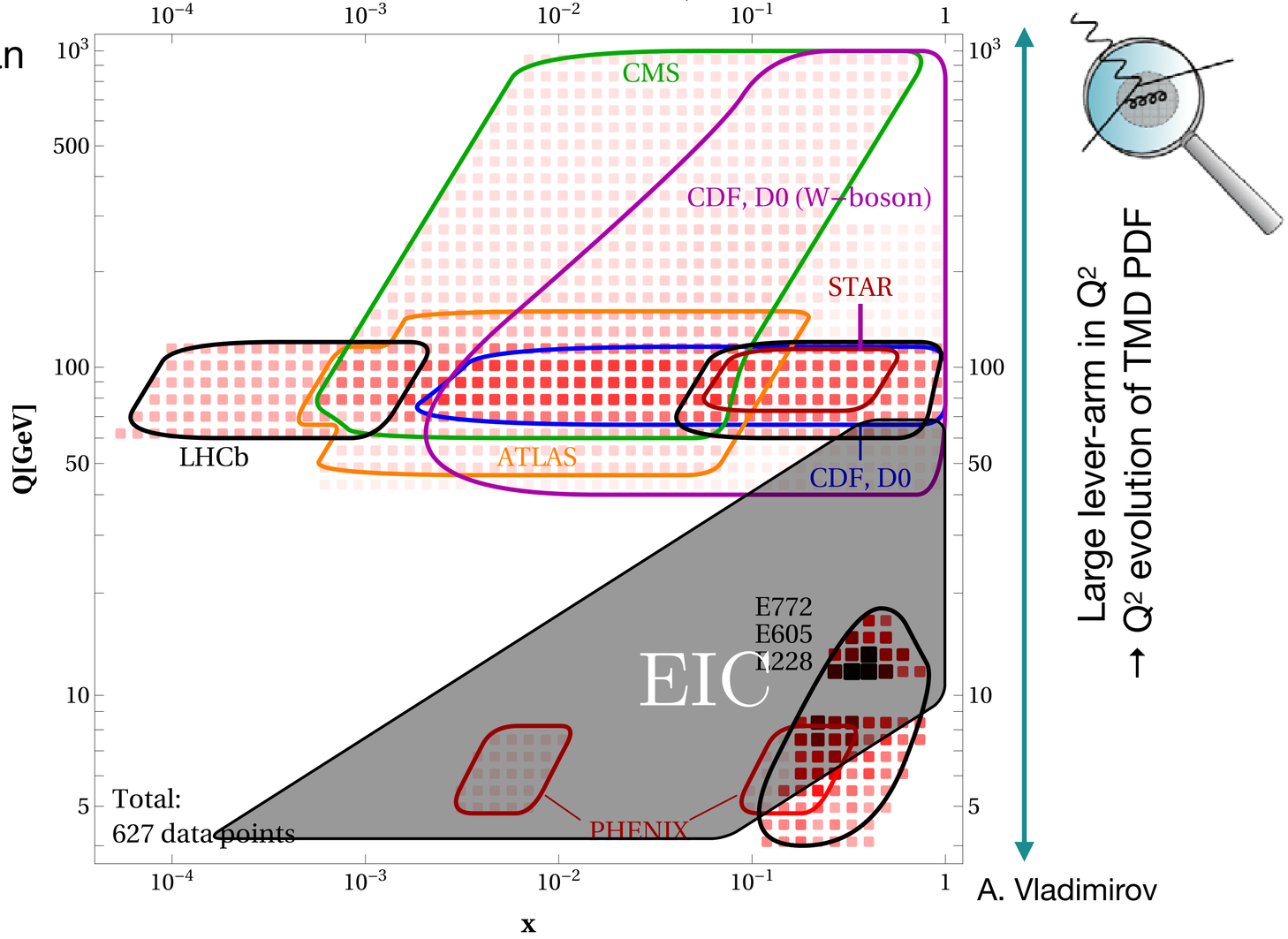

Large lever-arm in Q^2
→ Q^2 evolution of TMD PDF

A. Vladimirov

Quark Boer-Mulders TMD PDFs at the LHC

$A_2 \sim h_1^\perp h_1^\perp$ and $f_1 f_1$

Comparison data – fit:

S. Piloñeta, A. Vladimirov, JHEP **12** (2024) 059

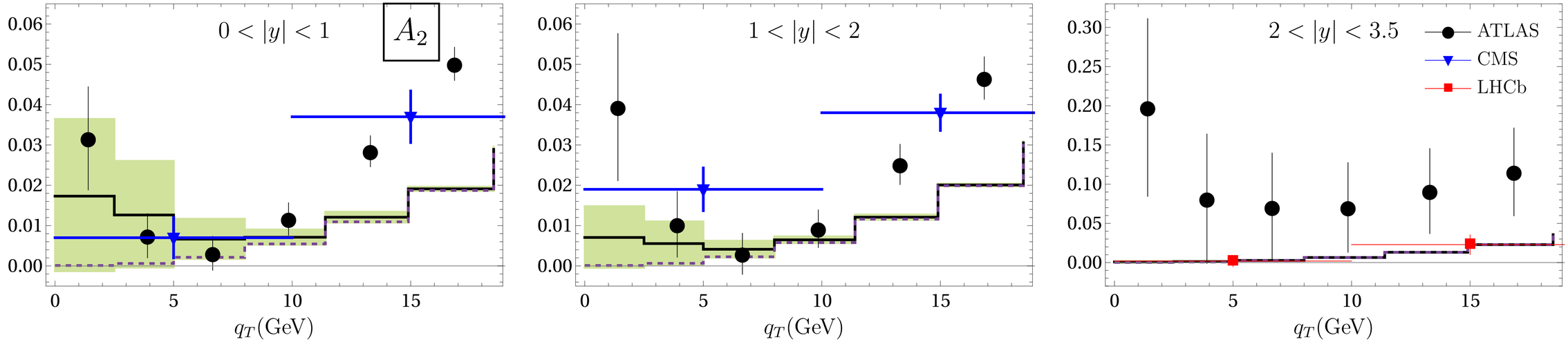

------ No Boer-Mulders

- ATLAS JHEP **08** (2016) 159.
- CMS, Phys. Lett. B **750** (2015) 154.
- LHCb, Phys. Rev. Lett. **129** (2022) 091801.

Quark Boer-Mulders TMD PDFs at the LHC

$A_2 \sim h_1^\perp h_1^\perp$ and $f_1 f_1$

Comparison data – fit:

S. Piloñeta, A. Vladimirov, JHEP **12** (2024) 059

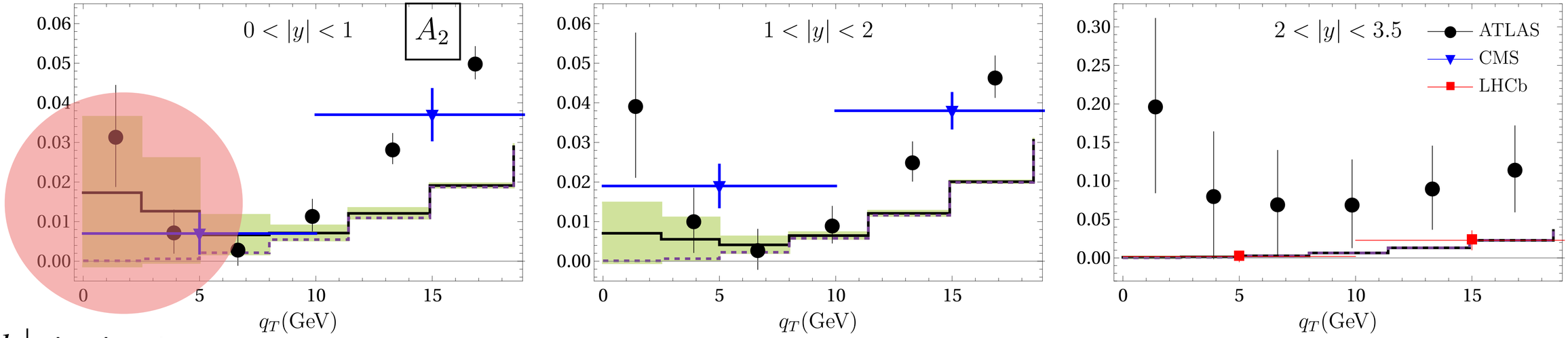

$h_1^\perp h_1^\perp$ dominant

------ No Boer-Mulders

- ATLAS JHEP **08** (2016) 159.
- CMS, Phys. Lett. B **750** (2015) 154.
- LHCb, Phys. Rev. Lett. **129** (2022) 091801.

Quark Boer-Mulders TMD PDFs at the LHC

$A_2 \sim h_1^\perp h_1^\perp$ and $f_1 f_1$

Comparison data – fit:

S. Piloñeta, A. Vladimirov, JHEP **12** (2024) 059

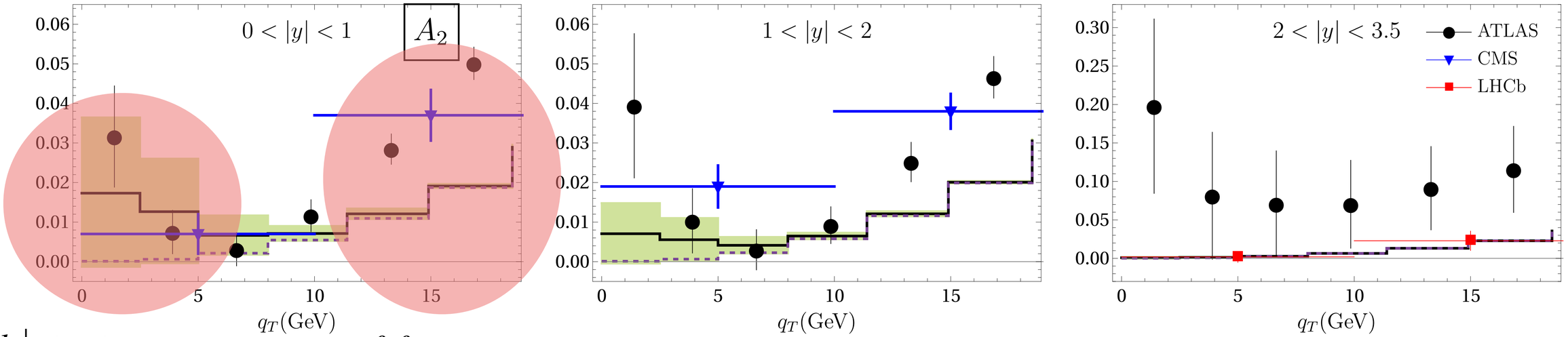

$h_1^\perp h_1^\perp$ dominant

$f_1 f_1$ dominant

------ No Boer-Mulders

- ATLAS JHEP **08** (2016) 159.
- CMS, Phys. Lett. B **750** (2015) 154.
- LHCb, Phys. Rev. Lett. **129** (2022) 091801.

Quark Boer-Mulders TMD PDFs at the LHC

$A_2 \sim h_1^\perp h_1^\perp$ and $f_1 f_1$

Comparison data – fit:

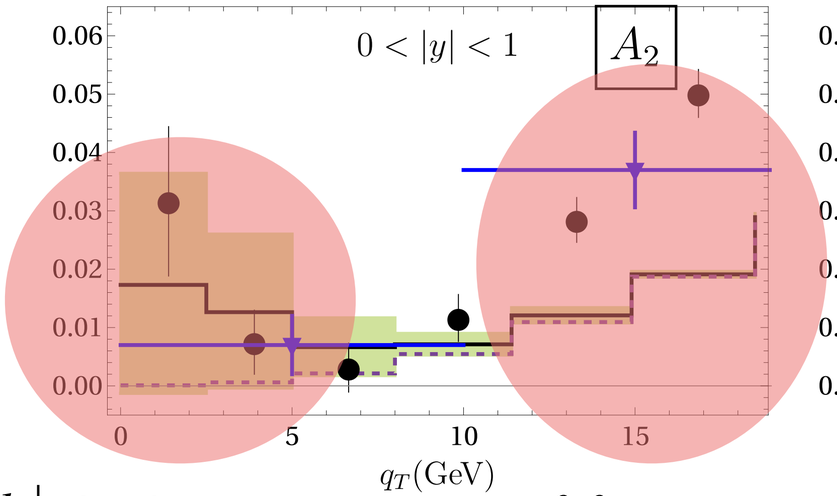

$h_1^\perp h_1^\perp$ dominant

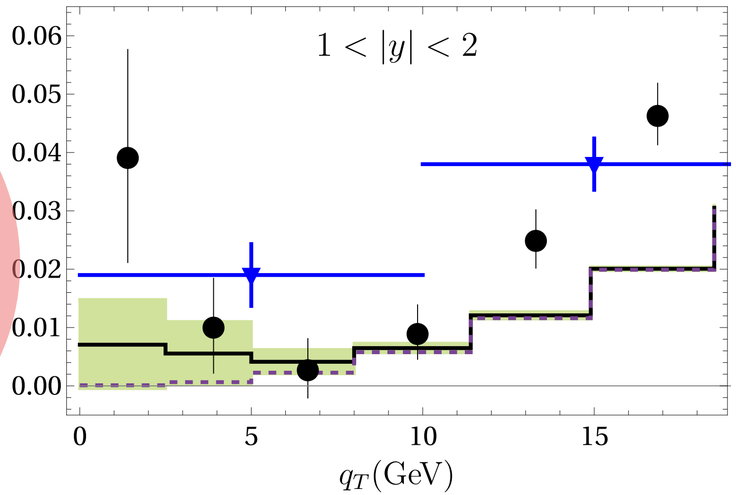

$f_1 f_1$ dominant

S. Piloñeta, A. Vladimirov, JHEP **12** (2024) 059

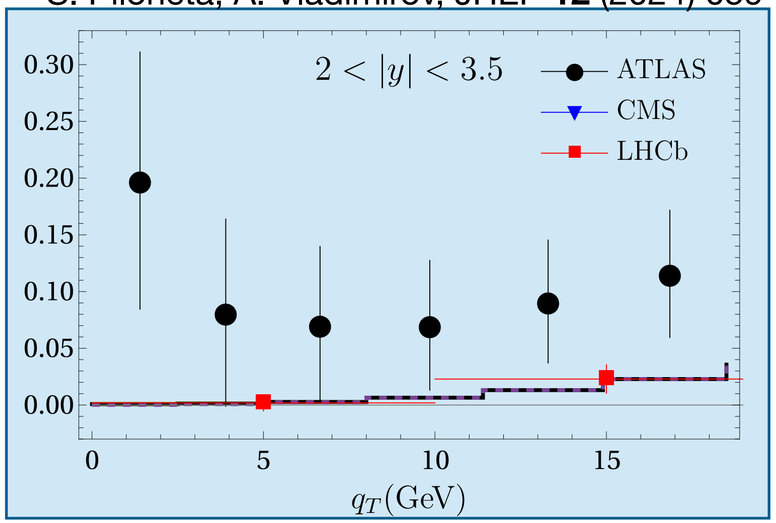

------ No Boer-Mulders

- ATLAS JHEP **08** (2016) 159.
- CMS, Phys. Lett. B **750** (2015) 154.
- LHCb, Phys. Rev. Lett. **129** (2022) 091801.

Problematic: inconsistent with ATLAS; consistent with LHCb.

Gluon TMD PDFs

gluon polarisation

nucleon polarisation

	U	circular	linear
U	f_1^g		$h_1^{\perp g}$
L		g_1^g	$h_{1L}^{\perp g}$
T	$f_{1T}^{\perp g}$	g_{1T}^g	h_1^g, $h_{1T}^{\perp g}$

Gluon TMD PDFs

gluon polarisation

nucleon polarisation

	U	circular	linear
U	f_1^g		$h_1^{\perp g}$
L		g_1^g	$h_{1L}^{\perp g}$
T	$f_{1T}^{\perp g}$	g_{1T}^g	$h_1^g, h_{1T}^{\perp g}$

- In contrast to quark TMDs, gluon TMDs are almost unknown

Gluon TMD PDFs

gluon polarisation

nucleon polarisation	U	circular	linear
U	f_1^g		$h_1^{\perp g}$
L		g_1^g	$h_{1L}^{\perp g}$
T	$f_{1T}^{\perp g}$	g_{1T}^g	h_1^g, $h_{1T}^{\perp g}$

- In contrast to quark TMDs, gluon TMDs are almost unknown
- Accessible through production of dijets, high-P_T hadron pairs, quarkonia

Access to gluon TMD PDFs

nucleon polarisation \ gluon polarisation

	U	circular	linear
U	f_1^g		$h_1^{\perp g}$

Unpolarised experiments

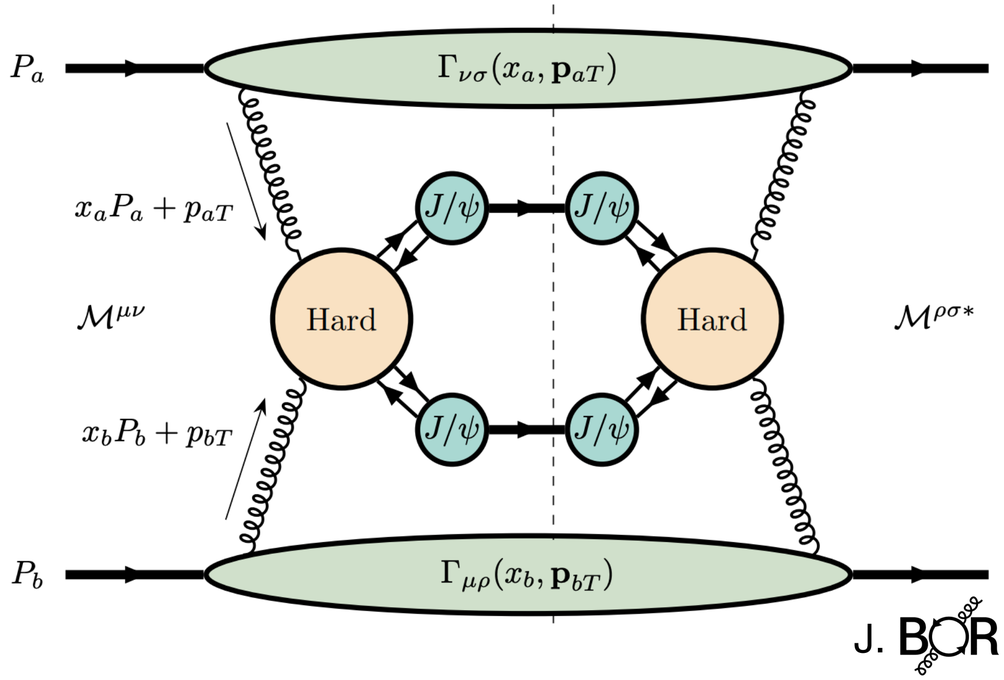

No problem with factorisation

if J/ψ in colour-singlet state

Access to gluon TMD PDFs

gluon polarisation

nucleon polarisation

	U	circular	linear
U	f_1^g		$h_1^{\perp g}$
L		g_1^g	$h_{1L}^{\perp g}$
T	$f_{1T}^{\perp g}$	g_{1T}^g	h_1^g, $h_{1T}^{\perp g}$

Polarised ep experiments

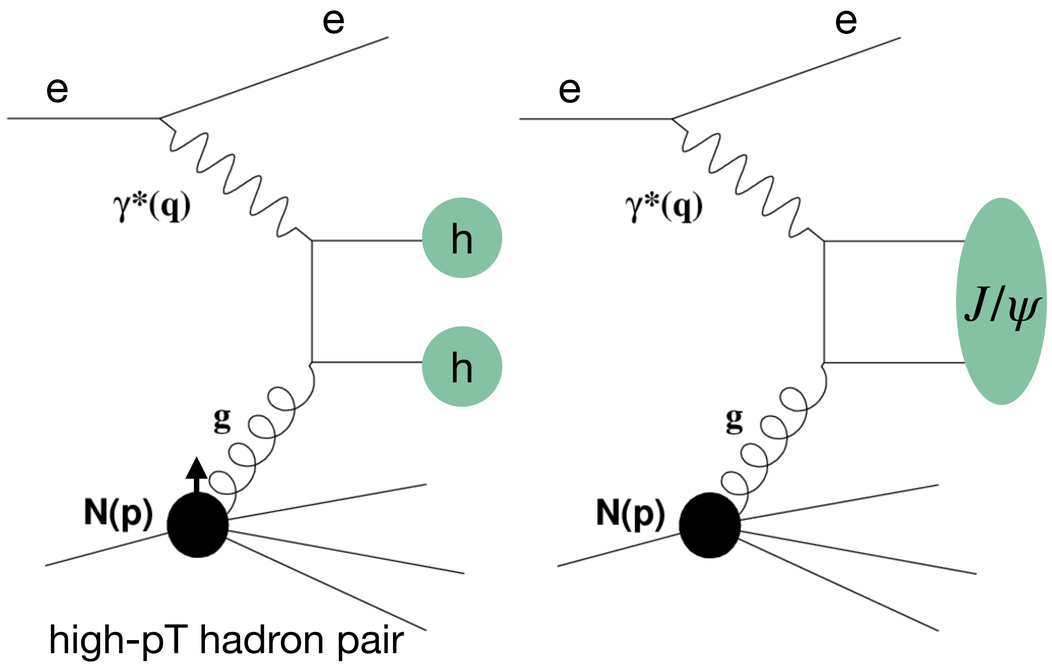

high-pT hadron pair

Linearly polarised gluon TMD PDF at LHCb

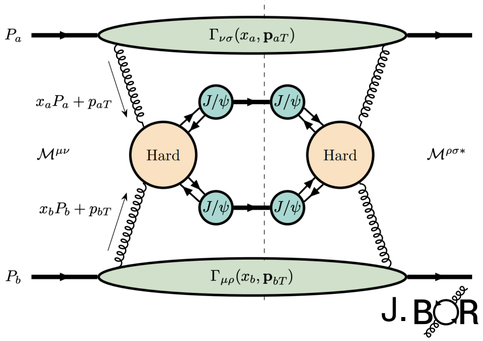

- $J/\psi J/\psi$ production largely dominated by gluon-induced processes

$$\sigma \propto F_1 \mathscr{C}[f_1^g f_1^g] + F_2 \mathscr{C}[w_2 h_1^{g\perp} h_1^{g\perp}] + \left(F_3 \mathscr{C}[w_3 f_1^g h_1^{g\perp}] + F_3' \mathscr{C}[w_3' f_1^g h_1^{g\perp}] \right) \cos\left(2\phi_{CS}\right) + \left(F_4 \mathscr{C}[w_4 h_1^{g\perp} h_1^{g\perp}] \right) \cos\left(4\phi_{CS}\right)$$

Linearly polarised gluon TMD PDF at LHCb

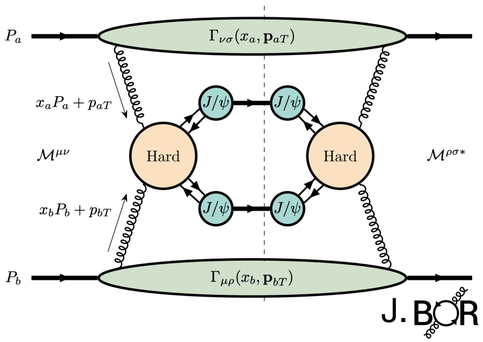

- $J/\psi J/\psi$ production largely dominated by gluon-induced processes

$$\sigma \propto F_1 \mathscr{C}[f_1^g f_1^g] + F_2 \mathscr{C}[w_2 h_1^{g\perp} h_1^{g\perp}] + \left(F_3 \mathscr{C}[w_3 f_1^g h_1^{g\perp}] + F_3' \mathscr{C}[w_3' f_1^g h_1^{g\perp}] \right) \cos\left(2\phi_{CS}\right) + \left(F_4 \mathscr{C}[w_4 h_1^{g\perp} h_1^{g\perp}] \right) \cos\left(4\phi_{CS}\right)$$

After subtraction of the double-parton scattering contribution

JHEP 03 (2024) 088

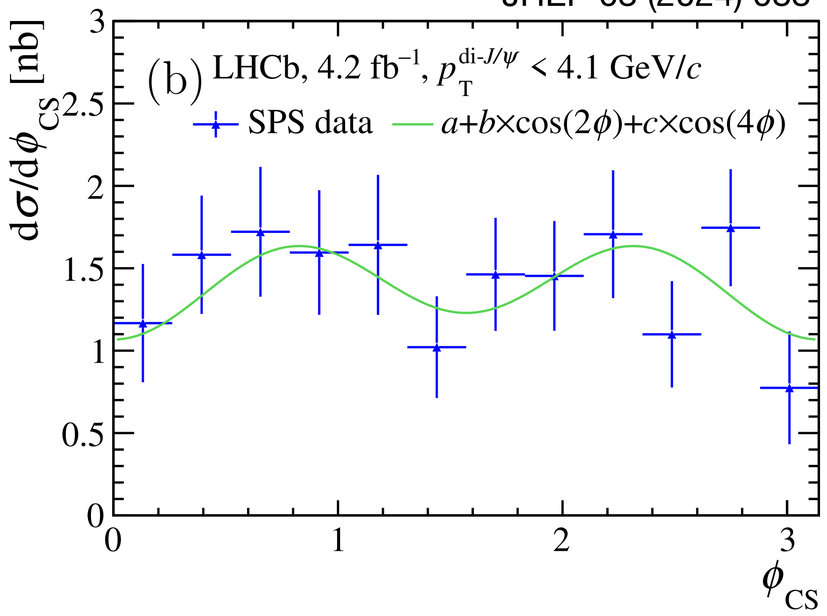

$$p_T^{J/\psi J/\psi} < \frac{\langle M_{J/\psi J/\psi} \rangle}{2},$$

$$\langle M_{J/\psi J/\psi} \rangle = 8.2 \text{ GeV}/c^2$$

$$\langle \cos 2\phi_{\text{CS}} \rangle = -0.029 \pm 0.050 \text{ (stat)} \pm 0.009 \text{ (syst)}$$
$$\langle \cos 4\phi_{\text{CS}} \rangle = -0.087 \pm 0.052 \text{ (stat)} \pm 0.013 \text{ (syst)}$$

Upcoming

AMBER

Apparatus for Meson and Baryon Experimental Research

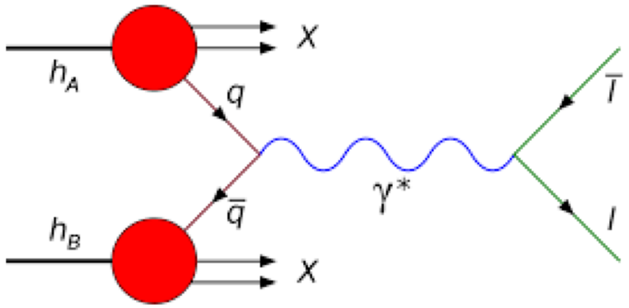

Meson structure

Upcoming

AMBER

Apparatus for Meson and Baryon Experimental Research

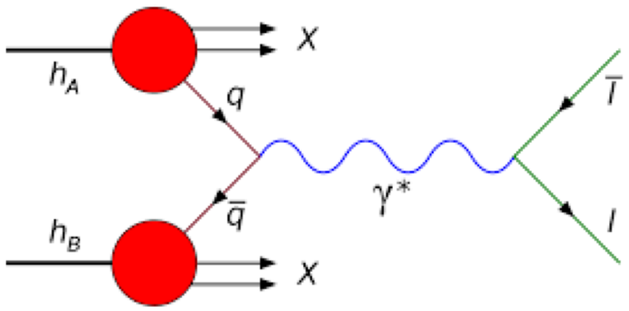

Meson structure

SpinQuest

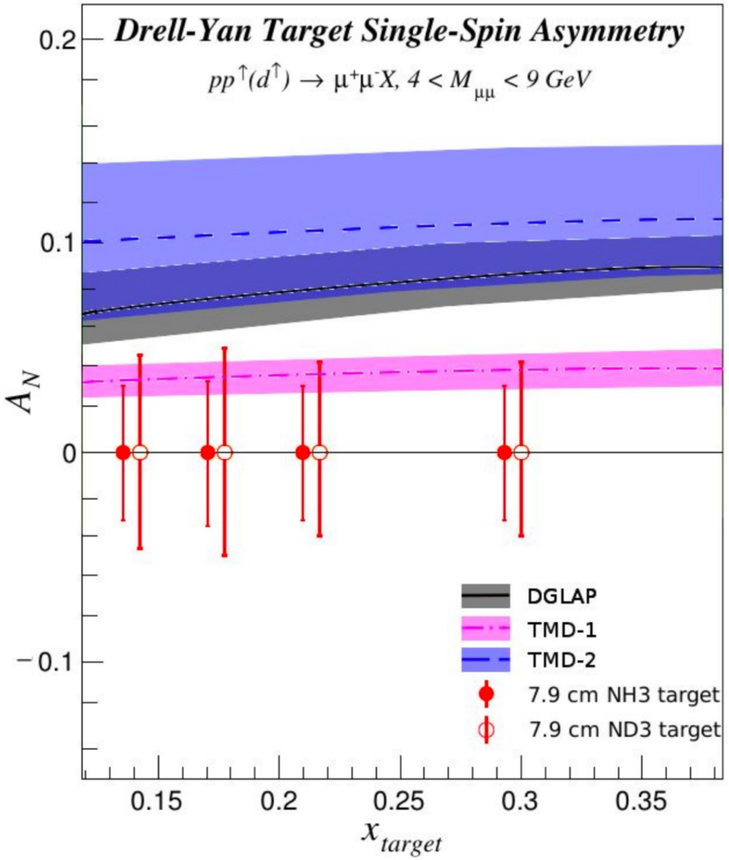

Study of $\bar{u}$ and $\bar{d}$ Sivers function

Upcoming

AMBER

Apparatus for Meson and Baryon Experimental Research

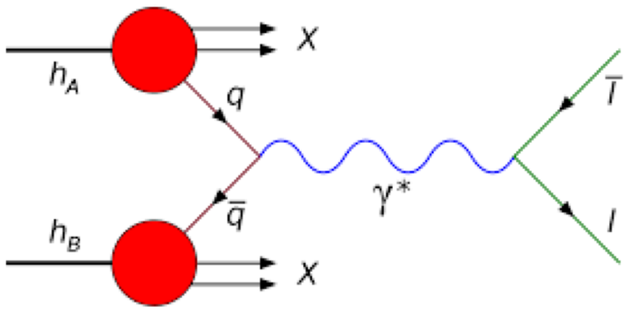

Meson structure

SpinQuest

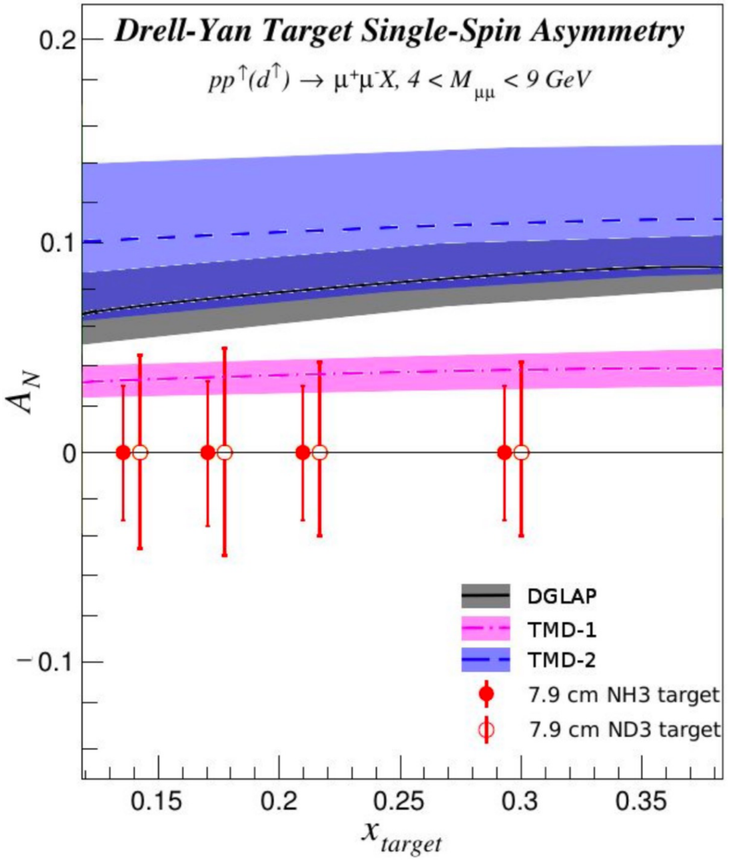

Study of $\bar{u}$ and $\bar{d}$ Sivers function

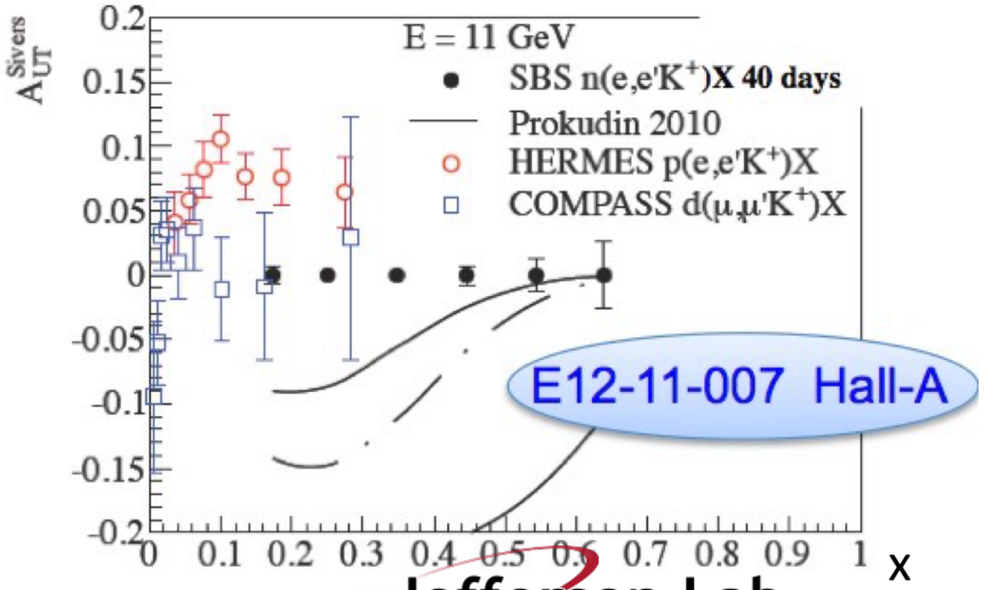

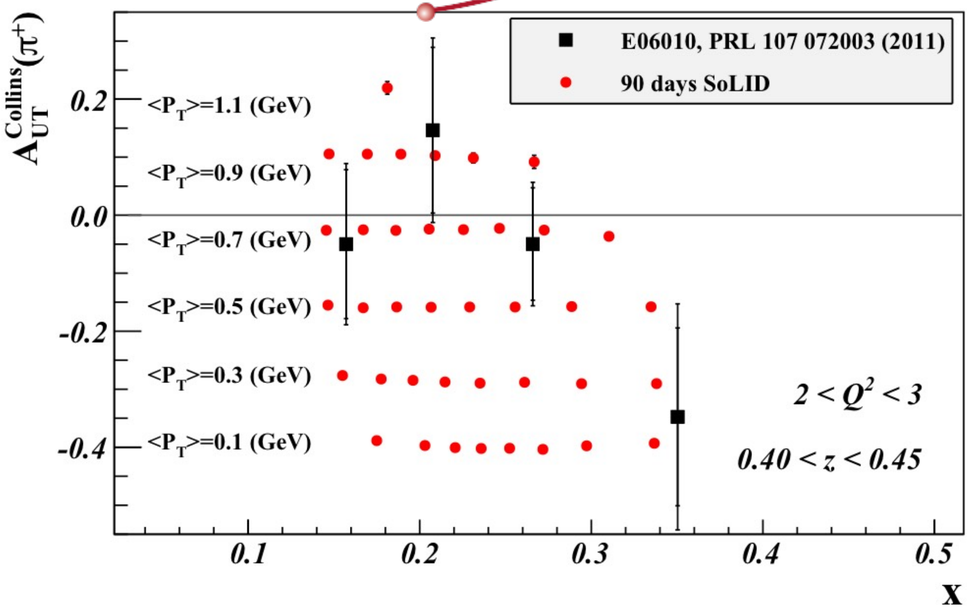

Future: LHCSpin

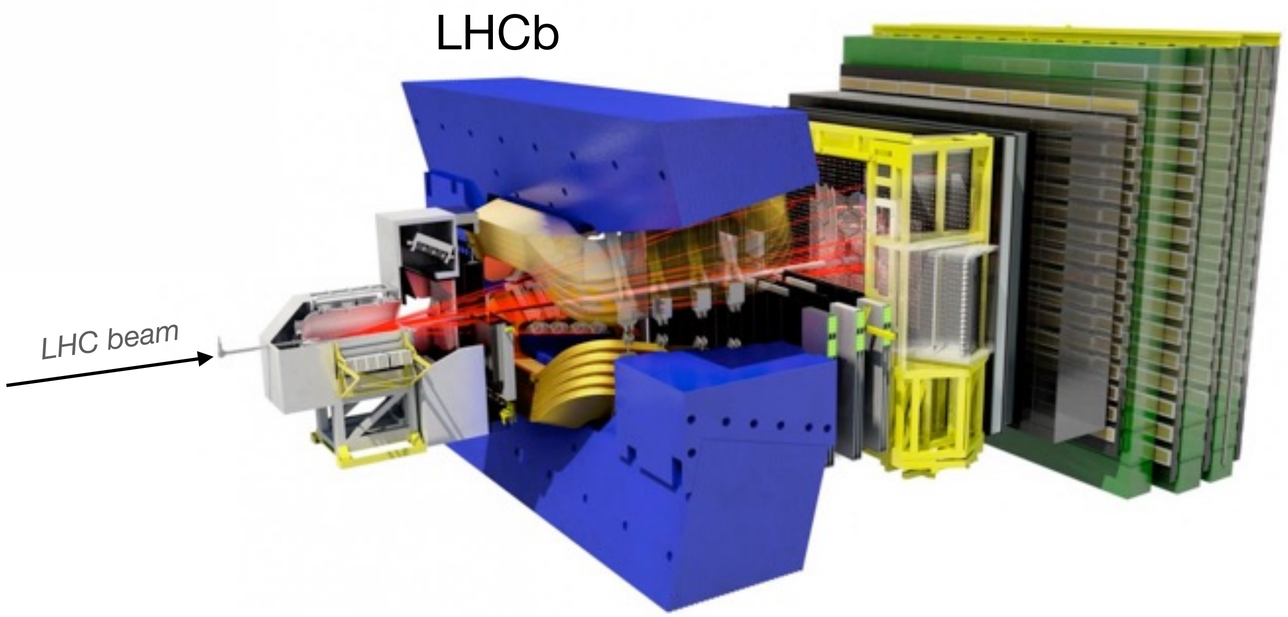

Future: LHCSpin

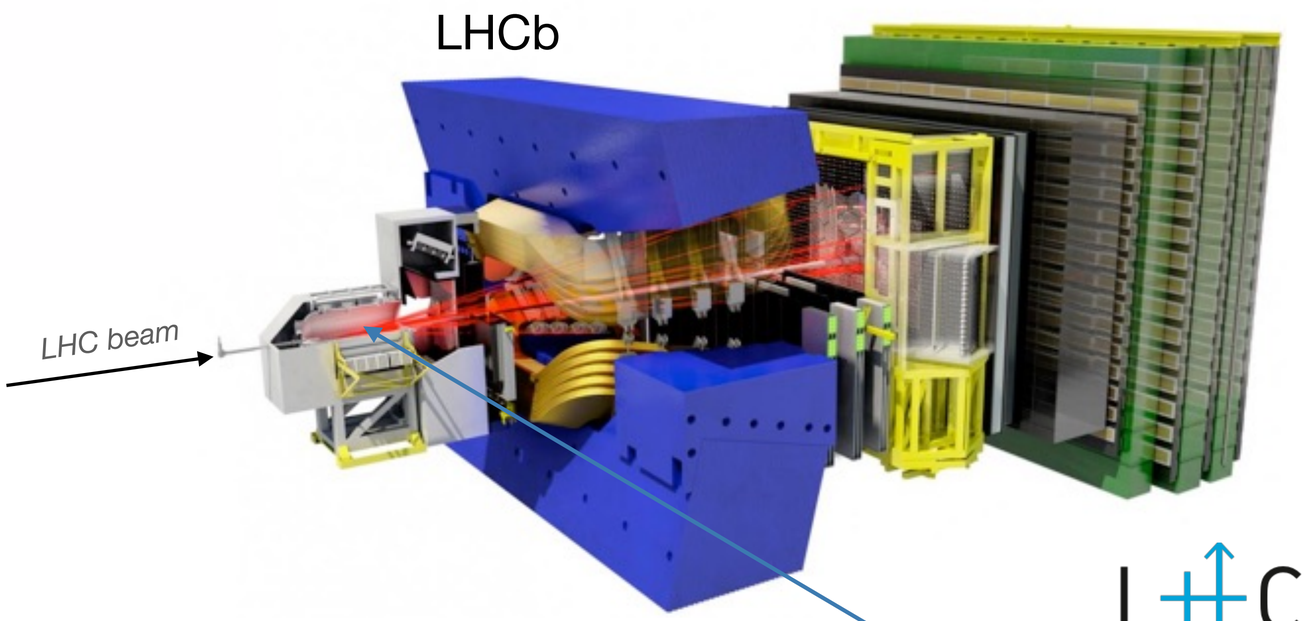

transversely polarised gas target

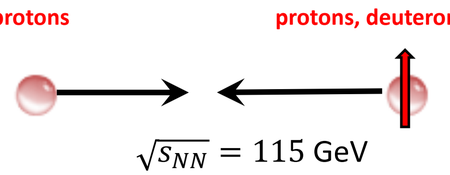

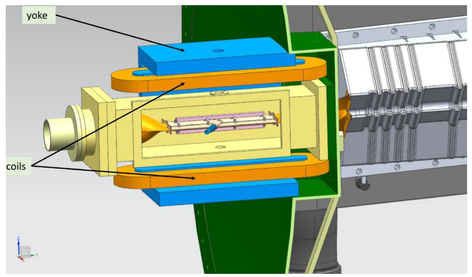

Future: LHCSpin

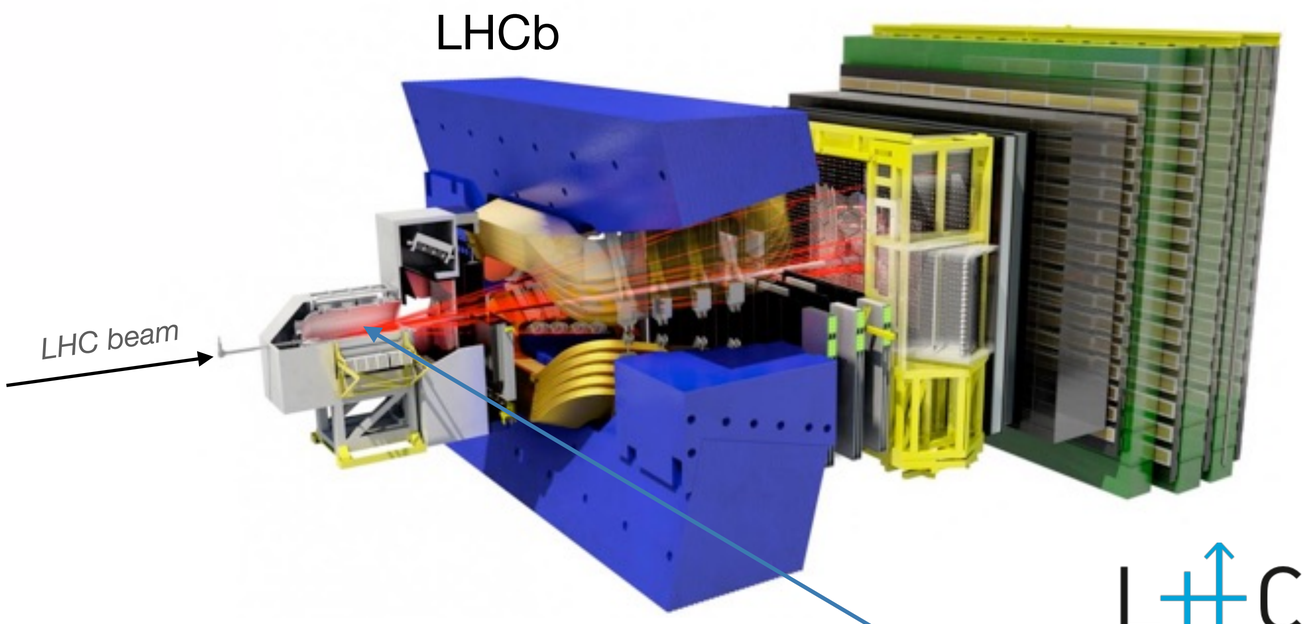

transversely polarised gas target

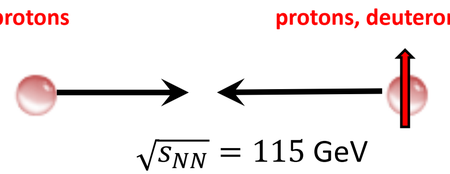

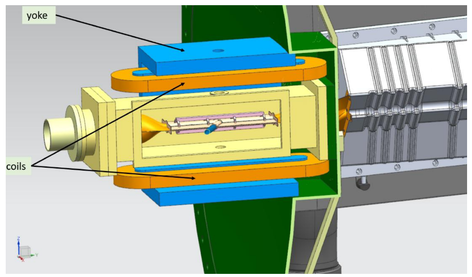

LHCspin

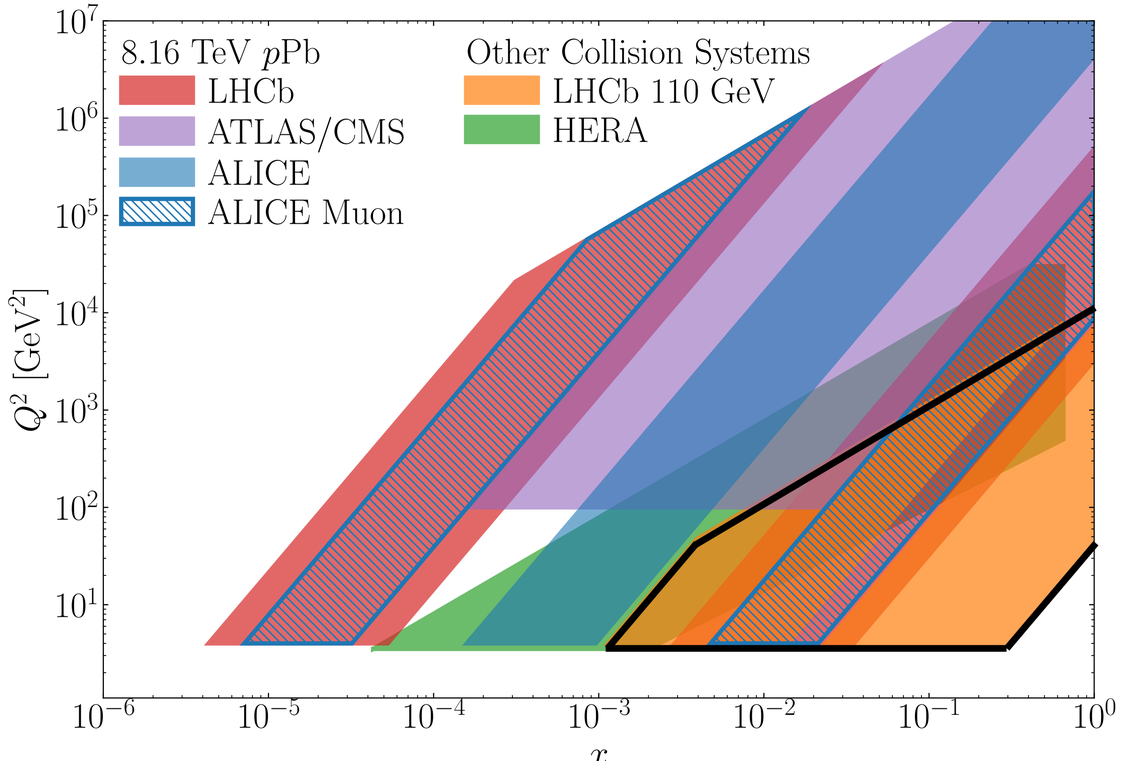

Study of quark and gluon TMDs in polarised proton, via Drell-Yan or quarkonium production at **high x**

Future: LHCSpin

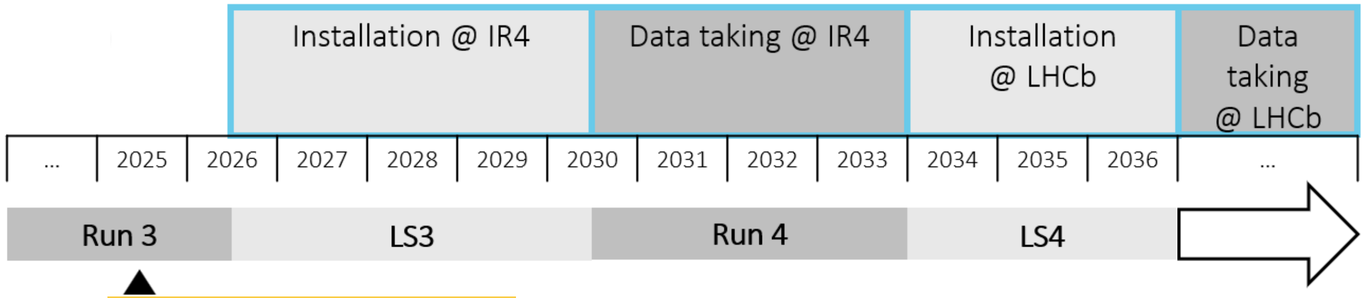

We are here: unpolarised gas target: SMOG2

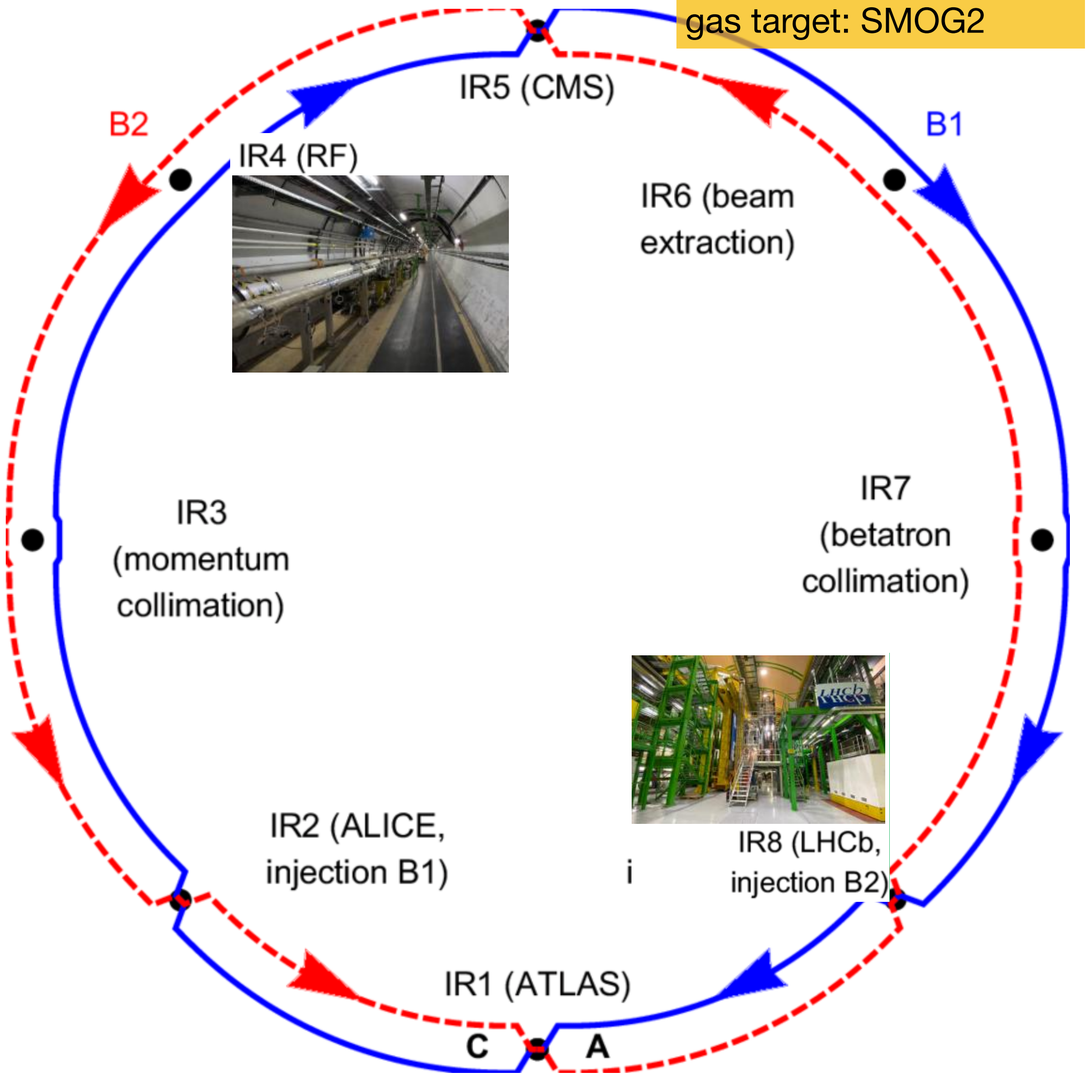

Future: LHCSpin

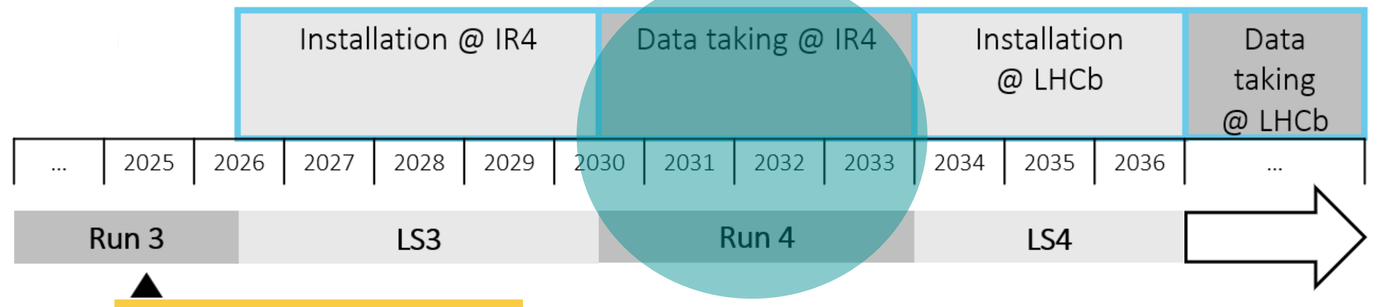

We are here: unpolarised gas target: SMOG2

phase I

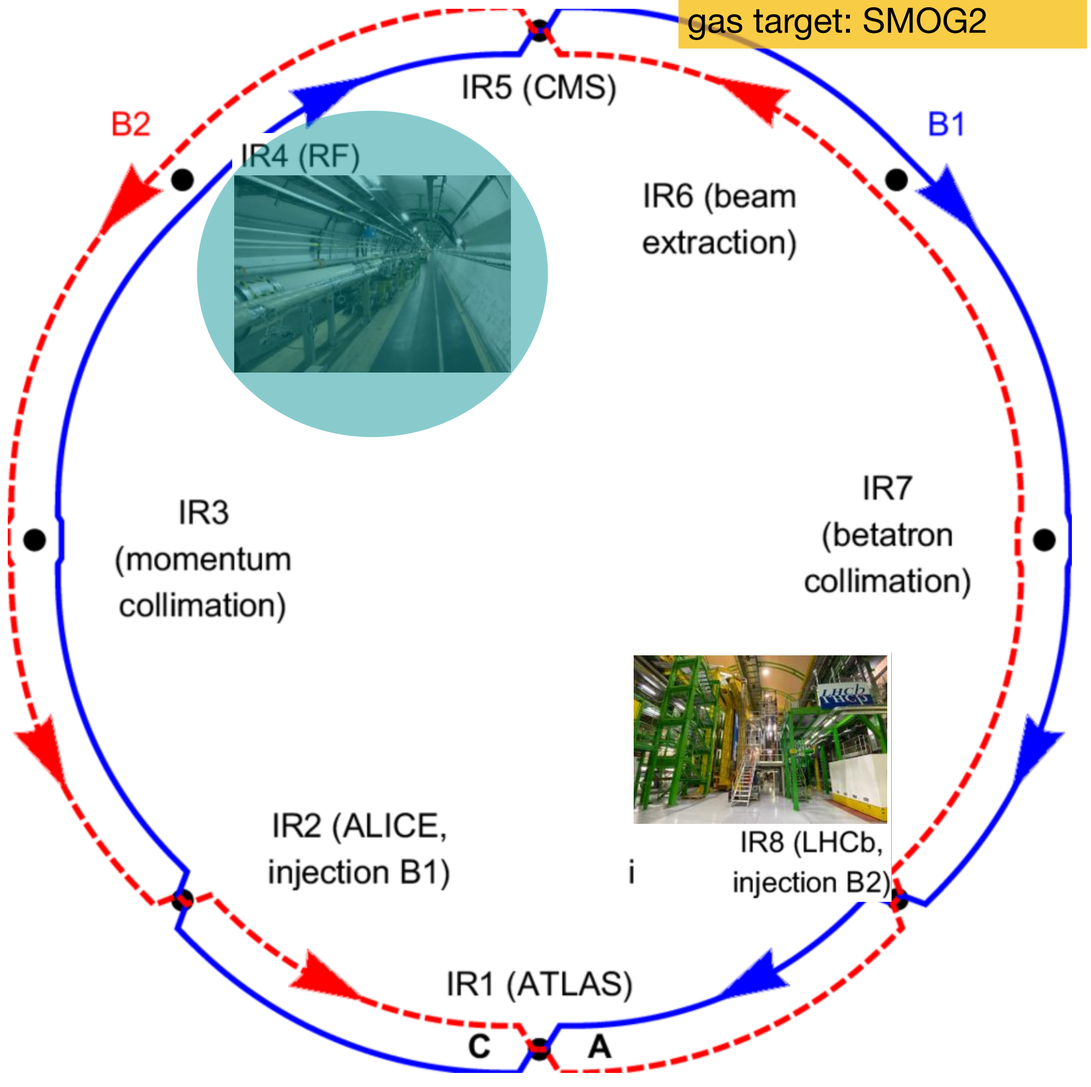

Future: LHCSpin

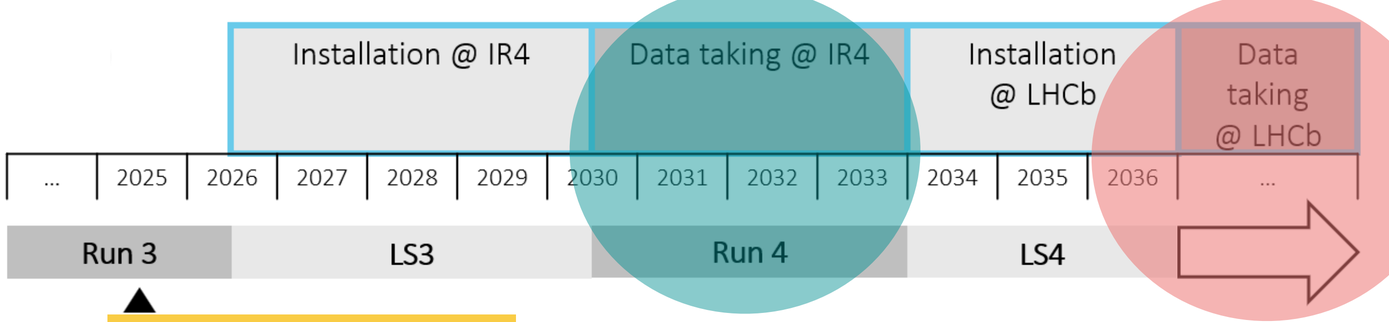

We are here: unpolarised gas target: SMOG2

phase I

phase II

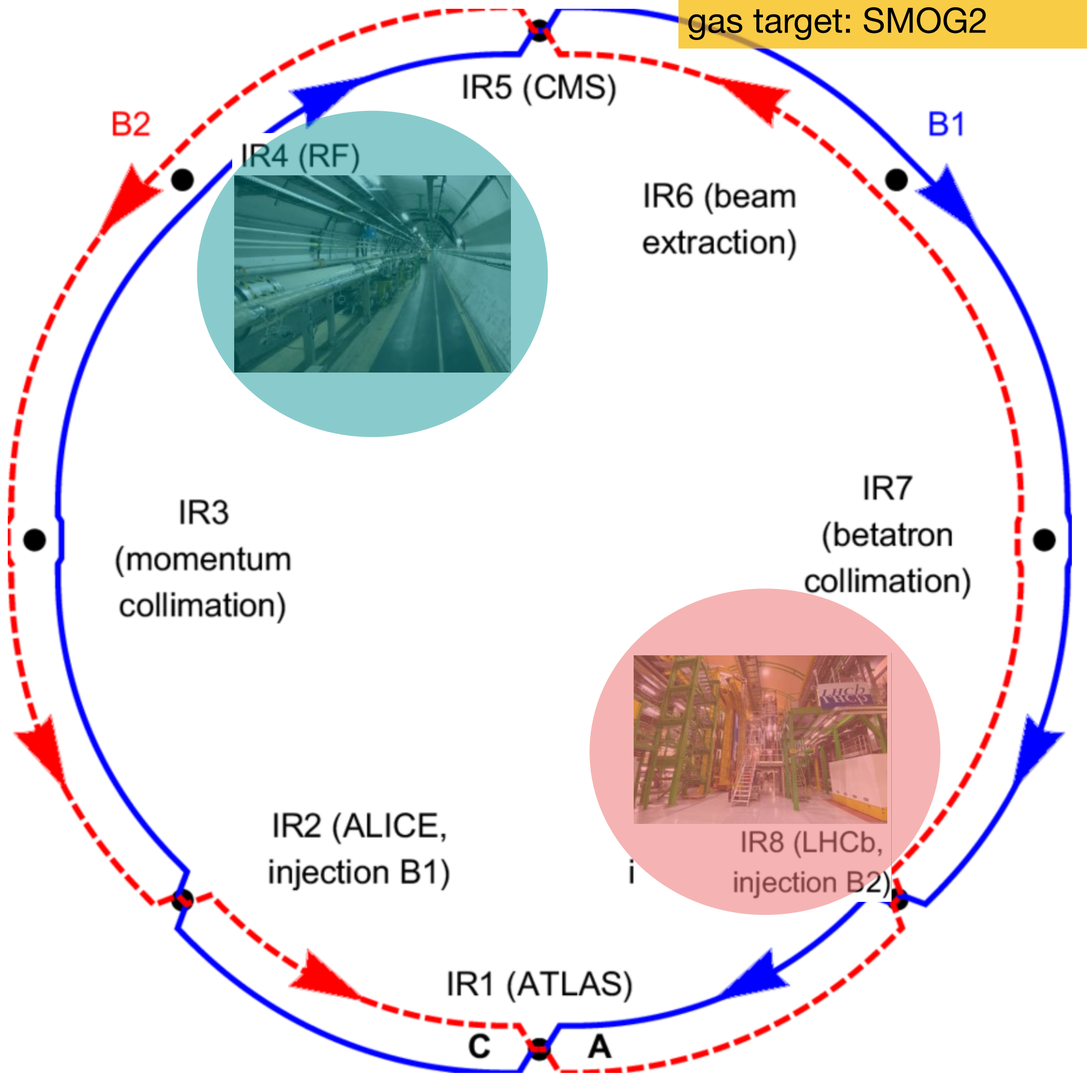

EIC: Sivers asymmetry

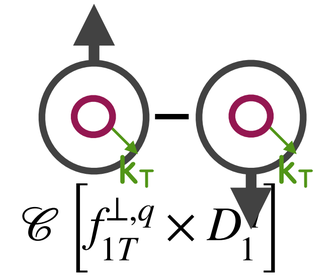

ECCE $\mathscr{C}\left[f_{1T}^{\perp,q} \times D_1^q\right]$

systematic uncertainty=
|generated - reconstructed|

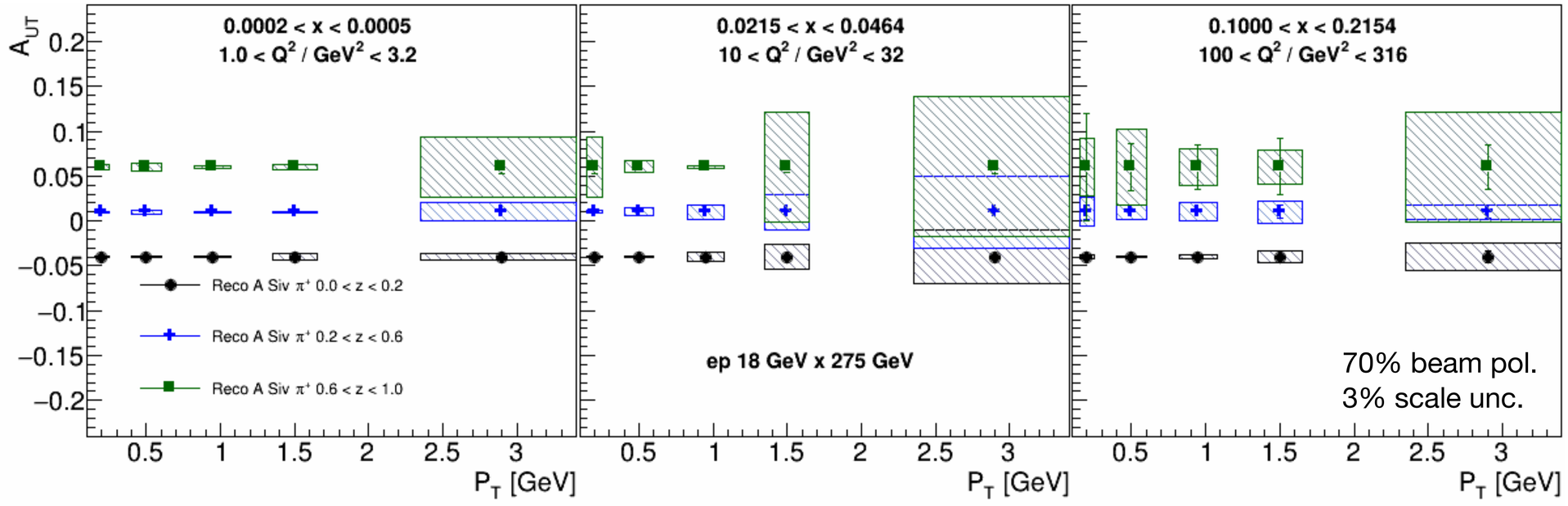

- Asymmetries at low x and low Q^2 well below 1% → need small uncertainties.
- Low x and Q^2: small statistical uncertainty.
- For not too large z and P_T, statistical uncertainty well below 1%.
- Systematic uncertainties increase with z and P_T: likely because of higher smearing effects.

Sivers TMD: impact of the EIC

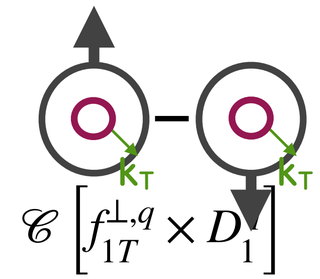

A. Vladimirov, R. Seidl et al., NIM A **1049** (2023) 168017
Parametrisation from M. Bury et al., JHEP **05** (2021)151

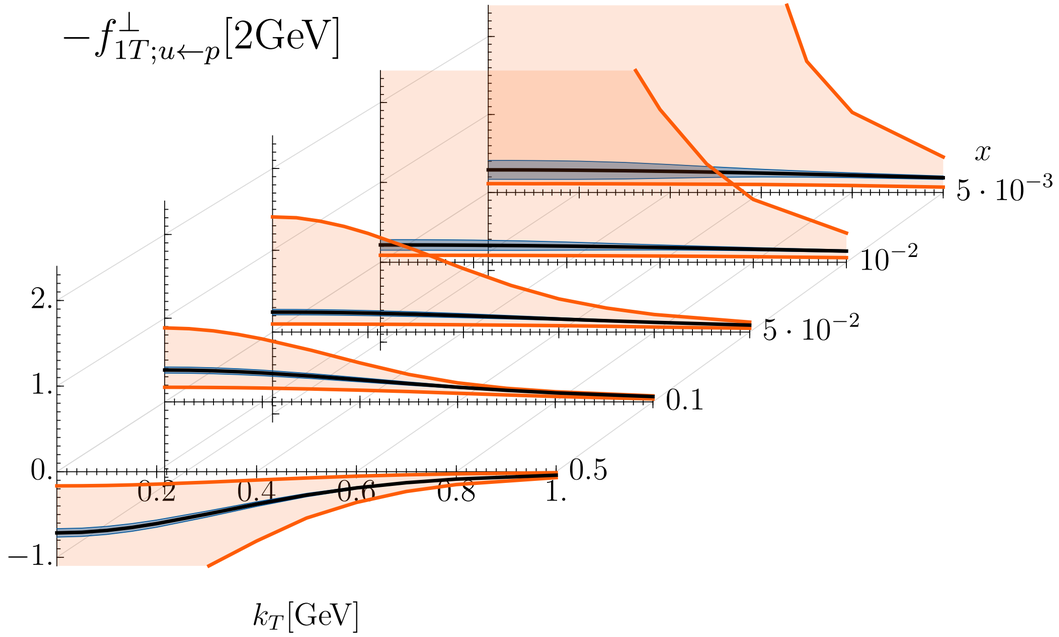

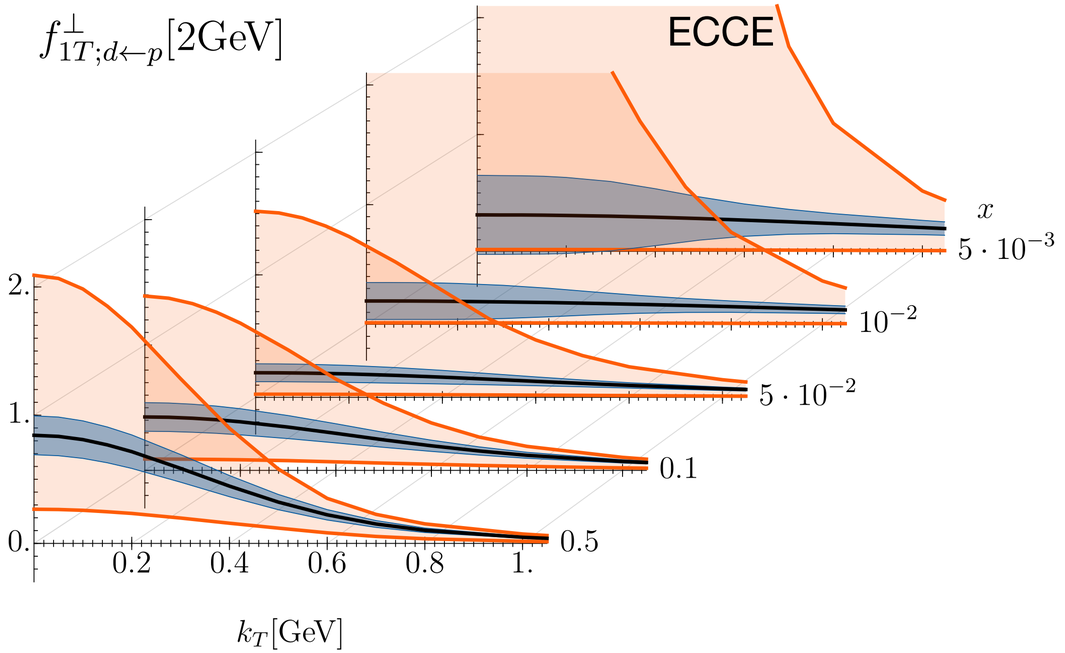

DIS variables via scattered lepton

$$Q^2 > 1\ \mathrm{GeV}^2$$
$$0.01 < y < 0.95$$
$$W^2 > 10\ \mathrm{GeV}^2$$

$$5 \times 41\ \mathrm{GeV}^2$$
$$10 \times 100\ \mathrm{GeV}^2$$
$$18 \times 100\ \mathrm{GeV}^2$$
$$18 \times 275\ \mathrm{GeV}^2$$

$\mathcal{L} = 10\ \mathrm{fb}^{-1}$ for each collision energy